

**CLASSIFICATION OF INDIAN COASTAL
TIDAL INLETS AND SOME ASPECTS OF
MORPHOLOGY CHANGES UNDER
CYCLONE EVENT**

Thesis

Submitted in partial fulfillment of the requirements for the degree of

DOCTOR OF PHILOSOPHY

by

N. Amaranatha Reddy



DEPARTMENT OF APPLIED MECHANICS AND HYDRAULICS

NATIONAL INSTITUTE OF TECHNOLOGY KARNATAKA,

SURATHKAL, MANGALORE – 575025

AUGUST 2018

DECLARATION

I hereby *declare* that the Research Thesis entitled “**CLASSIFICATION OF INDIAN COASTAL TIDAL INLETS AND SOME ASPECTS OF MORPHOLOGY CHANGES UNDER CYCLONE EVENTS**” which is being submitted to the **National Institute of Technology Karnataka, Surathkal** in partial fulfillment of the requirements for the award of the Degree of **Doctor of Philosophy in Department of Applied Mechanics and Hydraulics** is a *bonafide report of the research work carried out by me*. The material contained in this Research Thesis has not been submitted to any University or Institution for the award of any degree.

Register Number : **123038AM12P04**

Name of the Research Scholar : **N. Amaranatha Reddy**

Signature of the Research Scholar :

Department of Applied Mechanics and Hydraulics

Place : **NITK-Surathkal**

Date : **24 AUG 2018**

C E R T I F I C A T E

This is to *certify* that the Research Thesis entitled “**CLASSIFICATION OF INDIAN COASTAL TIDAL INLETS AND SOME ASPECTS OF MORPHOLOGY CHANGES UNDER CYCLONE EVENTS**” submitted by **Mr. N. Amaranatha Reddy (Register Number: 123038AM12P04)** as the record of the research work carried out by him, is *accepted as the Research Thesis submission* in partial fulfillment of the requirements for the award of degree of **Doctor of Philosophy**.

Prof. Subba Rao

Research Supervisor & Professor

Department of Applied Mechanics

NITK, Surathkal

Dr. Jaya Kumar Seelam

Research Supervisor & Principal Scientist

CSIR-National Institute of Oceanography

Dona Paula, Goa

Prof. A. Mahesha

Chairman - DRPC

DEPARTMENT OF APPLIED MECHANICS AND HYDRAULICS
NATIONAL INSTITUTE OF TECHNOLOGY KARNATAKA,
SURATHKAL, MANGALORE – 57502

ACKNOWLEDGEMENTS

Completing the Ph.D. thesis has been probably the most challenging activity of my life. During the journey, I worked and acquainted with many people who contributed in different ways to the success of this study and made it an unforgettable experience for me. It is a pleasure to convey my gratitude to them.

First and foremost, I would like to express my deep gratitude to my research supervisors **Dr. Jaya Kumar Seelam**, Principal Scientist, CSIR-NIO, Goa and **Prof. Subba Rao**, Department of Applied Mechanics and Hydraulics, National Institute of Technology Karnataka (N.I.T.K), Surathkal, for their patient guidance, stimulating suggestions and invaluable advices they have been provided throughout my doctoral research endeavor. Their insightful observations and constructive criticism helped me to establish the overall direction of the research and move forward with investigation in depth.

I take this opportunity to thank **Prof. A. Mahesha**, Professor and Head, Department of Applied Mechanics and Hydraulics for his continuous and timely suggestions.

I wish to thank the members of the Research Program Assessment Committee, **Dr. M.K. Nagaraj**, Professor, Department of Applied Mechanics and Hydraulics and **Dr. A. U. Ravi Shankar**, Professor, Department of Civil Engineering for their appreciation and constructive criticism all through my research work.

I wish to thank **Dr. M.V. Ranama Murthy**, Project Director, National Institute of Ocean technology (NIOT), Chennai, for his invaluable help and constructive comments on the work at the early stage of its development. I owe my sincere thanks to A. Arun Kumar, Scientist-D and Karunakar, Scientist-C of NIOT for their suggestions and advices.

I would like to thank the Additional Surveyor General, Survey of India (SoI) in both Hyderabad and Bangalore regional offices for providing the required SoI toposheets to carry out my research work. I would also like to thank Dr. G.S. Srinivasa Reddy, Director, Karnataka State Natural Disaster Monitoring Centre, Bangalore, for providing the hourly rainfall data for a year.

Special thanks to **Dr. Santosh G Thampi**, Professor, Department of Civil Engineering, National Institute of Technology Calicut (NITC), for his help and constructive suggestions provided to carry out the first objective of my research work.

I wish to express my sincere gratitude to all the faculty members of the Applied Mechanics and Hydraulics Department, N.I.T.K Surathkal for their help, encouragement and support all through this research work.

I am thankful to the Director, NIO, for granting me the permission to carry out and utilize the facilities of the Institute to accomplish my research work.

It would have been difficult for me to shape up my manuscript on classification of inlets without the help of Mr. Vikas Mendi, Research Scholar, NITK. His timely and efficient contribution greatly enhanced the quality of my research and I express my deepest appreciation for his assistance.

Mike 21 Software have been used extensively in this study. I would like to express my gratitude to Mrs. Jyothi, NIO for her willingness to patiently answer my queries on MIKE 21 anytime and for all her help and support during my stay at NIO.

I wish to thank the Secretary & Correspondent, Dr.N.Vijaya Bhaskar Choudary; Principal, Dr. C. Yavaraj; SAO (G), Mrs. M. Prathibha, Madanapalle Institute of Technology & Science (MITS), Madanapalle for their enough support and encouragement given during my research at final stage.

Words fail me when it comes to acknowledge my soul mate, my shadow and light, my ever loving wife **Suma**. These past years have not been an east ride for both of us; her sacrifice and patience are beyond words. I truly thank her for being my side even when I was irritated and depressed. I doubt that I will ever be able to convey my appreciation fully, but I owe everything for being so patient, understanding and self-sacrificing.

It is the time to admire my cuties **Loshika Reddy** and **Rohan Karthik Reddy**, the most adorable gifts of the God and for being so understanding at their small age. During the past years, I could not give my full attention and time to them. But they never troubled and always allowed me to

work with all their smiles. Therefore, now it is the time to compensate for all the lost days and embrace each and every moment of joy and happiness with them to the fullest. My life is meaningless without you, dear Loshi and dear Rohan.

I would like to thank my mother who have trusted me throughout my life. I would like to share this moment of happiness with my mother, Santhamma; My brother Madhu Sudhan Reddy; My Sister-in-law Sujatha for their constant encouragement.

I am indebted to my friends cum relatives Mr. V. Siva Reddy, Mr. G. Harinath Reddy, Mr. M. Ramesh Reddy for their constant help and encouragement during the entire research work and also the informal support and encouragement of my dear colleagues Prof. A. Mohan, Kishore, Prathap Kumar, Rajendra, Nowshad, Srinivasa Reddy and Suresh has been indispensable.

I would like to thank my colleagues at MITS for their constant support and help when I was not there in the college. Especially I would like to thank Mr. I. Bhargav Reddy, post graduate student and Karthik, graduate student at MITS who helped me a lot in drawing the plots and their support in writing the thesis.

My acknowledgement will be incomplete if I do not express my gratitude and deep appreciation to my dearest friends and students Adi, Swathi, Sai, Geetha (NITK), Venkatesh (NITK), Srinivasa Reddy (NITK), Santosh (NITC) and Yadhunath (NIO) whose support and caring have enlightened and entertained me over the many years of friendship. Last but not least, I would like to thank all my students at KSRM college and MITS for their support and encouragement. Finally, I would like to thank everybody who helped me directly or indirectly to the successful realization of this thesis.

Amaranatha Reddy N.

ABSTRACT

Coastal inlets are the openings along the coastline which connects wide-spread oceans and the adjacent water bodies. These coastal inlets vary in nature depending on many parameters including waves and tides. Coastal inlets play a major role in regulating the inland flow and in feeding the coast with hinterland sediments to maintain the coastal morphology. The studies for inlet dynamics are essential to understanding the coastal and inland waters interaction like physical processes as well as the exchange of nutrients or pollutants between the two water bodies.

To study the inlet dynamics, understanding its behaviour in the form of type of dominance (i.e. tide-dominated or wave-dominated or river dominated) along the coastline and morphology of the tidal inlets are very essential. Although many methods are available in the literature to classify the tidal inlets worldwide, comprehensive information on inlet classification and river discharge at majority of the inlets is not available for the Indian coast. This study identified 471 tidal inlets along the nine maritime coastal states of India, and focuses on the classification of these inlets. The classification is based on various parameters viz., tidal range, wave exposure conditions, morphology, hydrodynamics and non-dimensional parameterization of wave, tide and river discharge forces with and without mean wave period. All these 471 tidal inlets have an inlet width greater than or equal to 5m at the confluence of river with the sea.

The inlet morphology depends on the tidal range, significant wave height, mean wave period and river discharge. Therefore, these parameters were determined in the vicinity of each of the inlets. The tidal range for each of the inlet is obtained by simulating the water level variations for about 30 days along the coast using a state of the art hydrodynamic model of MIKE by DHI, i.e., MIKE-HD flow model. The wave data, viz., significant wave height (H_s) and mean wave period (T_z) are obtained from the validated MIKE21 spectral wave model simulations for the year 2010 using NCEP/NCAR wind as input data.

The Central Water Commission (CWC) and State's Water Resource Departments maintain gauging stations to measure the stage, discharge and water quality in the major streams and rivers across the country. The data maintained by CWC is available through online portal Water Resources Information System (India-WRIS). Out of 471 tidal inlets, only 36 inlets have the gauging stations within 1km from the inlet entrance (Source: Karnataka State Natural Disaster Monitoring Centre), and therefore, the available discharge is directly taken from the database for the classification by assuming no losses between the gauging station and the sea. Due to the limited information available on the measured river discharge, discharge at ungauged stations along Konkan and Malabar coast has been estimated using catchment characteristics rather than rainfall-runoff data. The catchment characteristics viz., catchment area, length of the main stream, a distance of the centroid from basin outlet and equivalent stream slope are determined using basin maps in ArcGIS® software.

The Synthetic Unit Hydrograph (SUH) methods like CWC method, Snyder method, Soil Conservation Service (SCS) method, Gray method, Croley method, Transmutation approach method, two parameter Gamma distribution method and Hybrid model are used to estimate the flood discharge. Since there is no measured data available, the discharge estimation at the tidal inlets has been done in two stages. Firstly, for the CWC measured data, the above said SUH methods are applied and validated with the measured data. Later, the discharge for ungauged basins is simulated based on the fitted parameters for selected methods. The results showed that even though the CWC, Snyder and SCS methods are used widely in practical engineering problems, the manual fitting of Unit Hydrograph with limited characteristics points needs a high degree of precaution as well as trial and error. Alternatively, the probability distribution functions (pdfs) based SUH methods used in the study give the full shape of unit hydrograph and also satisfies the prerequisite for UH criterion (i.e., area under the UH is unity). A new non-dimensional UH is formulated which is applicable for Konkan and Malabar coastline of India.

The classification of the Indian coastal tidal inlets based on the tidal range has been carried out based on the values given by Davies (1964) and Hayes (1975). Wave

exposure condition classification is carried out using the basic measure of wave energy which is quantified with the parameter H^2T^2 , where, H is the annual average significant wave height, and T is the mean wave period. Geomorphological classification of the tidal inlets is carried out visually using the satellite images. Hydrodynamic classification of tidal inlets is carried out according to the relative strength of tide and waves with tidal range serving as a surrogate for the tidal prism or tidal current. In the Hydrodynamic classification, wave heights during non-monsoon, southwest monsoon and northeast monsoon periods are considered to identify the variations in the classification of the inlets in addition to annual wave heights. Non-dimensional classification is carried out for 75 inlets for which the river discharge information is available. In addition to the three main forcing functions viz. tide, waves, and river discharge, the non-dimensional classification considers the mean wave period. Thus, the tidal inlets classified by hydrodynamics and non-dimensional methods are compared with the geomorphological classification. A new range is identified for the non-dimensional classification by incorporating the mean wave period.

Majority of the inlets along the Indian coastline fall under the category of micro- to meso-tidal environment. Hence for many river mouths and tidal inlets along the east coast and southern part of the west coast, inlet migration depends upon the magnitude of littoral drift, tidal current and depth of the inlet at the entrance. Tidal inlets along the west coast of India (219 in number) are subjected to high wave energy environments, whereas east coast inlets are subjected to moderate wave energy environments. None of the inlets fall under the category of mildly exposed wave environments. Majority of the tidal inlets on the east coast of India and the southern regions on the west coast (Kerala, Karnataka, and Goa) are observed to be wave-dominated inlets, whereas, the inlets towards the north on the west coast (Maharashtra and Gujarat) are tide-dominated. Intermittently Closed and Open Lakes and Lagoons (ICOLLs) are present in the coasts of southern states: Andhra Pradesh, Tamil Nadu, and Kerala.

The blockage of tidal inlets may lead to flooding due to excess rainfall in the upper reaches of the watershed. The blocked inlets will impact significantly the sediment discharge system in the coastal region. On the other hand, excessive alongshore

sediment transport could result in sediment deposition at the inlet mouths and lead to inlet closure. The coastal wave climate has a significant influence on the coastal sediment transport system as well as in the breaching of the closed tidal inlets. These interlinked phenomena are still in the interest of research community as the underlying physical processes are temporally and spatially variable. Also, the formation of flood and ebb deltas is yet to be understood. Moreover, the passing of storms in the vicinity of tidal inlets poses very different problems both in terms of increased river discharge due to storm associated rainfall or due to increased wave activity and storm surges.

The morphological changes of the tidal inlets associated with the storm activity is a challenging research area on which models have not yet fully mimicked all the processes. Therefore, to study the morphology changes in tidal inlet vicinity due to a cyclone, numerical modeling study is undertaken at a specific location on the east coast of India, where some of the measured data is available. To study morphological changes near the vicinity of a tidal inlet, a case study of cyclone Phailin has been taken which had a landfall near Gopalpur in Odisha state. The reasons to take up this study area are: (1) availability of measured wind and wave data, (2) the landfall point is closer to the coast where a tidal inlet exists and (3) satellite images showing a breach of the berm after the cyclone, which was not there before the cyclone. Using the MIKE21 numerical model, the conditions for breaching of the berm has been successfully reproduced, and thereon morphology around the inlet and in the near shore region is studied.

Keywords: Tidal inlets, Indian Coastline, Flood discharge, Ungauged basins, Cyclone, Morphology and Berm breach

CONTENTS

	Page No.
Declaration	
Certificate	
Acknowledgements	
Abstract	i
List of Contents	v
List of Figures	x
List of Tables	xix
List of Symbols	xxii
Abbreviations	xxv
1. INTRODUCTION	1
1.1. General	1
1.2. Current state of knowledge	3
1.3. Historical Cyclones – Their impact on Indian coastline	7
1.4. Necessity and relevance of the present study	10
1.5. Formulation of research objectives	13
1.6. Organization of thesis	13
2. ESTIMATION OF FLOOD DISCHARGE	15
2.1. Introduction	15
2.2. Study area and data collection	19
2.2.1. Karnataka state	19
2.2.2. Kerala state	20
2.3. Analysis of physiographic parameters of the catchments	22
2.3.1. Catchment area	23
2.3.2. Length of the main stream	24
2.3.3. Center of gravity of each catchment	24
2.3.4. Equivalent stream slope of the catchment	26
2.4. Different synthetic unit hydrograph approaches	30
2.4.1. Traditional SHU methods	31

	2.4.1.1 CWC SUH Method	32
	2.4.1.2 CWC Dimensionless unit hydrograph method	36
	2.4.1.3 Snyder Method	38
	2.4.1.4 Soil Conservation Service (SCS) method	39
2.4.2.	Probability Distribution Function based SUH methods	41
	2.4.2.1. Gray method	42
	2.4.2.2. Croley method	43
	2.4.2.3. Transmutation approach	43
	2.4.2.4. Two Parameter Gamma Distribution method	44
2.4.3.	Conceptual Synthetic Unit Hydrograph methods	45
	2.4.3.1 Hybrid model	45
2.5.	Estimation of UH parameters	47
	2.5.1. Parameter estimation for CWC methods	47
	2.5.2. Parameter estimation for Snyder's method	49
	2.5.3. Parameter estimation for SCS method	49
	2.5.4. Parameter estimation for probability distribution function based SUH methods	49
2.6.	Development of synthetic unit hydrographs	51
	2.6.1. Development of SUH's for measured data	51
	2.6.2. Development of SUH's at ungauged catchments	56
2.7.	Comparison of total flood discharges at ungauged catchments	60
	2.7.1. Comparison of flood discharged for the CWC measured data	60
	2.7.2. Comparison of flood discharges at ungauged catchments along Kerala coastal line	61
2.8.	Summary	62
3.	CLASSIFICATION OF TIDAL INLETS	66
	3.1. Introduction	66
	3.2. Study area	68
	3.3. Literature on classification of tidal inlets	75
	3.3.1. Classification based on tidal range conditions	76

3.3.2.	Classification based of coastal energy regime	77
3.3.3.	Geomorphological classification	78
3.3.4.	Hydrodynamic classification	81
	3.3.4.1. <i>Tide dominated inlets</i>	83
	3.3.4.2. <i>Wave dominated inlets</i>	84
	3.3.4.3. <i>Mixed energy inlets</i>	85
3.3.5.	Classification based on dimensionless parameters without wave period	85
3.3.6.	Classification based on dimensionless parameters with wave period	87
3.4.	Parameter estimation	88
3.4.1.	Tidal range	88
3.4.2.	Lagoon or Bay area	90
3.4.3.	Tidal prism	91
3.4.4.	Tidal discharge	91
3.4.5.	Significant wave height	96
3.4.6.	Flood discharge	96
3.5.	Classification of inlets based on different methods	97
3.5.1. (a)	Classification based on tidal range conditions (Davies, 1964)	97
3.5.1.(b)	(b) classification based on tidal range regime (Hayes, 1975)	102
3.5.2.	Classification based on wave energy regime	106
3.5.3.	Geomorphological classification	107
3.5.4.	Hydrodynamic classification	111
3.5.5.	Classification based on dimensionless parameters without wave period	122
3.5.6.	Classification based on dimensionless parameters with wave period	125
3.6.	Comparison of Tidal inlet classifications	127
3.6.1.	Geomorphological Vs Hydrological classification	127

3.6.2.	Geomorphological Vs Non-dimensional Vu method	128
3.6.3.	Geomorphological Vs Non-dimensional modified Vu method	129
3.6.4.	Comparison of all methods	129
3.7.	Summary	132
4.	CYCLONE INDUCED MORPHOLOGY CHANGES	134
4.1.	INTRODUCTION	134
4.1.1.	Naming of the cyclones	137
4.2.	CYCLONE INDUCED MORPHOLOGY STUDIES	140
4.2.1.	Introduction	140
4.2.2.	The Cyclone Phailin	141
4.3.	STUDY AREA	143
4.4.	DESCRIPTION OF THE NUMERICAL MODELS	144
4.4.1.	Parametric wind models	145
	4.4.1.1. <i>Young and Sobey model</i>	145
	4.4.1.2. <i>Holland single vertex model</i>	146
	4.4.1.3. <i>Holland double vertex model</i>	147
	4.4.1.4. <i>Rankine vortex model</i>	147
	4.4.1.5. <i>Wind correction</i>	148
4.4.2.	Description of Numerical models	149
	4.4.2.1. <i>Hydrodynamic model</i>	149
	4.4.2.2. <i>wave model</i>	152
	4.4.2.3. <i>Non-cohesive sediment transport model</i>	154
4.5.	METHODOLOGY	155
4.5.1.	Cyclone wind data	155
4.5.2.	Model domain and mesh generation	159
4.5.3.	Model parameters	159
	4.5.3.1. <i>MIKE21 Spectral Wave FM model parameters</i>	161
	4.5.3.2. <i>MIKE21 Coupled model FM model parameters</i>	162
4.6.	RESULTS AND DISCUSSION	163
4.6.1.	Cyclone winds	163

4.6.2.	Storm waves	164
4.6.3.	Surface elevation and Storm surge	166
4.6.4.	Bed level changes	167
	<i>4.6.4.1. Bed level changes along the berm</i>	168
	<i>4.6.4.2. Bed level changes across the berm</i>	172
4.6.5.	Flow pattern at points of interest	175
4.6.6	Berm breach process	178
4.7.	Summary	182
5.	CONCLUSIONS	184
5.1.	Classification of tidal inlets	184
5.2.	Estimation of flood discharge	187
5.3.	Cyclone induced morphology changes in the vicinity of inlet	188
5.4	Limitations of the study	189
5.4.	Research findings	189
5.5.	Matters of Further Research	190
	Appendix-I	193
	Appendix-II	202
	Appendix-III	219
	Appendix-IV	268
	Publication list	
	Resume	

LIST OF FIGURES

Figure No.	Description	Page No.
Figure 1.1	Month wise frequency cyclone disturbances over North Indian Ocean during 2001-2017	9
Figure 1.2	Month wise frequency cyclone disturbances over Bay of Bengal during 2001-2017	9
Figure 1.3	Month wise frequency cyclone disturbances over Arabian Sea during 2001-2017	10
Figure 1.4(a)	Year wise frequency of sustained wind speeds of cyclone disturbances over North Indian Ocean during 2001-2017	11
Figure 1.4(b)	Year Wise frequency of central pressures of cyclone disturbances over North Indian Ocean During 2001-2017	11
Figure 2.1	Study area showing Western catchments of Karnataka along with drainage and watershed boundaries (red dot is measured data location by CWC)	21
Figure 2.2	Study area showing different watersheds and drainage pattern along Kerala coast	22
Figure 2.3	Survey of India toposheet (toposheet No: 48 I/6) showing the basin outlets, drainage patterns at Tadri, Manjaguni, Belambar, Ankola and Belekari catchments	23
Figure 2.4	Catchment area of Kundapura watershed along with basin outlet location (Green circle)	24
Figure 2.5	Length of the main stream for Mavinakurve watershed (=17km)	25
Figure 2.6	Catchment centroid position (red point) for the Tadri basin	25
Figure 2.7	Physiographic parameters of the representative catchment plan and longitudinal section	27
Figure 2.8	Hydrometeorologically homogeneous zones in India (CWC, 1983) and Green colour zone is the present study area along Karnataka coastline	33

Figure 2.9	Synthetic Unit Hydrograph parameters	34
Figure 2.10	Dimensionless unit hydrographs at 13 bridge sites	37
Figure 2.11	Dimensionless Unit Hydrograph derived for the project catchments	37
Figure 2.12	Arrangement of first and second reservoirs of the hybrid model	47
Figure 2.13(a)	Synthetic Unit Hydrograph of 1 hour duration using traditional SUH methods and along with the measured UH at Bridge site No.9	54
Figure 2.13(b)	(b) Synthetic Unit Hydrograph of 1 hour duration using pdfs and conceptual based SUH methods and along with the measured UH at Bridge site No.9	55
Figure 2.14(a)	SUH of 1 hour duration during using Traditional SUH methods at Mahe Catchment (Catchment ID-1)	56
Figure 2.14(b)	SUH of 1-hour duration during using pdfs and conceptual based SUH methods at Mahe catchment (Catchments ID-1)	58
Figure 3.1	Locations of Inlets considered in study area	70
Figure 3.2(a)	Inlets considered along the coast of Gujarat (42 inlets)	71
Figure 3.2(b)	Inlets considered along the coasts of Maharashtra (65 inlets)	71
Figure 3.2(c)	Inlets considered along the coasts of Goa (11 inlets)	72
Figure 3.2(d)	Inlets considered along the coasts of Karnataka (27 inlets)	72
Figure 3.2(e)	Inlets considered along the coasts of Kerala (68 inlets)	73
Figure 3.2(f)	Inlets considered along the coasts of Tamil Nadu (121 inlets)	73
Figure 3.2(g)	Inlets considered along the coasts of Andhra Pradesh (106 inlets)	74
Figure 3.2(h)	Inlets considered along the coasts of Odisha (23 inlets)	74
Figure 3.2(i)	Inlets considered along the coasts of West Bengal (8 inlets)	75
Figure 3.3	Classification of inlet shapes based on the influence of waves, tide and river flow (de Vriend et al. 1999)	79
Figure 3.4	Hydrodynamic based classification of tidal inlet morphology (After Davies and Hayes, 1984)	82

Figure 3.5(a)	Representative planform morphology and bypassing mode of natural inlets based on tide dominance (Source: FitzGerald 1982)	84
Figure 3.5(b)	Representative planform morphology and bypassing mode of natural inlets based on wave dominance (Source: FitzGerald 1982)	84
Figure 3.5(c)	Representative planform morphology and bypassing mode of natural inlets based on mixed energy dominance (Source: FitzGerald 1982)	85
Figure 3.6	Inlet classification in terms of $\frac{\hat{Q}_{tide}}{\sqrt{gH^3}}$ and $\frac{Q_f}{\sqrt{gH^3}}$ for 178 estuaries in NSW, Australia (Vu 2013)	87
Figure 3.7	MIKE21 Model bathymetry for Mandovi and Zuari inlets	89
Figure 3.8	Generated mesh for Mandovi and Zuari inlets	90
Figure 3.9(a)	Tidal range along West coast of India	92
Figure 3.9(b)	(b) Tidal range along East coast of India	93
Figure 3.10(a)	(a) Wave heights along East coast of India	94
Figure 3.10(b)	(b) Wave heights along East coast of India	95
Figure 3.11(a)	Classification of tidal inlets along west coast of India based on Tidal range conditions	100
Figure 3.11(b)	Classification of tidal inlets along east coast of India based on Tidal range condition	101
Figure 3.12(a)	Classification of tidal inlets along west coast of India based on Tidal range conditions	103
Figure 3.12(b)	Classification of tidal inlets along east coast of India based on Tidal range conditions	104
Figure 3.13(a)	Classification of tidal inlets along west coast of India based on wave energy regime	108
Figure 3.13(b)	Classification of tidal inlets along east coast of India based on wave energy regime	109
Figure 3.14	Classification based on Hayes (1979) for all seasons along Gujarat coast	112

Figure 3.15	Classification based on Hayes (1979) for all seasons along Maharashtra coast	113
Figure 3.16	Classification based on Hayes (1979) for all seasons along Goa coast	114
Figure 3.17	Classification based on Hayes (1979) for all seasons along Karnataka coast	115
Figure 3.18	Classification based on Hayes (1979) for all seasons along Kerala coast	116
Figure 3.19	Classification based on Hayes (1979) for all seasons along Tamilnadu coast	117
Figure 3.20	Classification based on Hayes (1979) for all seasons along Andhra Pradesh coast	118
Figure 3.21	Classification based on Hayes (1979) for all seasons along Odisha coast	119
Figure 3.22	Classification based on Hayes (1979) for all seasons along West Bengal coast	120
Figure 3.23	Classification based on dimensionless parameters without wave period	123
Figure 3.24	Classification based on dimensionless parameters with wave period	126
Figure 4.1	Observed track of VSCS, Phailin during 8 th -14 th October 2013 (Source: IMD)	142
Figure 4.2(a)	Study area [Google Earth image as on 25-03-2013 (i.e. before Phailin cyclone)]	143
Figure 4.2(b)	Study area [Google Earth image as on 14-01-2014 (i.e. after Phailin cyclone)]	144
Figure 4.3	Bathymetry and mesh adopted for generation of cyclone induced parameters	156
Figure 4.4	Wind fields of the Phailin cyclone	158

Figure 4.5	Pressure fields of the Phailin cyclone	158
Figure 4.6	Model domain and mesh used in the study	160
Figure 4.7	Model domain showing the mesh and bathymetry contours at points of interest	160
Figure 4.8	Boundary conditions of the SW model	161
Figure 4.9	Boundary conditions of the Coupled Model FM	162
Figure 4.10	Comparison of measured and modelled cyclone winds at Gopalpur for cyclone Phailin	164
Figure 4.11	Points of interest in the study	165
Figure 4.12	Wave heights obtained from Phailin Cyclone wind wave model for Gopalpur (solid line) and Paradip (dash line) compared with measured wave heights at Gopalpur (dot-dash line)	166
Figure 4.13	Locations considered to study Bed level changes along the berm at (a) breach location and (b) inlet location	167
Figure 4.14	Locations considered for study of bed level changes along the berm	168
Figure 4.15	Bed level changes along the berm at 4 transect lines	169
Figure 4.16	Bed level changes at 2.2m berm height of the berm near breaching point	170
Figure 4.17	Bed level changes at 2.2m berm height of the berm near inlet location	171
Figure 4.18	Locations considered for study of bed level changes across the berm	172
Figure 4.19	Bed level changes across the berm at breaching location	172

Figure 4.20	Bed level changes across the berm at breach location at different time steps	173
Figure 4.21(a)	Bed level changes across the berm at Transect D-D	174
Figure 4.2a(b)	Bed level changes across the berm at Transect C-C	174
Figure 4.22	Bed level changes across the berm at inlet location	175
Figure 4.23	Bed level changes across the berm at inlet location at different time steps	176
Figure 4.24	Width of the berm at breach location after the cyclone Phailin (a) Google earth image and (b) MIKE modelled data	178
Figure 4.25	Bed level at the end of simulation for Wind only case	179
Figure 4.26	Bed level at the end of simulation for wave only case	179
Figure 4.27	Bed level at the end of simulation for Tide only case	180
Figure 4.28	Bed level at the end of simulation for Tide + Wind case	180
Figure 4.29	Bed level at the end of simulation for Tide + Wave case	181
Figure 4.31	Bed level at the end of simulation for Wave + Wind case	181
Figure 4.32	Bed level at the end of simulation for Tide + Wind + Wave case	182
Figure A2.1(a)	Rain Gauge network (* symbol) along the Dakshina Kannada, Udupi and Uttara Kannada districts of Karnataka state	200
Figure A2.1(b)	Location of rain gauge stations (* symbol) in watersheds of Kerala	200
Figure A2.2	SUH of 1 hour duration during using Traditional SUH methods at Catchments IDs 2, 3, 4, 5, 6 and 7	205
Figure A2.3	SUH of 1 hour duration during using Traditional SUH methods at Catchments IDs 8, 9, 10, 11, 12 and 13	206
Figure A2.4	SUH of 1 hour duration during using Traditional SUH methods at Catchments IDs 14, 15, 16, 17, 18 and 19	207
Figure A2.5	SUH of 1 hour duration during using Traditional SUH methods at Catchments IDs 20,21, 22, 23, 24 and 25	208

Figure A2.6	SUH of 1 hour duration during using Traditional SUH methods at Catchments IDs 26, 27, 28, 29, 30 and 31	209
Figure A2.7	SUH of 1 hour duration during using Traditional SUH methods at Catchments IDs 32, 33, 34, 35 and 36	210
Figure A2.8	SUH of 1 hour duration during using pdfs based SUH methods at Catchments IDs 2, 3, 4, 5, 6 and 7	211
Figure A2.9	SUH of 1 hour duration during using pdfs based SUH methods at Catchments IDs 8, 9, 10, 11, 12 and 13	212
Figure A2.10	SUH of 1 hour duration during using pdfs based SUH methods at Catchments IDs 14, 15, 16, 17, 18 and 19	213
Figure A2.11	SUH of 1 hour duration during using pdfs based SUH methods at Catchments IDs 20, 21, 22, 23, 24 and 25	214
Figure A2.12	SUH of 1 hour duration during using pdfs based SUH methods at Catchments IDs 26, 27, 28, 29, 30 and 31	215
Figure A2.13	SUH of 1 hour duration during using pdfs based SUH methods at Catchments IDs 32, 33, 34, 35 and 36	216
Figure A4.1	At 09-10-2013 18:00:00 time step the Figure shows vector plot (a) whole model domain, (b) near breach, (c) near inlet with time series plots of (d) significant Wave height, (e) surge and (f) surface elevation at various locations	266
Figure A4.2	At 10-10-2013 00:00:00 time step the Figure shows vector plot (a) whole model domain, (b) near breach, (c) near inlet with time series plots of (d) significant Wave height, (e) surge and (f) surface elevation at various locations	267
Figure A4.3	At 10-10-2013 06:00:00 time step the Figure shows vector plot (a) whole model domain, (b) near breach, (c) near inlet with time series plots of (d) significant Wave height, (e) surge and (f) surface elevation at various locations	268
Figure A4.4	At 10-10-2013 12:00:00 time step the Figure shows vector plot (a) whole model domain, (b) near breach, (c) near inlet	269

	with time series plots of (d) significant Wave height, (e) surge and (f) surface elevation at various locations	
Figure A4.5	At 10-10-2013 18:00:00 time step the Figure shows vector plot (a) whole model domain, (b) near breach, (c) near inlet with time series plots of (d) significant Wave height, (e) surge and (f) surface elevation at various locations	270
Figure A4.6	At 11-10-2013 00:00:00 time step the Figure shows vector plot (a) whole model domain, (b) near breach, (c) near inlet with time series plots of (d) significant Wave height, (e) surge and (f) surface elevation at various locations	271
Figure A4.7	At 11-10-2013 06:00:00 time step the Figure shows vector plot (a) whole model domain, (b) near breach, (c) near inlet with time series plots of (d) significant Wave height, (e) surge and (f) surface elevation at various locations	272
Figure A4.8	At 11-10-2013 12:00:00 time step the Figure shows vector plot (a) whole model domain, (b) near breach, (c) near inlet with time series plots of (d) significant Wave height, (e) surge and (f) surface elevation at various locations	273
Figure A4.9	At 11-10-2013 18:00:00 time step the Figure shows vector plot (a) whole model domain, (b) near breach, (c) near inlet with time series plots of (d) significant Wave height, (e) surge and (f) surface elevation at various locations	274
Figure A4.10	At 12-10-2013 00:00:00 time step the Figure shows vector plot (a) whole model domain, (b) near breach, (c) near inlet with time series plots of (d) significant Wave height, (e) surge and (f) surface elevation at various locations	275
Figure A4.11	At 12-10-2013 06:00:00 time step the Figure shows vector plot (a) whole model domain, (b) near breach, (c) near inlet with time series plots of (d) significant Wave height, (e) surge and (f) surface elevation at various locations	276

Figure A4.12	At 12-10-2013 12:00:00 time step the Figure shows vector plot (a) whole model domain, (b) near breach, (c) near inlet with time series plots of (d) significant Wave height, (e) surge and (f) surface elevation at various locations	277
Figure A4.13	At 12-10-2013 18:00:00 time step the Figure shows vector plot (a) whole model domain, (b) near breach, (c) near inlet with time series plots of (d) significant Wave height, (e) surge and (f) surface elevation at various locations	278
Figure A4.14	At 13-10-2013 00:00:00 time step the Figure shows vector plot (a) whole model domain, (b) near breach, (c) near inlet with time series plots of (d) significant Wave height, (e) surge and (f) surface elevation at various locations	279
FigureA 4.15	At 13-10-2013 06:00:00 time step the Figure shows vector plot (a) whole model domain, (b) near breach, (c) near inlet with time series plots of (d) significant Wave height, (e) surge and (f) surface elevation at various locations	280
Figure A4.16	At 13-10-2013 12:00:00 time step the Figure shows vector plot (a) whole model domain, (b) near breach, (c) near inlet with time series plots of (d) significant Wave height, (e) surge and (f) surface elevation at various locations	281
Figure A4.17	At 13-10-2013 18:00:00 time step the Figure shows vector plot (a) whole model domain, (b) near breach, (c) near inlet with time series plots of (d) significant Wave height, (e) surge and (f) surface elevation at various locations	282
Figure A4.18	At 14-10-2013 00:00:00 time step the Figure shows vector plot (a) whole model domain, (b) near breach, (c) near inlet with time series plots of (d) significant Wave height, (e) surge and (f) surface elevation at various locations	283

LIST OF TABLES

Table No.	Descriptions	Page No
Table 2.1	Comparison of equivalent stream slope at Belekeri inlet	28
Table 2.2	Inlet locations and physiographic parameters of catchments in Kerala	28
Table 2.3	Inlet locations and physiographic parameters of catchments in Karnataka	29
Table 2.4	Estimated parameters for the development of CWC SUH methods for catchments of Kerala	47
Table 2.5	Estimated parameters for the development of CWC SUH methods for catchments of Karnataka	48
Table 2.6	Estimated parameters for the development of Snyder's SUH for catchment of Kerala	49
Table 2.7	Estimated parameters for the development of Snyder's SUH for catchment of Karnataka	50
Table 2.8	Estimated parameters for the development of SCS method for catchments of Kerala	51
Table 2.9	Estimated parameters for the development of SCS method for catchments of Karnataka	52
Table 2.10	Comparison of flood discharge for CWC measured data	63
Table 2.11	Comparison of flood discharges at ungauged catchments along Kerala coastline	63
Table 2.12	Comparison of flood discharges at ungauged catchments along Karnataka coastline	64
Table 3.1	Classification based on tidal range variations along shoreline (Davies, 1964)	76
Table 3.2	Classification based on tidal range variations along shoreline (Hayes, 1975)	77
Table 3.3	Classification criteria based on wave energy (Walton & Adams, 1976)	78
Table 3.4	Morphological variations at tidal inlets	80

Table 3.5	Classification of coastal systems based on dimensionless parameters (Vu, 2013)	86
Table 3.6	Classification criteria used for modified non-dimensional method (modified Vu method, Reddy et al., 2015)	88
Table 3.7	Summary of Geomorphological classification (de Vriend et al., 1999)	110
Table 3.8(a)	Summary of Hydrodynamic classification (Annual)	121
Table 3.8(b)	Summary of hydrodynamic classification (South West Monsoon)	121
Table 3.8(c)	Summary of hydrodynamic classification (North East Monsoon)	122
Table 3.8(d)	Summary of hydrodynamic classification (Fair Weather)	122
Table 3.9	Comparison of tidal inlet classifications for locations with river discharge along the Indian coast	130
Table 4.1	Classification of cyclones as per RSMC, New Delhi, India	135
Table 4.2	Set of limiting values of wind speed based on the expected damage	135
Table 4.3	Storm intensity, expected damage and suggested actions for various types of disturbances	136
Table 4.4	Naming of cyclones over North Indian Ocean (2004-2017)	139
Table 4.5	Input parameters required (green blocks) for wind and pressure fields' generation using different parametric models	148
Table 4.6	Basic input data for the cyclone Phailin (Start date 07-10-2013 000000UTC)	157
Table A1.1	Historical cyclonic disturbances formed over NIO & its characteristics and effects on Indian coastline	191
Table A2.1	Physical and UH parameters studied to establish relationships in CEC sub-Zone 5 (a) and 5(b)	201
Table A2.2	List of railway bridge/M.O.T. catchments, availability of gauge, discharge and rainfall data	201
Table A2.3	Location and basin characteristics of 13 catchments of CWC report (CWC, 1992)	202

Table A2.4	Representative 1 hour unit hydrograph parameters for sub-zone 5(a) and 5(b)	202
Table A2.5	Ordinates of unit hydrograph at bridge site No, 8 (MOT-8)	203
Table A2.6	Ordinates of average dimensionless UG's at 13 CWC bridge catchments	204
Table A3.1	Classification of tidal inlets based on tidal range and wave exposure condition	217
Table A3.2	Morphological classification of tidal inlets along Indian coast	230
Table A3.3	Hydrodynamic classification on Hayes (1979) for all seasons along the Indian coast	242
Table A3.4	Classification of tidal inlets based on dimensionless parameters without wave period (Vu, 2013)	260
Table A3.5	Classification of tidal inlets based on dimensionless parameters wave period	263

LIST OF SYMBOLS

A	catchment area (sq. km)
B	Constant parameter
B	shape parameter
C	concentration of scalar quantity
C	constant
E	wave energy density spectrum
L	length of main stream
H	wave height (m)
H	mean annual significant wave height (m)
K	storage coefficient
P	exponent
P	tidal prism (m ³)
S	average water bed slope (m/m)
S	equivalent stream slope of the catchment
S	magnitude of the discharge due to point sources
T	mean wave period (s)
T	tidal period (s)
V	volume (m ³)
X	shape parameter
X & Y	independent and dependent variables
A _b	bay or lagoon area (m ²)
C _s	concentration of scalar quantity at the source
C _t , C _p	non-dimensional constants
D _h	horizontal diffusion coefficient
D _{i-1} , D _i	heights of successive bed locations at contours intersections
D _v	vertical turbulent diffusion coefficient
F _c	horizontal diffusion term
\hat{H}	source term due to heat exchange with the atmosphere
H ² T ²	measure of wave energy parameter (m ² s ²)
H _{FW}	wave height in fair weather season (m)
H _{NE}	wave height in northeast monsoon (m)
H _{SW}	wave height in southwest monsoon (m)
H _s	significant wave height
H _{s,avg}	average annual significant wave height (m)
K ₁ , K ₂	storage Coefficients
L _C	centroid of catchment from basin outlet
L _i	length of i th segment
L ₀	deep water wave length
N(σ, θ)	wave action density spectrum
P _a	atmospheric pressure
P _R	time from starting of surface runoff to the peak discharge
Q _f	yearly freshwater discharge or river discharge (m ³ /s)
Q _i	discharge ordinate at 1 hour interval (cumecs)
Q _P	peak discharge of unit hydrograph (cumecs)
Q ₂ (t)	time to peak with respect to 't'

\hat{Q}_{tide}	peak or mean tidal discharge (m ³ /s)
R_{mw}	radius of maximum wind speed
R_{to}	tidal range (m)
S_{xx}, S_{xy}, S_{yx} and S_{yy}	components of radiation stress tensor
T_B	base width of UH (h)
T_m	time from the starting of rise to the peak of UH (h)
T_{mean}	mean tidal range (m)
T_s	temperature of the source
T_z	mean wave period
S_M	slope of main stream in percentage
S_s	salinity of the source
V_{10}	near-surface wind
$V_g(r)$	wind gradient speed
V_{max}	maximum wind speed
W_{50}	width of UH at 50% of peak discharge ordinate (h)
W_{75}	width of UH at 75% of peak discharge ordinate (h)
W_{R50}	width of rising limb of UH at 50% of peak discharge ordinate (h)
W_{R75}	width of rising limb of UH at 75% of peak discharge ordinate (h)
a, b	coefficient and exponent of power equation
d	still water depth
g	acceleration due to gravity
h	total water depth
hPa	hectoPascals
kmph	kolometers per hour
n	number of reservoirs
n, K	Parameters defing the shape of IUH
m	meter
q	depth of runoff per unit time per unit effective rainfall
q	shape parameter
sq km	square kilomaters
t	time
u,v,w	velocity components in x,y and direction
x,y,z	Cartesian coordinates
k_p	linear decay rate of the scalar quantity
p_c	central pressure
p_n	neutral pressure
t_i	point of inflection after the peak
t_L	lag time
t_r	unit rainfaal duration in a specific study (h)
t'_p	midified basin lag
t'_r	any other time duration
q_p	peak flow (cumecs/sq. km) or peak discharge (cm/h/cm)
ν_t	vertical turbulent viscosity
$\overline{u, v}$	depth averaged velocity components
β and λ	factors governing the shape of dimensionless UH
η	surface elavation
ρ	density of water

ρ	air density
f	Coriolis parameter
σ	angular frequency
Γ	gamma function
ρ_o	reference density of water
γ'	dimensionless parameter
$\sqrt{gH^5}$	yearly averaged wave forcing (m ³ /s)
$\frac{\hat{Q}_{tide}}{\sqrt{gH^5}}, \frac{Q_f}{\sqrt{gH^5}}$	non-dimensional parameters
Q_t/P_R	percent of flow at any given time t/P_r

ABBREVIATIONS

ANN	Artificial Neural Networks
AS	Arabian Sea
BoB	Bay of Bengal
CA	Catchment Area
CFL	Courant Friedrichs Lewy
CGWB	Central Ground Water Board
CN	Curve Number
CS	Cyclonic Storms
CWC	Central Water Commission
CWC-SUH	Central Water Commission-Synthetic Unit Hydrograph
D	Depression
DD	Deep Depression
DEMs	Digital Elevation Models
DHI	Danish Hydraulic Institute
ERADS	Earth Resources Data Analysis System
ESCS	Extremely Severe Cyclonic Storm
FW	Fair Weather
GIUH	Geomorphological Instantaneous Unit Hydrograph
ICOLLs	Intermittently Closed and Opened Lakes and Lagoons
IMD	Indian Meteorological Department
IST	Indian Standard Time
IUH	Instantaneous Unit Hydrograph
JTWC	Joint Typhoon Warning Centre
KSNDMC	Karnataka State Natural Disaster Monitoring Centre
L	Low Pressure Area
ME (TD)	Mixed Energy (Tide Dominated)
ME (WD)	Mixed Energy (Wave Dominated)
MOT	Ministry Of Transport
NCAR	National Center for Atmospheric Research
NCEP	National Centers for Environmental Prediction
NE	North East
NIO	North Indian Ocean
NHO	National Hydrographic Office
NSW	New South Wales
NWP	Numerical Weather Prediction
OLI	Operational Land Imager
pdfs	Probability Distribution Functions
QGIS	Quantum GIS
RSME	Regional Specialised Meteorological Centre
SCS	Severe Cyclonic Storm
SCS	Soil Conservation Service
SDDS	Seamless geographic Data Distribution System
SoI	Survey of India
SRTM	Shuttle Radar Topography Mission
SUCS	Super Cyclonic Storm

SUH	Synthetic Unit Hydrograph
SW	South West
TDE	Tide Dominated Estuaries
TD (L)	Tide Dominated (Low)
TD (H)	Tide Dominated (High)
TIRS	Thermal Infrared Sensor
TS	Taylor and Schwarz
UHs	Unit Hydrographs
USA	United States of America
UTs	Union Territories
UTC	Universal Time Coordinated
VSCS	Very Severe cyclonic Storm
WD	Wave Dominated
WDD	Wave Dominated Deltas
WDE	Wave Dominated Estuaries
WB	West Bengal
WMO	World Meteorological Organization
WRIS	Water Resources Information System
2PGD	Two Parameter Gamma Distribution

CHAPTER - 1

INTRODUCTION

1.1. GENERAL

Coastal inlets are the openings along the coastline that connects wide-spread oceans and the neighbouring water bodies. These coastal inlets vary in nature depending on many parameters including waves and tides. Coastal inlets play a major role in regulating the inland flow and in feeding the coast with hinterland sediments to maintain the coastal morphology. The studies for inlet dynamics are essential to understand the coastal and inland waters interaction like physical processes as well as the exchange of nutrients or pollutants between the two water bodies.

To study the inlet dynamics, understanding the type of dominance (i.e. tide dominated or wave dominated or river dominated) along the coast and morphology of the tidal inlets are very essential. Although many methods are available in the literature to classify the tidal inlets for worldwide comprehensive information on classification including river discharge is not available for the Indian tidal inlets along coasts. This study focuses on classification of 471 tidal inlets along the nine maritime coastal states of India for the tidal range, wave exposure conditions, morphology, hydrodynamics and non-dimensional parameterization of wave, tide and river discharge forces with and without mean wave period. All 471 tidal inlets are having an inlet width greater than or equal to 5m at the confluence of river with sea.

The CWC (Central Water Commission) and State's Water Resource Department maintain the gauging stations to measure the stage, discharge and nutrients in the streams and rivers across the country. The data maintained by CWC is available through online portal Water Resources Information System (India-WRIS). The gauging stations maintained by CWC are within 1km from the inlet entrance (Source:

Karnataka State Natural Disaster Monitoring Centre) and limited data is available through the different sources. Due to the availability of limited information regarding the measured river discharge, an attempt has been made in this study to estimate the flood discharge using catchment characteristics rather than rainfall runoff data.

The blockage of tidal inlets may lead to flooding due to excess rainfall in the upper reaches of the watershed. The closure of inlets will impact significantly the sediment discharge system in the coastal region. On the other hand, excessive alongshore sediment transport could result in sediment deposition at the inlet mouths and lead to inlet closure. The coastal wave climate has significant influence on the coastal sediment transport system as well as in the breaching of the closed tidal inlets. Due to its prime importance in terms of morphohydrodynamics and exchange processes, Ranasinghe (1999, 2003) investigated tidal inlet closure pattern mainly in two aspects: (i) identifying the underlying physics in morphodynamic processes governing seasonal closure of inlet; (ii) quantifying the adverse effect of the estuarine hydrodynamics connected to the inlet due to inlet closure. These interlinked phenomena are still in the interest of research community as the underlying physical processes are temporally and spatially variable. Also the formation of flood and ebb deltas in the deltas is yet to be understood. Moreover, the passing of storms in the vicinity of tidal inlets pose very different problems both in terms of increased river discharge due to storm associated rainfall or due to increased wave activity and storm surges. The morphological changes of the tidal inlets associated with the storm activity is a challenging research area on which models have not yet fully mimicked all the processes. Therefore, in order to explore above mentioned research gaps, it is proposed to carry out a study to understand the dynamics of tidal inlets at specific locations on the east coast of India through numerical modelling augmented with available measured data.

1.2. CURRENT STATE OF KNOWLEDGE

Classification of tidal inlets has been carried out extensively along the United States of America (USA) and Australia coasts (e.g., Barton, et al. 2007; Burgess, et al. 2004; Duck and Silva, 2012; Hale and Bucher, 2008; Heap, et al. 2001; Isla, 1995; Kierfve, 1994; Roy, et al. 2001). Burgess et al. (2004) used over dissimilar approaches to study the coastal systems in the United States of America (USA). The classifications of USA coasts by Kierfve (1994) and Isla (1995) were based on the isolation level of coastal lagoons restricted by the coastal barrier wherein each type presents its own hydro- and geomorphological aspects. Classification of inlets along New South Wales (NSW) coast in Australia was reviewed by Barton et al. (2007). Hale and Bucher (2008) classified inlets mostly based on geomorphology, salinity and hydrology. Duck and Silva (2012) comprehensively reviewed the coastal lagoons classification for inlets along the coast of Australia with an emphasis on hydro-morphology. Roy et al. (2001) included biological criteria to classify estuaries within NSW, Australia. Heap et al. (2001) proposed another method using the ratio of wave power to tidal power at the entrance of the estuary and classified 780 coastal systems around the coast of Australia. Another method of classification based on biodiversity, functioning, resource exploitation, conservation and sustainability is used in literature (e.g., Silva et al. 2002; Dadouh-Guebas et al. 2005; Danovaro and Pusceddu, 2007; Iwasaki and Shaw, 2008; Perez-Ruzafa et al. 2011).

Various coasts around the world have been classified as wave-dominated, or tide-dominated or river-dominated, depending upon the forcing parameters that have a major effect on the shaping of the inlet. However, most of the studies on the inlet morphodynamics are carried out under the forcing functions of either tide or tide and waves (Guo, 2014). However, the river flow or discharge impact on tidal inlet morphodynamics is least examined. The river discharge has a major consequence on inlet hydrodynamics and morphology changes. The fresh water flow from river gives an added value to the incoming tidal waves through enriched tidal friction (Godin, 1985; Savenije, 2005; Sassi and Hoitink, 2013). River discharge constraints landward saltwater intrusion in the form of enhanced ebb currents (Horrevoets et al., 2004; Gallo

and Vinzon, 2005). It also plays like a dominant mechanism in exporting river supplied sediment seaward (Garel et al., 2009). The cyclones associated with heavy rainfall discharges most of the sediment over a short interval of time in the form of river flow (Chien et al., 2011). The saltwater mixed with river flow may lead to significant stratification and density currents, causing a local landward sediment transport (Dyer, 1995; Chant et al., 2011). Considering morphological view in their studies, Cooper (1993, 2002) observed that river discharge and associated floods are responsible for short-term to medium-term (i.e., year to a decade) inlet morphological changes. Estuarine morphodynamics should be adversely affected by river discharge through sediment supply, enhanced ebb currents and interaction with tides (Geo et al., 2014). Freshwater flows from the rivers can significantly alter the amount of surge particularly in northern Bay of Bengal (BoB), where largest river systems carry a lot of river discharge annually (Dube et al., 1986, 2005). On the other hand, the tropical cyclone associated with heavy precipitation can also influence the total water level. As of now, precipitation effect has not been considered in the computation of storm surge using any numerical model, which is essential and should be incorporated into the storm surge model (Shaji et al., 2014).

Any coastal system can be adversely affected by either newly evolved or elope of existing features on the coastline. Catastrophic events like cyclones and tsunamis bring significant changes along the shoreline in various aspects for about hundreds of kilometres from landfall point. The morphology changes in the vicinity of the tidal inlets under the tropical monsoon climatic conditions is highly dynamic and varied in nature. The tropical monsoon regime exerts its influence on the tidal inlet morphology through the seasonal variation of river flow and wave climate. However, the mechanisms of forcing functions are still poorly understood in determining the morphology changes of the tidal inlets.

Adverse environmental conditions may not support to keep the hydrometeorological characteristics under observation during cyclones or tsunami. However, those parameters are essential to know how precisely the tidal inlet behave during such events. Hence the numerical models are necessary to predict the hydrological

parameters and morphology changes in the vicinity of the tidal inlets to understand its behaviour. Moreover, morphological analysis of coastline is very much essential in understanding the evolution of new features along the shoreline in response to storm events causing significant changes in wave direction, sediment transport, bathymetry and shoreline orientation (Jain, 2008).

Different engineering approaches were applied all along world's coastline to study long-term morphological modelling of tidal basins or inlets. These approaches are as follows: (a) Behaviour oriented models (e.g., Di Silvio, 1989; Van Dongeren and de Vriend, 1994; Karssen, 1994a, 1994b; de Vriend et al., 1989; de Vriend, 1996; Steetzel, 1995; Stive et al., 1998; Stive and Wang, 2003); (b) process based models (e.g., Wang et al., 1995; Ranasinghe and Pattiaratchi, 1999, 2003; Van Leeuwen et al., 2003; Marciano et al., 2005; Van der Wegen and Roelvink, 2008; Van der Wegen et al., 2008, 2010, 2011; Dissanayake et al., 2009; Tung et al., 2008, 2009, 2011); (c) inverse methodology (e.g., Karunarathna et al., 2008, 2009, 2016), (d) formally integrated, long-term models (e.g., Krol, 1990; de Vriend, 1996; De Swart, 1996).

de Vriend (1996) has categorised the behaviour based models to study the long-term morphological modelling with a special focus on tidal basins as (i) data based models; (ii) empirical models and (iii) semi-empirical models. The data-based models took into account a large number of input parameters to predict the behaviour of the coastal system. Therefore, to study the evolution of tidal basins using data based models requires a good understanding of underlying physical mechanisms (de Vriend, 1996).

Empirical models are of two types namely equilibrium models and transient models. The equilibrium model assumes that the coastal system is already in equilibrium which is then used as a prototype for the other systems with similar conditions, whereas transient model assumes an exponential decay process between actual state and its equilibrium state to describe the evolution of morphological parameter (de Vriend, 1996). The semi-empirical modelling approach uses all kinds of information available such as measured data, equilibrium equations etc. for the evolution of morphological studies in tidal basin systems.

Process-based models work based on the underlying physical processes, which comprised of some modules to describe different processes viz. hydrodynamics, mud transport and sediment transport. All these modules interact with seabed bathymetry and lead to the morphological changes. Roelvink (2006) developed and summarised different techniques on ‘how to couple the basic modules of different processes in a model’ for the evolution of long-term morphological modelling.

However, the morphological evolution of tidal basins and inlets particularly pertaining to the east coast of India is least studied. Rao and Vaidyanadhan (1979a, 1979b); Sastry et al. (1991); Rengamannar and Pradhan (1991) had studied morphological changes in the Godavari delta region. Ramkumar (2000, 2003) had studied morphological evolution of Kakinada Bay. Rao et al. (2003); Rao (2006) has studied the Holocene evolution and coastal morphodynamics of Godavari estuary. Jain et al., 2008 studied morphodynamics of Godavari tidal inlets using satellite data. Morphological evolution of Mandovi-Zuari tidal inlet along Goa coast was studied using the process-based numerical model by Chowdhury and Behera (2006). Jaya Kumar et al. (2014) had considered the effect of tsunami and cyclone for two real case scenarios to study the morphological changes in the vicinity of the tidal inlets.

Various process-based numerical models have been extensively applied for various catastrophic events in the Arabian Sea and Bay of Bengal as well (e.g., Bhaskaran et al., 2013, 2014; Gayathri et al., 2015; Jaya Kumar et al., 2005, 2006, 2012, 2014; Patra and Jena, 2013; Gowthaman et al., 2015) to study the parameters like storm surge, wave characteristics, and coastal inundation and sediment transport. Tidal asymmetry parameters have a significant effect on sediment transport and morphology of the estuarine channels (e.g., Sivakholundu, 2009; Guo et al., 2014).

1.3. HISTORICAL CYCLONES - THEIR IMPACT ON INDIAN COASTLINE

The records of worldwide tropical cyclones revealed that the Indian subcontinent is exposed to near about 10% of the total cyclones. India has a coastline length of 7516 km out of which along mainland is 5400 km, Lakshadweep islands is 132km, and Andaman & Nicobar Islands is 1900km. There are nine coastal states viz., Gujarat, Maharashtra, Goa, Karnataka and Kerala along the west coast of India, and Tamil Nadu, Andhra Pradesh, Odisha and West Bengal along east coast of India and 5 Union Territories (UT) viz., Dadra and Nagar Haveli, Daman and Diu, Lakshadweep, Pondicherry and Andaman & Nicobar Islands comprising 84 coastal districts which are adversely affected by tropical cyclonic storms. Out of which four coastal states, i.e. West Bengal, Odisha, Andhra Pradesh, and Tamil Nadu including one (Union Territory) UT (i.e. Pondicherry) on the East Coast of India and only one coastal state on the west coast of India (i.e. Gujarat) are more prone to cyclone disasters. The cyclone seasons in India are May to June and October to November. However, the primary and secondary peaks are in November and May respectively. Though the tropical cyclones affect the total Indian coastline, the east coast is liable to more severe in terms of frequency as well as intensity than the west coast.

Floods and flood-related destructions in low-lying coastal area occurring from natural hazards such as tsunamis, cyclonic storms, intense local precipitation and high river flows have been well known since the 20th century. Among all the catastrophic activities, cyclone-induced storm surges remain next to Tsunamis as world's leading devastating activities, especially due to frequent occurrences in many parts worldwide. The substantial loss regarding lives and property and damage to seaside infrastructure also gives an added value to get more focused globally. Nowadays, extensive efforts are already in place to mitigate coastal flood hazards and would probably intensify in the coming days.

The records of most devastating cyclones, which formed over North Indian Ocean during 2001-2017 is presented in Table A1.1. The historical cyclones are shown by

their origin, period of occurrence, landfall, characteristics of tropical cyclone such as lowest central pressure, maximum wind speed, storm surge, rainfall information and damaged caused. The data presented in Table A1.1 is related to categories above cyclonic storms. This is because characteristics of cyclonic storms and above categories would impact the coastline severely.

Monthly frequency cyclone disturbances over northern Indian Ocean (NIO), Bay of Bengal (BoB) and Arabian Sea (AS) during 2011-2017 are depicted in the Figures 1.1 to 1.3. Total 141 cyclone disturbances (Figure 1.1) has occurred during 2011-17 comprised of 39 Depressions (D), 40 Deep Depressions (DD), 31 Cyclonic Storms (CS), 13 Severe Cyclonic disturbances, ten very severe cyclonic disturbances and 8 Extremely Severe Cyclonic storms. The months May-June and October-November are subjected to 91 cyclonic disturbances out of 141 (i.e. about 65%). Among 141 cyclonic disturbances 101 formed in the Bay of Bengal (71.65%) and 40 in the Arabian Sea (28.35%).

Over northern Indian Ocean (NIO) the cyclones are named for the categories of Cyclonic Storms (CS) and above since 2004. Before 2004, the specific names were not given for the cyclonic disturbances except for one to two in a year based on the severity of wind speed, central pressure and damage (Table A1.1). However, the names are also given based on the landfall point (e.g. Indian cyclone in 2001, Oman cyclone and West Bengal cyclone in 2002 and Sri Lanka cyclone in 2004). The sustained wind speeds (kmph) and central pressures (hPa) for the cyclonic disturbances are given the graphical form (Figure 1.4(a) & (b)). The Figure 1.4(a) and 1.4(b) show that on an average there are four cyclones per year over North India Ocean since 2001. The sustained wind speed has crossed over 200 kmph for about six times since 2001. The storm surge is reported for only 12 cyclones and if storm surge details are not reported or no storm surge data available from Regional Specialised Meteorological Centre (RSME) then it is given as dash (-) in Table A-1. The T-Number in Table A1.1 indicates the visual developmental patterns of satellite images during cyclones which are used to estimate the intensity of tropical cyclones. More the T-Number, more damage unless the cyclone dissipated over the ocean.

The damage caused over the Indian coastline in terms of lives and property are also reported in Table A1.1 for cyclones which had their landfall location along the Indian coast. However, for cyclones with landfall location elsewhere, it is stated as ‘No damage occurred’ in Table A1.1, even though they caused damage.

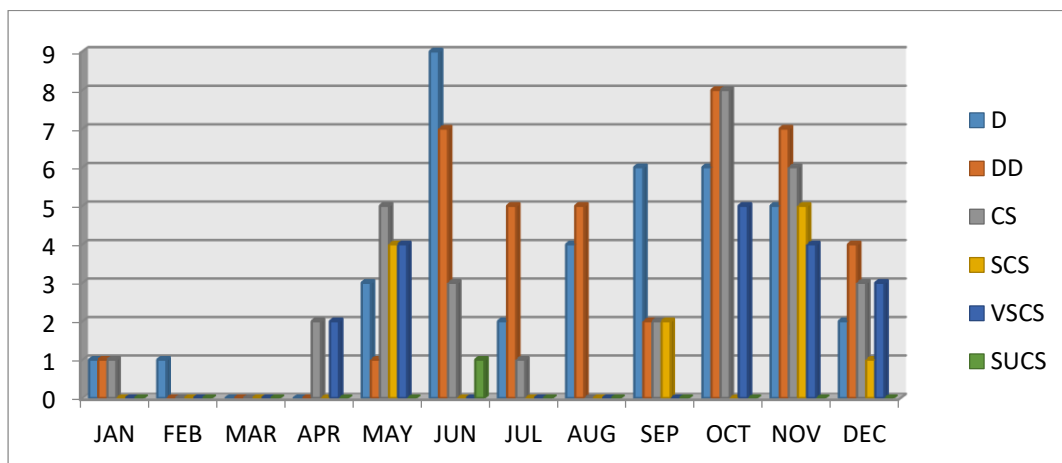


Figure 1.1 Monthwise frequency cyclone disturbances over North Indian Ocean during 2001-2017

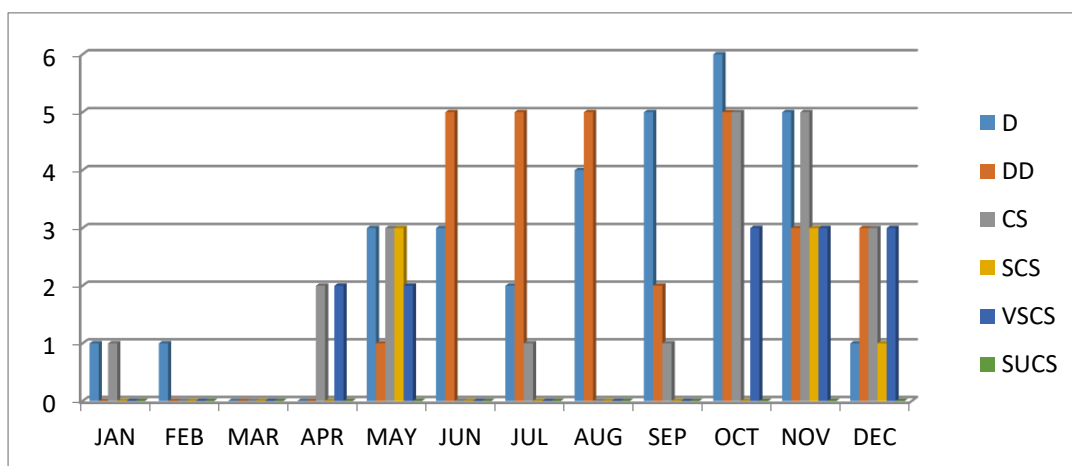


Figure 1.2 Monthwise frequency cyclone disturbances over the Bay of Bengal during 2001-2017

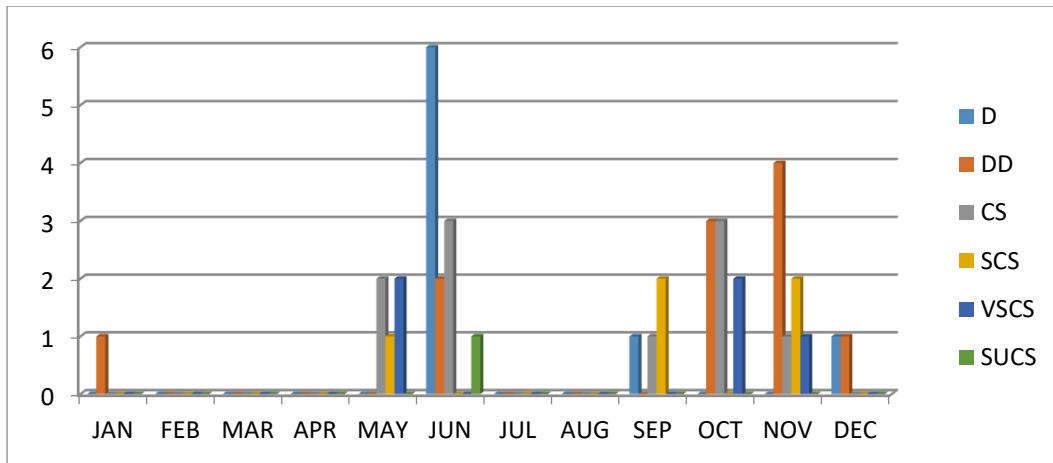


Figure 1.3 Monthwise frequency cyclone disturbances over the Arabian Sea during 2001-2017

1.4. NECESSITY AND RELEVANCE OF THE PRESENT STUDY

Although many methods are used to classify the tidal inlets all over the world, information on classification for the tidal inlets along the coast of India is not available. This study identified 471 tidal inlets along the nine maritime coastal states of India for their classification in terms of morphology, hydrodynamics and non-dimensional parameterisation of the wave, tide and river discharge forces. The classification of inlets thus became a primary objective of this study.

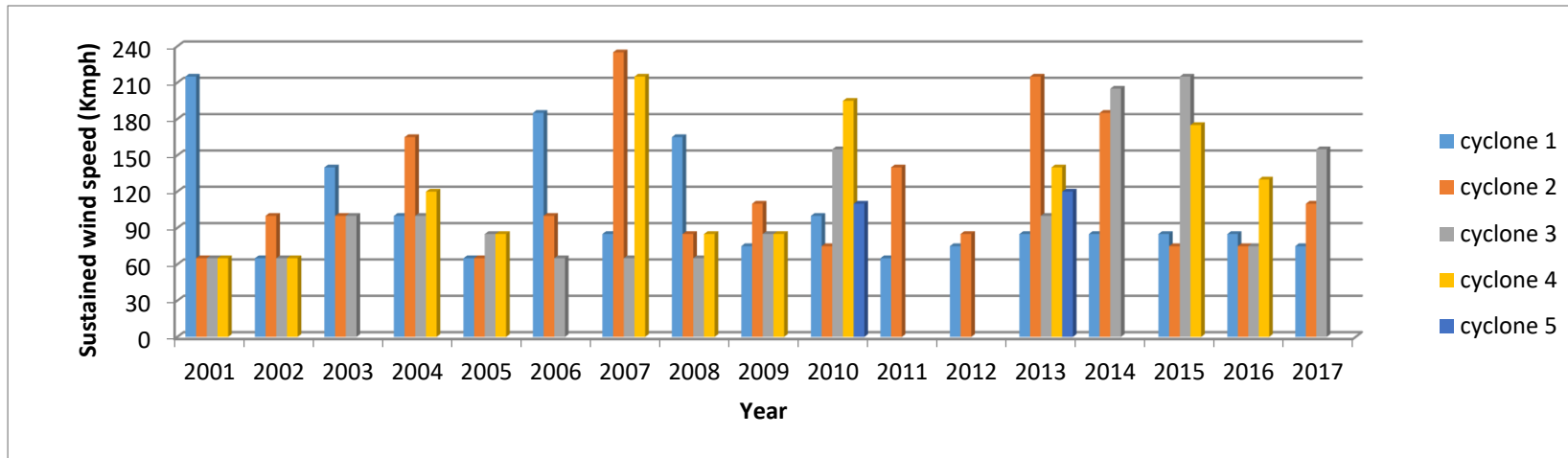


Figure 1.4(a) Yearwise frequency of sustained wind speeds of cyclone disturbances over North Indian Ocean during 2001-2017

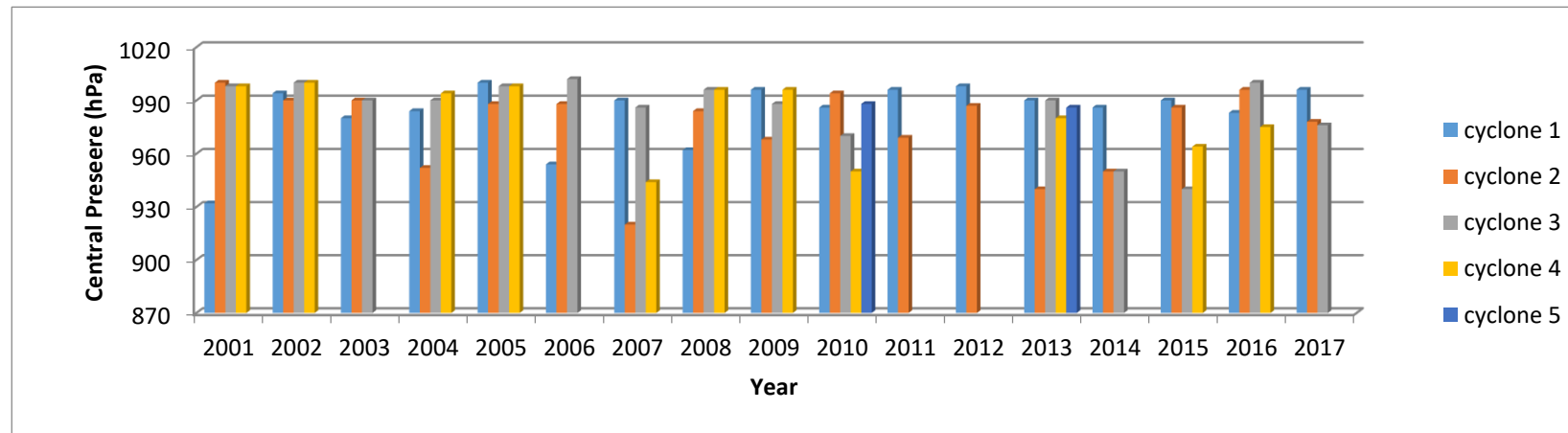


Figure 1.4(b) Yearwise frequency of central pressures of cyclone disturbances over North Indian Ocean during 2001-2017

Although information pertaining to the wave climate and tidal range required for classification can be sourced from the literature, the river runoff is not readily available. Hence estimation of the river discharge became another important objective without which the classification of inlets would be incomplete.

In India many of the catchments are devoid of rain gauge stations and also detail hydro-meteorological studies is not possible on a large scale at every catchment. However, there are numerous methods available in the literature which calculate the discharge based on the catchment characteristics rather than rainfall-runoff data. Even though such methods are applied for Indian catchments, there is limited information on the watershed discharge characteristics of inlets that drain into the adjoining seas. Apart from major rivers and few important inlets, there is no discharge information for the tidal inlets. Therefore, there is a need to estimate the watershed discharge to study the tidal inlet dynamics.

The inlet morphology could vary drastically with catastrophic events like cyclones and tsunamis impacting on the coastline, especially along tidal inlets. The inlets get opened or closed depending on the sediment transport and its interaction with the waves, tide and river discharge thereby altering the water quality parameters (Ranasinghe, 1998). There is limited information on the morphology changes in the vicinity of tidal inlets due to cyclones. Therefore, it is important to understand the dynamics of tidal inlets and the morphodynamics around the inlet under cyclone conditions. In view of the fact that the cyclone induced morphology is important for coastal stability studies, an attempt is made to study the morphology changes around an inlet using state of the art numerical model available.

It is almost impossible to keep the hydro and morphological parameters under observation all the time especially during heavy winds or during the action of cyclones. The most conventional and best way to monitor the tidal inlet morphology changes is to observe satellite images. But during the cyclone, the cloud covers the vision of the satellite image which is evident in the snapshots obtained from the imageries. The satellite images are

available in public domain and are only available before and post-monsoon but not during the monsoon. It is also a fact that surveying for field measurements during cyclones is impractical as the atmospheric conditions are severely dynamic and unstable. Hence, numerical modelling for morphology changes during the cyclone is a most practical and safest way of studying morphological changes at the tidal inlet.

1.5. FORMULATION OF RESEARCH OBJECTIVES

Therefore, in order to tackle the above mentioned research gaps, it is proposed to carry out a study to understand the morphodynamics of tidal inlets at specific locations through numerical modelling augmented with available measured data. To fulfil the mentioned research gaps the objectives are formulated as given below

- 1) Estimation of flood discharge at the tidal inlets.
- 2) Classification of tidal inlets along the Indian coastline.
- 3) Study the morphodynamics of selected tidal inlets under the influence of cyclonic storm

1.6. ORGANIZATION OF THE THESIS

This research work on “Classification of Indian Coastal Tidal inlets and some aspects of morphology changes under Cyclone events” is presented in five chapters:

Chapter 1 presents a general introduction to the tidal inlets and the research work carried out on tidal inlets in the Indian context is highlighted. The importance of classification of tidal inlets and the limitations on availability of flood discharge at tidal inlets is brought out. The adverse impacts the tidal inlets, bays and estuaries due to catastrophic disturbances like storm surge, cyclones etc. have been highlighted. Some of the historical cyclones and their characteristics along with impact on Indian coastline are presented. The need for morphology studies in the vicinity of tidal inlets under tropical storms/cyclones has been brought out. The organisation of the thesis is presented.

Chapter 2 deals with the estimation of flood discharge that would be used as input in the classification of tidal inlets. This chapter describes the different Synthetic Unit Hydrograph methods to estimate the flood discharge at ungauged catchments. The available methods for the flood discharge estimation in India particularly Central Water Commission (CWC) methods are reviewed for the measured data using other SUH methods and extended this knowledge to determine flood discharge at ungauged catchments along the tidal inlets of Indian coastline. Comparison of flood discharges at the tidal inlets using all the methods have been made and discussed.

Chapter 3 presents detailed discussion on different coastal classification systems. The input parameters required for various classifications are acquired through measurements and modelling. Identification and naming of tidal inlets have been carried out using satellite images. The classification have been done using four methods based on inlet shapes (geomorphological), tide and waves (hydrodynamic), waves, tide and river discharge with and without wave period (dimensionless classification). A comparison of different classification methods is carried out and a new classification range for the dimensionless method has been brought out.

Chapter 4 deals with the numerical modelling of the hydrodynamics and corresponding morphology changes in the area of coastal tidal inlet due the cyclone Phailin. Cyclonic winds generated from validated parametric wind models, tide inputs from global tidal constituents and cyclone induced waves generated from spectral wind wave model are used in the model study. A coupled model is used wherein the sediment transport is estimated from the wave and flow inputs and the bed level change is fed back to the flow model. The coupled model is used to obtain morphological changes in vicinity a tidal inlet. The results from this study are compared with the morphology changes observed from available satellite imageries. **Chapter 5** summarises salient aspects of the present research along with the conclusions derived from the present study. The scope for future research in this area is put forth at the end. The relevant Tables and Figures are presented Chapter wise in the Appendices at the end.

CHAPTER - 2

ESTIMATION OF FLOOD DISCHARGE

2.1. INTRODUCTION

Even though various coasts around the world are classified as wave-dominated or tide-dominated or river-dominated, most of the studies on the inlet morphodynamics are carried out under the forcing functions of either tide (Guo, 2014) or tide and waves. However, the river flow or discharge impact on tidal inlet morphodynamics is least examined. The river discharge has a major consequence on inlet hydrodynamics and morphology changes. The freshwater flow from river gives an added value to the incoming tidal waves through enriched tidal friction (Godin, 1985; Savenije, 2005; Sassi and Hoitink, 2013). River discharge constraints landward saltwater intrusion in the form of enlarged ebb currents (Horrevoets et al., 2004; Gallo and Vinzon, 2005). It also plays a predominant mechanism in exporting river supplied sediment seaward (Garel et al., 2009). The cyclones associated with heavy rainfall discharges most of the sediment over a short interval of time in the form of river flow (Chien et al., 2011). The saltwater mixed with river flow may lead to significant stratification and density currents, causing a local landward sediment transport (Dyer, 1995; Chant et al., 2011). Considering morphological view in their studies, Cooper (1993, 2002) observed that river discharge and associated floods are responsible for short-term to medium-term (i.e., year to a decade) inlet morphological changes. Estuarine morphodynamics should be adversely affected by river discharge through sediment supply, enhanced ebb currents, and interaction with tides (Geo et al., 2014). Freshwater flow from the rivers can significantly alter the amount of surge particularly in northern Bay of Bengal (BoB), where largest river systems carry a lot of river discharge annually (Dube et al., 1986, 2005). On the other hand, the tropical cyclone associated with heavy precipitation can also influence the total water level. As of now, precipitation effect

has not been considered in the computation of storm surge using any numerical model, which is essential and should be incorporated into the storm surge model (Shaji et al., 2014). However, the analysis of the impact of river discharge on inlet morphodynamics is still lacking.

From the above-cited literature, it is evident that river discharge is desirable to study the inlet morphodynamics. Many catchments in India are devoid of gauging stations, and moreover, it is uneconomical to collect the data and carry out detailed hydrologic and meteorological studies at every new site on a large scale. The data obtained regarding rain gauge stations and rainfall from Karnataka State Natural Disaster Monitoring Centre (KSNDMC) show that installed rain gauge stations are near about 1km or more from all the catchment outlet locations under study (Figure A2.1). Hence it is decided to carry out the research work regarding the flood discharge estimation at catchment outlet (Tidal inlets) points.

The non-availability or limited availability of the rainfall-runoff data emerged the concept of synthetic unit hydrograph for flood estimation in ungauged catchments. One of the popular methods which have widespread application in deriving Synthetic Unit Hydrograph (SUH) for Indian catchments is the method suggested by Central Water Commission (CWC, 1992) under the long-term hydrological plan for water resources development and management. India is divided into 26 hydro-meteorologically homogeneous sub-basins. Analysis of selected concurrent rainfall and flood data for the gauged catchments has been carried out to derive mostly the UH of 1-hour rainfall, gauge data and discharge data collected during the monsoon season. Various parameters viz. river drainage pattern, topography and relief, rainfall, temperature, soil and land use data has been investigated at each subzone while deriving the UH (CWC, 1992). The characteristics and Unit Hydrographs (UHs) have been prepared for several catchments in subzones of CWC and were correlated using regression analysis for estimating flood discharge at ungauged catchments.

With the advent of higher standards of hydrometeorology and better knowledge of the hydrometeorological phenomenon, the Central Water Commission (CWC, 2001) updated the flood estimation manual for the benefit of the design/field engineers. In the revised manual, various approaches such as hydrometeorological, probability, and regional studies have been discussed in detail with case histories and strategy to be adopted to evaluate a regional flood. In addition to CWC method, the traditional methods like Snyder (1938) and Taylor and Schwarz (TS) model (1952) utilize a set of empirical equations relating the physiographic characteristics of the catchment to UH parameters. Some of these parameters are peak flow rate, time to peak, base time, and UH width at 50% and 75% of peak discharge ordinates. However, the most available methods for SUH development involves a degree of subjectivity in the fitting of a hydrograph through a few data points, which require simultaneous adjustments to get the area under SUH to be unity. Hence during past few decades, the use of probability distribution functions (pdf) in developing SUH has gained much attention due to similarity with unit hydrograph properties.

Ramakar and Vladimir (2008) reviewed the methods of hydrological estimation at ungauged sites in India for low flow [e.g., Croker et al. (2001), Singh et al. (2001), Pandey and Ramasastri(2003), Rees et al. (2004), Holmes et al (2004), Arora et al. (2005)], long-term mean flow [Kothyari (1984, 1995), Kothyari and Garde (1991), Croker et al. (2001), Goel and Chander (2002)] and flood characteristics [e.g., Garde and Kothyari (1990), Swamee et al. (1995), Bhaskar et al. (1997), Goel (1998), Jain et al. (2000), Goel and Chander (2002), Bhunya et al. (2003), Kumar et al. (2003), Kothyari (2004), Kumar et al. (2004), Parida et al. (2004), Parida (2004), Raghuvanshi et al. (2006), Sahoo et al. (2006), Sudhakar et al. (2015), Jayantilal et al.(2016)].

Croker et al. (2001) developed an equations set to estimating the hydrological characteristics in Himalayan region. Singh et al. (2001) developed regional flow duration models for ungauged sites in the same region. Pandey and Ramasastri (2003) derived various sets of flow duration curves for various (daily/weekly/monthly) discharge data.

Rees et al. (2004) developed hydrological model for estimating dry season flows using recession curves. Holmes et al (2004) examined the range of hydrological characteristics and Arora et al. (2005) studied the effect of altitude on water availability in subbasin. Kothyari (1984), Kothyari and Garde (1991), Croker et al. (2001) used data from different Indian catchments to verify the existing relationships for annual runoff, to study the influence of different parameters and also to develop simple method for monthly discharge estimation. Swamee et al. (1995) described a dimensional approach for peak flood estimation. Goel (1998) and Goel and Chander (2002) gave some flood estimation procedures for Indian catchments. Jain et al. (2000), Kumar et al. (2004) and Sahoo et al. (2006) applied Geomorphological Instantaneous Unit Hydrograph (GIUH) and unit hydrographs are derived and checked its applicability for the Indian catchments. Kothyari (2004) used Artificial Neural Networks (ANN) for the estimation of hydrological parameters from ungauged catchments and Raghuvanshi et al. (2006) used ANN to predict runoff and sediment yield for a small basin.

Bhunya et al. (2003) introduced a simplified version of the existing two-parameter Gamma distribution method to derive accurate synthetic unit hydrographs. Empirical relations are developed for the estimation of β and λ (factors governing the shape of dimensionless UH) from the Nash parameter n (=number of reservoirs). Again in 2005, Bhunya et al. introduced a Hybrid model for the derivation of SUH by splitting the Nash single reservoir into two serially connected reservoirs of different storage coefficients for a physically realistic response. Empirical relations are given for the estimation of storage coefficients (K_1 & K_2) from the known peak flow (q_p) and time to peak (t_p). The Hybrid model was found to work significantly better than Snyder, Soil Conservation Service (SCS) and two-parameter Gamma distribution for both synthetically generated data and measured data from four catchments from India and one catchment from Turkey. The workability of proposed approach was tested for partial and no data availability situations. Well tested and applied relationships have been developed to estimate the parameters of pdfs such as Gamma, Chi-square, Weibull and Beta distributions (Bhunya et al. 2011). Singh et al.

(2014) critically reviewed flood hydrograph modelling techniques for ungauged basins, the SUH and its recent developments and advances by grouping into four main classes viz. (a) traditional models, (b) conceptual models, (c) probabilistic models and (d) geomorphological models. It was found that the geomorphological class is the most useful since it can employ topographic information.

Earlier literature studies on flood estimation at ungauged catchments in India are mostly for the catchments quite far away from the coastline. Hence the present study has an added advantage for the coastal/ocean engineers/researchers to study the dynamics of estuaries since river discharge is an essential parameter. Therefore, this unit presents the following: (i) a review of the conventional SUH methods and the SUH methods based on probability distribution functions; and (ii) estimation and comparison of the peak discharge values between different methods. SUHs derived from the traditional methods, and those derived from pdfs at 29 ungauged catchments of the coastal districts of Karnataka state and seven ungauged catchments along Kerala coastline in India are compared in this study. This information on the flood discharge along the 36 ungauged catchments of coastal Karnataka and Kerala are not available thus far (Source: WRIS-India), and hence this work adds new knowledge base on the flood discharges along Karnataka and Kerala coast.

2.2. STUDY AREA AND DATA COLLECTION

The study area represents the entire Karnataka coastline (Figure 2.1) and part of Kerala coastline (Figure 2.2).

2.2.1. Karnataka State

The Karnataka coastline extends over a length of 320 km along three coastal districts viz., Uttar Kannada, Udupi and Dakshina Kannada. The Karnataka state boundary lies between $11^{\circ}31'N$ and $18^{\circ}45'N$ latitude and $74^{\circ}12'E$ and $78^{\circ}40'E$ longitude and occupies the central part of the west coast of India. Fourteen rivers drain into the Arabian Sea namely Kali,

Gangavali, Aghnashini (Tadri River), Sharavati, Venkatapur, Chakra, Haladi, Sita Nadi, Swarna, Udayavara, Mulki, Pavenje, Gurgur and Netravathi. The present study considered 29 tidal inlets along the coast of Karnataka, which are named, based on the names available in Survey of India (SoI) toposheets nearby the inlet entrance. The entrance locations and names of the inlets are given in Table 2.3. The data products used in this study are Survey of India (SoI) topographic maps of 1981 (1:50000 Scale) and 2011 (1:50000 Scale), Shuttle Radar Topography Mission (SRTM) 90m Digital Elevation data. The extent of study area accounted for in the Survey of India maps No. 48I/4, 6, 7, 8, 10, 11, 12, 14, 15, 16; 48J/1, 2, 5 to 16; 48K/9 to 16; 48L/13; 48N/1 to 4, 5; 48O/1 to 8, 12; 48P/1, 2, 5, 6, 9, 10, 13, 14.

2.2.2. Kerala State

Another part of the study area is the central part of the Kerala state. It extends between 12°48' and 8°18' North Latitude and 74°52' and 77°25' East Longitude having a coastline length of about 580 km. The state of Kerala is bounded by Karnataka state in the north, Tamil Nadu to the East and South and Arabia Sea to the West. As per the Watershed Atlas of India provided by the Central Ground Water Board (CGWB), the state of Kerala Comes under 3 Sub-basins of the Malabar basin viz. (a) Netravathi and others sub-basin, (b) Varrar and others sub-basin, (3) Periyar and others sub-basin. The present study confined to only Varrar and other sub-basin. Figure 2.2 shows the catchments with drainage pattern and elevations in terms of a colour palette. The Varrar basin consists of seven catchments along the coastline of Kerala for which the total discharge ($m^3/s/h$) have been estimated. The inlet ID, names, and locations are given in Table 2.2. The extent of Kerala coastline (pertaining to present study area) accounted for in the Survey of India maps No. 49M/1, 5, 6, 9 to 16; 49N/13,14, 15; 58A/1 to 8, 11, 12 16; 58B/1 to 16; 58F/3, 4, 8; 58C/1, 5, 9, 13; 58G/1.

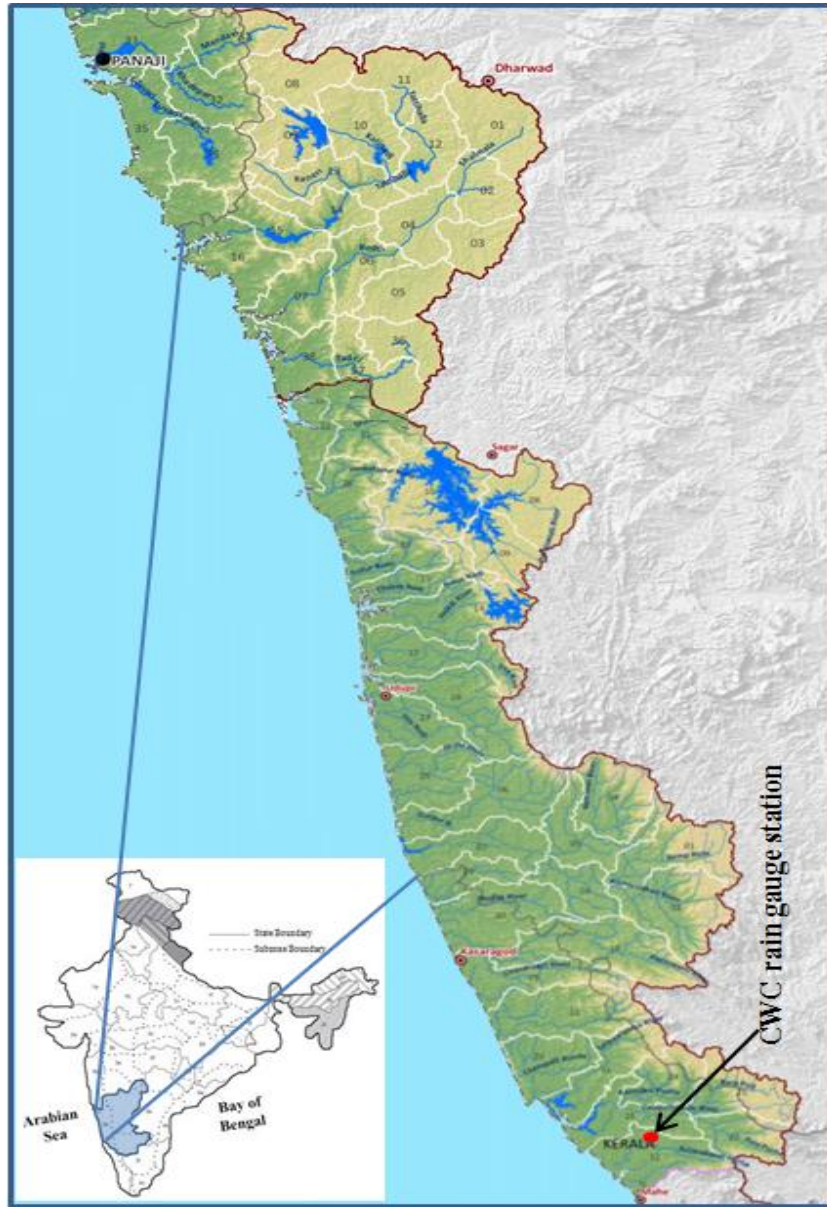


Figure 2.1 Study area showing Western catchments of Karnataka along with drainage and watershed boundaries (red dot is measured data location by CWC)



Figure 2.2 Study area showing different watersheds and drainage pattern along Kerala coast

2.3. ANALYSIS OF PHYSIOGRAPHIC PARAMETERS OF THE CATCHMENTS

The toposheets collected from Survey of India are digitized and geo-referenced using QGIS (Quantum GIS) and processed further using ERDAS (Earth Resources Data Analysis System) Imagine 2014 and given as input to ArcGIS® to determine the physiographic parameters.

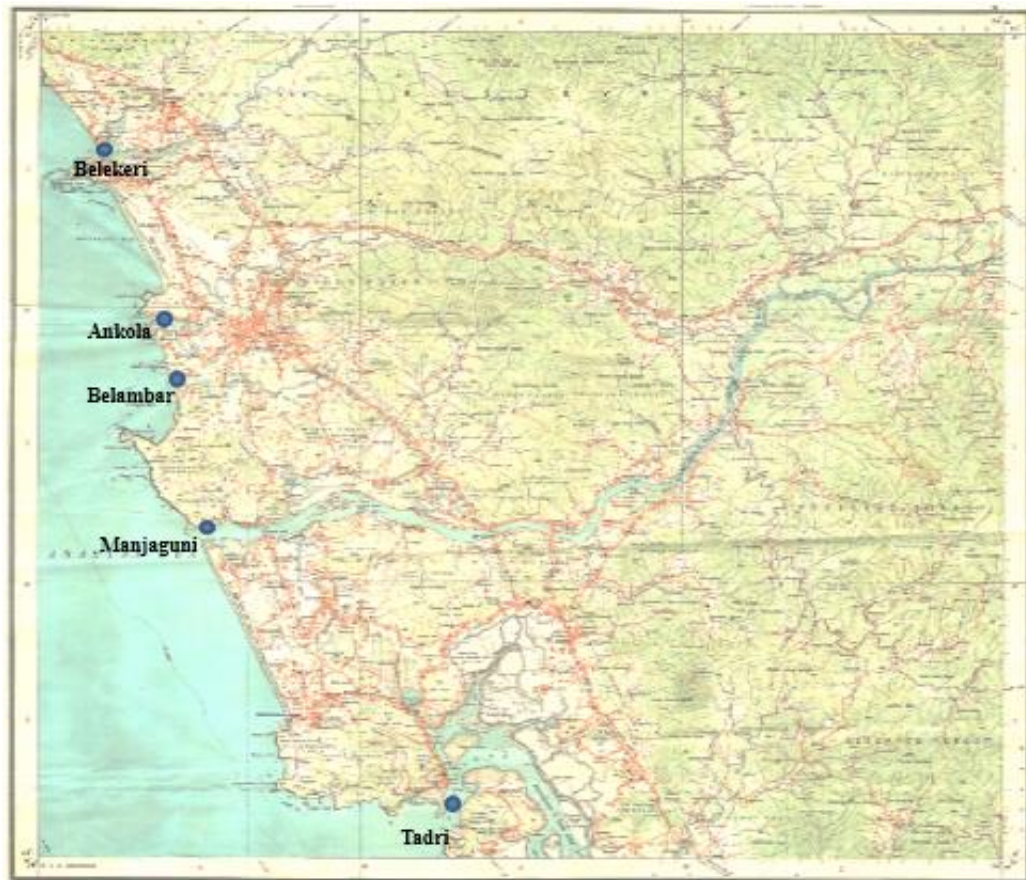


Figure 2.3 Survey of India toposheet (toposheet No: 48 I/6) showing the basin outlets, drainage patterns at Tadri, Manjaguni, Belambar, Ankola and Belekari catchments

All the representative catchments selected for the study are analysed for physiographic parameters (i.e., Catchment area, Main stream length, Centroid of catchment from basin outlet and Slope). The physiographic parameters are determined using ArcGIS® tools. The basic definitions of parameters and process of obtaining those from ArcGIS® tools are explained in subsequent sections.

2.3.1. Catchment Area (CA)

Catchment area is an independent hydrological unit that drains the water through series of natural drains to a common outlet (Figure 2.4).

Thus, the catchment boundary is the water divide line drawn between the neighbouring catchments using the drainage network map in the ArcGIS platform

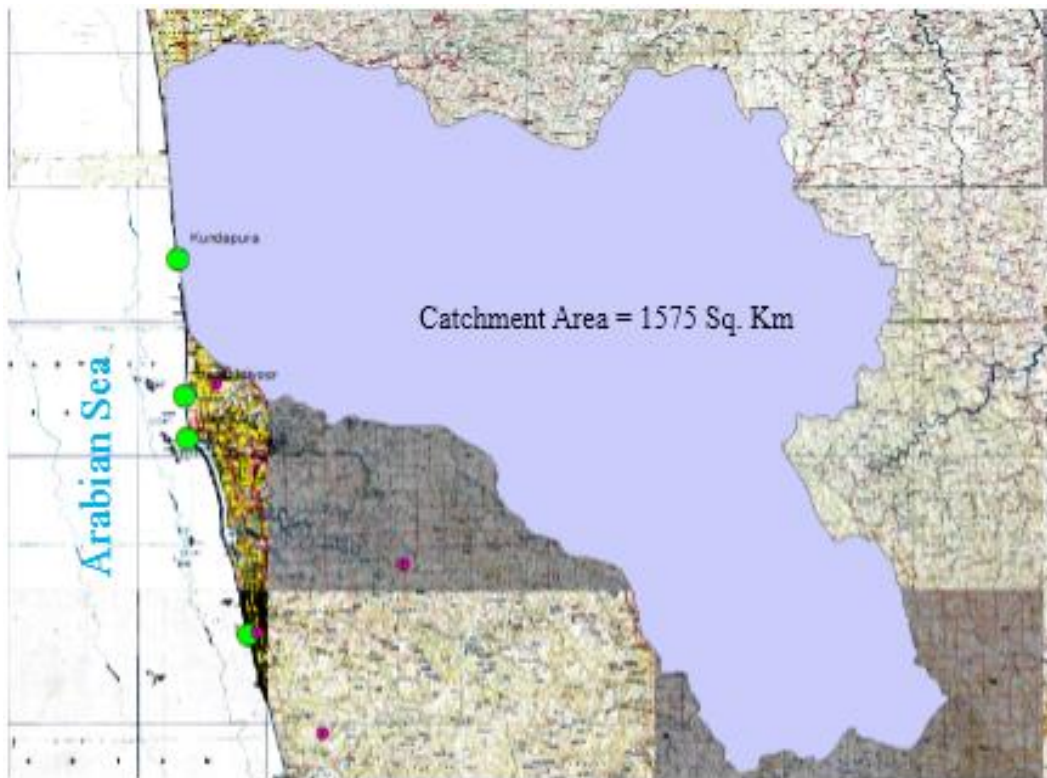


Figure 2.4 Catchment area of Kundapura watershed along with basin outlet location (Green circle)

2.3.2. Length of the mainstream (L)

It is measured as the longest length of the main river course from the farthest watershed boundary to the point of the study (Figure 2.5).

2.3.3. Centre of gravity of each catchment (L_c)

It is the longest length of the main river course from a point opposite to the centre of gravity to the basin outlet. It is found by converting catchment area feature into point feature using ArcGIS® tools (Figure 2.6).

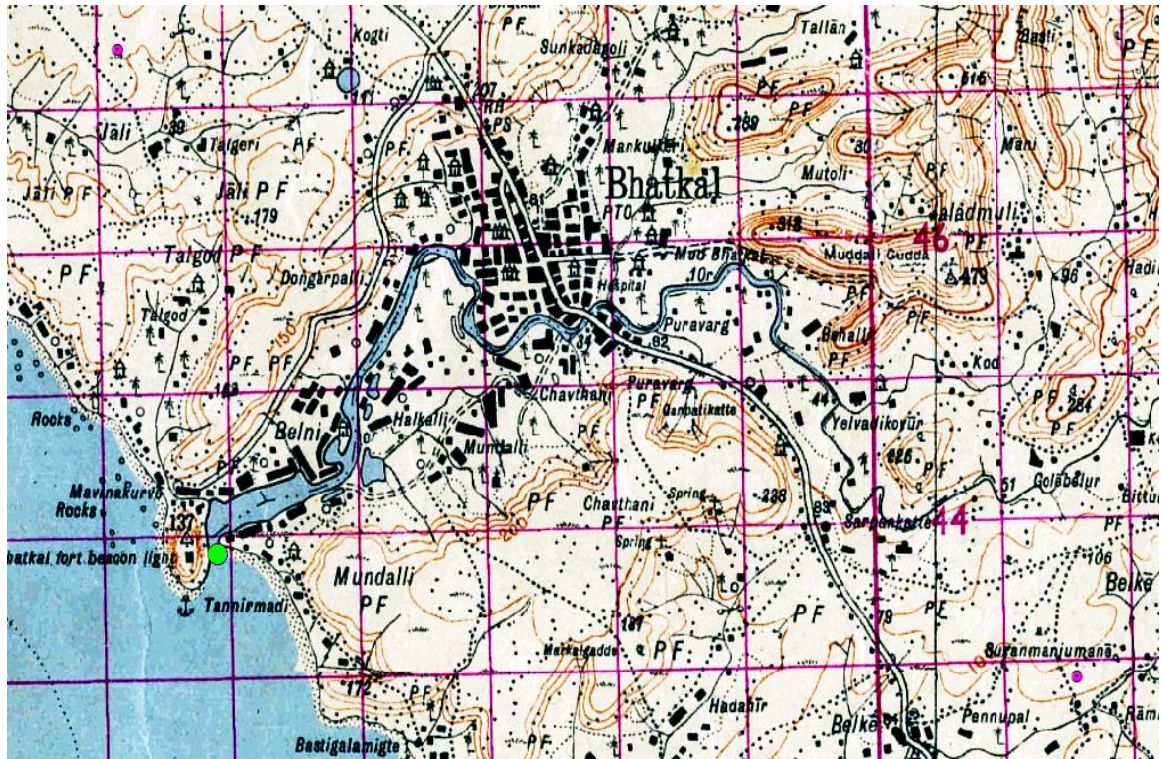


Figure 2.5 Length of the main stream for Mavinakurve watershed (=17 km)

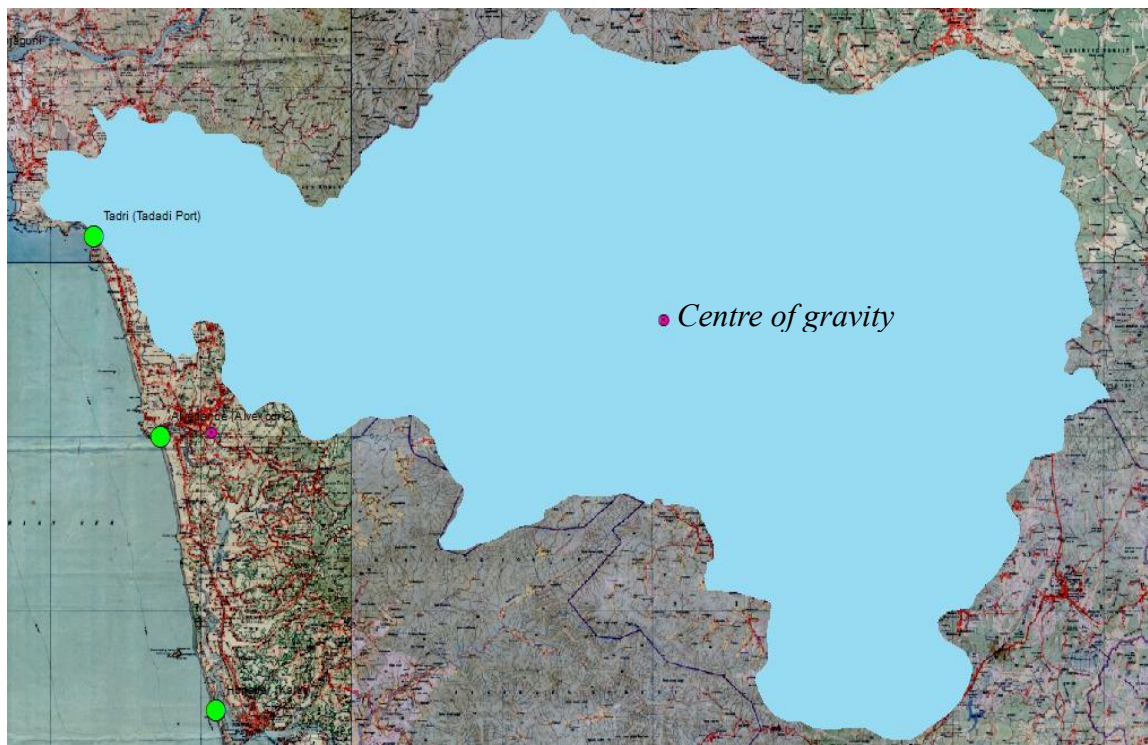


Figure 2.6 Catchment centroid position (red point) for the Tadri basin

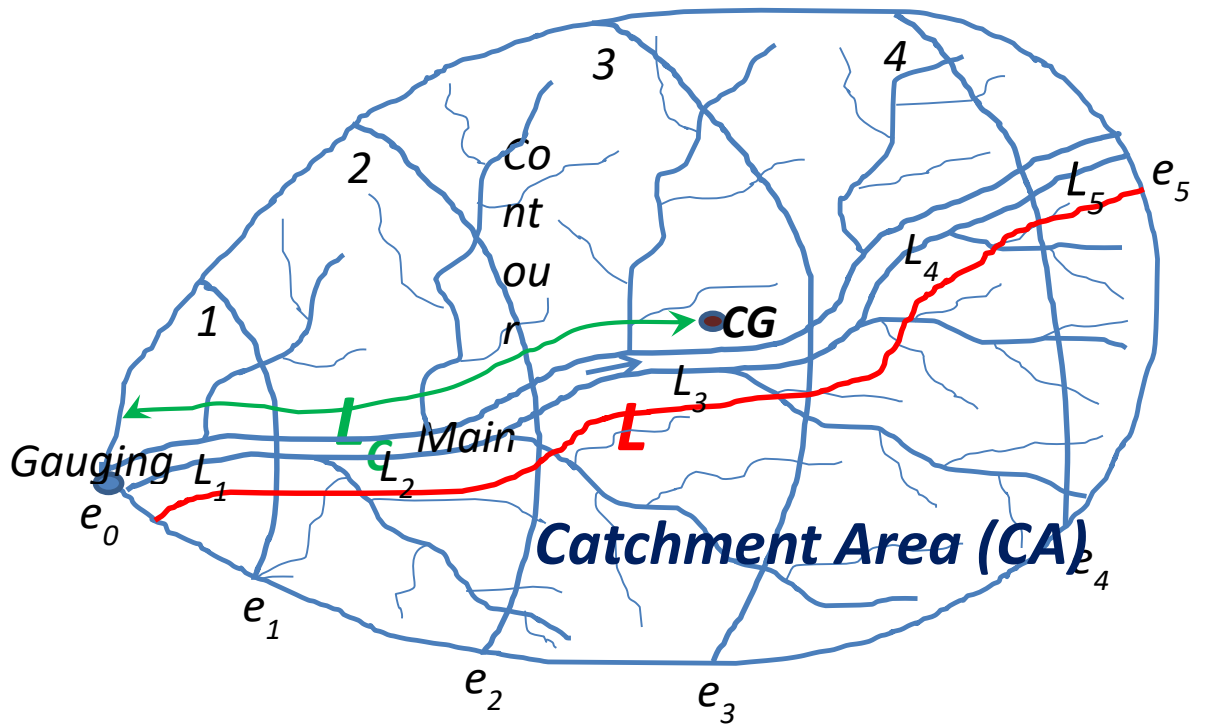
2.3.4. Equivalent stream slope of the catchment (S)

It is determined by dividing the longitudinal section of the main stream into a number of convenient segments representing the broad ranges of slopes of the segments (Figure 2.7). Contours for all the watersheds are digitized from 1: 50000 scale topographic maps. Western Karnataka coastline watersheds are covered by 49 maps, and Kerala coast under study is covered by 49 maps. The maps are produced from aerial photographs taken in 1981. The topographic maps have a contour interval of 20m. Based on National Map Accuracy Standards (NMAS) that 90% of true elevation values are within one-half the contour interval. Hence for determining the slope of watersheds, Shuttle Radar Topography Mission (SRTM) Digital Elevation Models (DEMs) are freely downloaded from Seamless geographic Data Distribution System (SDDS) website at <http://seamless.usgs.gov/>. All the data have been pre-processed to account for some typical problems (i.e., data voids and contrast) that could be found from the original SRTM DEMs.

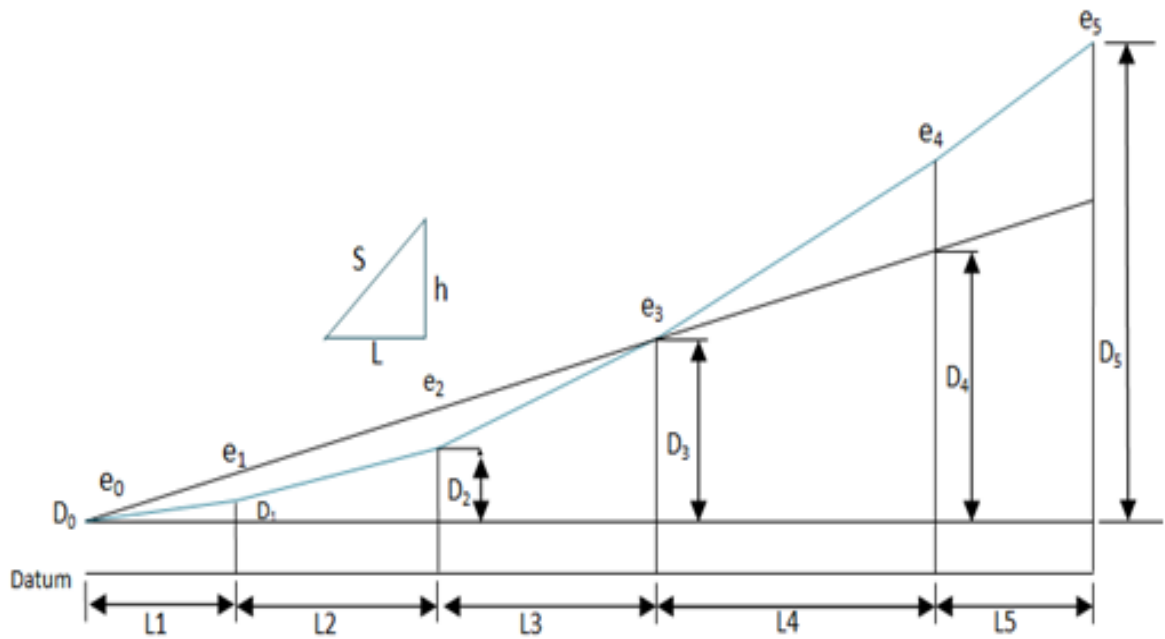
Using spatial analyst tool in ArcGIS®, 10m contour intervals are generated and then the georeferenced catchment basin is overlaid on the DEM data to determine slope using the Eq. 2.1. The representative slope calculation for the Belekkeri watershed is shown in Table 2.1

$$S = \frac{\sum_{i=1}^n (D_i + D_{i-1}) * L_i}{L^2} \quad (2.1)$$

Where, L_i is Length of i^{th} segment (km), L is Length of the main stream (km), $D_{i-1} + D_i$ is elevations of river bed at intersection points of contours reckoned from the bed elevation at a point of interest considered as datum, and D_{i-1} and D_i are the heights of successive bed locations at contours intersections.



(a) *Catchment Plan*



(b) *Longitudinal Section*

Figure 2.7 Physiographic parameters of the (a) representative catchment plan and (b) longitudinal section

Table 2.1 Computation of equivalent stream slope at Belekeri inlet

S.No.	Reduced Distance (from the point of study)	Reduced level	Length of each Segment (L _i)	Height above Datum (D)	D _{i-1} +D _i	L _i *(D _{i-1} +D _i)
	km	m	m	m	m	m*km
1	0.00	9	0.00	0	0	0.00
2	3.01	14	3.01	5	5	15.06
3	6.07	30	3.06	21	26	79.74
4	9.88	48	3.80	39	60	228.30
5	12.19	57	2.31	48	87	200.97
6	14.60	68	2.40	59	107	257.44
7	18.28	77	3.68	68	127	468.50
8	20.94	95	2.65	86	154	409.48
9	22.90	120	1.95	111	197	384.93
10	24.48	142	1.58	133	244	386.25
11	26.91	214	2.42	205	338	820.66

$\Sigma(L_i*(D_{i-1}+D_i))$ **3251.357**

Datum = 9m (Contour elevation at the basin outlet)

Equivalent stream slope,
$$S = \frac{L_i * [D_{i-1} + D_i]}{L^2} = \mathbf{4.489} \quad \text{m/km}$$

Table 2.2 Inlet locations and physiographic parameters of catchments in Kerala

Inlet Id	Inlet location		Inlet Name	CA (sq.km)	L Stream (km)	L _c (km)	S (m/km)
	Long (E)	Lat (N)					
1	75° 31' 51"	11° 42' 14"	Mahe	411.81	57.23	14.73	2.133
2	75° 35' 23"	11° 33' 54"	Iringal	1290.70	68.15	21.36	0.996
3	75° 43' 58"	11° 20' 59"	Elathur	615.91	61.64	11.21	3.166
4	75° 46' 48"	11° 13' 40"	Thekupuram	3036.97	141.17	45.88	1.894
5	75° 49' 31"	11° 7' 25"	Balathirutti	1241.35	137.74	33.49	0.849
6	75° 54' 50"	10° 47' 9"	Ponnani	6382.14	216.24	75.74	3.372
7	76° 2' 15"	10° 30' 24"	Chettuva	1676.66	96.18	14.73	1.973

Table 2.3 Inlet locations and physiographic parameters of catchments in Karnataka

Inlet Id	Inlet location		Basin Name (Inlet Name)	CA (sq.km)	L Stream (km)	Lc (km)	S (m/km)
	Long (E)	Lat (N)					
8	74°09'31"	14°50'29"	Karwar	5074.27	184.00	77.27	4.18
9	74°13'41"	14°45'08"	Kelaginakeri	33.61	5.49	2.60	4.64
10	74°15'51"	14°44'41"	KantrivadaGudda	29.67	3.40	1.60	8.97
11	74°16'45"	14°42'42"	Belekeri	226.34	26.91	14.40	4.49
12	74°17'02"	14°39'41"	Ankola	42.67	12.72	7.73	5.71
13	74°17'32"	14°38'49"	Belamber	23.98	7.68	5.06	1.75
14	74°21'28"	14°36'00"	Manjaguni	3983.59	159.59	84.22	3.89
15	74°23'34"	14°31'11"	Tadri(Tadadi Port)	1413.42	120.54	62.87	5.57
16	74°25'27"	14°25'03"	Alvekodi 2	34.54	10.84	4.96	5.24
17	74°28'11"	14°17'56"	Honavar(karki)	3042.23	131.10	76.14	6.07
18	74°30'05"	14°11'20"	Manki(Nakhuda)	13.92	8.60	4.30	7.69
19	74°29'16"	14°06'10"	Navayatkeri	23.95	6.82	3.70	8.72
20	74°31'04"	14°01'36"	Alvekodi 1	356.08	34.79	25.70	3.81
21	74°32'05"	13°59'05"	Jali	7.47	2.64	1.66	5.54
22	74°33'59"	13°58'01"	Mavinakurve	58.73	17.00	12.46	4.89
23	74°35'08"	13°56'59"	Hadin	10.65	4.54	2.92	3.60
24	74°34'58"	13°55'26"	Gorta	18.22	9.01	6.40	9.85
25	74°36'25"	13°55'20"	Alvegadde	92.03	15.40	13.88	6.36
26	74°37'27"	13°52'05"	Paduvari	114.08	17.75	7.60	1.91
27	74°40'11"	13°47'38"	Koderi	100.06	22.81	13.30	1.98
28	74°41'43"	13°38'02"	Gangoli	1565.74	65.29	43.00	5.72
29	74°44'11"	13°27'00"	Kundapura	1575.09	70.13	44.00	1.01
30	74°41'45"	13°22'15"	Badanidiyoor	5.64	4.40	2.25	5.39
31	74°41'44"	13°20'50"	Malpe	475.86	45.53	23.20	0.71
32	74°46'01"	13°13'26"	Kaup	3.94	2.30	0.90	4.07
33	74°46'36"	13°06'42"	Nadsal	31.66	14.49	7.90	1.57
34	74°48'22"	13°04'31"	Hejamadi	564.46	41.00	23.76	1.24
35	74°51'49"	12°50'43"	Gurpur&Netravathi	4327.51	143.62	68.40	2.18
36	74°53'15"	12°45'38"	Kanwatheertha	59.48	13.70	5.90	6.50

From Tables 2.2 and 2.3, it is understood that the study area comprises of all types of catchments (small, medium and large) and catchment areas ranging from less than 10 sq km to more than 5000 sq km. The major rivers like Kali (184km), Gangavali (159.60 km), Agnashini (120.54 km), Sharavali (131.10 km), Gangoli (65.29 km), and Netravati (143.62 km) are having longest length of the main-stream. The equivalent slopes values are ranging from 0.71 m/km at Maple to 9.85 m/km at Gorta in Karnataka and 3.37 m/km at Ponnani to 0.99m/km at Iringal in Kerala.

2.4. DIFFERENT SYNTHETIC UNIT HYDROGRAPH APPROACHES

More than 85 years since the inception of UH theory by Sherman (1932), it is still one of the most widely used methods for the development of flood prediction and warning systems for gauged basins with observed rainfall-runoff data. He was the first person to see the possibilities of extending the UH theory he had developed for the derivation of SUH at ungauged catchments. In his theory, he listed the physical catchment characteristics, viz., drainage area, size and shape of the basin, distribution of water courses, main stream slope, slope of the channel, pondage due to channel obstructions, etc., that would reflect in a UH, and which could be used to estimate the stream flow for an ungauged basin from the given rainfall data.

Sherman's idea has been the basis of many SUH methods (Hoffmeister and Weisman 1977). Numerous procedures have been derived whereby the unit hydrograph for an ungauged area can be constructed. Each procedure, however, differs somewhat from another either in the relationships or the methodology employed. The UH concept predominantly needs observed rainfall-runoff data at the gauging site for UH generation; the lack of such data sparked the idea of the SUH concept. The term "Synthetic" denotes the UH is derived from basin characteristics rather than rainfall-runoff data.

Since last three decades research on the hydrology of ungauged basins has received much attention. To provide a quick reference guide for researchers exploring new methods in ungauged basins; Singh et al. (2014) categorized the available SUH methods into four groups as traditional (or empirical), conceptual, probabilistic and geomorphological. Unit hydrographs are derived using rainfall and runoff records for the basin under consideration. But there are many basins, which are not gauged especially in developing country like India and for which a unit hydrograph may be required. This is usually done by relating the selected basin characteristics to the UH shape. Once such relations are established between the basin parameters and UH parameters for the basins having sufficient rainfall, runoff data, the same relations are applied to get a unit hydrograph for un-gauged catchments of the hydro-meteorologically homogenous region.

Among various SUH methods, the traditional and probabilistic based synthetic unit hydrographs which are used to estimate the total flood discharge at basin outlets (i.e., tidal inlets) have been discussed in subsequent sections.

2.4.1. Traditional SHU methods

To synthesize the UH from watershed characteristics; the SUH concept was traced back in the form of distribution graph by Bernard (1935). Some of such traditional methods of SUHs include Snyder (1938), Taylor and Schwarz (1952) and Soil Conservation Service (1957). Central Water Commission (CWC 1992, 2001) have been developed two methods which are also considered as traditional methods in the present study since some degree of subjectivity is involved in fitting the remaining points on the SUH. In addition to that, all traditional SUHs are also required simultaneous adjustments to ensure that the area under the SUH is unity corresponding to unit excess of rainfall. The empirical equations come across in various traditional SUHs have certain constants, which may vary over a wide range. However, despite their inconsistencies, these SUH methods are still widely used in engineering applications. The descriptions of traditional or empirical SUH methods used in the present study are given below.

2.4.1.1. CWC SUH Method

After reviewing the empirical methods available for estimation of design flood discharge under the chairmanship of Dr. A.N. Khosla in 1959, the committee of engineers recommended the adoption of rational methodology involving the use of design storm and unit hydrograph. To do so, under the long-term plan; India has been divided into 26 hydro meteorologically homogeneous sub-basins (Figure 2.8), and these are used to carry out regional studies at ungauged basins. For preparing the flood estimation report for all sub-zones, hydro-meteorological data has been collected at the representative catchments for 5 to 10 years. For UH analysis, rainfall, gauge and discharge data were collected during the monsoon season (CWC, 1992). The characteristics of the catchments and their unit hydrographs have been prepared for several catchments in a subzone and are correlated using regression analysis, and then the equations are developed for synthetic unit hydrograph for estimating flood discharge at ungauged catchments. From the published reports of CWC, two methods viz. synthetic unit hydrograph and dimensionless unit hydrograph are considered in the present study and are explained in the subsequent sections.

CWC has adopted a simple model for establishing the relationships between physiographic and UH parameters.

$$Y=C*X^P \quad (2.2)$$

Where X and Y are Independent and dependent variables, C = a constant, P = an exponent
The Eq. 2.2 is of the form, $\text{Log } Y = \text{Log } C + P \text{ Log } X$. Therefore there exists straight line relationship, when the graph is drawn between dependent and independent variables on a log-log scale. Various trials of relationships were made between physiographic parameters and one of the unit hydrograph graph parameters and among the unit hydrograph parameters themselves for the 13 gauged catchments in the CWC subzone 5(a) and 5(b) (CWC, 1992). List of physical and unit hydrograph parameters studied to establish relationships are given in Table A2.1. The relationship between the physiographic

parameter $\left(\frac{L}{S}\right)$ and UG parameter (q_p) was found to be significant. After that t_p was related to q_p and q_p was related to various UG parameters like W_{50} , W_{75} , W_{R50} , and W_{R75} . The T_B could be significantly correlated to t_p .

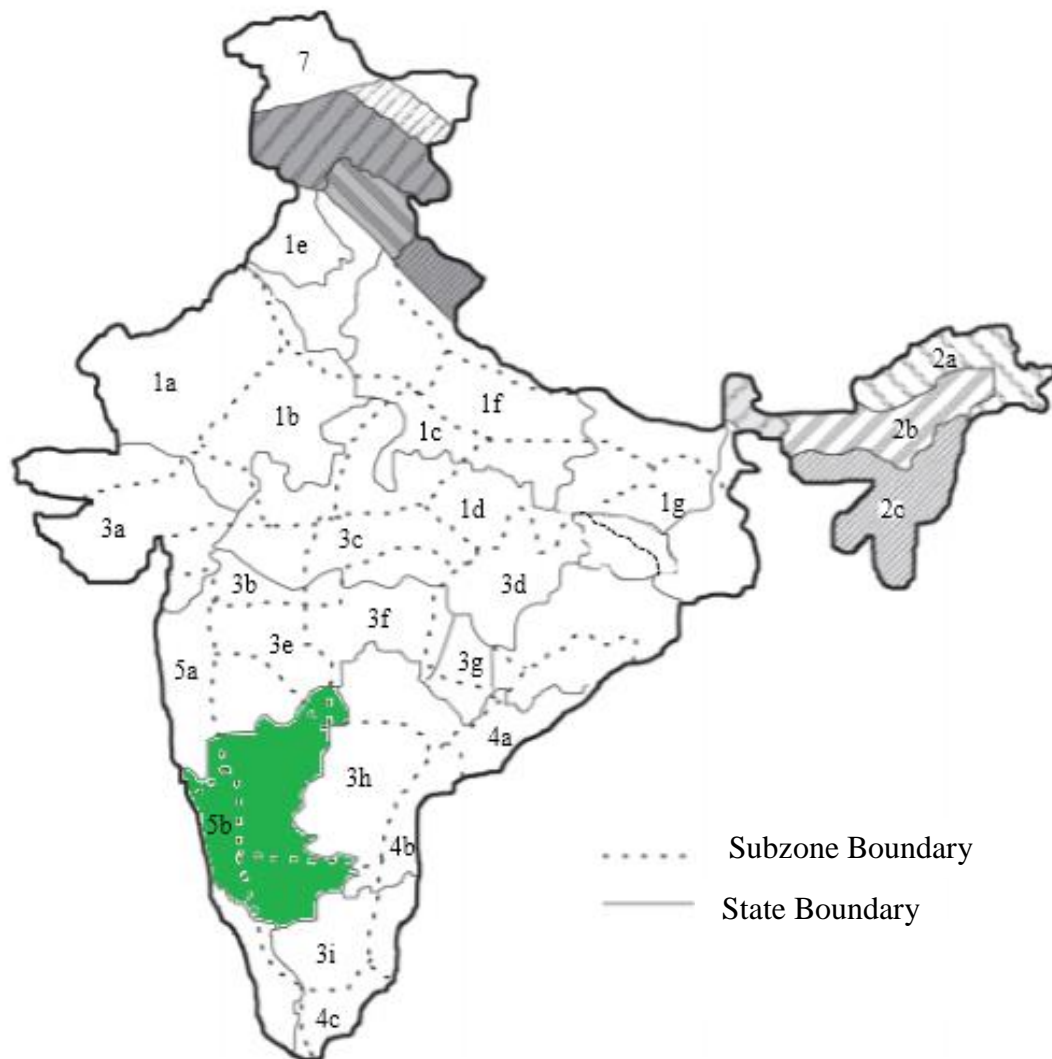


Figure 2.8 Hydrometeorologically homogeneous zones in India (CWC, 1983) and the Green colour zone is the present study area along Karnataka coastline.

The principle of least square was used in the regression analysis to get the above relationship in the equation $Y = C * X^P$ to predict the parameters of the synthetic unit

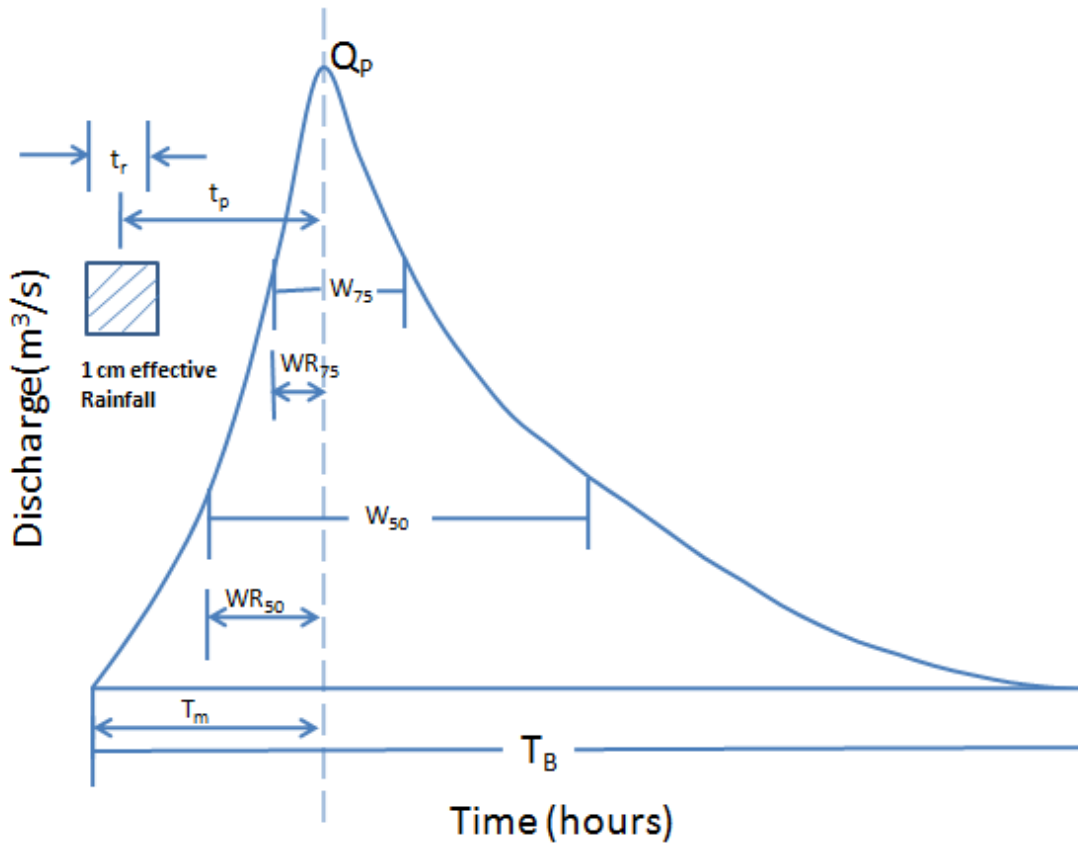


Figure 2.9 Synthetic Unit Hydrograph parameters

hydrograph in an unbiased manner. The following relationships are derived for estimating the 1-hour unit hydrograph parameters (Figure 2.9) in the subzones 5(a) and 5(b) (CWC, 1992).

$$q_p = 0.9178 \left[\frac{L}{S} \right]^{-0.4313} \quad (2.3)$$

$$t_p = 1.5607 [q_p]^{-1.0814} \quad (2.4)$$

$$w_{50} = 1.9251 [q_p]^{-1.0896} \quad (2.5)$$

$$w_{75} = 1.0189 [q_p]^{-1.0443} \quad (2.6)$$

$$w_{R50} = 0.5788 [q_p]^{-1.1072} \quad (2.7)$$

$$w_{R75} = 0.3469 [q_p]^{-1.0538} \quad (2.8)$$

$$T_B = 7.3801 [t_p]^{0.7343} \quad (2.9)$$

$$T_m = t_p + \frac{t_r}{2} \quad (2.10)$$

$$Q_p = q_p A \quad (2.11)$$

The above relationships (Eq.2.3 to Eq. 2.11) are used to estimate the parameters of 1-hour Synthetic Unit Hydrograph (SUH) for an ungauged catchment with its known catchment characteristics like A, L, L_C, and S.

Considering the hydrometeorological homogeneity of subzones 5(a) and 5(b), the stepwise procedure for derivation of 1-hour unit hydrograph for an ungauged catchment is given below.

- 1) Physiographic parameters of the ungauged catchment (i.e., A, L, L_C, and S) are determined from the catchment plan and then $\frac{L_i}{S}$ is calculated.
- 2) Substitute $\frac{L_i}{S}$ in the Eq.2.3 to obtain q_p and this q_p in Eq.2.4 to get t_p in hours.
- 3) Substitute the value of q_p in the Eq.2.5 to 2.8 to obtain W₅₀, W₇₅, W_{R50}, W_{R75} and t_p in Eq. 2.9 to get T_B in hours.
- 4) Plot the parameters of 1-hour unit hydrograph through seven characteristic points viz. T_m, T_B, Q_p, W₅₀, W₇₅, W_{R50}, W_{R75} using Microsoft spreadsheet.
- 5) Sum of discharge ordinates of t_r (h) unit hydrograph is accurately obtained by using the Eq. 2.12.

$$Q_i = \frac{2.78A}{t_r} \quad (2.12)$$

where Q_i = discharge ordinates at 1-hour interval (cumecs)

A = catchment area (sq km)

t_r = unit duration (h)

- 6) Suitable modifications should be made in rising and recession limbs to get the area under the UH as unity.

2.4.1.2. CWC Dimensionless Unit Hydrograph method

If unit hydrographs are available for several areas adjacent to the watershed for which a unit hydrograph is required but for which insufficient data or no data available, then transposition of available unit hydrographs will give better results than resorting to a wholly synthetic procedure. Unit hydrographs are reduced to dimensionless form, to compare them from basins of different sizes and shape or those resulting from different storm patterns. Among a number of dimensionless unit hydrographs that are developed for the purpose, the one explained here is more commonly used for Indian catchments. For developing the UH at all the ungauged catchments of Karnataka coastline using dimensionless UH, observed unit hydrographs of 13 catchments in the same hydrological region are considered. The data pertaining to availability of gauge, discharge, rainfall, basin characteristics and representative one hour UH parameters are given in Table A2.2 to A2.4.

The stepwise procedure for the development of dimensionless unit hydrograph is given below.

1. The unit hydrographs at the given bridge sites are converted to dimensionless form by dividing the time ordinate by T_m and discharge ordinate by (V/T_p) . The converted dimensionless form at MOT-8 is shown in Table A2.5 as an example.
2. The dimensionless forms of the unit hydrographs are plotted, and an average dimensionless UH for the site is drawn at an equal interval (i.e., 0.2 in the present study). The ordinates of average dimensionless UGs at all bridge sites (i.e., measured data) is depicted in Table A2.6.
3. T_m and V for the un-gauged catchments are computed using regional formulae of the respective subzone, proposed by Central Water Commission (CWC).
4. The time and runoff ordinates of UH at the required catchment are computed by multiplying the average dimensionless UH by T_m and (V/T_m) .
5. Suitably modify the rising and falling limbs of UH to get smoothed and its volume adjusted for unity.

In the present study after determining UHs for all individual bridge sites, the UGs at the 13 sites are converted to dimensionless form by dividing the time ordinate by T_m and discharge ordinate by (V/T_m) (Figure 2.10). The T_m and V values for the individual watersheds are computed by using CWC regional report (1992). The average dimensionless UH for estimation of flood discharge at the ungauged watersheds is given in Figure 2.11.

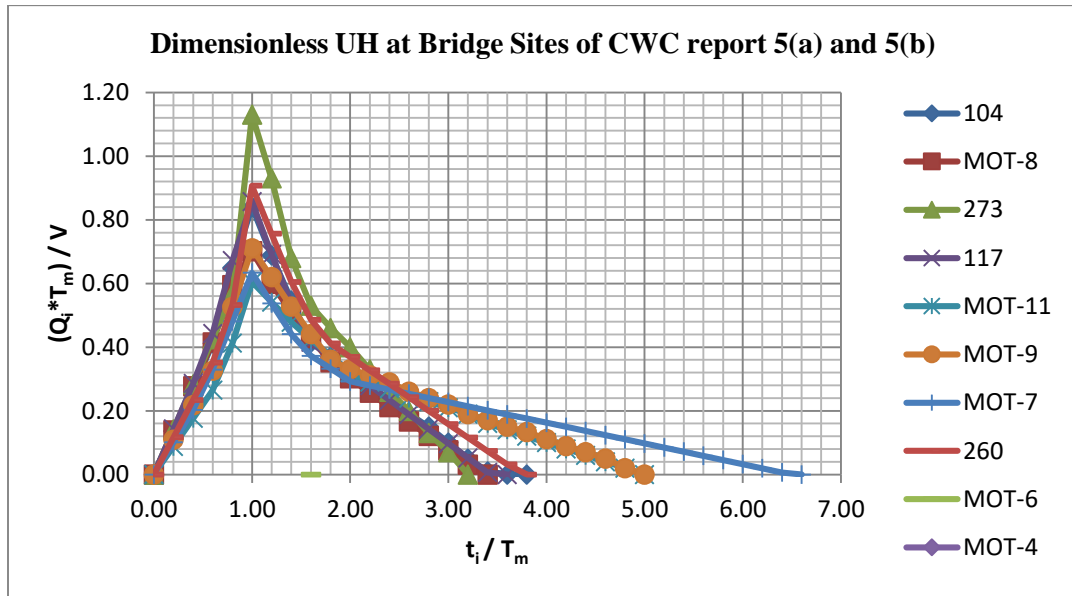


Figure 2.10 Dimensionless unit hydrographs at 13 bridge sites

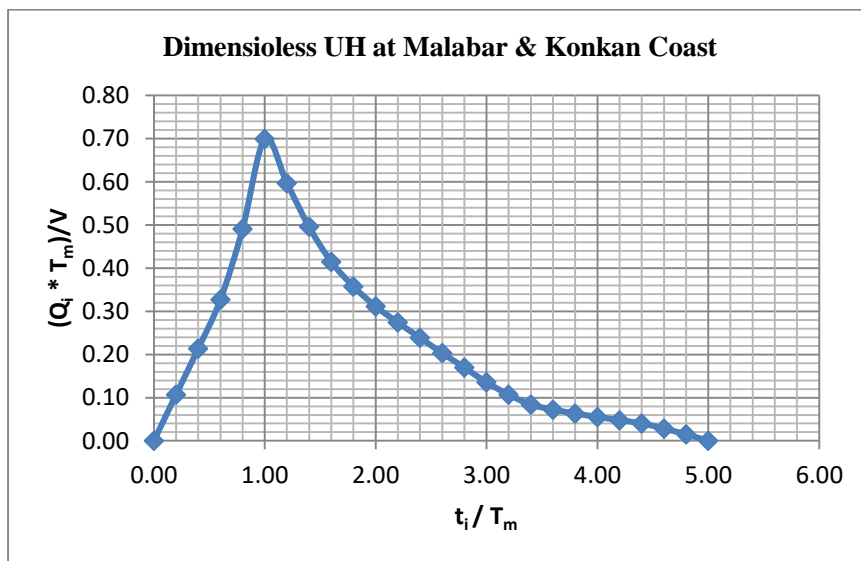


Figure 2.11 Dimensionless Unit Hydrograph derived for the project catchments

2.4.1.3. Snyder method

Snyder (1938) selected the peak discharge Q_p , the basin lag t_p , and base time T_B , to define the shape of the unit hydrograph. These equations are expressed, respectively, as

$$t_p = C_t (LL_c)^{0.3} \quad (2.13a)$$

$$q_p = \frac{Q_p}{A} = \frac{2.778 C_p}{t_p} \quad (2.13b)$$

$$T_B = 72 + 3t_p \quad (2.13c)$$

Where, L is the length of the main stream (km), L_c is the distance from the watershed outlet to a point on the main stream nearest to the centre of area of watershed (km), A is catchment area (sq km), q_p is the peak discharge per unit area of the catchment ($m^3/s/sq$ km), C_t and C_p are non-dimensional constants. The Eqs.2.13 (a) and 2.13(b) are obtained from the study of catchments varying in size from 26 to 259000 km^2 . Snyder (1938) found C_t to vary from 1.8 to 2.2 and C_p from 0.59 to 0.65. More recently, Das (2009) reported C_t and C_p as 0.65 and 0.94, respectively, for Ramganga catchment in the Himalayan range, India. The standard duration of the Snyder's unit hydrograph is $t_r = \frac{2}{11} t_p$, which gives unreasonably long base period (T_B) for small basins. Therefore some investigators recommended that a base period which is five times the time to peak is about reasonable. Thus modified base time is given as

$$T_B = 5 \left(\frac{t_r}{2} + t_p \right) = 5.455 t_p \quad (2.14)$$

If a SUH for any other duration t'_r is required, then the modified basin lag is given as

$$t'_p = t_p + \frac{t'_r - t_r}{4} \quad (2.15)$$

The Eq.2.15 gives the peak discharge of t'_p hours of unit hydrograph. Therefore Eq. 2.13 gets modified accordingly. One can sketch any number of UHs through the three known characteristic points, i.e., t_p , q_p and T_B . To overcome this ambiguity associated with Snyder's method, the US Army Corps of Engineers (USACE, 1940) proposed empirical relations between the width of UHs at 50% and 75% of $Q_p (= q_p A)$, and they are given as

$$W_{50}=2.14(q_p')^{-1.08} \quad (2.16)$$

$$W_{75}=1.22(q_p')^{-1.08} \quad (2.17)$$

where, W_{50} and W_{75} are the widths of UH in hours at 50% and 75% of the peak discharge. Thus, one can sketch a smooth curve through the seven characteristics points (Q_p , t_p , T_B , W_{50} , and W_{75}) relatively more efficiently with less degree of ambiguity to satisfy the UH criterion. However, in practical applications, this procedure is very tedious and involves a great degree of subjectivity and error due to the manual fitting of the points and simultaneous adjustments for the SUH area.

Bhunya et al. (2011) summarised the major inconsistencies associated with the Snyder method are:

- a) The manual fitting of the characteristics points needed a great degree of subjectivity and trial and error and may involve error.
- b) The constants C_t and C_p vary over a wide range and from region to region, and may not be equally suitable for all the reasons.
- c) The time base (Eq.2.13c) of Snyder's method is always greater than three days, which is reasonable for reasonably large catchments only (Gray 1961a, 1961b; Taylor and Schwarz 1952; and Ponce 1989).

2.4.1.4. Soil Conservation Service (SCS) method

The dimensionless unit hydrograph developed by United States Soil Conservation Service (SCS) provides a shape to the unit hydrograph, which leads to high reproducible results than the Snyder method. It is derived from the analysis of a large number of actual unit hydrographs for the watersheds of different size and locations, to synthesize the UH (Singh, 1998). The plotting positions of dimensionless unit hydrograph are expressed in terms of ratios of time to ratios of flow (t/t_p vs. Q/Q_p), where Q_p is the peak discharge and t_p is the time to peak. The time to peak (t_p) and peak discharge (Q_p) are computed as

$$t_p = \frac{t_r}{2} + t_L \quad (2.18)$$

$$Q_p = 2.08 \frac{A}{t_p} \quad (2.19)$$

where t_r = duration of rainfall (h); A = catchment area (Sq km); and t_L = lag time (h). The value of t_L can be estimated from catchment characteristics using the Curve Number (CN) procedure as

$$t_L = \frac{L^{0.8}(2540-22.86CN)^{0.7}}{14104CN^{0.7}S^{0.5}} \quad (2.20)$$

where L = length of watershed (m); CN = Curve Number ($50 < CN < 95$); and S = average watershed slope (m/m). Thus with the known values of t_p and Q_p , and a specified dimensionless UH, the Synthetic Unit Hydrograph (SUH) can be easily derived.

Bhunya et al. (2011) enumerated the inconsistencies associated with the SCS method as:

- a) Since curve number method applies to watersheds of areas ranging from 8 km² to 16 km² (Ponce 1989), its application to large and medium watersheds may lead to erroneous results.
- b) Since the SCS method, the ratio of time base to time to peak (T_B/t_p) for triangular UH equal to 2.67, ratios other than this may lead to the other shapes of the UH. In particular, larger ratio implies greater catchment storage. Therefore, since the SCS method fixes the ratio (T_B/t_p), it should be limited to midsize watersheds in the lower end of the spectrum.
- c) The SCS method is one of the popular methods for synthesizing the UH for only small watersheds of an area less than 500 square miles (Wu, 1969; Wang, 1972; McCuen and Bondelid, 1983).

2.4.2. Probability Distribution Function based SUH Methods

The probability distribution function based SUH methods have been used since it has a long successful history. Due to the similarity in the shape of statistical distributions and a conventional UH, several attempts have been made in the past to use their probability density functions (pdfs) for the derivation of the SUH. In practice, two approaches are followed (a) a non-parametric approach based on a discretization technique (Snyder, 1955; Eagleson et al., 1966; Collins, 1939; Mays and Taur, 1982 and Yang and Han, 2006); (b) a parametric approach that fits some prescriptive functional curves with a limited numbers of parameters, and these parameters are estimated through any suitable approach.

The non-parametric methods are believed to be more accurate because they use a large number of points for UH derivation. Therefore, despite their disadvantages in terms of a large number of correlated parameters in the UH model, they are widely used for UH derivation. Further, the large number of parameters involved in the derivation of the UH using these methods can lead to the problems of computational instability, which restricts the practical application of these techniques. On the other hand, the parametric approach fits the UH through selected salient points such as (t_p, q_p) , (t_p, t_i) and (q_p, t_i) , where t_p is the time to peak, q_p is peak discharge per unit area, and t_i is the point of inflection after the peak. Their simplicity and ease of development can characterize these SUHs as they require fewer data and yield a smooth and single-valued shape corresponding to one unit runoff volume, which is essential for UH derivation. The SUH methods of Gray (1961), Croley (1980), Aron and White (1982), Singh and Chowdhury (1985), McCuen (1989), Haktanir and Sezen (1990), Singh (2000), Bhunya et al. (2003, 2008, 2009) are but a few of them.

In the present study, the pdfs based SUH methods like Gray (1961), Croley (1980), Singh (2000) and Bhunya et al. (2003) are used to estimate the total discharge. The descriptions of the above-said methods are given below.

2.4.2.1. Gray method

Gray (1961) used two-parameter Gamma distribution function and catchment characteristics to derive a non-dimensional SUH. The geometry of dimensionless graph is expressed as

$$Q_{t/P_R} = \frac{25(\gamma')^q}{\Gamma(q)} \left(e^{-\gamma' t/P_R} \right) \left(\frac{t}{P_R} \right)^{(q-1)} \quad (2.21)$$

where Q_{t/P_R} is the percent flow at any given time $\frac{t}{P_R}$; P_R is the time from starting of surface runoff to the peak discharge; γ' is a dimensionless parameter; q is a shape parameter ($=1+\gamma'$); Γ is gamma function. The empirical graphs described in this manner are referred to as dimensionless graphs.

He defined the parameter called storage factor as the ratio of $\frac{P_R}{\gamma'}$ which gives the storage property of a watershed and related it with the catchment characteristics in the form a power equation as

$$\frac{P_R}{\gamma'} = a \left(\frac{L}{\sqrt{S_M}} \right)^b \quad (2.22)$$

where a and b are the coefficient and exponent of the power equation and S_M is the slope of the main stream in percentage. The above equation was applied to 33 watersheds covering three regional groups, and finally, he developed a regression relationship between the period of rise and dimensionless parameter γ' as

$$\frac{P_R}{\gamma'} = \frac{1}{\frac{2.676}{P_R} + 0.0139} \quad (2.23)$$

Thus the Eqs.2.21 and 2.23 are used to develop the dimensionless SUH.

2.4.2.2. Croley method

Synthetic hydrographs are usually a function of watershed and storm characteristics, and one of the most commonly used SUH is based upon the two-parameter Gamma distribution. Croley (1980) developed SUH by fitting two-parameter Gamma distribution for a different set of boundary conditions: (t_p, q_p) , (t_p, t_i) or (q_p, t_i) , where t_p is the time to peak, q_p is peak discharge per unit area, and t_i is the point of inflection. He summarized gamma synthetic hydrograph fit by applying four sets of boundary conditions as: (1) for given q_p and t_p , (2) for given t_p and t_i , (3) for given t_p , t_γ and γ , (4) for given q_p and t_i . These boundary conditions are used to estimate the parameters α and β of the distribution. The expression for the SUH is expressed as

$$q(t) = q_p \left\{ \left(\frac{t}{t_p} \right) \exp \left[1 - \left(\frac{t}{t_p} \right) \right] \right\}^{\alpha-1} \quad (2.24a)$$

$$\text{where } t_p = \beta(\alpha - 1) \quad (2.24b)$$

$$\text{and } q_p = V(\alpha - 1)^{\alpha-1} \exp(1 - \alpha) / [\beta\Gamma(\alpha)] \quad (2.24c)$$

The methodology provides an initiation to work with probability distribution functions for SUH derivation at ungauged catchments. The works of Singh (2000) and Bhunya et al. (2003) seem to be much inspired by Croley's work.

2.4.2.3. Transmutation approach

Singh (2000) transmuted the popular SUHs, such as Snyder, Soil Conservation Service (SCS) and Gray method into a gamma distribution in a simplified manner. Nash (1959) and Dooge (1959), based on the concept of n-linear reservoirs with equal storage coefficient K, expressed the Instantaneous Unit Hydrograph (IUH) in the form of a Gamma distribution function as

$$q(t) = \frac{1}{K\Gamma(n)} \left(\frac{t}{K} \right)^{n-1} e^{-\frac{t}{K}} \quad (2.25)$$

where n and K are the parameters defining the shape of the IUH and q is the depth of runoff per unit time per unit effective rainfall. Assuming that the Eq. 2.25 represents UH of unit duration, the condition at the peak ($t=t_p$) can be expressed as

$$K = \frac{t_p}{n-1} \quad (2.26)$$

From Eqs. 2.25 and 2.26, one can obtain:

$$\frac{q}{q_p} = e^{(n-1)\alpha(t/t_p)} \quad (2.27)$$

Where, α is a function of t/t_p is given by

$$\alpha(t/t_p) = \left[1 - t/t_p + \ln(t/t_p) \right] \quad (2.28)$$

Using Eqs. 2.25 and 2.26, a simple analytical expression relating the parameter n and a non-dimensional term β was developed as

$$\beta = \frac{(n-1)^{(n-1)} e^{-(n-1)}}{\Gamma(n-1)} \quad (2.29)$$

in which $\beta (=q_p t_p)$ is called as the shape factor and had a range of values between 0.35 to 1.25. Substituting the approximate expression for the gamma distribution function in Eq. 2.29, the following simple analytical equation for inverting Eq. 2.29 was obtained as

$$n = 7/6 + 2\pi\beta^2 \quad (2.30)$$

Eq. 2.30 can be used to calculate β if n is known from other sources.

2.4.2.4. Two Parameter Gamma Distribution method

Based on the concept of a cascade of n -linear reservoirs of equal storage coefficient K , Nash (1958, 1959) and Dooge (1959) derived the expression in the form of Gamma function for Instantaneous Unit Hydrograph (IUH) as

$$q = \frac{1}{K\Gamma n} \left(\frac{t}{K} \right)^{n-1} e^{-t/K} \quad (2.31)$$

Where, n is number of reservoirs and K is storage coefficient, which defines the shape of IUH; and q = depth of runoff per time per unit effective rainfall. From the known values of n and K , the SUH is derived based on the Eq. 2.31. A simple equation is derived by relating the parameters n and β ($=q_p t_p$) of the gamma distribution for SUH derivation and is given as follows (Bhunya et al. 2003).

$$n=5.53\beta^{1.75}+1.04 \quad 0.01<\beta<0.35 \quad (2.32 \text{ a})$$

$$n=6.29\beta^{1.998}+1.157 \quad \beta\geq 0.35 \quad (2.32 \text{ b})$$

With the known values of q_p (peak discharge in cm/h/cm) and t_p (time to peak in hours) by using the Eq.2.32 one can estimate the shape of Synthetic Unit Hydrograph (SUH).

2.4.3. Conceptual Synthetic Unit Hydrograph methods

The popular conceptual models were developed by Clark (1945), Nash (1957), Dooge (1959), Singh (1964), Bhunya et al. (2005) and Singh et al. (2007). These conceptual models have ample potential to be transmuted into SUH, and thus require the attention of the Predictions in Ungauged Basins (PUB) research community for their analysis. In the present study, a Hybrid model proposed by Bhunya et al. (2005) was used for the estimation of flood discharge, and the same has been discussed below.

2.4.3.1. Hybrid model

A single linear reservoir of the Nash model yields an Instantaneous Unit Hydrograph (IUH) without rising limb, which is a physically unrealistic response. To simulate a complete IUH with rising limb, a hybrid model was introduced by splitting the Nash single reservoir into two serially connected reservoirs of unequal storage coefficients. The rainfall enters the first reservoir for its routing to the second reservoir for its further routing to the end of the first hybrid unit (i.e., reservoir) to yield the output in the shape of a hydrograph. This output

forms the variable inputs to the second hybrid unit of the same characteristics as the first one (Figure 2.12). The final output can be derived analytically and the final form of the output from the second unit is given as follows (Bhunya et al. 2005)

$$Q_2(t) = \frac{1}{(K_1 - K_2)^2} \left\{ t \left[\exp\left(-\frac{t}{K_1}\right) + \exp\left(-\frac{t}{K_2}\right) \right] - 2 \left(\frac{K_1 K_2}{K_1 - K_2} \right) \left[\exp\left(-\frac{t}{K_1}\right) - \exp\left(-\frac{t}{K_2}\right) \right] \right\} \quad (2.33)$$

where K_1 and K_2 = the storage coefficients of the first and second reservoirs respectively and its time to peak is given as (by differentiating with respect to t for the condition, at $t = t_p$, $Q_2(t) = Q_p$):

$$t_p = \frac{K_1 + K_2}{K_2 - K_1} \sqrt{K_1 K_2} \quad (2.34)$$

The unknown parameters K_2 and K_1 for solving the Eqs.2.33 and 2.34 are given by an expression in a simple form as follows (Bhunya et al. 2005).

$$K_2 = \frac{\beta t_p}{9.4452\beta^3 - 8.2173\beta^2 + 4.306\beta - 0.4466} \quad (2.35a)$$

$$K_1 = \frac{K_2}{-0.2073\lambda^3 + 1.772\lambda^2 - 5.2535\lambda + 7.1051} \quad (2.35b)$$

where $\beta = q_p t_p$ and $\lambda = t_p / K_2$. The complete shape of SUH can be derived with the known values of $q_p, t_p, K_1,$ and K_2 . Simple spreadsheet software can be used to compute the Synthetic Unit Hydrograph.

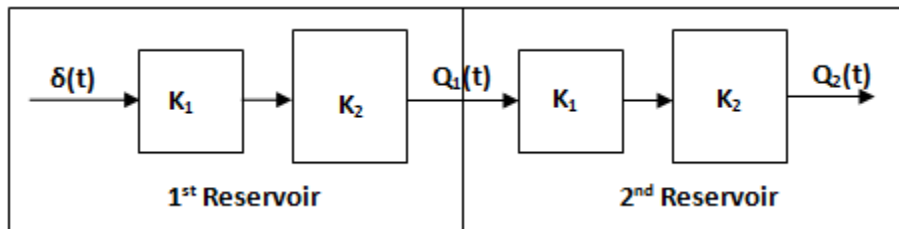


Figure 2.12 Arrangement of first and second reservoirs of the hybrid model

2.5. ESTIMATION OF UH PARAMETERS

The input data needed for parameter estimation such as catchment area, length of the main stream, a distance of the centroid from basin outlet and equivalent slope, etc. are obtained with the help of ArcGIS® tools. The data presented in Tables 2.2 and 2.3 are used for parameter estimation along the coastal catchments of Kerala and Karnataka.

2.5.1. Parameter estimation for CWC methods

Based on the equations (Eqs.2.3 to 2.11) suggested by CWC (CWC,1992), the parameters required for the development of CWC SUH and CWC dimensionless methods are calculated and presented in Table 2.4 and 2.5.

Table 2.4 Estimated parameters for the development of CWC SUH methods for catchments of Kerala

Catchment ID	q_p Cumec /sq km	t_p (h)	W_{50} (h)	W_{75} (h)	W_{R50} (h)	W_{R75} (h)	T_B (h)	T_m (h)	Q_p (Cumecs)
1	0.22	7.94	9.92	4.90	3.06	1.69	33.80	8.44	91.46
2	0.11	17.06	21.43	10.26	6.70	3.57	59.26	17.56	135.93
3	0.24	7.17	8.94	4.44	2.76	1.53	31.34	7.67	315.26
4	0.20	8.69	10.86	5.35	3.36	1.85	36.11	9.19	125.87
5	0.12	15.55	19.52	9.38	6.09	3.26	55.36	16.05	200.04
6	0.18	9.77	12.23	5.99	3.79	2.07	39.36	10.27	556.74
7	0.12	15.31	19.22	9.24	6.00	3.21	54.73	15.81	772.55

Table 2.5 Estimated parameters for the development of CWC SUH methods for catchments of Karnataka

Catchment Id	q_p (Cumeecs/sq km)	t_p (h)	W_{50} (h)	W_{75} (h)	W_{R50} (h)	W_{R75} (h)	T_B (h)	T_m (h)	Q_p (Cumeecs)
8	0.18	10.01	12.52	6.13	3.88	2.12	40.05	10.51	910.17
9	0.85	1.85	2.29	1.20	0.69	0.41	11.60	2.35	28.70
10	1.39	1.09	1.34	0.72	0.40	0.24	7.86	1.59	41.39
11	0.42	3.95	4.90	2.50	1.50	0.86	20.23	4.45	95.95
12	0.65	2.49	3.08	1.60	0.93	0.55	14.41	2.99	27.72
13	0.49	3.41	4.23	2.17	1.29	0.74	18.18	3.91	11.63
14	0.18	9.68	12.11	5.94	3.75	2.05	39.08	10.18	736.91
15	0.24	7.18	8.97	4.45	2.76	1.54	31.40	7.68	344.43
16	0.67	2.40	2.98	1.55	0.90	0.53	14.05	2.90	23.16
17	0.24	7.18	8.96	4.45	2.76	1.53	31.38	7.68	741.97
18	0.87	1.80	2.23	1.17	0.67	0.40	11.38	2.30	12.17
19	1.02	1.53	1.88	1.00	0.57	0.34	10.07	2.03	24.44
20	0.35	4.81	5.98	3.02	1.83	1.04	23.37	5.31	125.87
21	1.26	1.21	1.49	0.80	0.45	0.27	8.50	1.71	9.43
22	0.54	3.06	3.79	1.95	1.15	0.67	16.78	3.56	31.50
23	0.83	1.91	2.36	1.24	0.71	0.42	11.86	2.41	8.85
24	0.95	1.64	2.03	1.07	0.61	0.36	10.63	2.14	17.38
25	0.63	2.59	3.20	1.66	0.97	0.57	14.83	3.09	57.68
26	0.35	4.84	6.02	3.04	1.85	1.05	23.50	5.34	40.04
27	0.32	5.35	6.66	3.35	2.04	1.15	25.29	5.85	32.02
28	0.32	5.33	6.64	3.34	2.04	1.15	25.23	5.83	502.62
29	0.15	12.37	15.50	7.52	4.82	2.61	46.80	12.87	232.17
30	1.00	1.56	1.92	1.02	0.58	0.35	10.22	2.06	5.66
31	0.15	11.89	14.90	7.24	4.63	2.51	45.46	12.39	72.76
32	1.17	1.31	1.62	0.86	0.48	0.29	9.01	1.81	4.63
33	0.35	4.83	6.01	3.04	1.84	1.04	23.47	5.33	11.13
34	0.20	8.76	10.95	5.39	3.39	1.86	36.33	9.26	114.48
35	0.15	12.06	15.11	7.34	4.70	2.54	45.94	12.56	653.08
36	0.67	2.42	3.00	1.56	0.91	0.53	14.14	2.92	39.59

2.5.2. Parameter estimation for Snyder's method

Snyder expressed equations (Eqs.2.13 to 2.17) to define the shape of the UH in the form of peak discharge per unit area, basin lag, time base and width of UHs at 50% and 75% of Q_p . Based on these equations, the parameters required for the development of UH using Snyder's method are calculated and presented in the Table 2.6 and Table 2.7.

Table 2.6 Estimated parameters for the development of Snyder's SUH for catchments of Kerala

Catchment ID	t_p (h)	D (h)	$t_{p'}$ (1 hr)	$Q_{p'}$ (m^3/s)	$q_{p'}$ ($m^3/s/km^2$)	T_m (h)	t_B (h)	W_{50} (h)	W_{75} (h)
1	17.01	3.09	16.48	45.11	0.11	16.98	50.72	23.32	13.29
2	29.35	5.34	28.27	79.30	0.06	28.77	86.97	41.74	23.80
3	18.68	3.40	18.08	128.93	0.10	18.58	55.62	25.76	14.68
4	18.12	3.29	17.55	63.38	0.10	18.05	53.99	24.95	14.22
5	24.86	4.52	23.98	126.26	0.08	24.48	73.78	34.95	19.92
6	30.19	5.49	29.07	188.63	0.06	29.57	89.45	43.03	24.53
7	36.34	6.61	34.94	329.82	0.05	35.44	107.51	52.48	27.92

2.5.3. Parameter estimation for SCS method

Soil Conservation Service (SCS) method was derived from the analysis of a large number of actual unit hydrographs for the watersheds of different size and locations, to synthesize the UH. The time to peak, peak discharge and lag time were computed using the Eqs.2.18 to 2.20 and the parameters estimated for SCS method are given in Table 2.8 and 2.9.

2.5.4. Parameter estimation for pdfs based SUH methods

The parameter estimation for all the probability distribution function based SUH methods viz. Gray's method, Croley method, Transmutation approach, Simplified two-

parameter Gamma distribution method along with Hybrid model, which is a conceptual SUH method required few known parameters such as t_p and Q_p . The values of t_p and Q_p which are required to develop the above said SUHs are taken from Snyder's method.

Table 2.7 Estimated parameters for the development of Snyder's SUH for catchments of Karnataka

Catchment ID	t_p (h)	D (h)	t_p' (1 hr)	Q_p' (m ³ /s)	q_p' (m ³ /s/km ²)	T_m (h)	t_B (h)	W_{50} (h)	W_{75} (h)
8	23.78	4.32	22.95	399.28	0.08	23.45	70.61	33.33	19.00
9	3.00	0.55	3.11	19.51	0.58	3.61	9.57	3.85	2.20
10	2.24	0.41	2.39	22.41	0.76	2.89	7.36	2.90	1.65
11	8.07	1.47	7.95	51.39	0.23	8.45	24.47	10.61	6.05
12	5.35	0.97	5.35	14.39	0.34	5.85	16.47	6.92	3.95
13	4.05	0.74	4.11	10.52	0.44	4.61	12.66	5.21	2.97
14	23.38	4.25	22.57	318.73	0.08	23.07	69.44	32.73	18.66
15	19.69	3.58	19.04	134.02	0.09	19.54	58.59	27.25	15.53
16	4.46	0.81	4.51	13.83	0.40	5.01	13.87	5.75	3.28
17	21.38	3.89	20.66	265.86	0.09	21.16	63.58	29.76	16.97
18	3.99	0.73	4.06	6.19	0.45	4.56	12.48	5.13	2.92
19	3.56	0.65	3.64	11.87	0.50	4.14	11.21	4.57	2.60
20	10.37	1.89	10.15	63.36	0.18	10.65	31.22	13.81	7.87
21	2.10	0.38	2.26	5.97	0.80	2.76	6.95	2.72	1.55
22	6.73	1.22	6.68	15.89	0.27	7.18	20.54	8.78	5.01
23	2.93	0.53	3.05	6.31	0.59	3.55	9.38	3.77	2.15
24	4.56	0.83	4.60	7.16	0.39	5.10	14.15	5.87	3.35
25	6.75	1.23	6.69	24.83	0.27	7.19	20.59	8.81	5.02
26	5.88	1.07	5.86	35.14	0.31	6.36	18.04	7.63	4.35
27	7.50	1.36	7.41	24.39	0.24	7.91	22.79	9.83	5.60
28	14.62	2.66	14.20	199.08	0.13	14.70	43.70	19.85	11.32
29	15.04	2.73	14.60	194.77	0.12	15.10	44.93	20.46	11.66
30	2.68	0.49	2.81	3.62	0.64	3.31	8.66	3.45	1.97
31	10.90	1.98	10.66	80.64	0.17	11.16	32.79	14.56	8.30
32	1.68	0.31	1.85	3.84	0.97	2.35	5.70	2.20	1.25
33	5.60	1.02	5.59	10.22	0.32	6.09	17.21	7.26	4.14
34	10.64	1.93	10.41	97.95	0.17	10.91	32.02	14.19	8.09
35	21.28	3.87	20.56	379.98	0.09	21.06	63.28	29.61	16.88
36	5.04	0.92	5.06	21.21	0.36	5.56	15.58	6.52	3.71

Table 2.8 Estimated parameters for the development of SCS method for catchments of Kerala

Catchmen t ID	t_c (h)	t_l (h)	t_p (h)	Q_p (m^3/s)
1	15.98	9.59	10.09	84.90
2	42.13	25.28	25.78	100.15
3	15.70	9.42	9.92	270.59
4	17.71	10.63	11.13	115.12
5	33.99	20.39	20.89	166.92
6	26.85	16.11	16.61	380.28
7	45.83	27.50	28.00	474.10

2.6. DEVELOPMENT OF SYNTHETIC UNIT HYDROGRAPHS

The SUH ordinates are obtained for all the traditional, probability distribution functions based SUH and conceptual SUH methods from the respective estimated parameters. The development of SUHs with the measured data to review the methodology adopted by CWC and for ungauged catchments along Karnataka and Kerala coastline is explained in subsequent sections.

2.6.1. Development of SUHs for measured data

Thirteen catchments in Konkan and Malabar Coastal region (CWC, 1992), India are considered to review the methodology adopted by CWC with other SUH methods considered in the study. The procedure described by CWC for Ministry of Transport (MOT) bridge site No.9 with geographical location $75^{\circ}34'40''E$ and $11^{\circ}52'25''$ (CWC 1992, page 1, Illustrative example) is used to demonstrate the CWC-SUH method. The catchment has moderately sloped topography and oblong shape.

Table 2.9 Estimated parameters for the development of SCS method for catchments of Karnataka

Catchment ID	t_c (h)	t_l (h)	t_p (h)	Q_p (m^3/s)
8	30.32	18.19	18.69	564.66
9	1.95	1.17	1.67	41.88
10	1.04	0.63	1.13	54.77
11	6.71	4.03	4.53	103.98
12	3.44	2.06	2.56	34.65
13	3.67	2.20	2.70	18.45
14	27.92	16.75	17.25	480.22
15	19.60	11.76	12.26	239.82
16	3.14	1.88	2.38	30.13
17	20.23	12.14	12.64	500.77
18	2.27	1.36	1.86	15.56
19	1.81	1.08	1.58	31.45
20	8.71	5.23	5.73	129.29
21	1.04	0.62	1.12	13.85
22	4.56	2.74	3.24	37.76
23	1.86	1.11	1.61	13.73
24	2.14	1.28	1.78	21.28
25	3.82	2.29	2.79	68.57
26	6.77	4.06	4.56	52.03
27	8.10	4.86	5.36	38.85
28	12.10	7.26	7.76	419.63
29	24.92	14.95	15.45	212.03
30	1.55	0.93	1.43	8.21
31	20.42	12.25	12.75	77.61
32	1.05	0.63	1.13	7.26
33	6.25	3.75	4.25	15.50
34	15.24	9.15	9.65	121.72
35	32.16	19.29	19.79	454.74
36	3.46	2.08	2.58	48.02

To derive the SUH from the basin characteristics, the following parameters are used: catchment area (A), length of the main-stream (L), length of longest stream from centre of gravity of the catchment to the point of study (L_c), and equivalent stream slope (S), the equations recommended by CWC i.e. Eqs.2.3 to 2.11.

Physiographical parameters considered are, $A = 176 \text{ km}^2$, $L = 38.48 \text{ km}$, $L_C = 20.29 \text{ km}$, and $S = 4.21 \text{ m/km}$ (Table A2.3). The parameters estimated for SUH derivation of one hour duration are $q_p = 0.353 \text{ cumecs/ sq km}$, $t_p = 4.8 \text{ h}$, the widths of the UH at $0.5Q_p$ and $0.75Q_p$ are $W_{50} = 5.98 \text{ h}$ and $W_{75} = 3.02 \text{ h}$ for recession limb and $W_{R50} = 1.83 \text{ h}$ and $W_{R75} = 1.04 \text{ h}$ for rising limb, base width $T_B = 22 \text{ h}$, time from start of rise to peak $T_m = 5 \text{ h}$, and peak discharge $Q_p = 62.20 \text{ cumecs}$ (Table A2.4). For other SUH methods considered in the study, the descriptions are: (a) For non-dimensional CWC method, the parameter estimation is similar as that of CWC-SUH; (b) For Snyder method, $C_p = 0.65$ and $C_t = 1.8$ are used. Computations of C_t and C_p for a measured data (i.e., 13 CWC catchments) have been done using standard unit hydrograph basin lag and discharge equations (Ramirez, 2000). The same constants have been used since the ungauged catchments in the present study appear in the similar regions of gauged catchments.

The parameters of the Snyder method computed for SUH derivation are $t_p = 10.25 \text{ h}$, $q_p = 0.19 \text{ cumecs/sq km}$, the width of UH at $0.5Q_p$ and $0.75Q_p$ are $W_{50} = 13.23 \text{ h}$ and $W_{75} = 7.54 \text{ h}$, respectively; (c) For the SCS method, time to peak (t_p) = 16.32 h and peak discharge (Q_p) = 22.43 m^3/s ; (d) For Gary's method, the time from starting of surface runoff to the peak discharge (P_R) = 395.23 min, dimensionless parameter (γ') = 2.82 and shape parameter (q) = 3.82. (e) For Croley method, the point of inflection (t_i) = 7.52 h, peak discharge (Q_p) = 62.33 m^3/s and the constants $\alpha = 3.23$ and $\beta = 2.02$. (f) For transmutation approach, the values of t_p and Q_p are taken from CWC SUH method. (g) For two-parameter gamma distribution, the computed parameters are $\beta = q_p t_p = 0.61$ and $n = 3.51$. For determining q_p and t_p in two-parameter gamma method, CWC-SUH (1992) method is used; (h) For the Hybrid model, the parameters β and n are similar to Two Parameter Gamma Distribution method.

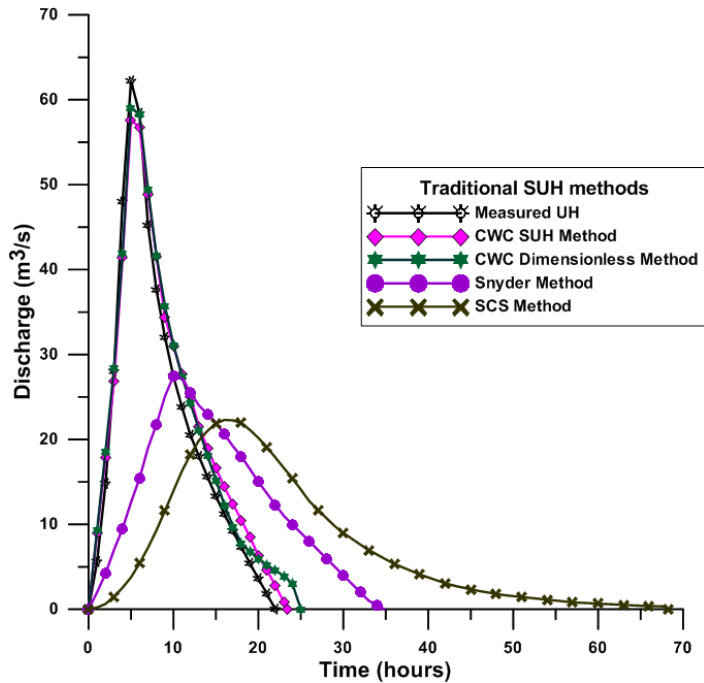


Figure 2.13(a) Synthetic Unit Hydrograph of 1-hour duration using traditional SUH methods and along with the measured UH at Bridge site No.9

The Croley method (1980), Transmutation approach (Singh 2000), simplified two-parameter Gamma distribution (Bhunya et al. 2003) and Hybrid Model (Bhunya et al. 2005) almost completely match in terms of peak discharge ordinate ($60.99\text{m}^3/\text{s}$, $60.92\text{m}^3/\text{s}$, $61.34\text{m}^3/\text{s}$ and $62.62\text{m}^3/\text{s}$ respectively), time to peak (5h for all four methods) at basin outlet with the observed Unit Hydrograph ($62.2\text{m}^3/\text{s}$ and 5h). The complete match is because of the parameters peak discharge per unit area (q_p) and time to peak (t_p) values used in Croley method, Transmutation approach and simplified two Parameter Gamma Distribution (2PGD) method and Hybrid model are taken from the SUH derived from the CWC-SUH method. However, the Gray method overestimated both in terms of the peak discharge ($78.67\text{m}^3/\text{s}$) and time to peak (7h) (Figure 2.13(b)). This might be because of the empirical relationships (Eqs. 2.21 to 2.23) are catchment size specific and should be used within the range of areas for which these are developed (Gray 1961 and SCS 1957).

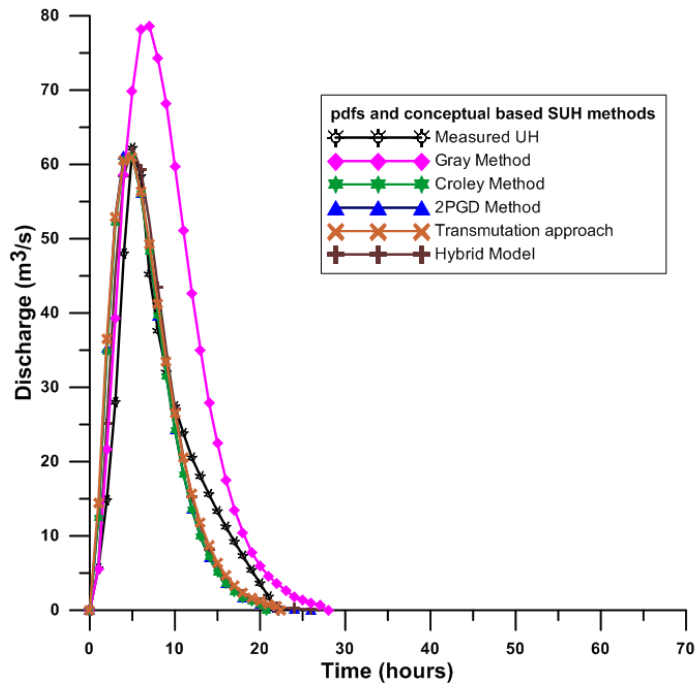


Figure 2.13(b) Synthetic Unit Hydrograph of 1-hour duration using pdfs and conceptual based SUH methods and along with the measured UH at Bridge site No.9

Figure 2.13(a) shows that the results of CWC-SUH ($t_p = 5$ h, $Q_P = 57.61$ m³/s) is slightly underestimated the peak discharge and Dimensionless CWC ($t_p = 5$ h, $Q_P = 59.88$ m³/s) is in close agreement with the measured data ($t_p = 5$ h and $Q_P = 62.20$ m³/s) in terms of peak discharge ordinate. The ascending limbs of CWC SHU, CWC dimensionless and measured data match well whereas the falling limb in both the CWC methods overestimated than CWC measured data (Figure 2.13(a)). Hence manual adjustments are required for falling limb for both CWC methods to get the area under the UH as unity. The SCS method (22.30 m³/s) and Snyder method (27.47 m³/s) appreciably underestimate the peak discharge ordinates compared to other methods used in the study and also rising, and recession limbs are underestimated and overestimated considerably in comparison with the CWC SUH, and non-dimensional CWC methods respectively. This trend is continued for all 13 catchments when SUH derived from Snyder and SCS methods. However, it is practically found that the Grey method overestimated the flood discharge values and time to peak values whereas Snyder and SCS methods underestimated the discharge values and time to

peak for measured data. The feasibility of the above three methods for the estimated data at the ungauged catchments is checked to assess the accuracy of these estimated values along with the other SUH methods.

2.6.2. Development of SUHs at ungauged catchments

Among all the ungauged catchments, the Mahe catchment (Catchment ID 1) has been taken as a representative of all and explained in detail below. The comparative analysis of CWC-SUH method with the other methods in the present study has been discussed using the plotted SUH at catchment ID 1 (Figure 2.14(a)).

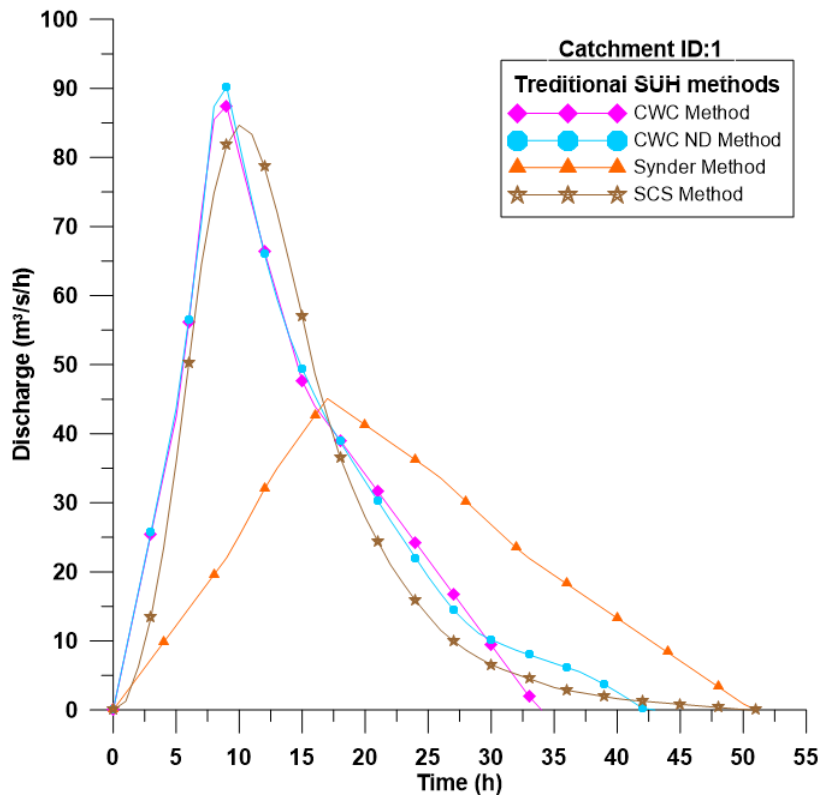


Figure 2.14(a) SUH of 1-hour duration during using Traditional SUH methods at Mahe catchment (Catchments ID-1)

The representative catchment have the physiographic parameters as $A = 411.81$ sq km, $L = 57.23$ km, $L_C = 14.73$ km and $S = 2.13$ m/km (Table 2.2) and the corresponding unit hydrograph parameter are $q_p = 0.22$ cumecs/ sq km, $t_p = 7.94$ h, the widths of the UH measured at 50% and 75% of maximum discharge (Q_p) ordinates are $W_{50} = 9.92$ h and $W_{75} = 4.9$ h for recession limb and $W_{R50} = 3.06$ h and $W_{R75} = 1.69$ h for rising limb, base width $T_B = 33.80$ h, time from start of rise to peak $T_m = 8.44$ h, and peak discharge $Q_p = 91.46$ m³/s (Table 2.4).

Comparison between CWC-SHU vs. CWC Dimensionless methods: the CWC dimensionless method also used the same unit hydrograph parameters for SUH derivation. The hydrograph from the CWC-SUH method completely matched both regarding time to peak (9h), and peak discharge ordinates, i.e., 87.49 m³/s for CWC-SUH and 90.21m³/s for CWC dimensionless SUH. This is because of the same input parameters for both SUH derivations.

Comparison between CWC-SUH vs. Snyder methods: The non-dimensional constants, $C_p = 0.65$ and $C_t = 1.8$ are respectively used in the computations. The computed parameters of Snyder method for derivation of SUH are $q_p = 0.11$ cumecs/sq km, $t_p = 16.48$ h, the width of UH at $0.5Q_p$ and $0.75Q_p$ are $W_{50} = 23.32$ h and $W_{75} = 13.29$ h, respectively (Table 2.6). The Snyder method remarkably underestimates the peak discharge value (45.09 m³/s) nearly about 50% (Figure 2.14(a)). The reason could be non-dimensional constants (C_p and C_t values) and also the minimum time base of Snyder's method is always greater than three days, which is reasonable for large catchments only.

Comparison between CWC-SUH vs. SCS methods: the computed parameters t_p , and Q_p are 10.09 h and 84.90m³/s respectively (Figure 2.14(a)). The lag time is estimated from catchment characteristics using Curve Number (CN) procedure. The derived flood hydrograph is given in Figure 2.14(a), and as observed from results, the SCS method slightly underestimated the peak discharge (84.69 m³/s), the rising and falling limbs of the hydrograph do not completely match with CWC methods. The reason could be the curve

number method which is applied for the determination of lag time applies to the catchments of the area ranging from 8 to 16 km², and its application to medium and large catchments may lead to erroneous results (Bhunya et al., 2011).

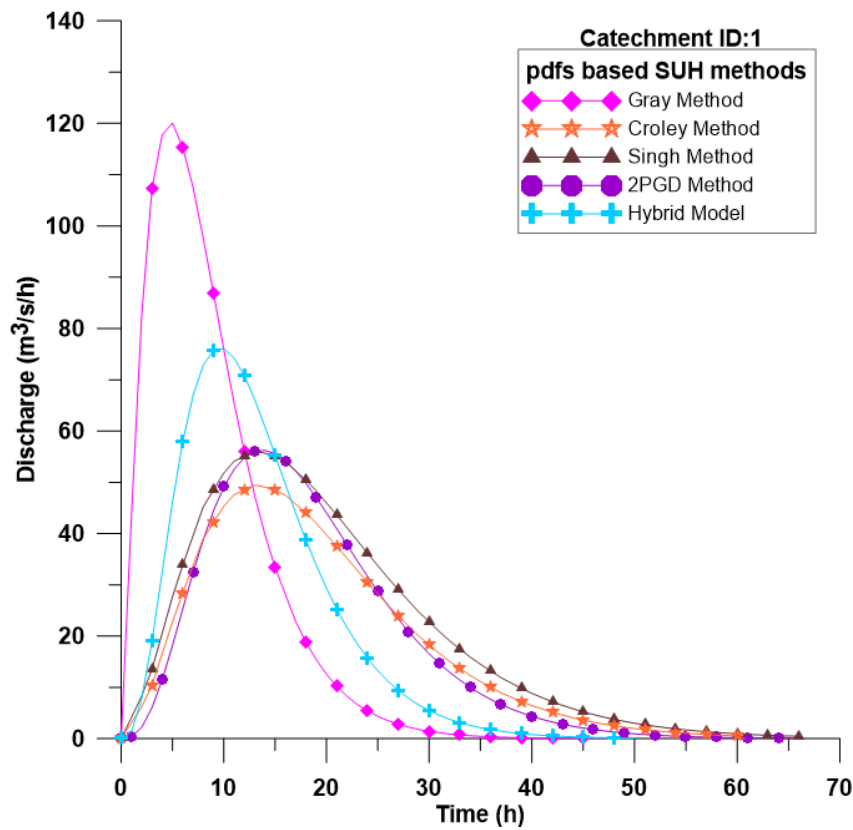


Figure 2.14(b) SUH of 1-hour duration during using pdfs and conceptual based SUH methods at Mahe catchment (Catchments ID-1)

Comparison between CWC-SUH vs.Gray method: this method uses a length of the main stream, main stream channel slope in percentage and area of the catchment in deriving the UH. The estimated parameters are the time from starting of surface runoff to the peak discharge (P_R) is 223.51 min, the dimensionless parameter (γ^1) is 1.27 and shape parameter (q) is 2.27. The peak discharge ordinate and time to peak for Gray’s method are 120.06

m³/s and 5h respectively (Figure 2.14(b)). The peak discharge ordinate is overestimated approximately by 37% and the time to peak is underestimated by 2.94hours.

Comparison between CWC-SUH vs.Croley method: parameter estimation was done using Snyder's method, and the values are $t_i = 22.07$ h and the constants $\alpha = 3.23$ and $\beta = 5.93$. The peak discharge ordinate and time to peak for Croley method are 49.45 m³/s and 13h respectively (Figure 2.14(b)). The peak discharge ordinate is underestimated and time to peak is overestimated when compared to CWC-SUH method.

Comparison between CWC-SUH vs.Transmutation approach: here also parameter estimation was done using Snyder's method. The peak discharge ordinate and time to peak for Croley method are 56.05 m³/s and 13h respectively (Figure 2.14(b)). Similar to Croley method, the peak discharge ordinate is underestimated and time to peak is overestimated when compared to CWC-SUH method.

Comparison between CWC-SUH vs.two-parameter Gamma distribution method: the computed parameters are $\beta = q_p t_p = 0.675$ and $n = 4.03$. The estimated parameters (i.e., t_p and q_p) are taken from Snyder's method. The derived SUH is given in Figure 2.14(b). The peak discharge ordinates for the 2PGD method is 56.22 m³/s whereas for CWC-SUH is 87.49m³/s because the q_p and t_p values used in the 2PGD method are taken from the Snyder's method.

Comparison between CWC-SUH vs. Hybrid model: the parameters required for SUH derivation are taken from the Snyder's method (i.e., $q_p = \frac{Q_p}{A} = \frac{74.55 \times 100 \times 3600}{411.81 \times 10^6} = 0.07$ cm/h/cm, $t_p = 10.48$ h and $\beta = 0.68$). The peak discharge ordinate value (Q_p) and time to peak in the Hybrid model are 76.08 m³/s and 10h respectively (Figure 2.14(b)).

This trend continued at all the seven catchments along Kerala coastline as seen in Figures A2.2&A2.3 and Figures A2.8&A2.9 and for 29 catchments along Karnataka coastline as

seen in Figure A2.2 to Figure A2.8 and Figure A2.9 to Figure A2.13, since the catchments considered in the study subjected to same hydrometeorological regions as per CWC.

2.7. COMPARISON OF TOTAL FLOOD DISCHARGES AT UNGAUGED CATCHMENTS

After estimated parameters of unit hydrograph are plotted as a graph using Grapher 8, the plotted points are joined to draw synthetic unit hydrograph at every catchment. The discharge ordinates (Q_i) of the unit hydrograph at $t_i = 1h$ interval are summed up to get total discharge values at each catchment. Comparison of total discharge values for the CWC measured data and at ungauged catchments along Karnataka and Kerala coastline are given below.

2.7.1. Comparison of flood discharges for the CWC measured data

The traditional SUH, probability distribution functions based SUH and conceptual based SUH methods considered in the study are compared with the CWC measured data at 13 catchments in Konkan and Malabar coastal region. The comparison is based on the total discharge values at the basin outlet. The MOT Bridge site No.9 has been taken as a representative catchment to analyse the results obtained by various synthetic unit hydrograph methods (Table 2.10 and Figures 2.13(a) and 2.13(b)). The methods considered for reviewing the methodology adopted by CWC shows relatively slight overestimated (i.e., 8.17% by CWC-SUH, 11% by CWC dimensionless) whereas Snyder method underestimated total discharge values ($m^3/s/h$) by 4.47% and SCS method gave almost same discharge compared to CWC measured data (Table 2.10).

The Gray method is overestimating the total discharge value by 64.40%, which could be because of the shape and size of the catchment. The Croley method is also overestimating by 4.33% at MOT Bridge site No.9, but at most of the remaining catchments it is matched

with CWC measured data with not more than 5% overestimated values. The Transmutation approach, 2PGD and Hybrid model gave exactly same discharge as that of measured data (Table 2.10) at almost all catchments. In addition to that, these three methods are satisfied the UH criterion (i.e. area under the UH is unity). At all the catchments it is observed that the Gray method is overestimating with abrupt changes in the discharge values (Table 2.10). The remaining methods have less than 10% difference betweenwith the measured data, and hence all the methods mentioned above are used to estimate the flood discharge at seven catchments along Kerala coastline and twenty nine ungauged catchments along Karnataka coastline.

2.7.2. Comparison of flood discharges at ungauged catchments along Kerala coastline

The ungauged catchment with Catchment ID 1 (i.e., Inlet ID 1) having geographical location 75°31'51" and 11°42'14" has been taken as a representative catchment to analyse the results obtained by various synthetic unit hydrograph methods (Table 2.11 and Table 2.12). Since there is no measured data, the total flood discharge values are compared with the volume of 1cm depth of runoff. The volume of 1cm runoff depth is given as $Q = \frac{A*d}{0.36t_r}$ where A is catchment area in sq km, d is 1cm depth and $t_i = t_r$ is the unit duration of the UH (=1h). The methods considered for the estimation of total discharge (m³/s/h) at ungauged catchments shows moderately overestimated values (i.e., 12.94% by CWC-SUH, 17% by CWC dimensionless, 3% by Snyder method and 6.9% by SCS method). These overestimated values are because of the manual adjustments have not been done the rising and falling limbs of UHs.

The Gray method overestimated at few catchments and underestimated at few catchments based on catchment area range, slope variation along the catchments and also variations in length of the main channel. The Croley method, 2PGD and Hybrid model gave almost similar relative discharge values as that of the volume of 1cm runoff depth at all catchments (Table 2.11& Table 2.12). In addition to that, these three methods are satisfied the UH

criterion (i.e., area under the UH is unity). At the ungauged catchments, the transmutation approach (Singh 2000) is overestimating the total discharge values appreciably. The same trend is continued at the remaining six catchments along Kerala coastline and 29 ungauged catchments along Karnataka coastline. Among all the adopted methods simplified two-parameter gamma distribution method proposed by Bhunya et al. 2003 gave the very close agreement with total discharge values at all the ungauged catchments (i.e., tidal inlets) and also satisfied the necessary criteria of unit hydrograph (area under UH is unity).

2.8. SUMMARY

Based on the results obtained, it could be observed that the UHs generated through SUH methods have been found useful and effective at the ungauged catchments along Konkan and Malabar coasts. The statistical evaluation of the UH ordinates obtained from the traditional, probabilistic and conceptual methods indicated that there were considerable differences in these methods except for two-parameter Gamma distribution method and Hybrid model, which have relatively close values both regarding peak discharge and time to peak. Even though the CWC, Snyder and SCS methods are used widely in practical engineering problems, the manual fitting of Unit Hydrograph with limited characteristics points needs a high degree of subjectivity and trial and error. Alternatively, the pdfs based SUH methods used in the study gives the complete shape of unit hydrograph and also satisfies the prerequisite for UH criterion, i.e., area under the UH is unity. Further, the results showed that the two-parameter Gamma distribution method and hybrid models perform better on field data as well as in conditions where no observed data are available compared to CWC, Snyder, and SCS methods.

Table 2.10 Comparison of flood discharges for CWC measured data

Inlet ID	Bridge Site No.	Discharge (m ³ /s/h)									
		CWC measured	CWC SUH*	CWC Dimensionless*	Snyder*	SCS	Gray	Croley	Transmutation Approach	2PGDM	Hybrid model
1	104	1079.17	1220.88	1197.24	1039.05	1076.08	1201.32	1613.35	1065.39	1011.83	1211.66
2	MOT-8	908.33	935.74	1010.78	860.80	917.47	2059.57	1051.58	902.77	907.29	905.04
3	273	556.14	727.08	617.44	527.02	561.17	1879.95	1035.51	551.60	556.04	560.04
4	117	525.19	601.59	583.97	495.47	529.62	792.94	765.12	523.01	524.96	545.66
5	MOT-11	491.67	575.28	546.09	465.91	495.96	830.75	525.43	490.14	441.02	493.21
6	MOT-9	488.87	528.85	543.15	467.06	493.17	803.71	510.08	484.90	488.42	487.02
7	MOT-7	172.22	236.13	194.76	161.31	173.98	350.18	147.56	169.22	167.92	177.74
8	260	133.39	164.45	148.86	124.47	134.56	312.04	193.47	132.91	133.33	138.38
9	MOT-6	2744.44	3305.81	3072.17	2672.91	2768.25	3125.06	2712.57	2735.29	2734.04	2788.28
10	MOT-4	1694.44	1679.06	1881.23	1641.43	1709.68	1982.72	2003.20	1680.60	1693.12	1687.58
11	MOT-5	1333.33	1534.72	1487.98	1292.50	1344.67	1590.32	1105.17	1326.90	1323.76	1370.70
12	MOT-2	861.11	657.50	973.82	819.71	869.22	1418.68	360.50	846.11	785.14	840.49
13	MOT-1	719.44	798.31	798.75	687.63	725.72	1252.64	956.86	713.57	719.09	718.73

Note: * Manual adjustments are not made for the discharge values and Bold values represent the representative catchment for which SUH of 1h duration using different methods.

Table 2.11 Comparison of flood discharges at ungauged catchments along Kerala coastline

Inlet ID	Catchment Name	Discharge (m ³ /s/h)									
		Vol. of 1cm direct runoff depth	CWC SUH*	CWC Dimensionless*	Snyder*	SCS	Gray	Croley	Transmutation Approach	2PGDM	Hybrid model
1	Mahe	1083.74	1223.99	1268.18	1116.46	1158.86	1346.34	1137.78	1363.31	1140.08	1139.26
2	iringal	3585.30	3871.49	3975.37	3510.47	3632.14	4154.30	3576.30	4269.79	3580.15	3570.83
3	Elathur	1710.86	1816.21	1899.12	1673.61	1733.76	1935.34	1709.23	2039.05	1708.35	1704.20
4	Thekupuram	8436.03	8862.10	9360.82	8418.40	8546.61	8177.39	8417.64	10051.08	8422.44	8400.32
5	Balathirutti	3448.19	3454.22	3827.07	3437.10	3493.55	3154.87	3432.13	4105.47	3436.35	3433.40
6	Ponnani	17728.17	17918.26	19681.26	17822.20	17960.75	15838.74	17704.19	21122.02	17711.95	17652.32
7	Chettuva	4657.42	4702.58	5171.87	4611.93	4718.86	4458.19	4652.89	5547.55	4651.08	4638.94

Table 2.12 Comparison of flood discharges at ungauged catchments along Karnataka coastline

Inlet ID	Catchment Name	Discharge (m ³ /s/h)									
		Vol. of 1cm direct runoff depth	CWC SUH*	CWC Dimensionless*	Snyder*	SCS	Gray	Croley	Transmutation Approach	2PGDM	Hybrid model
8	Karwar	14095.19	14767.70	15636.79	13933.82	14280.24	13392.28	16788.92	14050.08	14080.45	14035.74
9	Kelaginakeri	93.37	115.54	102.10	85.22	94.55	59.42	110.89	92.77	92.98	94.33
10	KantrivadaGudda	82.42	105.33	87.83	74.65	83.46	24.28	97.88	82.00	79.37	83.71
11	Belekeri	628.72	716.65	694.76	595.70	636.95	1588.57	748.07	626.25	628.02	628.64
12	Ankola	118.54	143.00	132.62	110.84	92.33	365.20	141.16	118.12	118.36	119.15
13	Belamber	66.60	77.79	74.09	61.28	67.49	144.09	79.13	66.15	66.52	66.64
14	Manjaguni	11065.53	11637.31	12281.50	10932.88	11210.73	10601.84	13184.53	11031.94	11053.84	11019.27
15	Tadri(Tadadi Port)	3926.16	4238.49	4353.94	3852.53	3977.70	4069.77	4676.27	3912.59	3921.80	3912.44
16	Alvekodi 2	95.93	115.02	106.83	89.23	97.21	196.77	114.00	95.52	95.77	96.48
17	Honavar(karki)	8450.64	9123.72	9370.91	8319.48	8561.58	8646.96	10066.72	8422.70	8441.24	8421.16
18	Manki(Nakhuda)	38.66	48.14	42.41	35.54	39.20	37.89	45.92	38.42	38.48	39.07
19	Navayatkeri	66.52	86.77	74.97	61.32	67.33	42.69	78.96	66.02	65.89	67.45
20	Alvekodi 1	989.12	1111.28	1095.57	946.65	1002.20	1724.95	1173.34	983.45	987.99	987.59
21	Jali	20.74	26.66	22.49	18.52	21.00	5.52	24.56	20.57	20.23	21.09
22	Mavakurve	163.14	191.62	179.57	153.65	165.23	366.46	194.30	162.44	162.95	163.54
23	Hadin	50.62	64.68	56.17	47.03	51.23	46.81	60.06	50.01	50.27	51.26
24	Gorta	29.59	36.43	32.29	26.92	29.96	16.66	35.07	29.38	29.48	29.87
25	Alvegadde	255.65	306.68	284.61	240.79	259.00	1688.60	304.11	254.52	255.29	256.84
26	Paduvari	316.90	355.67	350.95	296.54	321.01	1029.13	377.05	315.46	316.54	316.37
27	Koderi	277.94	309.13	308.66	263.16	281.60	601.43	329.30	275.43	277.62	277.32
28	Gangoli	4349.29	4837.77	4828.57	4218.47	4406.58	5546.10	5180.21	4333.56	4344.34	4339.88
29	Kundapura	15.68	20.34	17.59	14.19	15.92	7.23	18.60	15.55	15.54	15.89
30	Badanidiyoor	4375.26	4502.47	4857.77	4249.32	4432.71	4505.72	5209.79	4359.72	4370.94	4356.05
31	Malpe	1321.82	1364.54	1466.62	1267.98	1339.18	1484.83	1573.78	1316.48	1320.51	1316.12
32	Kaup	10.95	14.03	12.04	9.77	11.08	2.82	12.94	10.82	10.76	11.13
33	Nadsal	87.94	98.73	97.40	82.36	89.09	426.48	104.42	87.52	87.84	87.80
34	Hejamadi	1567.93	1662.61	1739.92	1502.75	1588.55	1960.76	1866.74	1562.16	1566.25	1561.57
35	Gurpur&Netravathi	12020.87	12390.72	13337.54	11833.04	12178.62	11364.76	14318.44	11979.68	12008.95	11968.96
36	Kanwatheertha	165.22	198.29	184.20	153.77	167.38	571.78	196.63	164.47	164.95	166.14

Since the measured data is not available for the catchments under study, the catchments with the measured data provided by Central Water Commission (CWC 1992) has been reviewed using the conventional SUH, probabilistic SUH, and conceptual SUH methods. Based on the obtained results, it is decided to use all SUH methods for the estimation of flood discharge at ungauged catchments. Adopting various methods available in the literature, and validating them with available measurements, unreported discharge estimates along the Karnataka Coast hitherto are provided in this study.

The computed flood discharges could be used as prime input parameter to determine the type of dominance (i.e., wave-dominated, tide-dominated or river dominated) along the coastal tidal inlets, which seldom are available along the Indian coastline.

CHAPTER-3

CLASSIFICATION OF TIDAL INLETS

3.1. INTRODUCTION

Tidal entrances or tidal inlets constitute a crucial dynamic boundary condition concerning the coastal regime due to their role as interfaces for exchange between seawater and embayed water. Tidal inlets provide the access between the ocean and the bay, by both nature and human interventions. The major functions of atidal inlet are natural flushing in the form of a flow of currents into and out of the bay through an inlet there by maintaining good water quality, migration of fish, fish larvae, and other sea life through the inlet channel. The closure of tidal inlets could lead to flooding of the upstream regions, in case of excess drainage from the watershed region. The closing of inlets would also mean less discharge of sediments into the coastal area, which may significantly influence the coastal sediment transport. On the other hand, excessive alongshore sediment transport could result in sediment deposition at the inlet mouths and lead to inlet closure.

Generalized morphodynamic relationships applicable to the entrances serve as useful tools for characterizing the physical state and the dynamic behavior of tidal inlets. Classification of inlets provides a means of understanding the nature of the inlets whether they are dominated by the wave action or tidal forcing or river discharge. Such classification offers coastal planners and stakeholders for planning and optimally using as well as takes

appropriate measures. Many tidal inlets indent the mainland coast of India, and no comprehensive information exists on the details of these inlets morphology or their dynamics. This chapter deals with the classification of a majority of tidal inlets along the mainland coast of India based on tidal range, wave exposure conditions, geomorphologic, hydrodynamic and non-dimensional criteria both with and without considering the wave periods.

Classification of tidal inlets has been carried out extensively along the USA and Australia coasts (e.g., Barton et al., 2007; Burgess et al., 2004; Duck and da Silva, 2012; Hale and Butcher, 2008; Heap et al., 2001; Isla, 1995; Kjerfve, 1994; Roy et al., 2001). Burgess et al. (2004) used over different methods to cover a vast range of coastal systems in the USA. The classifications of USA coasts by Kjerfve (1994) & Isla (1995) were based on the isolation level of coastal lagoons restricted by the coastal barrier wherein each type presents its hydro-morphological conditions and geomorphological features. Barton et al. (2007) reviewed the classification of inlets along New South Wales (NSW) coast in Australia. Hale and Bucher (2008) classified inlets mostly based on geomorphology, salinity, and hydrology. Duck and Silva (2012) reviewed the classification of coastal lagoons with an emphasis on hydro-morphology for inlets along the coast of Australia. Roy et al. (2001) included biological criteria to classify estuaries within NSW, Australia. Heap et al. (2001) proposed another method using the ratio of wave power to tide power at the entrance of the inlet and classified 780 coastal systems around the coast of Australia. The different way of classification based on biodiversity, functioning, resource exploitation, conservation, and sustainability exists in the literature (e.g., da Silva et al., 2002; Dadouh-Guebas et al., 2005;

Danovaro and Pusceddu, 2007; Iwasaki and Shaw, 2008; Perez-Ruzafa et al., 2011). Although many methods are available to classify the tidal inlets, no comprehensive information is available for the classification of tidal inlets along the coast of India. This study focuses on the classification of 471 tidal inlets along the coast of India in terms of morphology, hydrodynamics and non-dimensional parameterization of the wave, tide, and river discharge forces. The other parameters like salinity, biodiversity, functioning, resource exploitation, conservation, sustainability, are not considered in the classification of tidal inlets in this chapter.

3.2. STUDY AREA

The study area considered is the mainland coast of India, excluding the Islands, Sundarbans region, and the Gulf of Kachchh and Khambhat. The coastline of India comprises of headlands, promontories, rocky shores, sandy spits, barrier beaches, open beaches, embayment, estuaries, inlets, bays, marshy land and offshore islands (Chandramohan et al., 2001). India has a considerable variation in climate from region to region and experiences weather in different places at different times of a year. It is dominated by three seasons, viz. southwest monsoon (June to September), northeast monsoon (October to January) and fair weather season (February to May). The Indian mainland comprises nearly 43% sandy beaches, 11% rocky coast with cliffs and 46% mud flats and marshy coast (Jayappa and Deepika, 2018). The western part of the coastline experiences high wave activity during the southwest monsoon with relatively calm sea conditions during rest of the year. On the east coast, wave activity is significant during both the southwest and the northeast

monsoons. Extreme wave conditions occur under severe tropical cyclones, which are frequent in the Bay of Bengal during the northeast monsoon period (Singh et al., 2000). Along the west coast, waves approach from west and west-southwest during southwest monsoon; west, and west-northwest during northeast monsoon and predominantly from the southwest during fair weather period. Along the east coast, waves approach from the southeast during southwest monsoon as well as post-monsoon (fair-weather) period and from the northeast during the northeast monsoon.

A total of 471 inlets having an inlet width greater than or equal to 5m at the confluence are identified in the nine coastal states of Gujarat, Maharashtra, Goa, Karnataka, Kerala, Tamil Nadu, Andhra Pradesh, Odisha and West Bengal, using Google Earth[®]. There are 219 inlets along the west coast and 252 inlets along the east coast (Figure 3.1). The closest place names provided on Google Earth[®] are given for the inlets. The inlets are numbered sequentially starting from Gujarat state on the west coast of India (i.e., Arabian Sea Side) to West Bengal in the east coast of India (i.e., Bay of Bengal side). Most of the coastal inlets considered in each of the nine coastal states are shown in Figure 3.2(a) to 3.2(i). The geographical locations, the names of inlets for all nine coastal states are given in Table A3.2.



Figure 3.1 Locations of Inlets considered in the study area

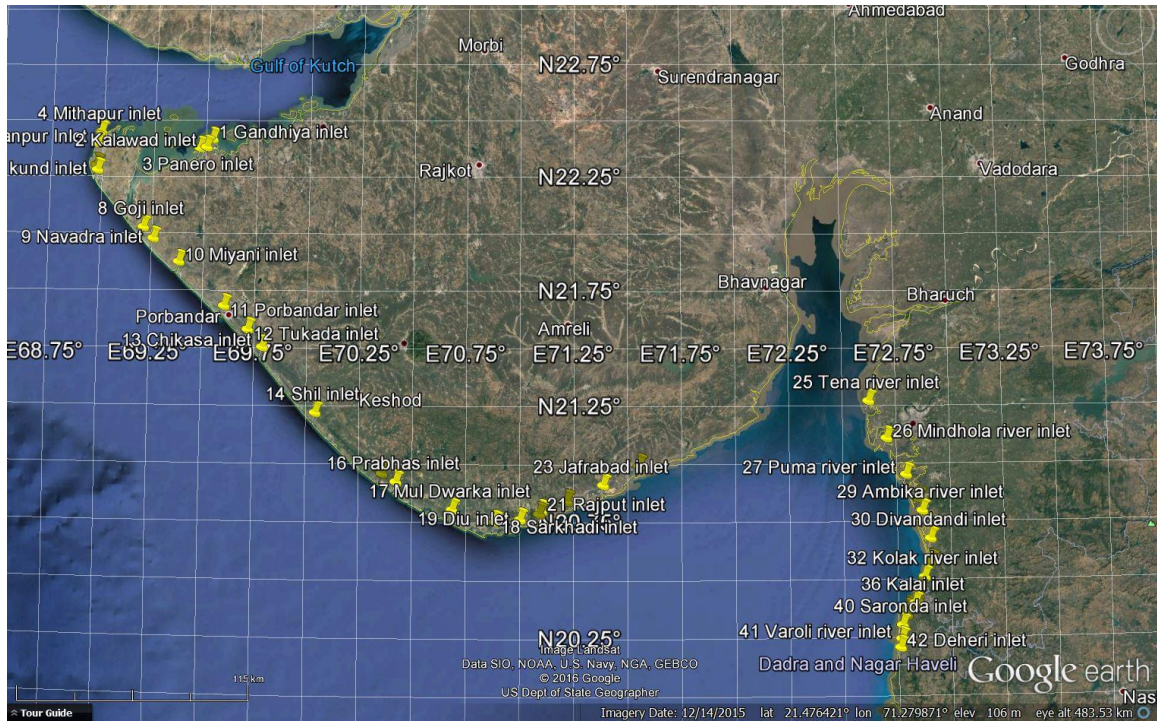


Figure 3.2(a) Inlets considered along the coast of Gujarat (42 inlets)

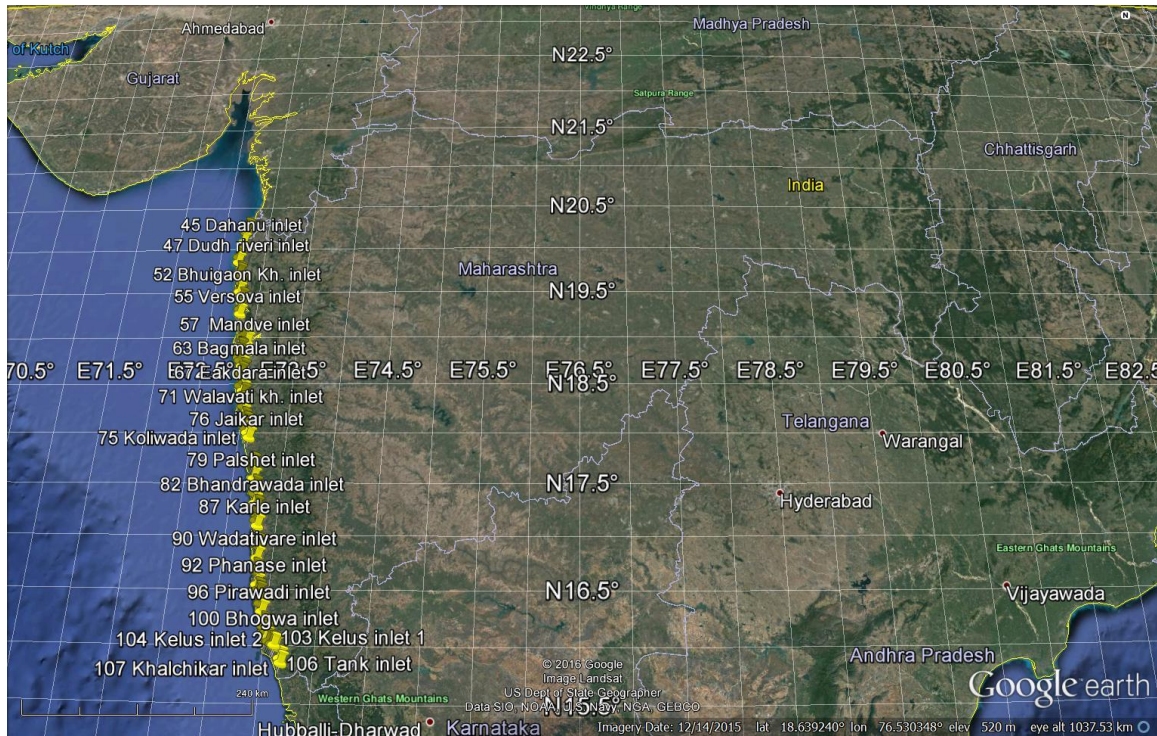


Figure 3.2(b) Inlets considered along the coasts of Maharashtra (65 inlets)

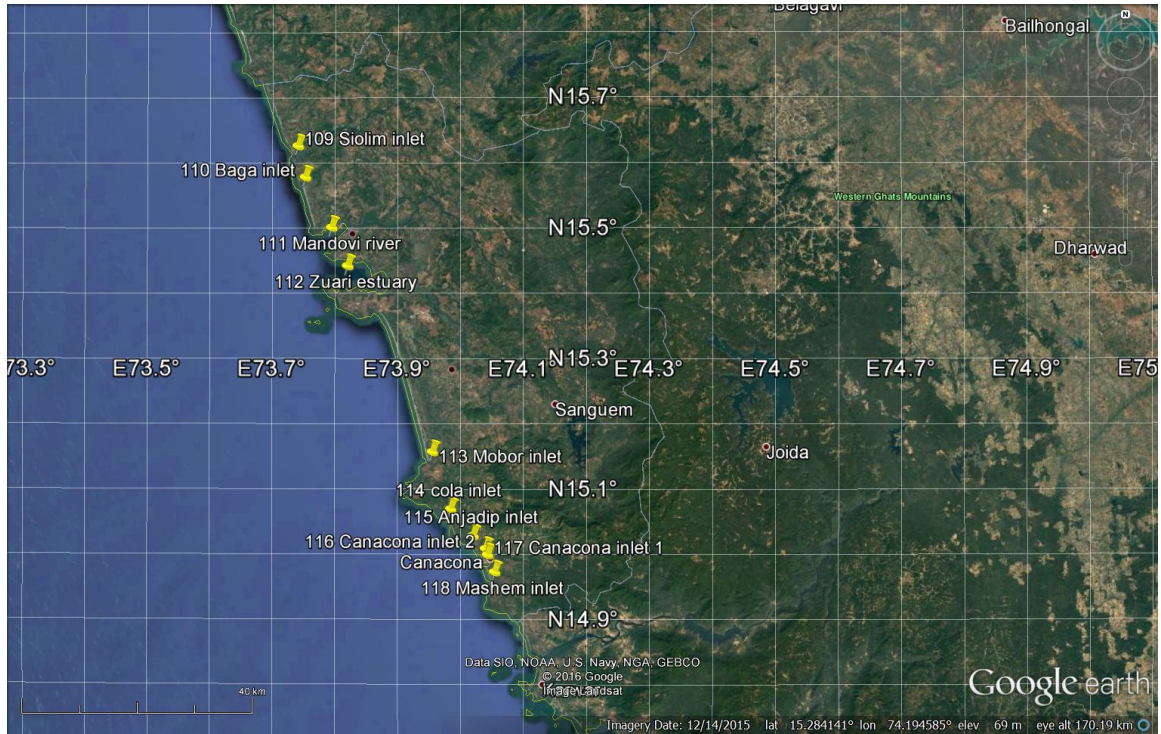


Figure 3.2(c) Inlets considered along the coast of Goa (11 inlets)

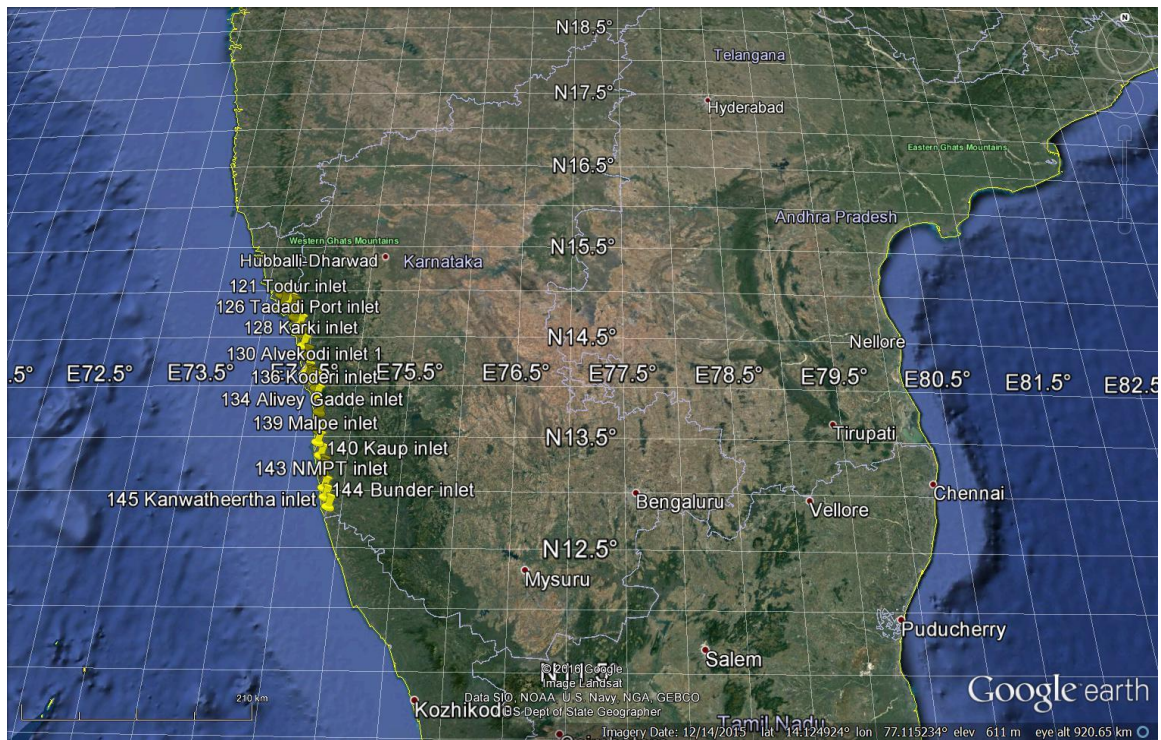


Figure 3.2(d) Inlets considered along the coast of Karnataka (27 inlets)



Figure 3.2(e) Inlets considered along the coast of Kerala (68 inlets)



Figure 3.2(f) Inlets considered along the coast of Tamil Nadu (121 inlets)

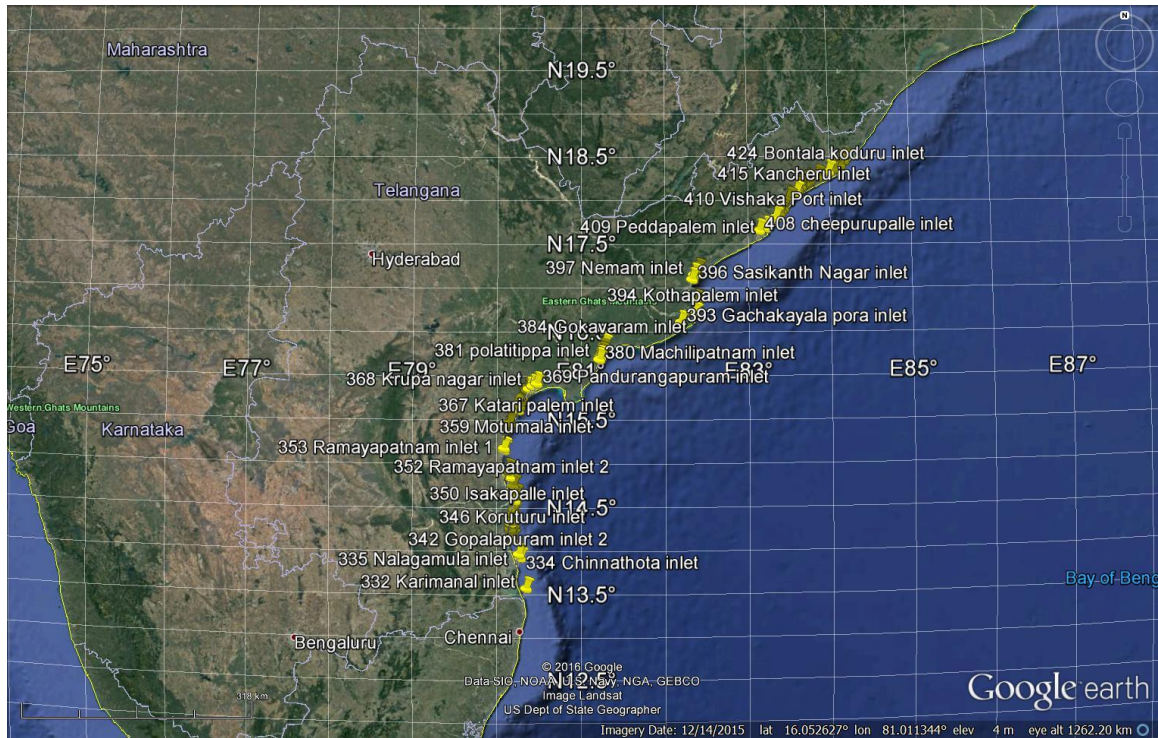


Figure 3.2(g) Inlets considered along the coast of Andhra Pradesh (106 inlets)

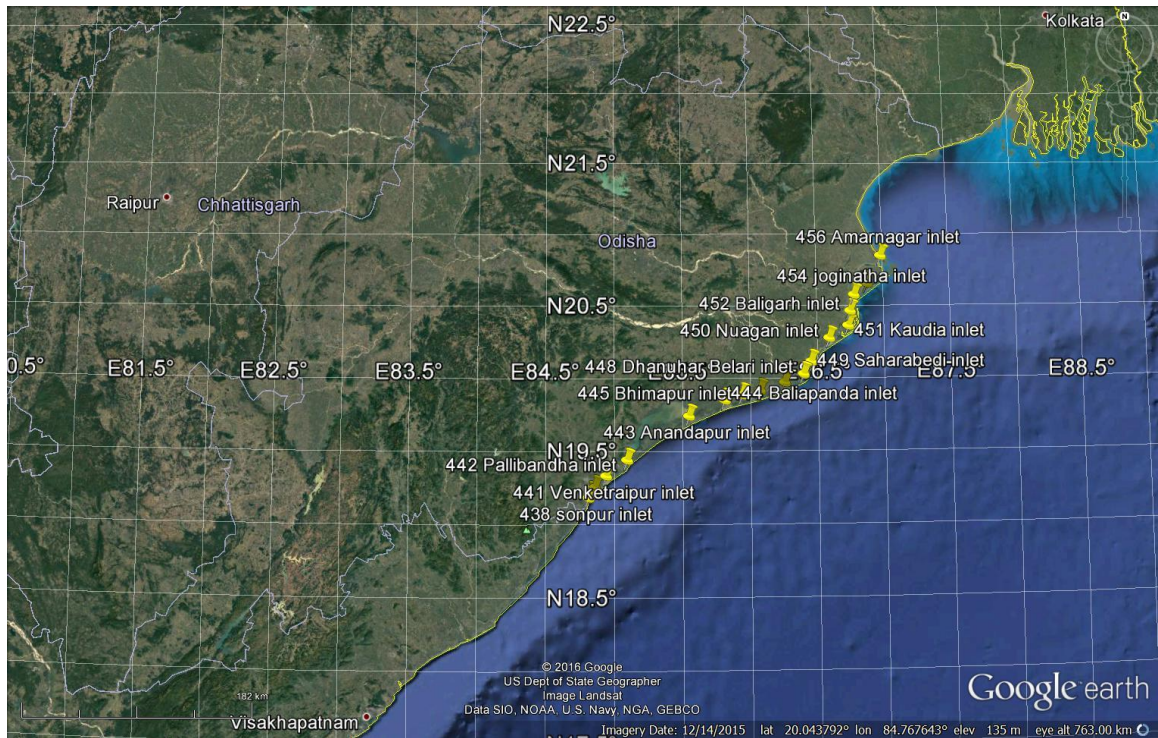


Figure 3.2(h) Inlets considered along the coast of Odisha (23 inlets)

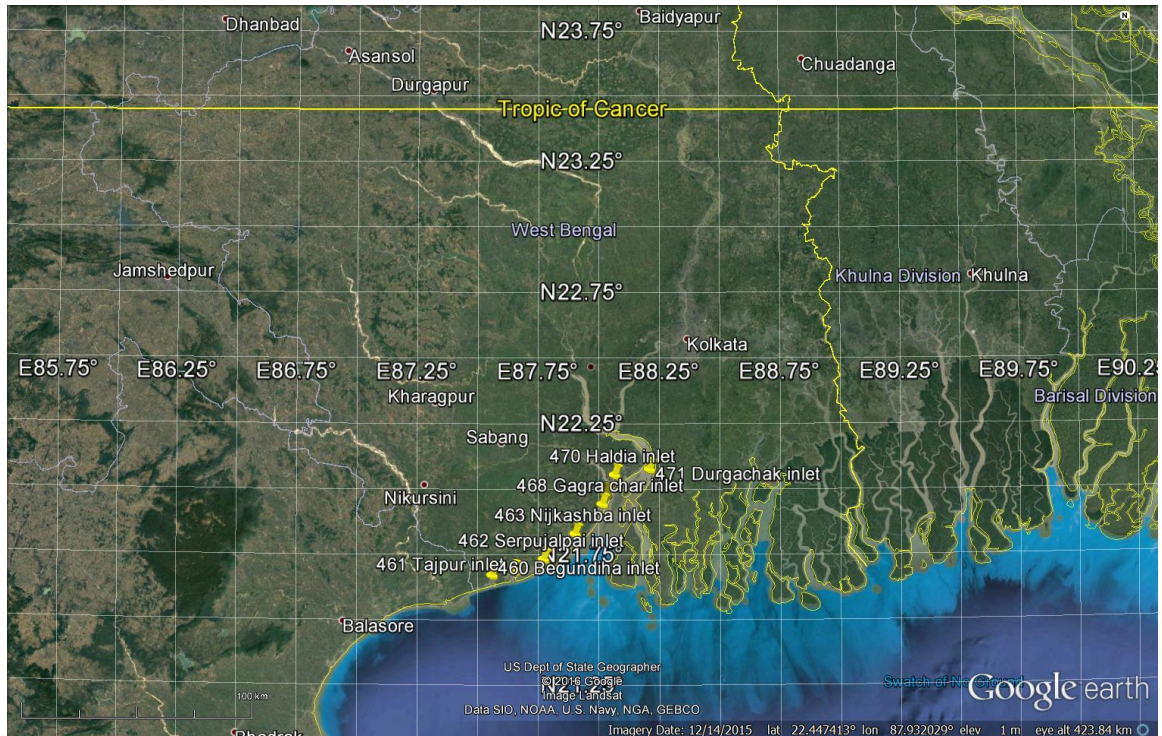


Figure 3.2(i) Inlets considered along the coast of West Bengal (8 inlets)

3.3. LITERATURE ON CLASSIFICATION OF TIDAL INLETS

In nature, there exists a large variety of coastal classification systems. Even then there is a further scope to categorize coastal morphological systems to bring a better understanding of the factors that have significant control over the morphology changes. This has led to the development of coastal classification schemes.

The diversity is the result of accumulated activities in coastal systems which are being influenced by a variety of factors and their combinations. Because of this, no unique classification can be made for the coastal systems. The decision of which classification scheme to be followed depends on the perception and concern of managers or researchers. However, all researchers agree that tidal inlet systems experience three different prominent forces viz. waves, tide and river discharge. The categorization can be subdivided into following points explained below.

3.3.1. Classification based on Tidal range conditions

While compiling information on worlds' shorelines, Armstrong Price was the first person who observed the tidal range as a significant influence on coastal geomorphology. It was stated that the morphology of sand deposits is controlled by the interaction of various process parameters such as tidal range, tidal currents, wave climate and storm actions. Among these parameters, the variations in tidal range had the severe effect in finding the large-scale differences in the morphology of sand accumulation (Hayes, 1975) and it also controlled the length of time waves act on any portion of shore profile (Davies, 1964). Based on the differences in tidal range along the shoreline, Davies (1964) proposed a set of limiting values for classification based on tidal range variations along the coastline (Table 3.1). After a decade, Hayes (1975) carried out a detailed study of coastal morphology on the coast of North America; It was concluded that mesotidal and macrotidal boundaries have to be changed or perhaps splitting those into two categories. Subsequently, Hayes (1975) documented the distribution and frequency of shoreline features into five tidal classes are depicted in Table 3.2 and also the variations of microtidal and mesotidal environments on the medium wave energy coasts (wave height, $H = 0.6$ to 1.5m) are documented in geomorphological aspects.

Table 3.1 Classification based on tidal range variations along the shoreline
(Davies, 1964)

S.No.	Tidal Range (m)	Shoreline classification
1	0 – 2	Microtidal
2	2 – 4	Mesotidal
3	> 4	Macrotidal

3.3.2. Classification of tidal inlets based on coastal energy regime

Walton and Adams (1976) attempted to quantify the amount of sand that was deposited in an offshore bar considering inlet hydraulics and tidal prism as major governing parameters along the South Carolina, Gulf coast of Florida and Pacific coast inlets.

Table 3.2 Classification based on tidal range variations along the shoreline (Hayes, 1975)

S.No.	Wave Height (m)	Tidal Range (m)	Shoreline classification
1	0.6 – 1.5	0 - 1	Microtidal
2		1 - 2	Low-mesotidal
3		2 - 3.5	High- mesotidal
4		3.5 - 5	Low-macrotidal
5		> 5	Macrotidal

In the areas of high wave activity, it was observed that there was a clear limiting relationship between the amount of sand stored in the outer bar and tidal prism, whereas inlets exposed to low wave activity showed more scattered correlation. For newly opened inlets on mildly exposed or moderately exposed or highly exposed coasts, the relationship was proposed for estimating the equilibrium volume of sand stored in the outer shoal.

To suitably classify the data on inlets into a set of limiting values with respect to wave energy acting on the offshore shoals, they used certain parameters such as wave height, wave period and nearshore continental shelf slope. As the continental shelf slope contained in the measure of wave heights, the basic measure of wave energy was quantified with the parameter H^2T^2 to categorize the energy environments along the coastline. The proposed arbitrary value set of each of the energy environment criteria is given in Table 3.3.

Table 3.3 Classification criteria based on wave energy (Walton & Adams, 1976)

S. No.	H^2T^2 (m^2s^2)	Energy environment
1	< 2.8	Mildly Exposed
2	2.8 to 27.9	Moderately Exposed
3	> 27.9	High Exposed

3.3.3. Geomorphological classification

Tidal entrances constitute an important dynamic boundary condition with respect to the coastal regime because of their crucial role for the exchange of seawater and embayed water. Generalized morphodynamic relationships applicable to the entrances serve as useful tools for characterizing the physical state and the dynamic behavior of entrances.

Coastal lagoons can be conveniently separated based on geomorphology into leaky, restricted or choked systems (Kjerfve and Magill, 1989). Roy et al.' (2001) have widely classified the estuaries within New South Wales based on the homogeneity in the geomorphology. According to decreasing marine influence, sea water bodies are being divided into five groups: 1) bays, 2) tide-dominated estuaries, 3) wave-dominated estuaries, 4) intermittent estuaries and 5) freshwater bodies with four states of sediment infiling viz. youthful, intermediate, semi-mature and mature. The scheme has been tested which confirmed the effectiveness of the method to distinguish and classify the estuaries (Saitilan, 2004). Apart from this, Heap et al. (2001) classified 780 coastal systems for Australia based on the ratio of wave versus tide energy scheme at the inlet entrance.

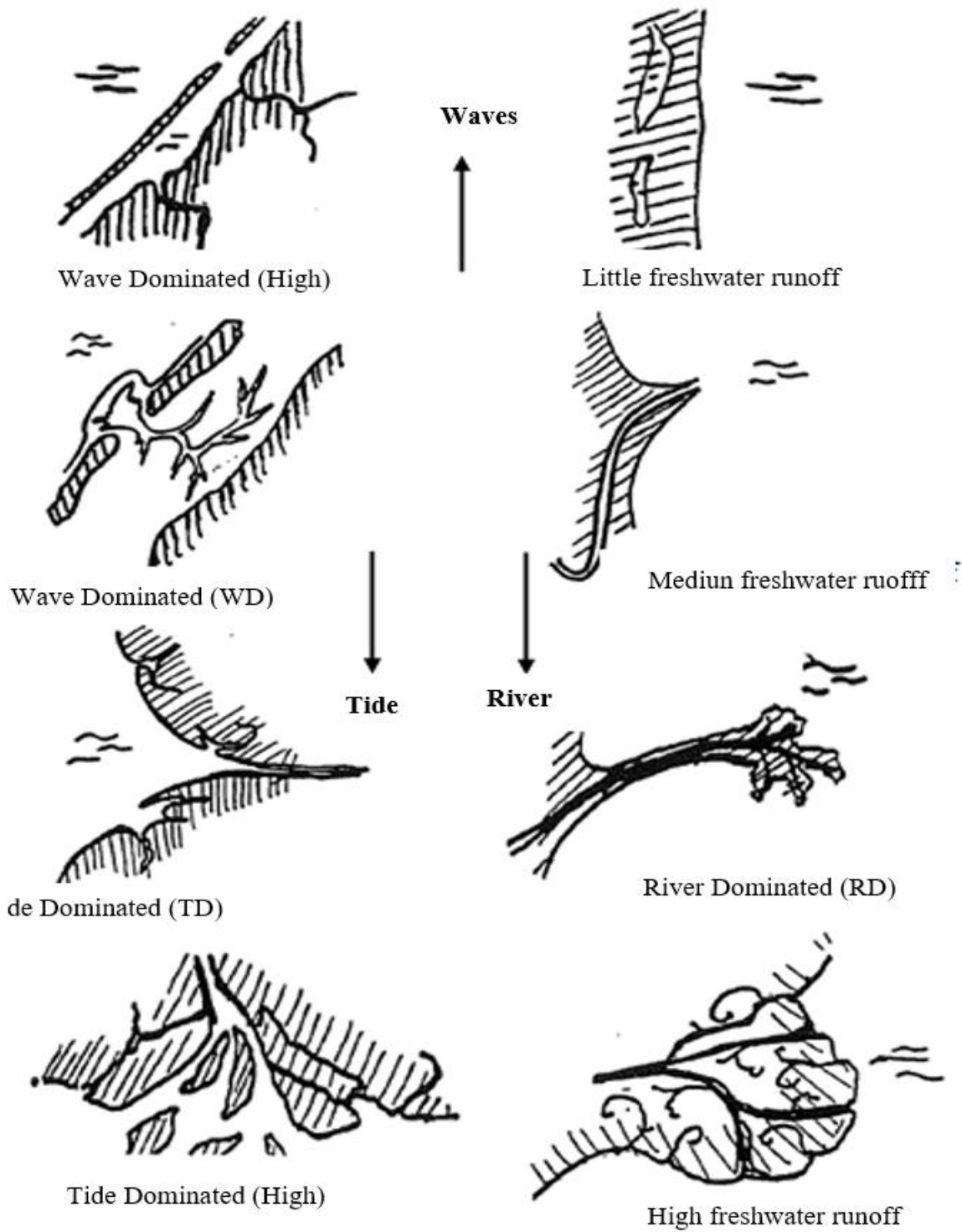


Figure 3.3 Classification of inlet shapes based on the influence of waves, tide and river flow (de Vriend et al. 1999)

In the view of geologists and geo-morphologists, the land-sea interface is the essential factor to classify coastal inlets (Carter, 1989; Davies, 1984). This is quite similar to Figure 3.3 sketched by de Vriend et al. (1999). Morphodynamic relationships are useful for the prediction of changes in the throat area and the ebb delta volume when morphologic changes are periodically consistent with the re-establishment of equilibrium.

The hydraulic geometry of a tidal inlet reflects a self-adjusting control system, reflecting periodic flow reversals, sedimentation, and the incident wave climate. Hubbard et al. (1979) have divided passes into three classes as shown in Table 3.4. Their classification is based mainly on the tidal passes in the south-eastern USA. However, their admission may not be universally applicable. Also, they showed that the balance between wave and tide forces determines the position, size, and shape of pass morphology and bedforms.

Table 3.4 Morphological variations at tidal inlets

Inlet types			
Variables	Wave-dominated	Mixed Energy	Tide-dominated
Main shoal position	Inside bay as flood delta	In throat	Seaward as linear bars
Ebb-tide delta	Small, near the beach	Variable	Usually absent
Channel type	Poorly defined, often multiple	Variable and unstable	Deep and stable
Width/Depth ratio	Moderate	Very large	Small
Lagoon	Wide, open	Fringing marsh or marsh filled	Marsh filled, with channels
Swash bars	Poorly developed	Variable	Variable
Swash platforms	Poorly developed	Variable	Well developed
Channel margin bars	Absent	Variable	Large
Sand body type	Tabular	Variable	“Pod” like
Sand by-passing	Via bar	Variable	By ebb currents in the channel

3.3.4. Hydrodynamic classification

The tidal range outside an inlet depends primarily on the ocean tides and their interaction with the continental shelf. The wave conditions are generated seaward (and thus independently) of the inlet. Since both parameters are independent of the inlet system's configuration, they are very suitable to be used for classification. An inverse relation between tidal range and length of a barrier island seems present (i.e. large tidal ranges apparently result in shorter barrier islands).

Davies (1964) first classified shorelines by tidal range (Table 3.1). The focus on shoreline classification based on the tide range is justified because tidal range controls the length of waves acting on any portion of the shore profile. Therefore, the effectiveness of wave energy decreases with increasing tidal range. Generally, wave action acts as a bulldozer on the tidal inlet morphology (Hageman, 1969); it moves sediment onshore and limits the area over which the ebb tidal delta can spread out. The wave climate is characterized by the mean significant wave height (H_s) on a yearly average basis (Table 3.2).

Using Davies' (1964) tidal classification of the coast, Hayes (1975) invented and diagrammed the distribution and frequency of shoreline features for all three tidal classes namely wave-dominated, tide-dominated and mixed energy. Also, he developed morphological models for both estuaries and barrier islands.

Hayes (1979) and Davis and Hayes (1984) characterized inlet planform morphology according to the relative strength of tide and waves (Figure 3.4), where tidal range serves as a surrogate for tidal prism (volume of water entering or leaving an inlet in the corresponding half tidal cycle) or tidal current (which moves the sediment). Hayes' classification is not only concerned with the morphologic behavior of a tidal inlet but also with the frequency of occurrence and the number of inlets along a barrier coastline. The

nature of tidal inlets and characteristics around the inlets is dependent on the relative influence of average significant wave height and average tidal range.

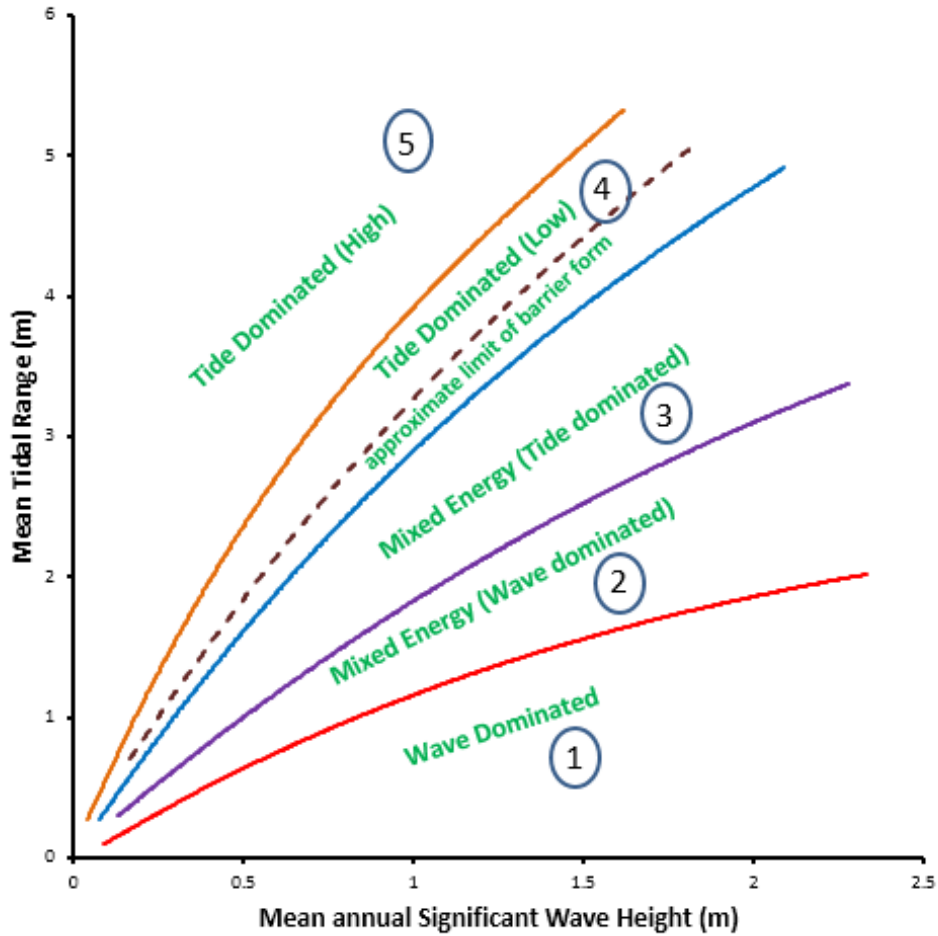


Figure 3.4 Hydrodynamic based classification of tidal inlet morphology
(After Davies and Hayes, 1984)

Each class in the hydrodynamic classification develops its specific morphologic features viz. (Figure 3.4):

1. Wave dominant inlets have long continuous barriers, with only a few tidal inlets and a lot of washovers.

2. Mixed energy inlets (Wave dominant) have a more substantial number of inlets and a smaller number of washovers. The size of the ebb tidal delta will become somewhat larger.
3. Mixed energy inlets (Tide dominant) have abundant tidal inlets, larger ebb tidal deltas and usually drumstick barriers.
4. Tide-dominated inlets (Low dominance) occasionally show wave built bars and transitional forms can be recognized.

3.3.4.1. Tide dominated inlets

Tide-dominated inlets tend to have larger ebb shoals that include channel migration bars. Tidal inlets take bypass route, which means the sediment enters the channel on one side of the flood tide and a portion eventually returns opposite to the ebb tide (Figure 3.5a). Large volumes of sand can also be added to the barrier segment on either side of the inlet by reorientation of the outer channel that isolates a portion of the ebb shoal from the strong tidal flow (FitzGerald et al. 2001). Sand bodies can move onshore over the shallower portion of the ebb shoal exposed to breaking waves. During storms, parts of the channel-margin bars or other features of the ebb shoal may break off and migrate towards an onshore direction.

Tide-dominated inlets (High dominance) are characterised by predominant tidal current ridges, extensive salt marshes, and tidal flats. Inlets of this kind often have large ebb tidal deltas and very deep inlet gorges. It is crucial to mention here that the classification of tidal inlets not only depends on the relative dominance of waves and tides but also on the surface area of the inlet basin.

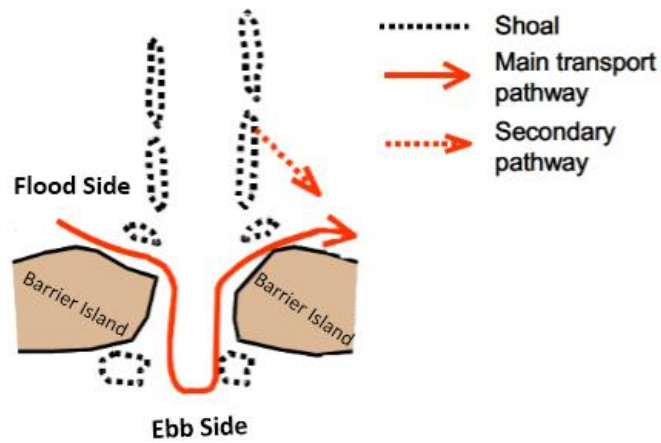


Figure 3.5(a) Representative planform morphology and bypassing mode of natural inlets based on tide dominance (Source: FitzGerald, 1982)

3.3.4.2. Wave dominated inlets

Wave-dominated inlets incline to be fringed by semi-circular ebb shoals. Bypassing of sediment around wave-dominated inlets occurs through sandbar bypassing; sand moves around the shoal with the longshore current that is generated by waves breaking on it. On wave-dominated coasts, the flood shoal tends to be large, because a large amount of littoral sand is brought to the inlet, which can be swept inside by the tidal current, as well as bypassed through tidal bypassing (Figure 3.5(b)).

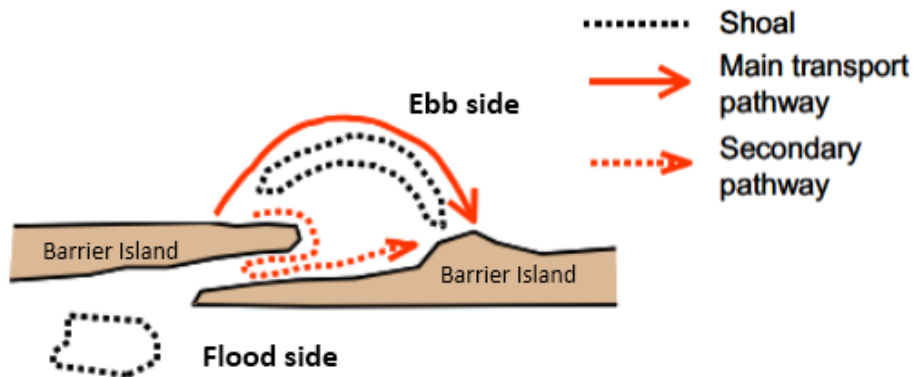


Figure 3.5(b) Representative planform morphology and bypassing mode of natural inlets based on wave dominance (Source: FitzGerald, 1982)

3.3.4.3. Mixed energy inlets

Mixed-energy inlets (Figure 3.5c) share the features of each of the tide-dominated and wave-dominated idealized end states (FitzGerald, 1982)

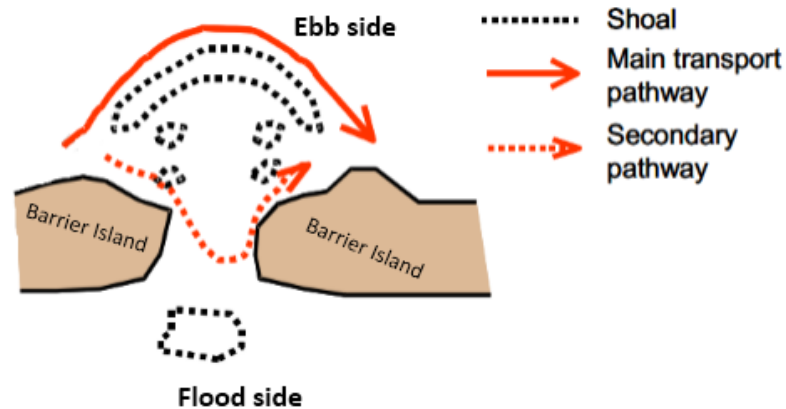


Figure 3.5(c) Representative planform morphology and by-passing mode of natural inlets based on mixed energy dominance (Source: FitzGerald, 1982)

3.3.5. Classification based on dimensionless parameters without wave period

There exist numerous methods to classify coastal systems; the most preferred and used classification is based on the hydro-morphological perspective related to ecological parameters. The literature review revealed that none of the previous methods consider quantitatively the three main driving agents that govern inlet morphodynamics. New methods of classification are introduced by Vu (2013) based on dimensionless parameters which represent the relative strength of the three main forcing agents, viz., tide, river flow and waves. The non-dimensional parameters $\frac{\hat{Q}_{tide}}{\sqrt{gH^5}}$ and $\frac{Q_f}{\sqrt{gH^5}}$ are introduced in which tidal forcing is quantified in terms of the peak tidal discharge and wave forcing represented in terms of sediment transport capacity where \hat{Q}_{tide} is peak or mean tidal discharge and Q_f is freshwater discharge and H is mean annual significant wave height. Along NSW coast of

Australia, 178 inlets are classified based on this new classification system, which revealed a clear peculiarity of three main groups (Table 3.5 and Figure 3.6).

Table 3.5 Classification of Coastal systems based on dimensionless parameters
(Vu, 2013)

S. No	Description	Type of Coast
1	$\frac{\hat{Q}_{tide}}{\sqrt{gH^5}} < 75$	Wave-dominated
2	$\frac{\hat{Q}_{tide}}{\sqrt{gH^5}} > 75$	Tide-dominated
3	$\frac{Q_f}{\sqrt{gH^5}} \geq 2$	River-dominated

In the Figure 3.6, ICOLLs represents Intermittently Closed and Opened Lakes and Lagoons. The dimensionless classification appears reliable when compared with other widely used classification schemes in the literature. The present method reduces discrepancies between hydrodynamic and morphodynamic classifications. This improved classification system allows better long-term prediction of inlet morphodynamics, enabling effective coastal zone management.

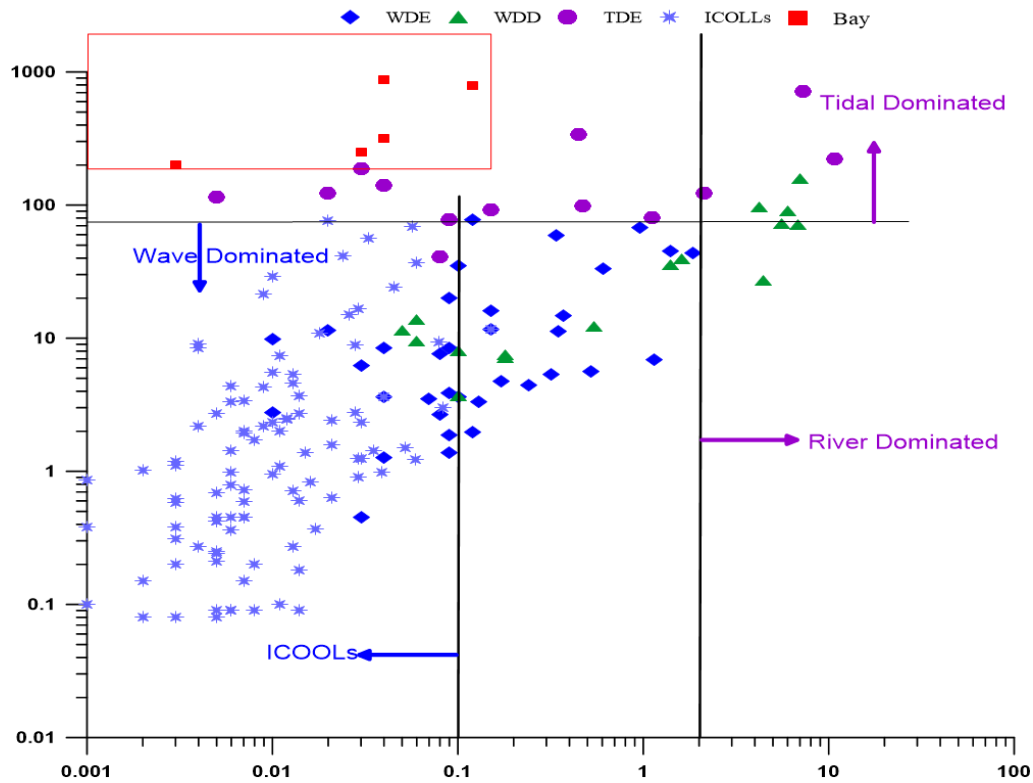


Figure 3.6 Inlet classification in terms of $\frac{\hat{Q}_{tide}}{\sqrt{gH^5}}$ and $\frac{Q_f}{\sqrt{gH^5}}$ for 178 estuaries in NSW, Australia (Vu 2013)

3.3.6. Classification based on dimensionless parameters with wave period

To compare the peak tidal discharge with waves at the inlet, there are two obvious fair choices. The simple one is $\frac{Q_{tide}}{\sqrt{gH^5}}$, which compares Q_{tide} to the sediment transport capacity of the waves as per CERC formula for littoral drift (Nielsen, 2009). More complicated measure compared to earlier one is $\frac{Q_{tide}}{\sqrt{gH^5}}$ which brings in the mean wave period (T) also into consideration, which is to be important in relation to runup height (Nielsen, 2009) and the ability of waves to build berms (Takeda and Sunamura, 1992), which eventually close the inlets (Vu, 2013). Vu (2013) discussed the methodology of classification by including

the wave period but not classified the inlets and hence we are calling this method as modified Vu method. Modified Vu (2013) method considered wave period (T) in addition to the wave height (H) in the dimensionless parameters $\frac{Q_{tide}}{\sqrt{gH^5}}$ and $\frac{Q_f}{\sqrt{gH^5}}$ by the runup scale $\sqrt{HL_0} = \sqrt{H \frac{gT^2}{4\pi}}$ which leads to new dimensionless parameters viz. $\frac{Q_{tide}}{(g^{1.75}H^{1.25}T^{2.5})}$ and $\frac{Q_f}{(g^{1.75}H^{1.25}T^{2.5})}$ respectively. The value set for each of the dominance criteria is shown in Table 3.6.

Table 3.6 Classification criteria used for modified non-dimensional method (modified Vu method, Reddy et al., 2015)

S.NO.	$\frac{Q_f}{(g^{1.75}H^{1.25}T^{2.5})}$	$\frac{\hat{Q}_{Tide}}{(g^{1.75}H^{1.25}T^{2.5})}$	Type of Dominance
1	< 0.0001	< 0.045	Wave Dominated (ICOLLs)
2	> 0.0001	< 0.045	Wave Dominated
3	> 0.0001	> 0.045	Tide Dominated
4	< 0.0001	> 0.045	River Dominated

3.4. PARAMETER ESTIMATION

The primary input parameters required for classification of tidal inlets are the tidal range, area of lake or lagoon or backwater, nearshore significant wave height and mean wave period, tidal prism, and river or flood discharge.

3.4.1. Tidal range

The tidal range for each of the inlet is obtained by simulation of the water level variation for about 30 days along the coast using a state of the art hydrodynamic model of MIKE by DHI, i.e., MIKE-HD flow model (DHI, 2012). The description of the MIKE21 FM including the the basic equations, boundary condtions, basic input and outputs along with application areas are represented in section 4.4.2.1.

Coastal bathymetry of different regions along the coast, where inlets are present, was obtained from Naval Hydrographic charts and flow models were setup with the offshore boundary being in water depths of about 10m. The tide variations at the boundaries of each of the flow models are generated using the global tidal constituents (Andersen, 1995). The model bathymetry for the Goa coast is shown in Figure 3.7 and Figure 3.8 shows the mesh generated for the Goa coast.

These tide variations at boundaries are used to simulate the water level variations within each flow model, and the tidal variation at each of the inlet mouth was obtained. The tidal variation results obtained at tide gauge stations are cross-checked with the tidal range provided in hydrographic charts for some of the tide gauge locations, published by the National Hydrographic office, Dehra Dun, India. The tidal range values along the west and east coast of India are represented in Figures 3.9(a) and 3.9(b).

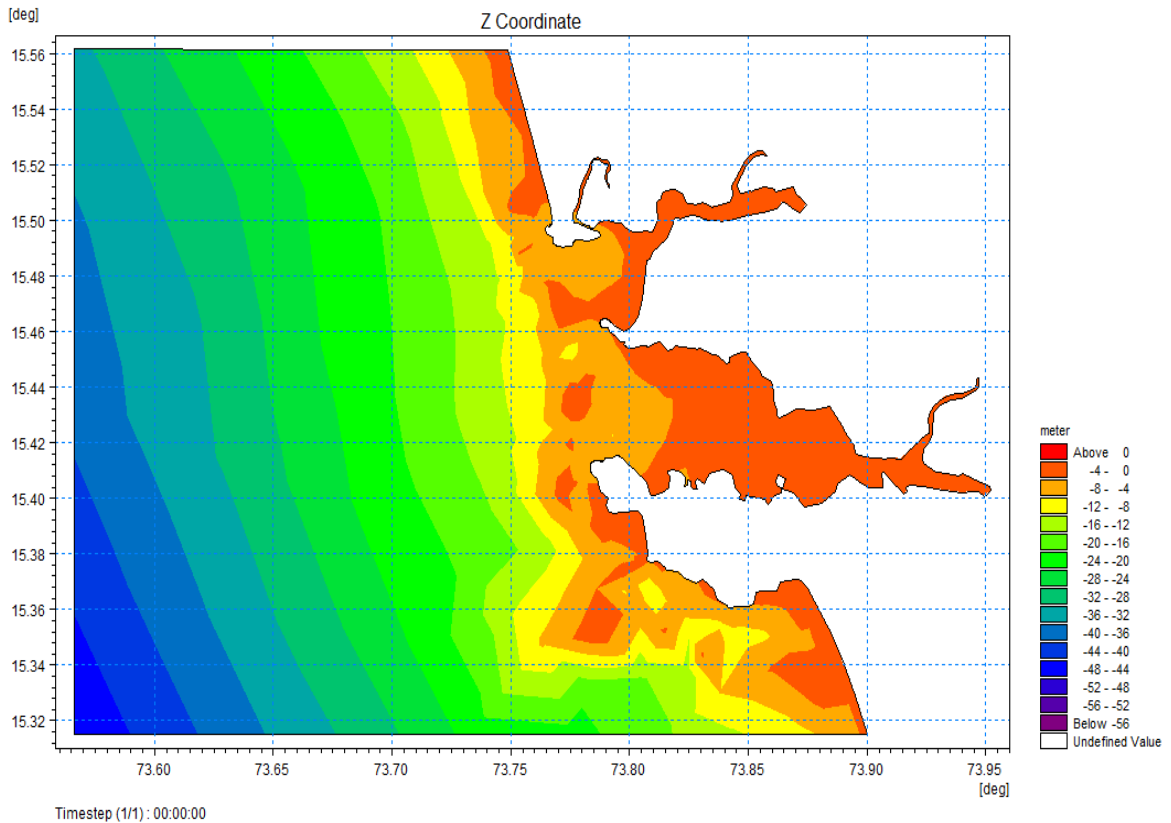


Figure 3.7 MIKE21 Model bathymetry for Mandovi and Zuari inlets

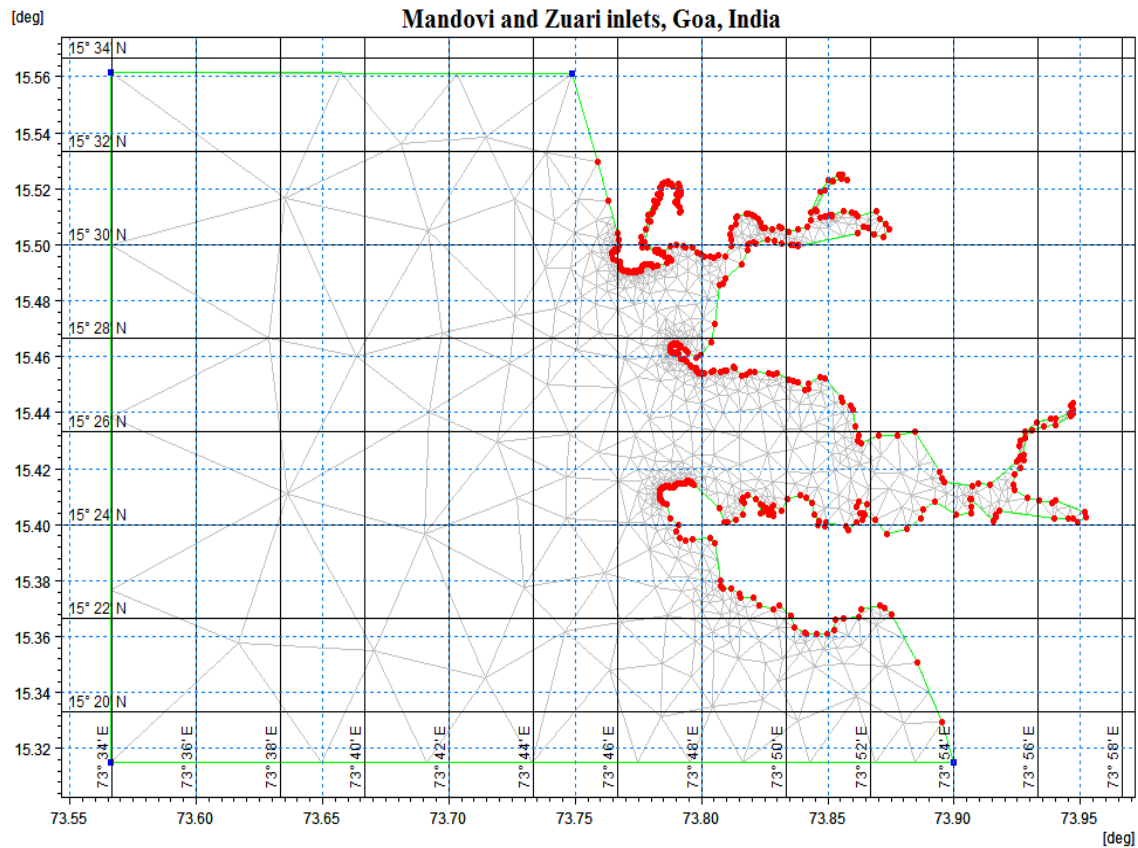


Figure 3.8 Generated mesh for Mandovi and Zuari inlets

3.4.2. Lagoon or Bay area

The lake, lagoon or bay area (A_b) for the inlets is calculated using high-resolution satellite data obtained from Landsat 8 OLI (Operational Land Imager), TIRS (Thermal Infrared Sensor) from U.S. Geological Survey Department and also Google Earth[®] imageries. The satellite image data consisting of various high-definition images of different bands is overlaid, and the final image is obtained by ArcMap[®] 10.1. From such composed images, the lagoon or bay area is calculated by creating shapefiles in ArcMap[®] 10.1 and further verified the same by estimating the bay or lagoon areas in topography and bathymetry using MIKE21 tool and area calculation tool from Draftlogic[®]. The bay area (A_b) calculated for the inlets are shown in Table A3.4. The lagoon or bay area is restricted approximately 15

km for few inlets whose extent is considerable and those inlets which are less than 10 km, have been fully considered.

3.4.3. Tidal prism

Tidal prism (P) is estimated as the product of tidal range and the basin area (A_b) and subtracting the volume of shoals.

i.e., Tidal prism = Tidal range X (Basin area – the volume of shoals)

3.4.4. Tidal discharge

The tidal discharge in m^3/s , Q_{tide} , is calculated using the relation as per equation 3.1 given in Vu (2013).

$$Q_{\text{tide}} = \frac{P\pi}{T} \quad (3.1)$$

where P is tidal prism (m^3), and T is the tidal period ($T=12\text{hrs } 25\text{min}$ for semi-diurnal tides)

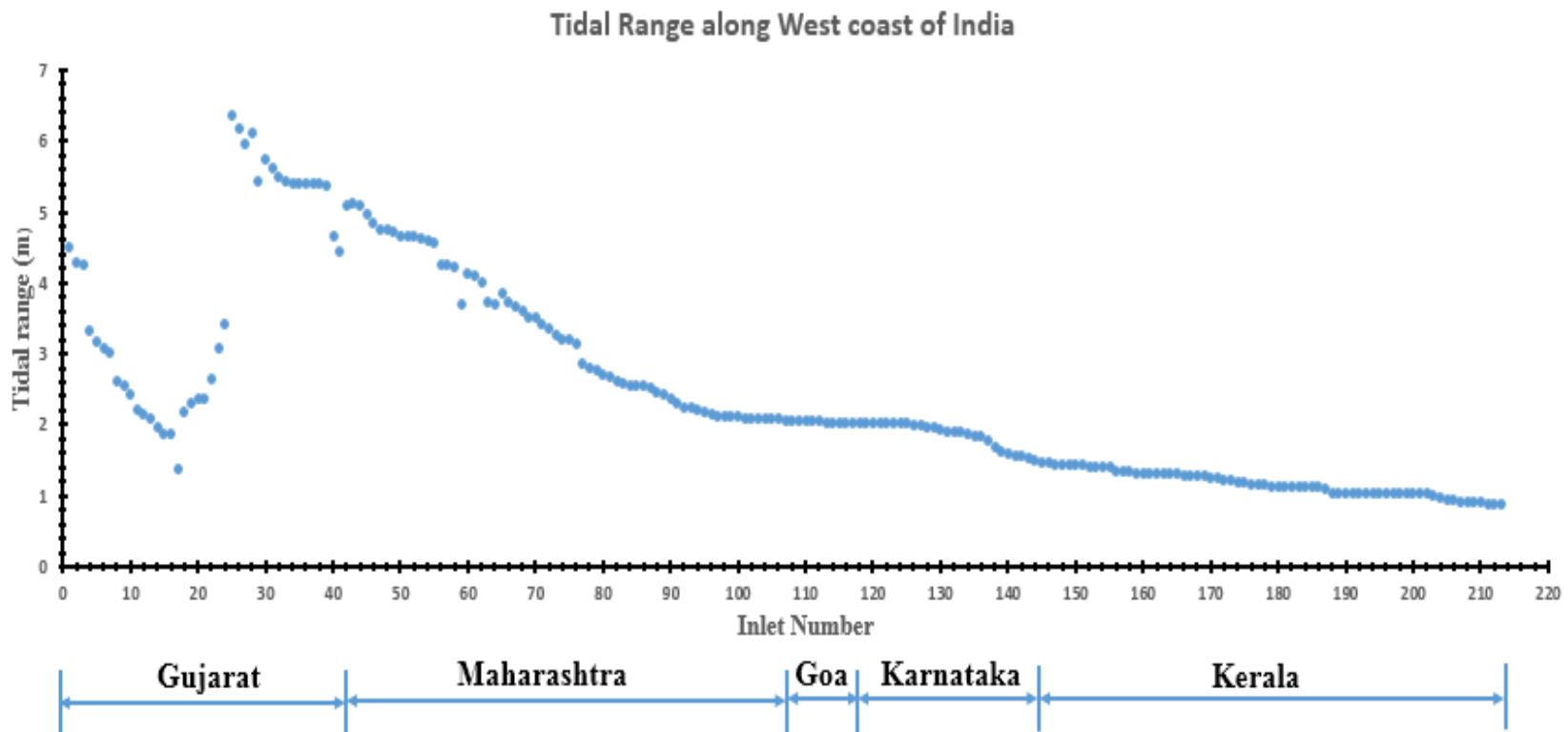


Figure 3.9(a) Tidal range along West coast of India

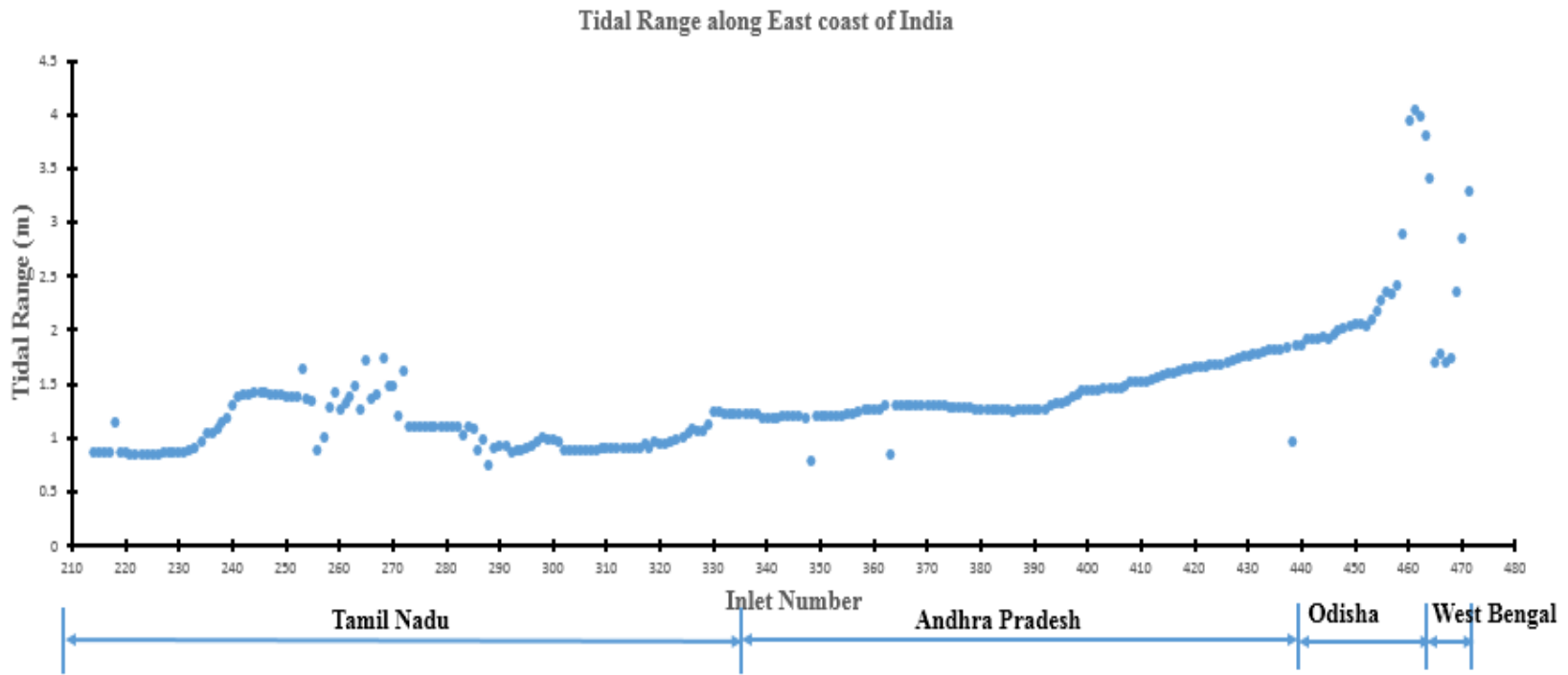


Figure 3.9(b) Tidal range along East coast of India

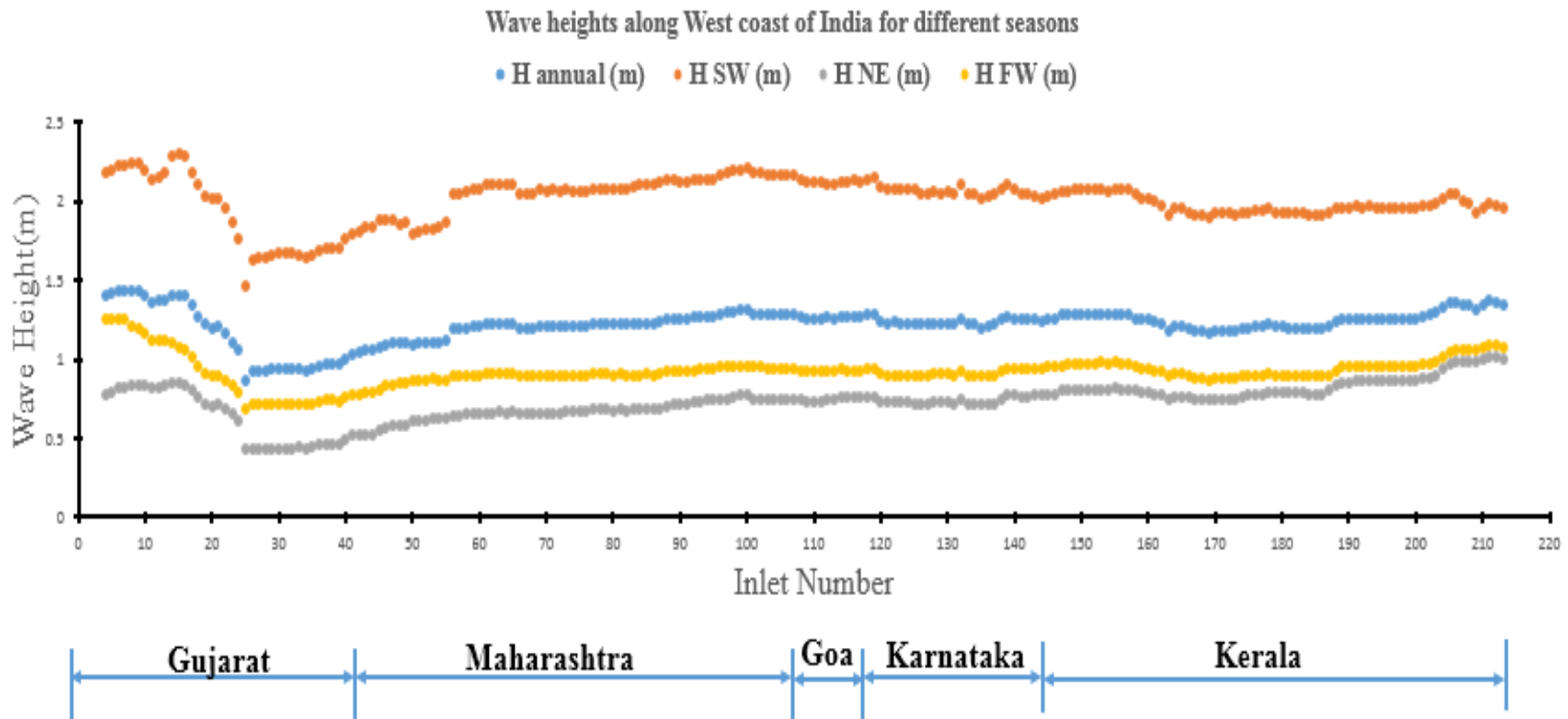


Figure 3.10(a) Annual and seasonal wave heights along East coast of India

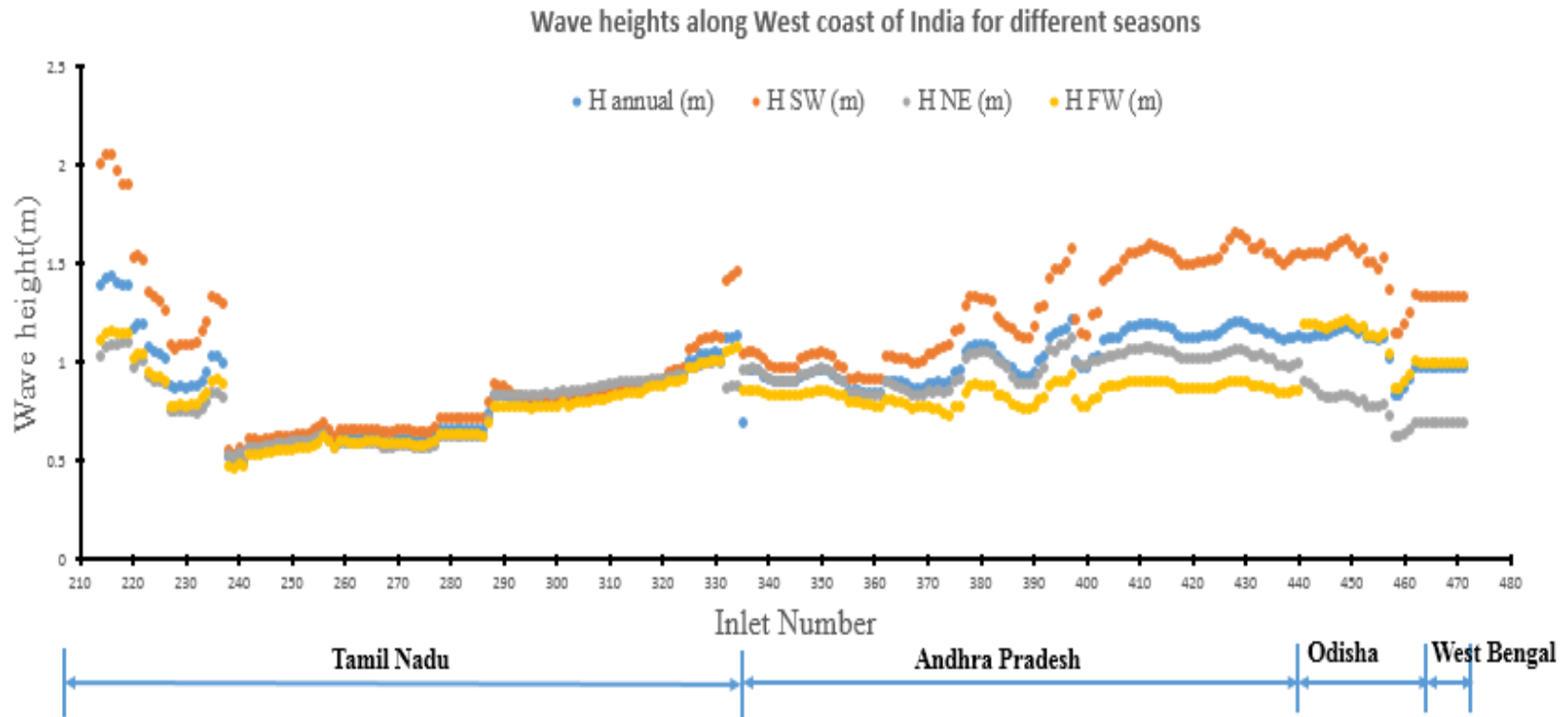


Figure 3.10(b) Annual and seasonal wave heights along East coast of India

3.4.5. Significant wave height

The wave data, viz., Significant wave height (H_s) and mean wave period (T_z) are obtained from the MIKE21 spectral wave model simulations for the year 2010 using NCEP (National Centers for Environmental Prediction)/NCAR (National Center for Atmospheric Research) wind input (Kalnay et al., 1996). The description of the MIKE21 SW including the basic equations, boundary conditions, basic input and outputs along with application areas are represented in section 4.4.2.2. The MIKE21 spectral wave model has been validated with measurements. The average significant wave height data is extracted at 10m water depth at each of the respective inlets considered in the study. The annual significant wave heights and southwest, northeast and fair weather seasonal wave heights along the east and west coast of India are represented in Figures 3.10a and 3.10b.

3.4.6. Flood discharge

Flood discharge was available for 75 tidal inlets out of which 39 were obtained from the gauge stations maintained by the Central Water Commission (CWC) and available through the Water Resources Information System (India-WRIS) database and other sources and remaining 36 were theoretically estimated and validated by Amaranatha Reddy et al. (2018). For 39 CWC inlets, the discharge data are available at gauging stations few kilometers away from the coast, and it is assumed that there are no losses in between the gauging station and the tidal inlet. The theoretical estimation of flood discharge is done using different methods of synthetic unit hydrograph models and was inter-compared, and river discharge data is obtained for 29 inlets along Karnataka coast (Amaranatha Reddy et al., 2018) and seven inlets along Kerala coast.

3.5. CLASSIFICATION OF INLETS BASED ON DIFFERENT METHODS

The classification methods viz. (i) based on tidal range (Davies 1964 and Hayes 1975); (ii) based on wave energy regime (Walton & Adams, 1976); (iii) based on geomorphology (de Vriend 1999); (iv) based on annual significant wave height and mean tidal range (Hayes 1979); (v) based on waves, tide and river discharge excluding wave period (Vu 2013); and (vi) based on waves, tide and river discharge including wave period are considered in the study and the results of various classification methods are presented in the following sections.

3.5.1. (a) Classification based on Tidal range conditions (Davies, 1964)

The classification of inlets along the west coast of India considering tidal range showed that 90 inlets could be considered to be influenced by microtidal environment, 82 inlets by mesotidal environment and 41 inlets by the macrotidal environment. The 42 inlets considered along the coast of Gujarat experiences tidal range values between 1.38m to 6.37m. The wide range of variations in tidal range conditions for micro-, meso- and macro-tidal environments are shown in Figure 3.11(a). From Figure 3.11(a) it is understood that only 12% of inlets come under microtidal regime whereas meso- and macro-tidal environments are 40% and 48% respectively. This is because, except north Gujarat, most of the inlets experience (37 out of 42 tidal inlets) are having a tidal range more than 2m and also only coastal state which experiences all three environmental regimes.

The coast of Maharashtra has tidal ranges more than 2m at all the 65 inlets, and the coast is experiencing meso- and macro-tidal environments. Unlike Gujarat coast, Maharashtra experiences the decreasing rate of tidal range values from the north to south along the coast (Figure 3.11(a)). The Maharashtra coast showed mesotidal dominance at 20 inlets (i.e. 30% of inlets) and macrotidal environment at 70% of the inlets (45 inlets). The tidal range values are 2.07m to 5.14m. Goa has a small coastline length of about 100km and contains only 11

tidal inlets. Since the coastline length is comparatively small, Goa coast does not show much variation in the tidal range. The average tidal range is 2.05m with a minimum of 2.03m at Mashem and maximum of 2.07m at Tiracol. The mesotidal regime has been observed all along the Goa coast (Figure 3.11(a)).

The Karnataka coastline spreads over a length of 320km which comprises of three coastal districts viz. Uttar Kannada, Udupi and Dakshina Kannada. The tidal range along this coast varies between 1.48m at Kanwatheertha to 2.03m at Karwar. Nineteen out of twenty-seven inlets experience microtidal behavior which is about 70%. Since the tidal range decreases in comparison with the states Goa, Maharashtra, and Gujarat, the inlets along the Karnataka coast are observed as mixed energy inlets at most locations.

The Kerala coast comprises of 68, and the tidal inlets completely showed microtidal environment (Figure 3.11(a)). The tidal range along the coast is less than 1.5m with a minimum value of 0.88m to a maximum of 1.74m. Tidal range acts as a major morphological driver at tidal inlets. Because of the low tidal range values, most the inlets along the Kerala coast show the seasonal closure and opening behavior.

Tamil Nadu on the east coast of India experiences the tidal range between 0.75m to 1.74m. This is the state which experiences the least tidal range of magnitude 0.75m at Kodikkarai inlet in Nagapattinam district of Tamil Nadu. All the inlets fall under the microtidal environmental cluster because of less variation in tidal range at all inlets (Figure 3.11(b)). This is the reason for observing the changing seasonal behavior of inlets along the coast of Tamil Nadu. Most of the inlets in summer season close due to non-exchange of water between sea and lagoon and due to high wave activity as well. Similar to Tamil Nadu coast, Andhra Pradesh also experiences microtidal environment at all 106 tidal inlets (Table A3.1). The tidal range values are ranging from 0.8m to 1.86m. It can be observed that the behavior does not vary much at many of the inlets along Andhra Pradesh coast. The satellite

images of the inlets show that there are no visual changes in the images seasonally and also most of the inlets are open throughout the year.

Odisha and West Bengal on the East coast show mixed environmental regime. The tidal range along the Odisha coast varies between 1.92m to 3.8m whereas along the West Bengal coast between 1.7m to 3.41m. Six inlets in Odhisa are observed under the microtidal environment (26%), sixteen inlets under the mesotidal environment (70%) and only one inlet as the macrotidal environment (4%).

However, West Bengal coast experiences 50% (i.e.four inlets) microtidal and 50% mesotidal environments. Because of relatively high tidal range, the inlets along both the coasts mostly remain open throughout the year.

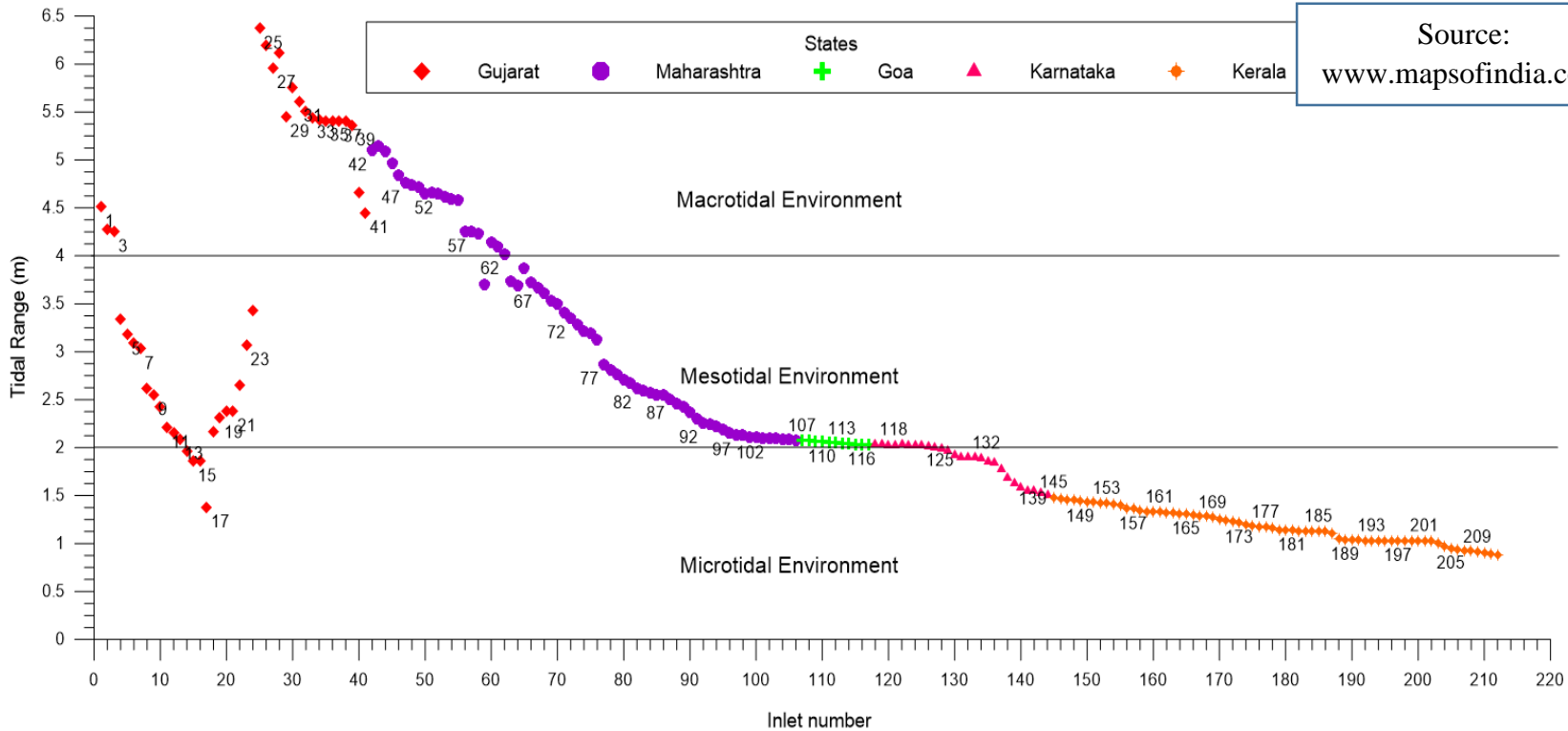
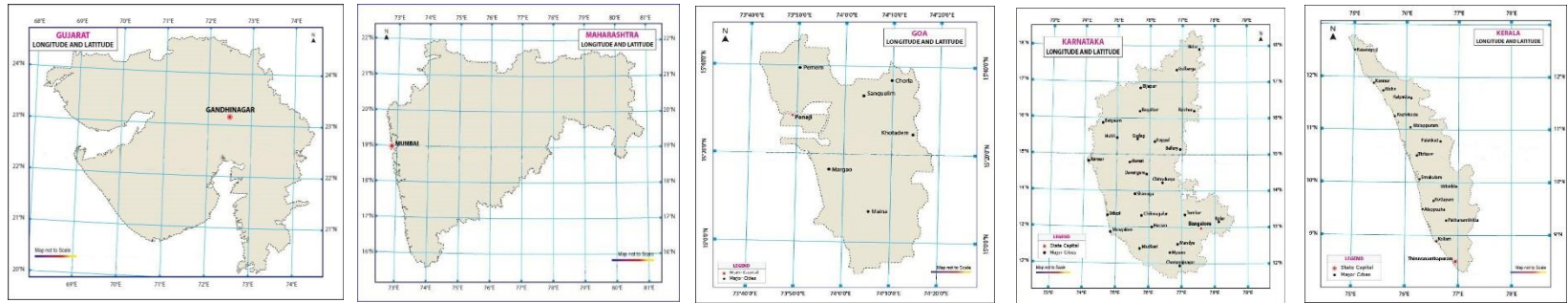
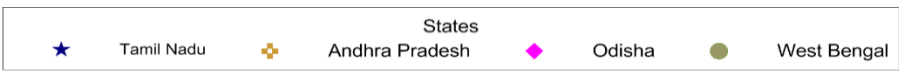
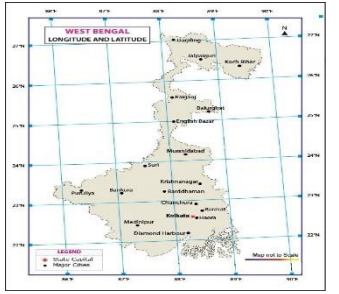
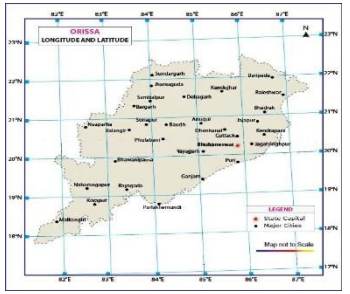
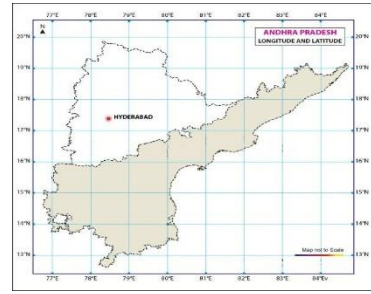
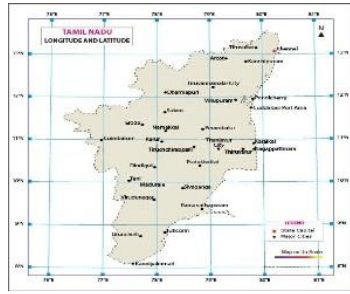


Figure 3.11(a) Classification of tidal inlets along the west coast of India based on Tidal range conditions



Source:
www.mapsofindia.com

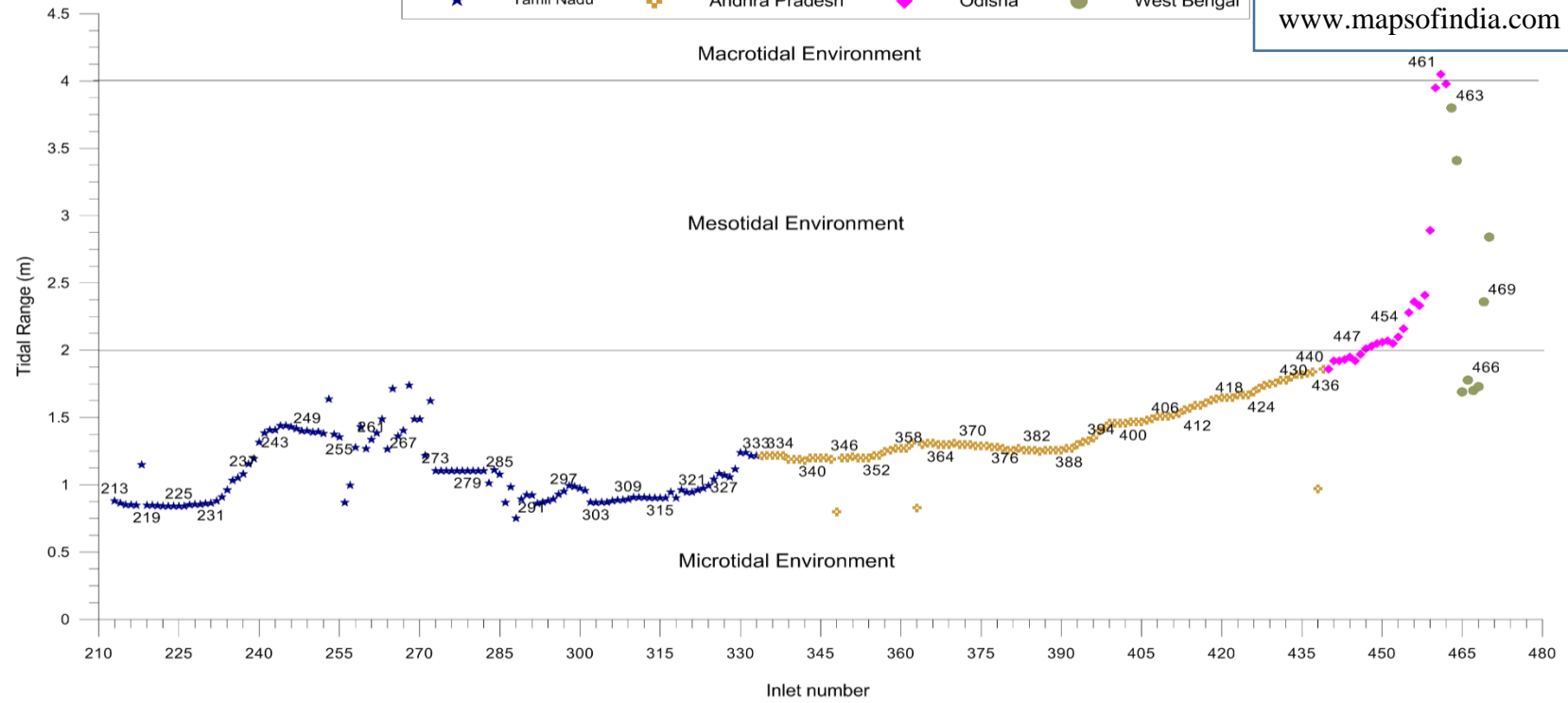


Figure 3.11(b) Classification of tidal inlets along the east coast of India based on Tidal range condition

3.5.1. (b) Classification based on tidal range regime (Hayes, 1975)

The Gujarat coast experiences four environmental regimes viz. low-mesotidal, high-mesotidal, low-macrotidal and macrotidal along the entire coast except for microtidal regime. The coast showed different coastal environments as: (i) low-mesotidal - 4; (ii) high-mesotidal - 17; low-macrotidal - 5 and macrotidal -16. Due to high tidal range values (ranges between 1.38m at Mul Dwaraka to 6.37m at Tena River) throughout the year, the inlets may remain opened irrespective of seasons. The coast of Maharashtra is subjected to the environmental regimes between high-mesotidal to macrotidal. Among these three regimes, 57% of the inlets fall under high-mesotidal, 38% fall under low-macrotidal and rest 5% inlets subjected to macrotidal cluster (Figure 3.12(a)).

The entire Goa coastline falls under high-mesotidal environment because the tidal range variations along the coast are minimal and the values are ranging from 2.03m to 2.07m. According to Davies (1964) classification, all inlet along Goa coast fall under microtidal regime whereas Hayes (1975) classification showed a high-mesotidal regime for the same inlets. The Karnataka coast experiences only two among five environmental regimes namely low-mesotidal and high-mesotidal. The Uttara Kannada district is experiencing by the high-mesotidal regime (33.33%) whereas Udupi and Dakshina Kannada districts are subjected to the low-mesotidal regime (66.67%).

None of the inlets along the four coastal states in the West viz. Gujarat, Maharashtra, Goa, and Karnataka fall under microtidal environment. Along the Kerala coast also 59 inlets (i.e. 87% of the inlets) fall under low-mesotidal environment and only nine inlets fall under microtidal environment.

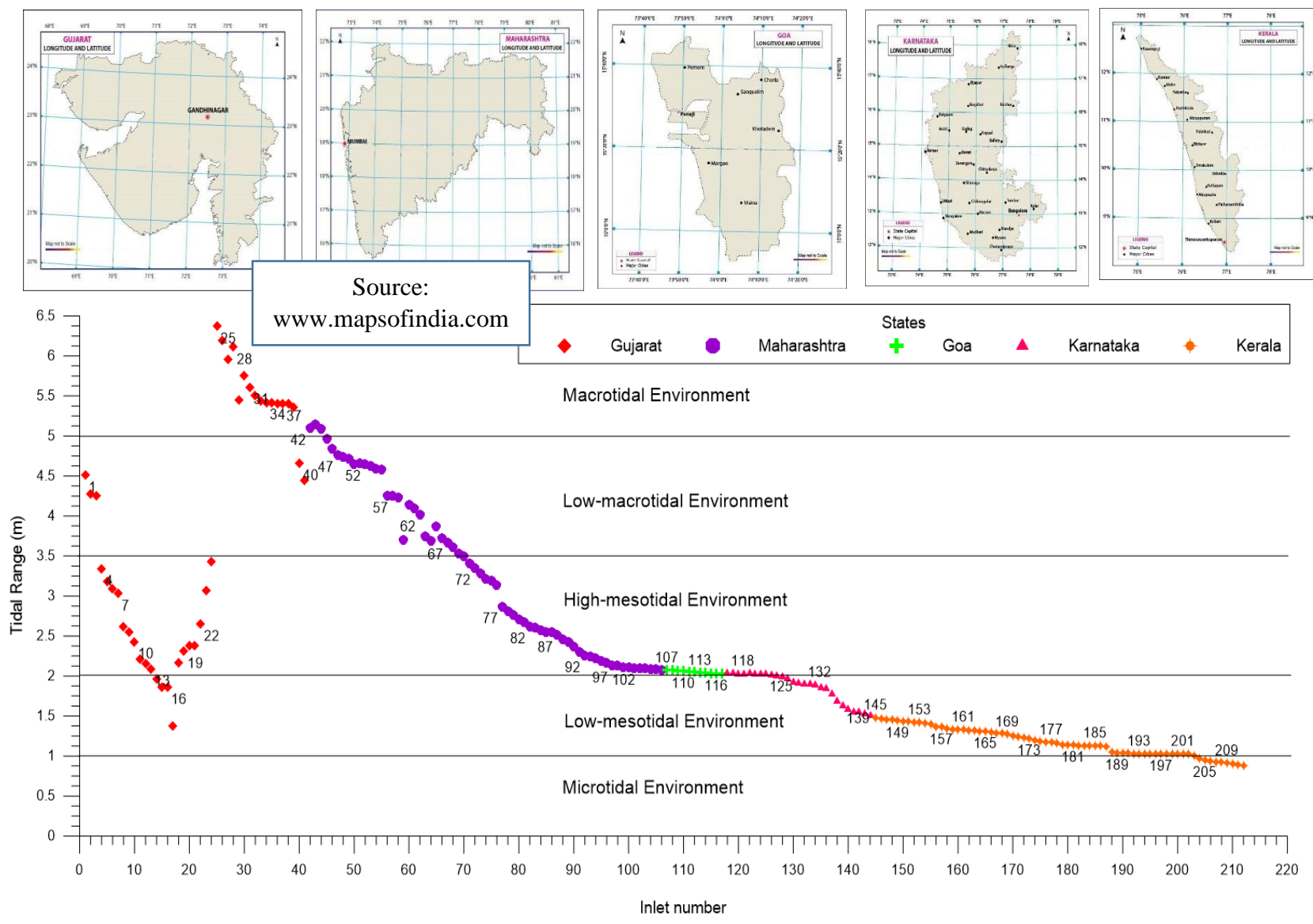


Figure 3.12(a) Classification of tidal inlets along the west coast of India based on Tidal range conditions

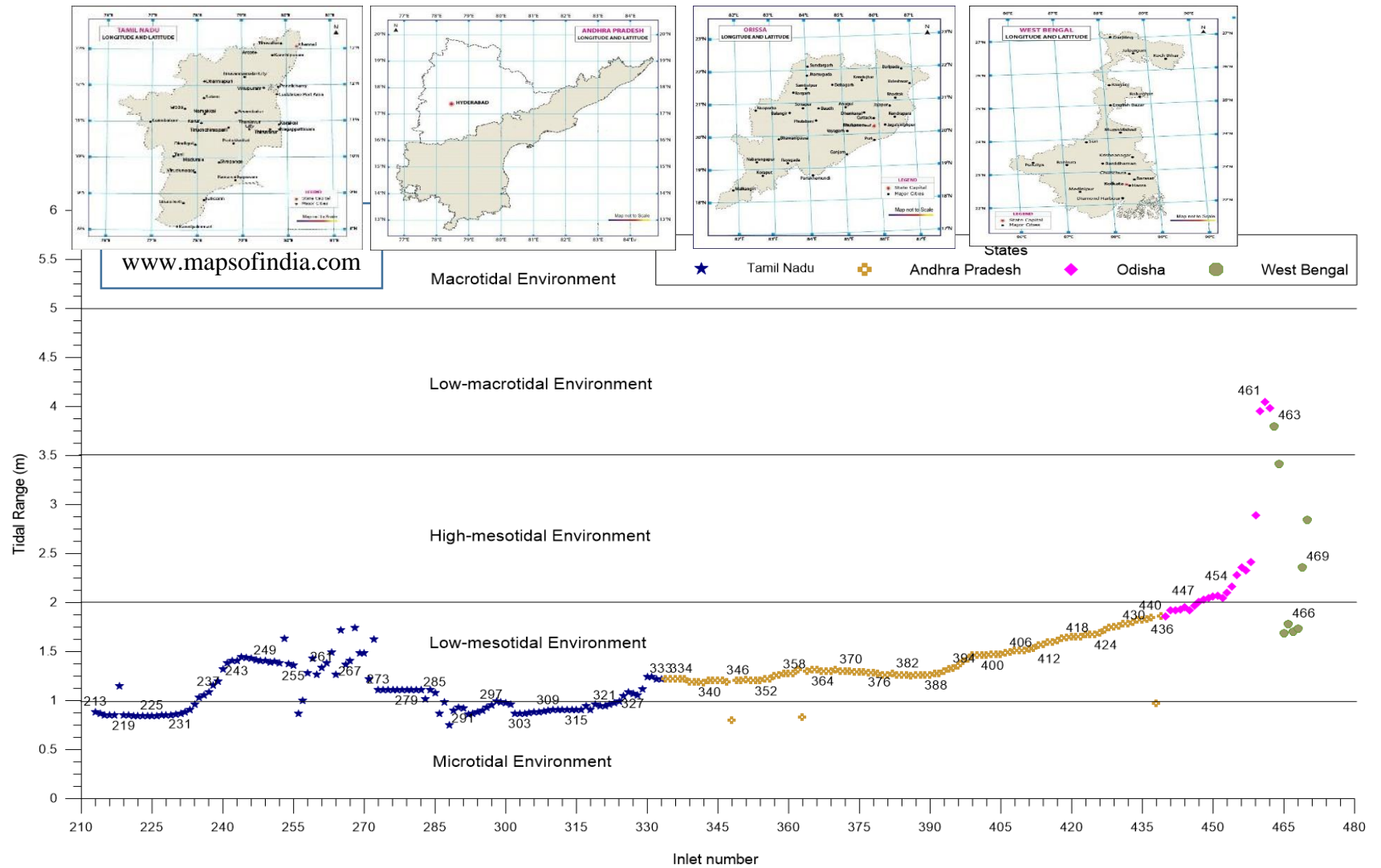


Figure 3.12(b) Classification of tidal inlets along the east coast of India based on Tidal range conditions

In total, along west coast of India (Table A3.1) experiences microtidal environment at 9 inlets (4.2%), low-mesotidal environment at 81 inlets (38%), high-mesotidal environment at 74 inlets (34.74%), low-macrotidal environment at 30 inlets (14.1%) and macrotidal environment at 19 inlets (8.96%). From this, it is understood that the seasonal closure and opening of inlets may be observed mostly along Kerala and Karnataka coasts because of less tidal ranges (Figure 3.12(a)).

Along the east coast of India, out of the 258 inlets 64 tidal inlets (25%) experienced microtidal environment, low-mesotidal environment is for tidal 173 inlets (67%), 17 tidal inlets (6.5%) experience high-mesotidal environment, low-macrotidal environment at four tidal inlets (1.5%) and none of the inlets showed macrotidal environment. Because of less tidal ranges, intermittently closed and opened behavior of tidal inlets may be observed mostly along coastal districts of Tamil Nadu and Andhra Pradesh because of less tidal ranges.

The coast of Tamil Nadu experience microtidal environmental state at 61 inlets which is about 50% of the total inlets and low-mesotidal environmental state at 60 inlets (Figure 3.12(b)). This is only the state observed with most of the inlets in a microtidal regime based on Hayes (1975) classification. The Andhra Pradesh coast showed mostly low-mesotidal behavior except at three tidal inlets under microtidal regime namely Pathapalem, Chintayigiri palem along Nellore coast and Borivenka along Srikakulam coast.

The coast of Odisha is experienced by the three intermediate states of environmental regimes viz. low-mesotidal, high-mesotidal and low-macrotidal (Figure 3.12(b)) and West Bengal are experienced by only two environments namely low-mesotidal and high-mesotidal regimes. The tidal ranges vary between 1.92m to 3.80m along Odisha coast and between 1.70m to 3.74m along West Bengal coast (Figure 3.12(b)). The Odisha coast experience low-mesotidal environmental at six inlets, the high-mesotidal environment at 13 inlets and low-macrotidal environment at four inlets whereas the West Bengal coast

observed with 50% (i.e. four inlets) of the inlets in the low-mesotidal region and 50% (i.e.,four inlets) of the inlets in the high-mesotidal region.

3.5.2. Classification based on wave energy regime

The west coast of India comprised of 213 tidal inlets spread over five coastal states viz. Gujarat, Maharashtra, Goa, Karnataka, and Kerala. The entire west coast of India characterized by high wave energy environment (Figure 3.13(a)) with a minimum wave energy parameter (H^2T^2) of $28.46 \text{ m}^2\text{s}^2$ and maximum wave energy parameter of $112.70 \text{ m}^2\text{s}^2$.

The Gujarat coast experience the annual significant wave height and mean wave period between 0.93m to 1.40m and 5.72s to 7.01s respectively and comprised of minimum and maximum wave energy parameters values of $28.46 \text{ m}^2\text{s}^2$ to $95.64 \text{ m}^2\text{s}^2$ respectively. The Maharashtra coast comprises of 65 tidal inlets which are categorized as high wave energy environment (Figure 3.13(a)). The entire coast is also experienced by medium wave height regime with a minimum value of 1.05m and maximum value of 1.31m. The wave energy ranges between $36.64 \text{ m}^2\text{s}^2$ to $84.29 \text{ m}^2\text{s}^2$. The Goa coast is also experienced by highly exposed wave energy environment at all 11 tidal inlets, but fewer variations are observed in the wave energy at all the inlets. Therefore, not much variations in terms of wave heights and wave period at all the tidal inlets.

All 27 inlets along the Karnataka coast and 68 inlets along the Kerala coast fall under the category of high energy wave environment. The extracted wave heights and wave periods from MIKE21 spectral wave model at 10m water depth are between 1.20m to 1.28m and 6.73s to 6.93s respectively. However, Kerala coast experiences by high wave climate than Karnataka coast (Figure 3.13(a)). Along these two states, it is observed that wave energy

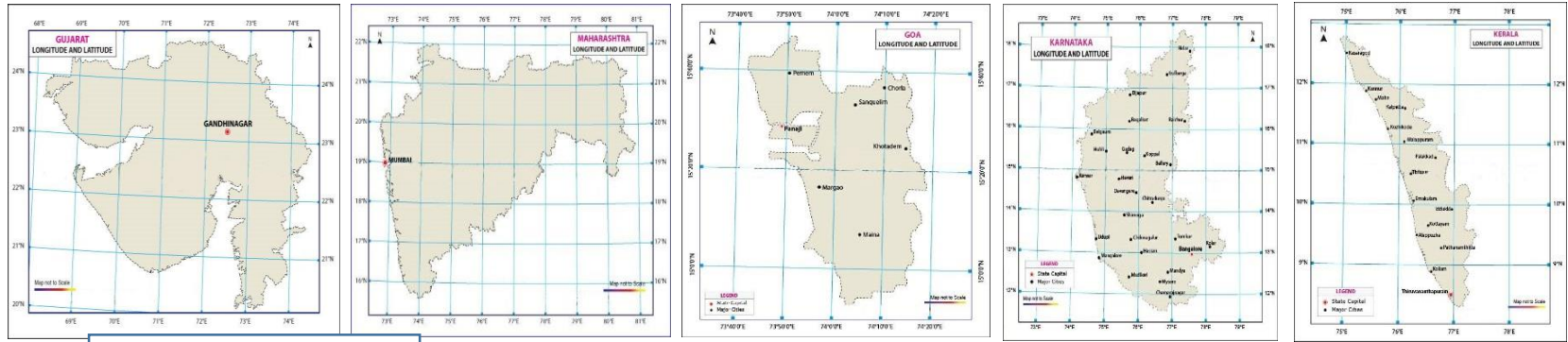
shows zigzag pattern at the inlet entrances when moved from north to south and also observed highest wave energy regime at the southernmost part of Kerala (Figure 3.13(a)).

The coast of Tamil Nadu is exposed to two types of environments. Southern Tamil Nadu coastal inlets which spread over four districts Kanniyakumari, Thirunelveli, Thoothukudi, and Ramanathapuram fall under highly exposed wave energy environment and also northernmost part of Tamil Nadu showed similar wave energy exposure. The remaining coastal states have been observed with moderately exposed wave energy environment. Overall 91 inlets fall under moderately exposed wave energy environment, and only 30 inlets fall under the category of highly wave exposed environment.

Among 106 coastal tidal inlets, the Andhra Pradesh coast experience moderate wave exposed regime at 17 inlets (16% of inlets), and high waveexposedregime at 89 inlets (84% of inlets). Only Tamil Nadu and Andhra Pradesh coasts along Indian coastline are subjected to moderate wave exposure environment and remaining seven coastal states are experienced by high wave energy regime (Figure 3.13(a) and 3.13(b)). The Odisha and West Bengal coasts are also subjected to high wave energy dominance at all inlets. The wave energy parameter (H^2T^2) ranges between $28.21\text{m}^2\text{s}^2$ and $63.76\text{m}^2\text{s}^2$ respectively (Table A3.1).

3.5.3. Geomorphological Classification

According to the geomorphological classification method given by de Vriend et al. (1999), inlets along the west coast of India are mostly subjected to tide dominance environment and low wave activity. Whereas, the inlets along the east coast of India are mostly wave-dominated. Seasonal closure of tidal inlets is observed in about 16% of the inlets along the east coast because of high wave activity during the summer season.



Source:
www.mapsofindia.com

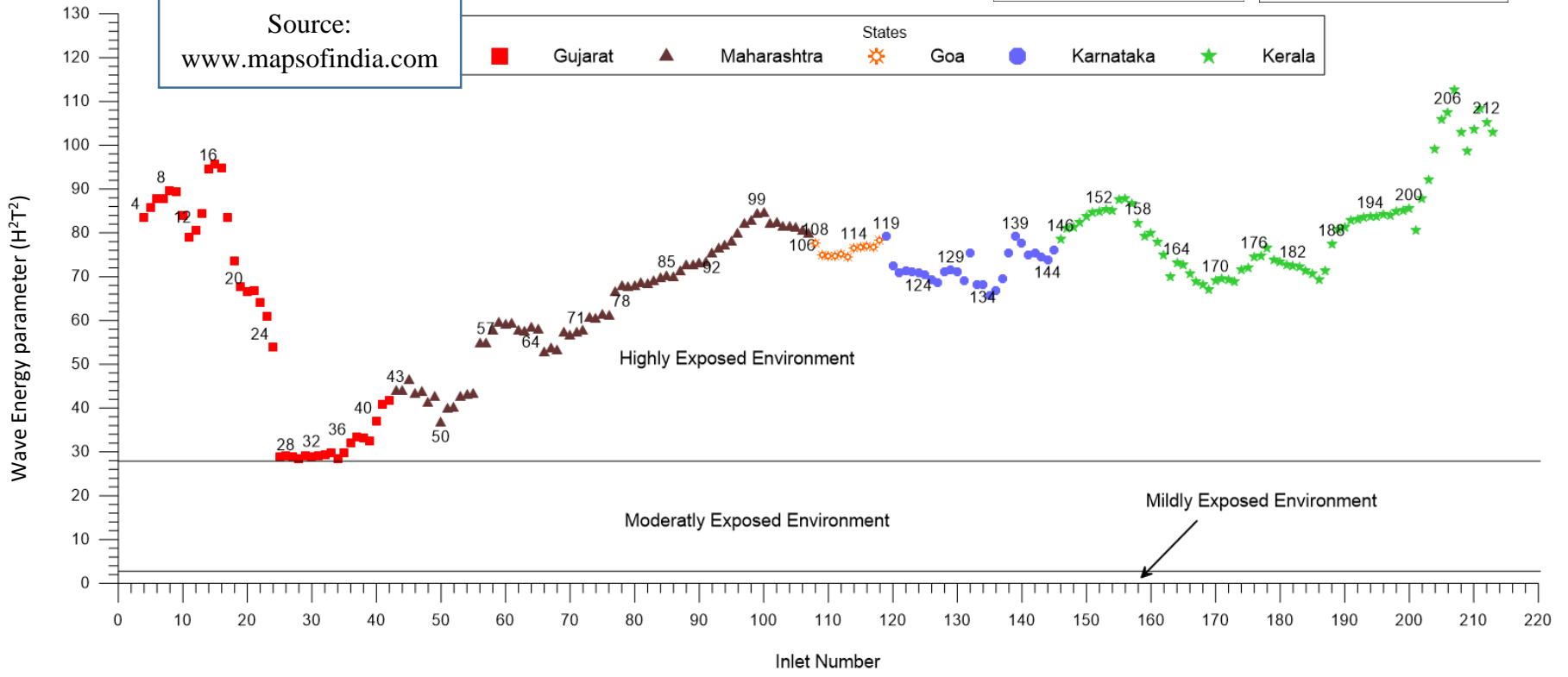
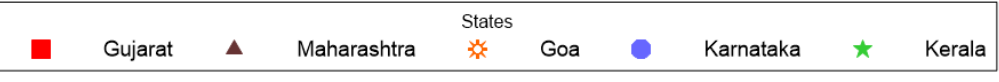


Figure 3.13(a) Classification of tidal inlets along the west coast of India based on wave energy regime

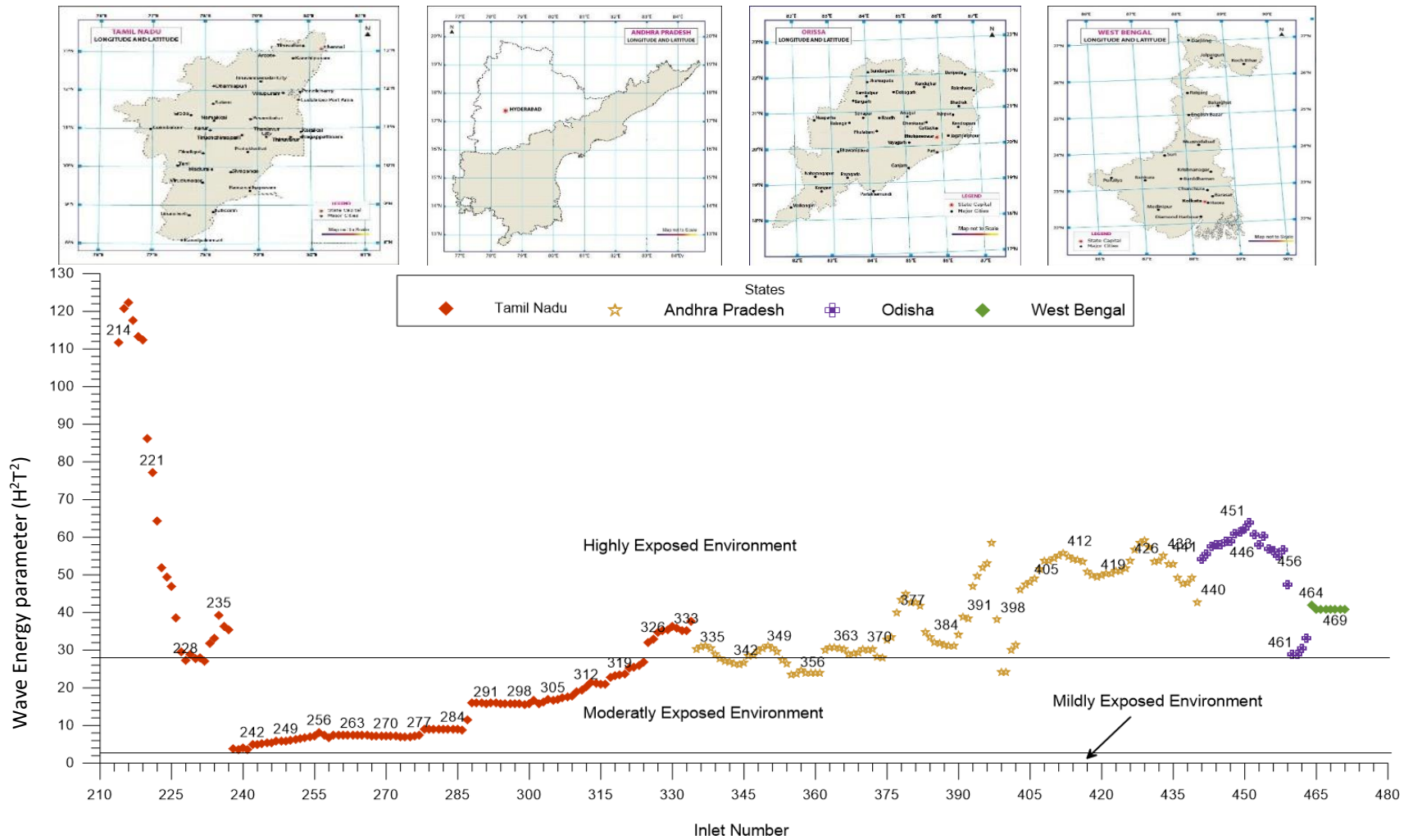


Figure 3.13(b) Classification of tidal inlets along the east coast of India based on wave energy regime

As per the geomorphological classification of the tidal inlets along the coast of India, 246 inlets are observed to be wave-dominated, 97 inlets are found to be tide dominated, 75 are classified as Intermittently Closed and Open Lakes and Lagoons (ICOLLs) and 53 are dominated by the mixed energy of both waves and tides (Table 3.7).

The ICOLLs are specific because of the alternative stage of an open and closed entrance. The inlet entrance is mostly either dominantly open or dominantly closed because the river discharge and tidal forcing are not significant enough to keep the entrance open all the time. Both the bay area and catchment area is small. Therefore, the river discharge is very sensitive to extreme periods of rain. The tidal range is not too large; generally up to 1m, this indicated a micro-tidal regime. The character of all the ICOLLs may not be available in Google Earth®. Such data could be obtained from alternative sources, e.g., through satellite imageries. The inlet cannot be perpetually classified as a wave or tide-dominated because the wave and tide forces modify the inlet discharge and corresponding sediment transport and morphology for the tidal dominated system and wave-dominated the system.

Table 3.7 Summary of Geomorphological classification (de Vriend et al., 1999)

S. No.	State	TideDominated	Wave Dominated	Mixed Energy	ICOLLs
1	Gujarat	30	02	04	06
2	Maharashtra	48	16	-	01
3	Goa	01	10	-	-
4	Karnataka	-	19	08	-
5	Kerala	-	41	03	24
6	Tamil Nadu	15	69	20	17
7	Andhra Pradesh	-	65	14	27
8	Odisha	02	18	02	-
9	West Bengal	01	06	01	-

Most of the inlets along Gujarat and Maharashtra coastline are tide-dominated (Table A3.2), this is because of the submerged coast. Another reason is since the Arabian Sea is less wide in comparison with Bay of Bengal, the tides occur and pull up the sea water, the force is spread over the smaller domain, and the equivalent rise in water is more. On the other hand, most of the inlets along the east coast of India are wave dominated because of high wave activity in relative comparison with the tide. Mixed energy inlets are also more along the Tamil Nadu and Andhra Pradesh coasts (Table A3.2). Few inlets along Kerala, Tamil Nadu, and Andhra Pradesh coastlines are ICOLLs, this is because of the river discharge, and tidal forcing is not significant enough to keep the entrance open all the time. Both the bay area and catchment area is small. Therefore, the river discharge is very sensitive to extreme periods of rain.

3.5.4. Hydrodynamic Classification

The classification of inlets as per hydrodynamic classification considering annual average wave climate showed that 285 inlets fall under mixed energy classification followed by 129 wave-dominated inlets and 54 tide-dominated inlets (Table A3.3).

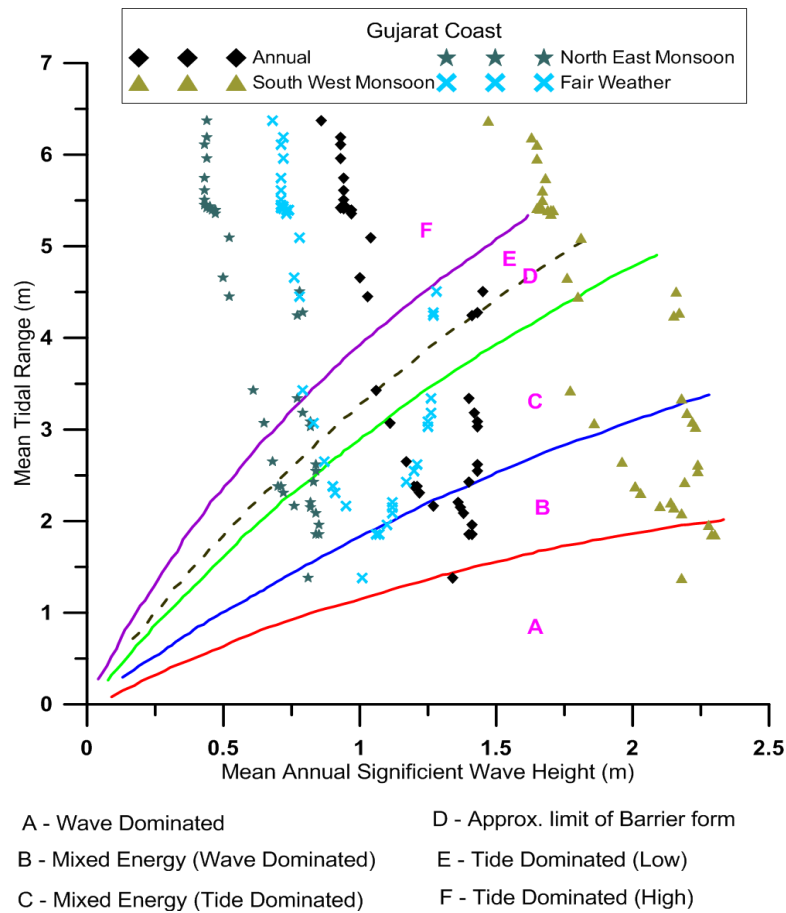


Figure 3.14 Classification based on Hayes (1979) for all seasons along Gujarat coast

However, four of the inlets fell into the classification of ICOLLs (Table 3.8(a)). The inlets considered along the Gujarat coast experience tidal ranges between 1m to 7m and the wave climate ranges between 0.5m during the NE monsoon period to about 2.5m during SW monsoon. This large variation in the tide and wave places the inlets into various classifications ranging from Tide dominated to Wave dominated (Figure 3.14). The inlets in the north Gujarat coast experience high tidal range and even though the wave heights vary from ~0.5m to ~1.75m these inlets fall in the tide-dominated classification. The inlets along the south Gujarat coast having a tidal range less than 5m experience varying wave heights during different seasons thereby undergoing changing dominance of tides and waves.

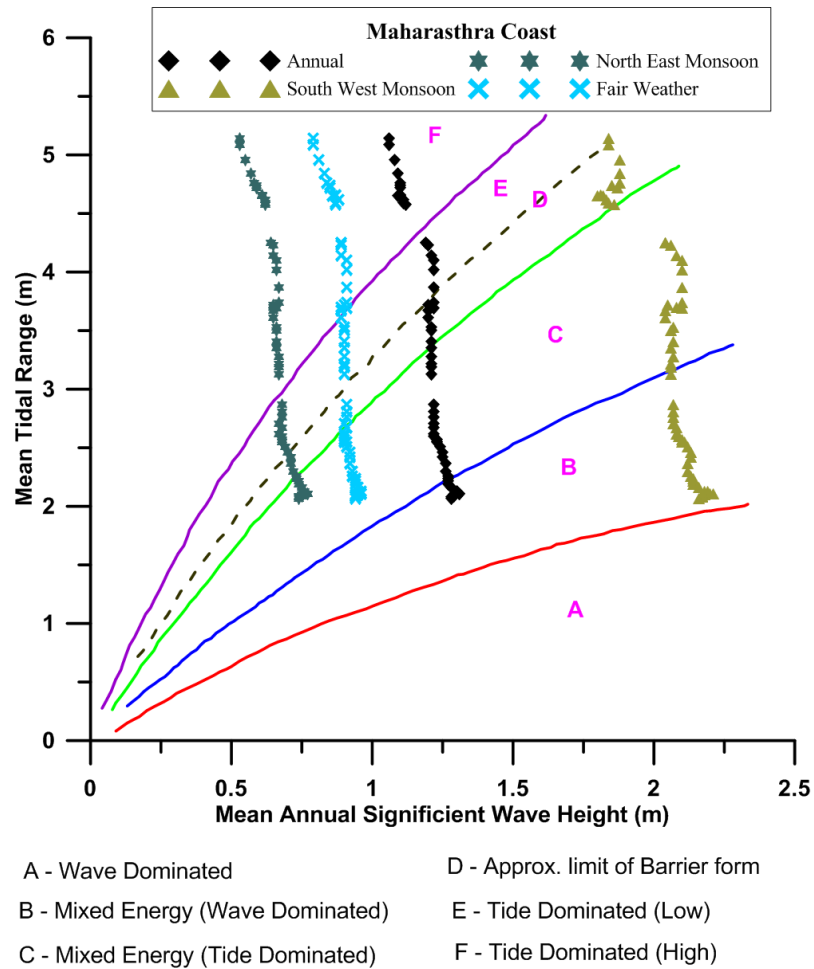


Figure 3.15 Classification based on Hayes (1979) for all seasons along Maharashtra coast

Some of the inlets along Gujarat coast are having similar tidal range but different wave climate, these are shown within a rectangle in Figure 3.14. The behavior of inlets in the northern part of Gujarat coast is different when compared with the southern Gujarat inlets and other states like Maharashtra, Goa, and Karnataka, which due to the wave activity being quite different for northern and southern parts of Gujarat (Figure 3.14).

The inlets along the Maharashtra coast are exposed to similar wave climate that of Gujarat respectively in different seasons although their tidal range varies between 2m and 5m. Despite the variation in seasonal wave climate, the inlets in the northern region are mostly tide-dominated (Figure3.15).

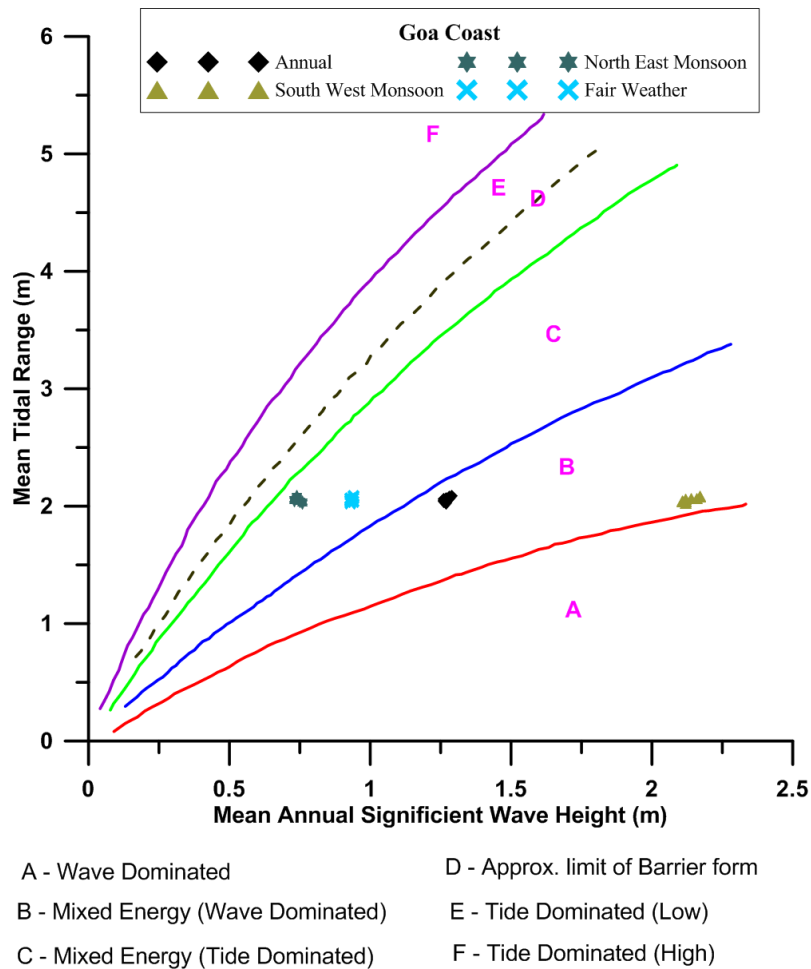


Figure 3.16 Classification based on Hayes (1979) for all seasons along Goa coast

The inlets along central Maharashtra are mixed energy tide-dominated during most of the period but are wave dominated during the southwest monsoon. Whereas, the inlets along south Maharashtra coast are predominantly wave-dominated.

The tidal range and wave climate is similar for all the Goa inlets, but the wave climate varies seasonally. The inlets along Goa coast are mixed energy tide-dominated during fair-weather and northeast monsoon periods while they are mixed energy wave dominated during the rest of the year (Figure 3.16).

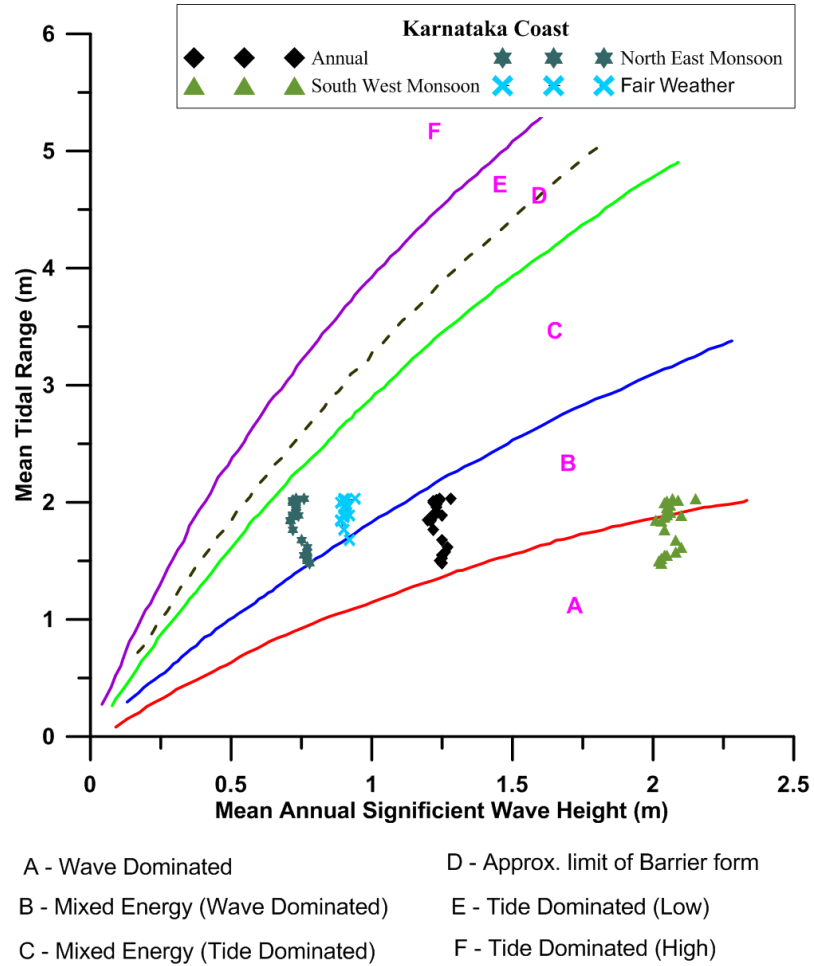


Figure 3.17 Classification based on Hayes (1979) for all seasons along Karnataka coast

The tidal range for Karnataka coast is between ~1.2m and ~2m with reducing tidal elevation southwards. The wave climate slightly varies during southwest monsoon period and almost similar for all the inlets during the rest of the year. During northeast monsoon period, all the inlets in Karnataka are mixed energy tide dominated, whereas, during fair-

weather period half of these inlets are mixed energy (either tide dominated or wave-dominated). During southwest monsoon majority of the inlets are wave dominated while some of the inlets are mixed energy wave dominated (Figure 3.17). Kerala coast experiences tides between 0.5m to 1.5m and most of the time are wave dominated (Figure 3.18).

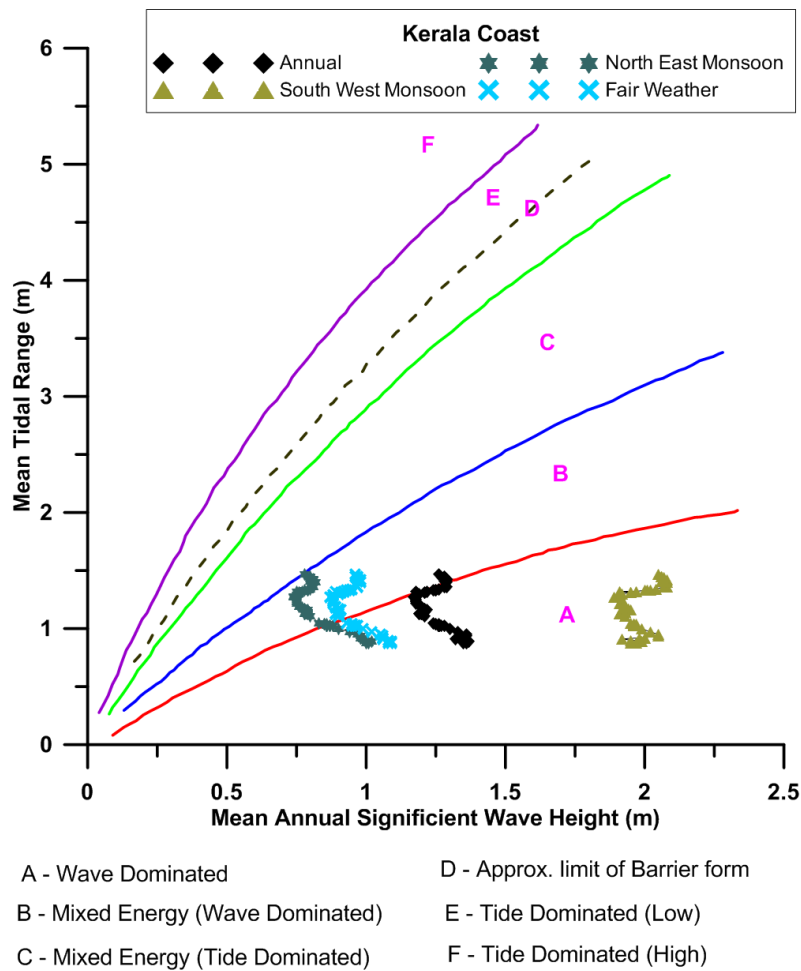


Figure 3.18 Classification based on Hayes (1979) for all seasons along Kerala coast

The season-wise variations of wave heights along with the respective tidal ranges along Gujarat, Maharashtra, Goa, Karnataka, and Kerala respectively are shown in Figures 3.14-3.18. It can be observed that in Gujarat and Maharashtra, the dominance of wave and tide

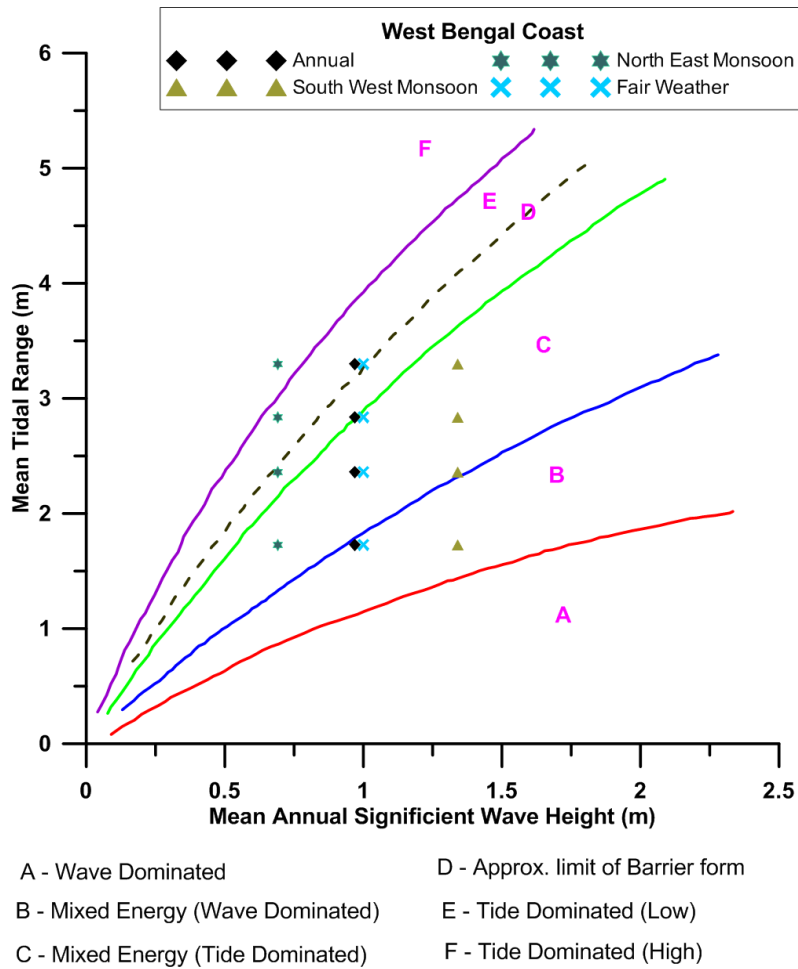


Figure 3.22 Classification based on Hayes (1979) for all seasons along West Bengal coast

The classification of inlets as per hydrodynamic classification considering South West monsoon, North East monsoon, and Fair Weather season wave climate showed that 232, 288, 307 inlets fall under mixed energy classification followed by 202, 89, 95 wave-dominated inlets and 35, 93, 67 tide-dominated inlets respectively (Table 3.8(b), 3.8(c), and 3.7(d)). However, only two inlets in South West monsoon, one inlet in North East monsoon and two of the inlets in Fairweather season fell into the classification of ICOLLs.

Table 3.8(a) Summary of Hydrodynamic classification (Annual)

S.No.	State	WD	ME (WD)	ME (TD)	TD (L)	TD (H)	Barrier formation
1	Gujarat	1	7	12	1	18	3
2	Maharashrta	-	14	22	16	13	-
3	Goa	-	11	-	-	-	-
4	Karnataka	-	27	-	-	-	-
5	Kerala	57	11	-	-	-	-
6	Tamil Nadu	69	20	33	-	-	-
7	Andhra Pradesh	3	103	-	-	-	-
8	Odisha	-	11	6	2	3	-
9	West Bengal	-	5	2	-	-	1

Table 3.8 (b) Summary of Hydrodynamic classification (South West Monsoon)

S.No.	State	WD	ME (WD)	ME (TD)	TD (L)	TD (H)	Barrier formation
1	Gujarat	3	13	6	8	11	1
2	Maharashrta	-	32	20	12	-	1
3	Goa	-	11	-	-	-	-
4	Karnataka	15	12	-	-	-	-
5	Kerala	68	-	-	-	-	-
6	Tamil Nadu	74	17	31	-	-	-
7	Andhra Pradesh	42	64	-	-	-	-
8	Odisha	-	16	2	4	-	-
9	West Bengal	-	5	3	-	-	-

Table 3.8 (c) Summary of Hydrodynamic classification (North East Monsoon)

S.No.	State	WD	ME (WD)	ME (TD)	TD (L)	TD (H)	Barrier formation
1	Gujarat	-	1	8	9	24	-
2	Maharashrta	-	-	15	15	34	1
3	Goa	-	-	11	-	-	-
4	Karnataka	-	-	27	-	-	-
5	Kerala	23	45	-	-	-	-
6	Tamil Nadu	63	25	34	-	-	-
7	Andhra Pradesh	3	99	4	-	-	-
8	Odisha	-	-	15	2	5	-
9	West Bengal	-	-	4	2	2	-

Table 3.8 (d) Summary of Hydrodynamic classification (Fair Weather)

S.No.	State	WD	ME (WD)	ME (TD)	TD (L)	TD (H)	Barrier formation
1	Gujarat	-	4	13	5	20	-
2	Maharashrta	-	-	27	13	25	-
3	Goa	-	-	11	-	-	-
4	Karnataka	-	8	19	-	-	-
5	Kerala	26	42	-	-	-	-
6	Tamil Nadu	66	22	34	-	-	-
7	Andhra Pradesh	3	89	14	-	-	-
8	Odisha	-	12	6	-	3	1
9	West Bengal	-	4	2	1	-	1

3.5.5. Classification based on dimensionless parameters without wave period

The dimensionless classifications are excellent tools to divide the tidal inlet systems into various groups by specifying their characteristics. The tidal inlet systems classification was carried out using hydraulics, and morphodynamics perspective along the coast of New South Wales (NSW) since the sustainability of the environment is given more attention (Vu, 2013).

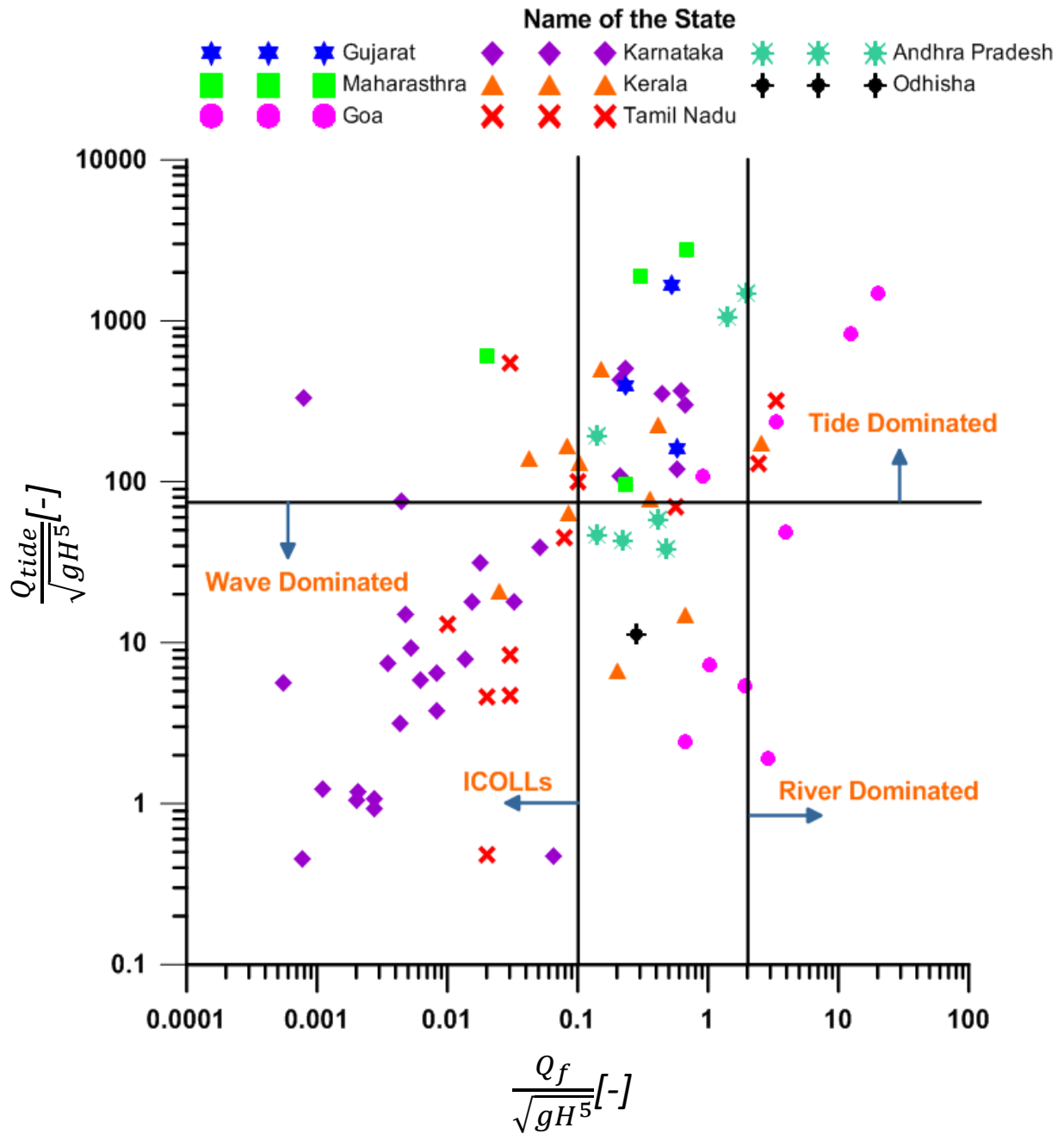


Figure 3.23 Classification based on dimensionless parameters without wave period

The classification introduced by Vu(2013) is based on dimensionless parameters which represent the relative strength of the three main forcing agents, viz., tide, waves, and river flow.

Three parameters were derived Q_f (yearly averaged river discharge in m^3/s), $\sqrt{gH^5}$ (yearly averaged wave forcing in m^3/s), and Q_{Tide} (yearly averaged peak tidal discharge in m^3/s). These three parameters are compared to each other leading to the three classes of classification. The classes are non-dimensional wave-dominated, tide-dominated and river-dominated inlet systems.

The non-dimensional parameters $\frac{Q_{tide}}{\sqrt{gH^5}}$ and $\frac{Q_f}{\sqrt{gH^5}}$ are introduced in which tidal forcings is quantified in terms of the peak tidal discharge and wave forcing represented in terms of sediment transport capacity. The conditions for different inlet classification are given in Table 3.5. The wave dominated tidal inlets have three subclasses viz. Intermittently Closed and Opened Lakes and Lagoon (ICOLLs) for which $\frac{Q_f}{\sqrt{gH^5}} < 0.1$ and $\frac{Q_{tide}}{\sqrt{gH^5}} = \frac{0.08}{75}$, Wave Dominated Deltas (WDD) for which $\frac{Q_f}{\sqrt{gH^5}} = \frac{0.05}{7}$ and $\frac{Q_{tide}}{\sqrt{gH^5}} = \frac{3}{100}$ and Wave Dominated Estuaries (WDE) for which $\frac{Q_f}{\sqrt{gH^5}} = \frac{0.005}{2}$ and $\frac{Q_{tide}}{\sqrt{gH^5}} = \frac{1}{75}$. However, Vu (2013) also mentioned that the subclasses of the wave dominated group is not clear using the above classification.

In the present study, only one subclass, i.e., ICOLLs is considered to study the 75 among 471 tidal inlets along the Indian coastline where sufficient information is available regarding the river discharge (Figure 3.23). The tide-dominated inlets have two subclasses namely Bays for which $\frac{Q_f}{\sqrt{gH^5}} = \frac{0.003}{0.12}$ and $\frac{Q_{tide}}{\sqrt{gH^5}} = \frac{200}{875}$ and Tide Dominated Estuaries (TDE) for which $\frac{Q_f}{\sqrt{gH^5}} \geq 0.005$ and $\frac{Q_{tide}}{\sqrt{gH^5}} = \frac{75}{715}$. The Ravdanda inlet in Maharashtra and Sadurangapattinam inlet in Tamil Nadu shows tide dominance under the subclass Bay. This is because of very small influence of wave and fresh water flow. The Ravdanda inlet and Sudurangapattinam inlets have the largest values of $\frac{Q_{tide}}{\sqrt{gH^5}} = 600$ and 548 corresponding to the largest tidal prism values ($44127002m^3$, $26934939m^3$) and very small $\frac{Q_f}{\sqrt{gH^5}} = 0.02$ and 0.03 respectively.

In river dominated groups, there are two wave dominated inlets (both in Goa state), and six tide-dominated inlets (three in Goa, two in Tamil Nadu and one in Kerala). The Mandovi River and Zuari estuary has the strongest river dominance with $\frac{Q_r}{\sqrt{gH^5}} = 20.31$ and 12.38 respectively. Six out of eleven inlets in Tamil Nadu, twenty out of twenty-nine inlets in Karnataka and two out of eleven in Kerala fall into wave dominated ICOLLs classification. The ICOLLs become isolated from the sea for a longer period of time by the combination of climatic and other reasons. The ICOLLs, when closed, are non-tidal for a long time of period. After a heavy rainfall the beach berms are breached by storm waves and/or high-water level differences between ocean and lagoon. This process is often manipulated by man to prevent the lagoon from flooding. The unpredictability of the rainfall in this area means that the opening behavior is intermittent and inconsistent. All inlets from Gujarat and Maharashtra come under tide dominance because the tidal ranges are relatively more compared to wave heights. In totality the classification method introduced by Vu (2013) classify the 75 tidal inlet systems (Figure 3.23) for the present study as: Tide dominated (32); tide dominated-bays (2); river dominated (2); wave dominated (11) and wave dominated ICOLLs (28).

3.5.6. Classification based on dimensionless parameters with wave period

To compare the peak tidal discharge with waves at inlet morphology, there are two choices. The simple one is $\frac{Q_{\text{tide}}}{\sqrt{gH^5}}$ which compares Q_{tide} to the sediment transport capacity of the waves as per CERC formula for littoral drift (Nielsen, 2009). More complicated measure compared $\frac{Q_{\text{tide}}}{gTH^2}$ which brings in the mean wave period (T) also into consideration, which is important in relation to runup height (Nielsen, 2009) and the waves' ability to build berms (Takeda and Sunamura, 1982), which eventually close the inlets (Vu, 2013). Vu (2013) discussed the methodology of classification by including the wave period but did not classified the inlets and hence this method is referred as modified Vu method.

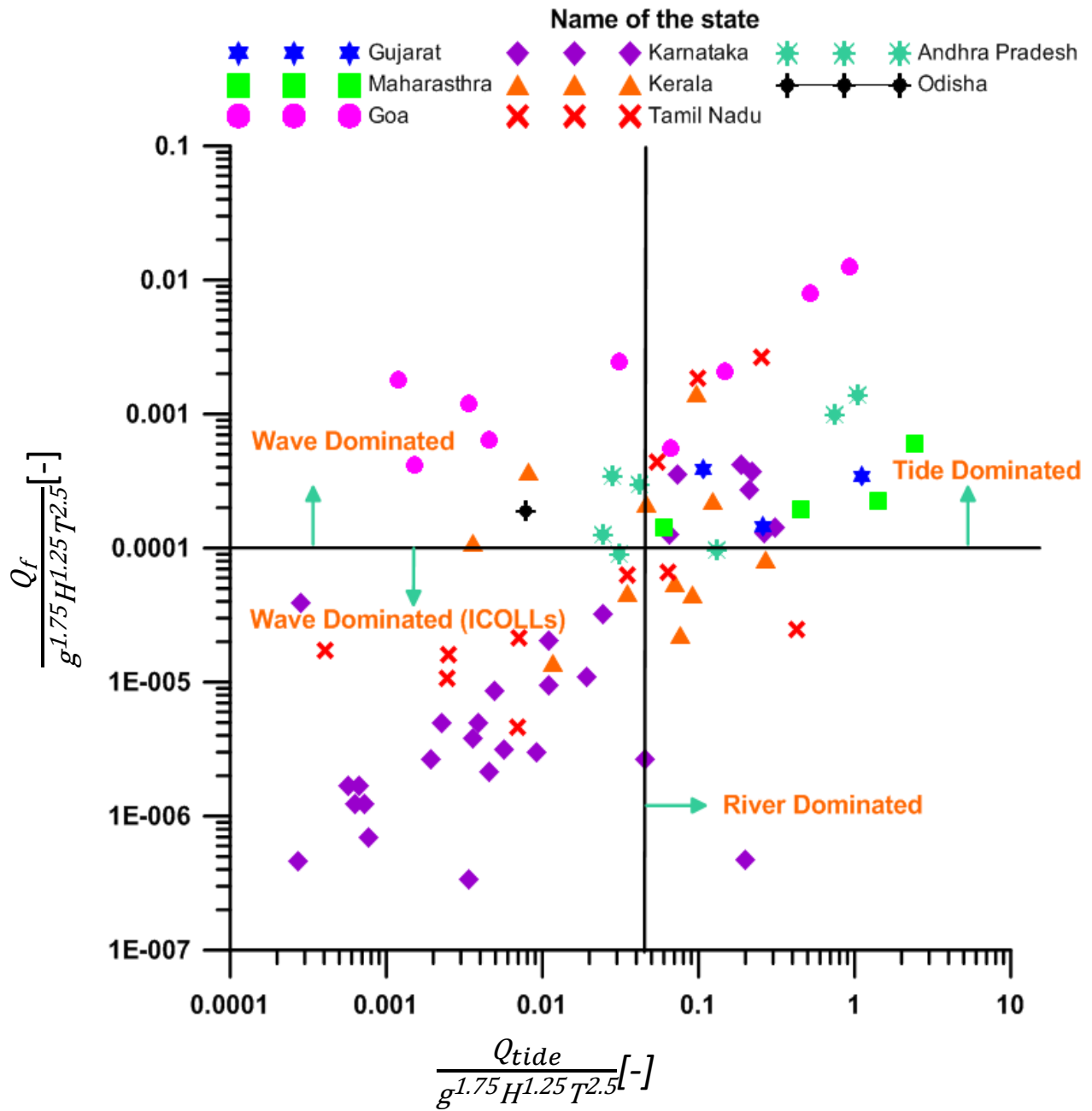


Figure 3.24 Classification based on dimensionless parameters with wave period

Modified Vu method considered wave period (T) in addition to the wave height (H) in the dimensionless parameters $\frac{Q_{\text{tide}}}{\sqrt{gH^5}}$ and $\frac{Q_f}{\sqrt{gH^5}}$ by the runup scale which leads to new dimensionless parameters $\frac{Q_f}{(g^{1.75}H^{1.25}T^{2.5})}$ and $\frac{Q_{\text{tide}}}{(g^{1.75}H^{1.25}T^{2.5})}$ respectively. A set of new range is identified for each of the dominance criteria considering the geomorphology classification as shown in Table 3.6.

Considering the new set of classification range, classification of 75 inlets along Indian coast based on dimensionless parameters considering wave period clearly differentiates the different inlets (Figure 3.24). Due to limited river discharge data available all the inlets were not classified, using this modified method. In totality the classification by modified Vu classify the 75 tidal inlet systems for the present study as: Tide dominated (27); wave dominated (11); wave dominated-ICOLLs (30); river dominated (7).

3.6. COMPARISON OF TIDAL INLET CLASSIFICATIONS

Geomorphological classification being the visual method of classifying the inlets has been considered as the base method with which other classification methods are compared. The hydrologic, non-dimensional Vu and non-dimensional modified Vu methods are compared in this section.

3.6.1. Geomorphological Vs Hydrological classification

All the inlets considered for the classification using hydrodynamics (i.e., tide range Vs. mean wave height) led to only two limiting conditions of Tide Dominated (TD) and Wave Dominated (WD). The inlets along the states of Gujarat and Maharashtra exhibited tide dominance while rest of them exhibit wave dominance. Along the Gujarat and Maharashtra states on the west coast of India and the states of Andhra Pradesh and Odisha on the east coast of India show 100% agreement in comparison with hydrological classification (Table

3.9). Majority of the inlets along the states of Karnataka (24 out of 29 inlets) and Tamil Nadu (10 out of 11 inlets) showed the same type of dominance with respect to both the methods. Only about 55% of the inlets along the coasts of Goa (5 inlets) and Kerala (6 inlets) showed similar Wave Dominated inlets. Overall 80% of the inlets (60 inlets) showed the same classification for both the methods (Table 3.9), because Hayes classification has limited applicability for describing the morphology of tidal inlets, and even though tidal range serves as a surrogate for tidal prism. Moreover, this method did not improve the classification (Carr-Betts, 2012). Also, the river discharge, which is a significant influencing parameter for the shaping of the inlet, is not included in this classification method.

3.6.2. Geomorphological Vs Non-dimensional Vu method

Similar to the hydrological classification, the non-dimensional method as per Vu (2013) also showed 100% agreement with geomorphological classification along four maritime states of India viz. Gujarat, Maharashtra, Andhra Pradesh and Odisha (Table 3.9). The Vu method showed better agreement than hydrological classification along the states of Goa (7 inlets) and Karnataka (26 inlets) whereas along the Tamil Nadu coast it exhibits slightly less agreement (8 inlets). The type of dominance along the Kerala coast remains unchanged. In total 81.33% of the inlets (61 inlets) showed the same classification through both the methods (Table 3.9).

In the river dominated group, there are six tide dominated-rivers and two wave dominated-rivers. The Mandovi (Inlet No: 111) and Zuari (Inlet No: 112) rivers have the strongest river dominance with $\frac{Q_f}{\sqrt{gH^5}}$ values of 20.31 and 12.58 respectively. The inlets along the Maharashtra coast namely Bhadve inlet (Inlet No: 50) and Mandve inlet (Inlet No: 57) has the strongest influence of tide with $\frac{Q_{\text{tide}}}{\sqrt{gH^5}}$ being 2750.78 and 1884 respectively.

3.6.3. Geomorphological Vs. Non-dimensional modified Vu method

Non-dimensional Vu method including mean wave period referred as modified Vu method showed 100% agreement with geomorphological classification along five coastal states of India viz. Gujarat, Maharashtra, and Goa on the west coast of India and Andhra Pradesh and Odisha on the east coast of India (Table 3.9). Majority of the inlets (86.2%) along the Karnataka coast has the same time of dominance, whereas along the Kerala (6 inlets) and Tamil Nadu (6 inlets) coasts exhibits only about 55 % similarity regarding the type of dominance at the inlets.

Like non-dimensional Vu method, here also the Bhadve inlet (Inlet No: 50) and Mandve inlet (Inlet No: 57) along the coast of Maharashtra have the strongest influence of tide with $\frac{Q_{\text{tide}}}{g^{1.75}H^{1.25}T^{2.5}} = 2.413$ and 1.404 respectively. The river dominated inlets are observed along Karnataka (1 inlet), Kerala (4 inlets) and Tamil Nadu (2 inlets) coasts with strongest river dominance of $\frac{Q_f}{g^{1.75}H^{1.25}T^{2.5}}$ values of 0.0127 and 0.0079 at Mandovi river and Zuari river respectively.

3.5.4. Comparison of all methods

The four classification methods (Table 3.9) viz., geomorphological, hydrological and dimensionless method without wave period and dimensionless method with wave period showed good agreement for the classification at 44 inlets. The inlets along the states Gujarat (Inlet Nos: 26, 27, 33), Maharashtra (Inlet Nos: 50, 57, 64 and 87) and Odisha (Inlet No: 445) show 100% agreement for all the methods mentioned above. Majority of the inlets (19 inlets) along the coastal state of Karnataka showed the same type of dominance. About 50% of the inlets along the Tamil Nadu (6 inlets) and Andhra Pradesh (4 inlets) coasts fall under the same type of dominance. Only 33.33% (3 inlets) agreement was found in the inlets along the state of Goa and 27.27% (3 inlets) agreement along the Kerala coast.

Both the non-dimensional methods (i.e., with and without wave period) gave a similar type of dominance at 61 tidal inlets when compared with geomorphological classification. However with reference to the geomorphological classification, the inlets are visually examined, and the dominance of wave, tide or river is decided. The visual examination of the tidal inlet may not be correct all the time. As of now, the tidal inlets are classified from the available satellite images. It would be more specific if the images of the tidal inlets are obtained in all the seasons. This seasonal geomorphological classification, on comparing with other methods gives a better idea about the character of the tidal inlets seasonally. In addition to that, a detailed investigation is needed in all aspects to determine the exact behaviour of the inlet.

Table 3.9 Comparison of tidal inlet classifications for locations with river discharge along the Indian coast

Inlet No	Inlet Name	Classification type			
		Geomorphological (deVriend et.al. 1999)	Hydrological (Hayes 1979)	Dimensionless without wave period (Vu 2013)	Dimensionless with wave period (Modified Vu)
26	Mindhola river	TD	TD(H)	TD	TD
27	Puma river	TD	TD(H)	TD	TD
33	Daman	TD	TD (H)	TD	TD
50	Bhadve	TD	TD(H)	TD	TD
57	Mandve	TD	TD(L)	TD	TD
64	Revdanda	TD	TD(L)	TD (Bay)	TD
87	Bhatiwadi	TD	ME(TD)	TD	TD
108	Tiracol inlet	TD	ME (WD)	TD	TD
109	Siolim inlet	TD	ME (WD)	TD	TD
110	Baga inlet	WD	ME (WD)	WD	WD
111	Mandovi river	TD	ME (WD)	TD	TD
112	Zuari estuary	TD	ME (WD)	TD	TD
113	Mobor inlet	WD	ME (WD)	RD	WD
114	Cola inlet	WD	ME (WD)	WD	WD
117	Canacona inlet 1	WD	ME (WD)	RD	WD
118	Mashem inlet	WD	ME (WD)	WD	WD
119	Karwar	TD	ME (WD)	TD	TD
120	Chendia	WD	ME (WD)	WD (ICOLLs)	WD (ICOLLs)
121	Todur	WD	ME (WD)	WD (ICOLLs)	WD (ICOLLs)
122	Belekeri	Mixed Energy	ME (WD)	WD (ICOLLs)	WD (ICOLLs)

123	Ankola	WD	ME (WD)	WD (ICOLLs)	WD (ICOLLs)
124	Belamber	WD	ME (WD)	TD	TD
125	Manjaguni	TD	ME (WD)	TD	TD
126	Tadadi port	Mixed Energy	ME (WD)	WD (ICOLLs)	WD (ICOLLs)
127	Alvekodi 2	Mixed Energy	ME (WD)	WD (ICOLLs)	WD (ICOLLs)
128	Karki	WD	ME (WD)	TD	TD
128_1	Manki	WD	ME (WD)	WD (ICOLLs)	WD (ICOLLs)
129	Nakhuda	Mixed Energy	ME (WD)	WD (ICOLLs)	WD (ICOLLs)
130	Alvekodi 1	WD	ME (WD)	WD (ICOLLs)	WD (ICOLLs)
131	Jali	Mixed Energy	ME (WD)	WD (ICOLLs)	WD (ICOLLs)
132	Mavakurve	WD	ME (WD)	WD (ICOLLs)	WD (ICOLLs)
133	Hadin	WD	ME (WD)	WD (ICOLLs)	WD (ICOLLs)
133_1	Gorta	WD	ME (WD)	WD (ICOLLs)	WD (ICOLLs)
134	Alvegadde	Mixed Energy	ME (WD)	WD (ICOLLs)	WD (ICOLLs)
135	Paduvari	Mixed Energy	ME (WD)	WD (ICOLLs)	WD (ICOLLs)
136	Koderi	Mixed Energy	ME (WD)	WD (ICOLLs)	WD (ICOLLs)
137	Gangoli	TD	ME (WD)	TD	TD
138	Kundapura	TD	ME (WD)	TD	RD
138_1	Badanidiyoor	WD	ME (WD)	WD (ICOLLs)	WD (ICOLLs)
139	Malpe	WD	ME (WD)	TD	TD
140	Kaup	WD	ME (WD)	WD (ICOLLs)	WD (ICOLLs)
141	Nadsal	WD	ME (WD)	WD (ICOLLs)	WD (ICOLLs)
142	Hejamadi	Mixed Energy	ME (WD)	TD	WD(ICOLLs)
144	Gurpur & Netravati	TD	ME (WD)	TD	TD
145	Kanwatheertha	WD	ME (WD)	WD (ICOLLs)	WD (ICOLLs)
150	Thalangara	WD	ME(WD)	TD	TD
162	Mahe	TD	ME(WD)	WD (ICOLLs)	WD (ICOLLs)
166	Iringal	WD	WD	WD (ICOLLs)	WD (ICOLLs)
169	Elathur	WD	WD	TD	RD
170	Thekupuram	WD	WD	WD	WD
171	Balathiruthi	WD	WD	TD	RD
174	Ponnani	TD	WD	TD	TD
178	Chettuva	TD	WD	TD	RD
186	Munambam	TD	WD	TD	TD
203	Thottapally lake	WD	WD	WD	WD
206	Neendakara	RD	WD	TD	RD
214	Erayumanthurai	WD	WD	WD (ICOLLs)	WD (ICOLLs)
218	Manakudi	WD	WD	WD (ICOLLs)	WD (ICOLLs)
226	Punnakayal	WD	WD	TD	RD
229	Vaippar	WD	WD	WD (ICOLLs)	WD (ICOLLs)
301	Keezhaiyur 2	WD	WD	WD (ICOLLs)	WD (ICOLLs)
304	Akkampettai	WD	WD	WD (ICOLLs)	WD (ICOLLs)
312	Pazhaiyar	WD	WD	TD	TD
314	Ariyakoshti	WD	WD	TD	TD
320	Subauppallavadi	WD	WD	WD (ICOLLs)	WD (ICOLLs)
322	C veerampattinam	WD	WD	WD	TD

328	Sudurangapattinam	TD	WD	TD (Bay)	RD
340	Swanamukhi river	WD	ME(WD)	WD	WD (ICOLLs)
351	Utukuru	Mixed Energy	ME(WD)	TD	TD
363	Chintayigari palem	WD	WD	WD	WD
377	LVD	Mixed Energy	ME(WD)	TD	TD
378	Elachetladibba	Mixed Energy	ME(WD)	TD	TD
427	Bontalakoduru	WD	ME(WD)	WD	WD
430	Kalingapatanam	Mixed Energy	ME(WD)	WD	WD
445	Pallibandha	WD	ME(WD)	WD	WD

3.6. SUMMARY

A total of 471 tidal inlets are classified along the nine maritime states of India viz. Gujarat, Maharashtra, Goa, Karnataka and Kerala on the west coast of India and Tamil Nadu, Andhra Pradesh, Odisha and West Bengal on the east coast of India using different coastal classification systems such as tidal range, wave exposure conditions, geomorphological, hydrodynamic, dimensionless classification with and without wave period. Inlets with greater than 5m width were considered. The non-dimensional classification which represents the relative strength of the tide, waves, and river flow along with the wave period into consideration gave better agreement with the geomorphology classification along the Indian coastline. Different season's wave heights and wave periods are considered to identify the seasonal variations in the classification of the inlets. The non-dimensional classification incorporating the mean wave period gave rise to a new range of values. The modified Vu method is observed to classify the inlets more appropriately compared to the dimensionless classification without considering wave period. Majority of the tidal inlets on the east coast of India and the southern regions on the west coast (Kerala, Karnataka, and Goa) are observed to be wave-dominated inlets, whereas, the inlets towards the north on the west coast (Maharashtra and Gujarat) are tide-dominated.

The summary of the different classification systems for 471 Indian coastal tidal inlets are:

(i) As per Davies (1964) classification, 41 inlets are macrotidal, 102 being mesotidal, 328

inlets are dominated by the microtidal environments; (ii) As per Hayes (1975) classification, 75 being microtidal, 253 being low mesotidal, 91 inlets are high mesotidal, 34 being low macrotidal and 18 are classified as macrotidal environments; (iii) As per de Vriend et al. (1999) classification, 97 inlets are tide dominated, 246 being wave dominated, 52 being dominated by the mixed energy of both waves and tides and 75 are classified as Intermittently Closed and Open Lakes and Lagoons (ICOLLS); (iv) As per hydrodynamic classification 285, 232, 288, 307 inlets fall under mixed energy classification followed by 129, 202, 89, 95 wave-dominated inlets and 54, 35, 93, 67 tide dominated inlets for annual, south west, north east and fair weather seasons respectively. However, only four inlets in annual, two in south west monsoon, one in northeast monsoon and two in fair weather season fell into the classification of formation of barrier at inlet entrance; (v) As per non-dimensional classification without wave period 32 inlets fall under tide dominated, two inlets being tide dominated-bays, two inlets being river dominated, 11 inlets being wave dominated followed by 28 inlets wave dominated ICOLLS; (vi) As per non-dimensional classification with wave period 27 inlets fall under tide dominated, seven inlets being river dominated, 11 inlets being wave dominated followed by 30 inlets wave dominated ICOLLS.

CHAPTER-4

CYCLONE INDUCED MORPHOLOGY CHANGES

4.1. INTRODUCTION

The atmospheric disturbances with rapid circulation of air around a region having low pressure are responsible for the cyclone genesis. The British meteorologist observed tropical storms in the form of coiled serpents of the sea both in the Arabian Sea (AS) and in the Bay of Bengal (BoB) and named them as cyclones. From the Greek word “Cyclos”, the word “Cyclone” is originated. Tropical cyclones normally decay when they move into unfavourable environment such as land or over cooler waters in higher latitudes. Depending the location where it occurred cyclones are named differently across the world.

The wind speed around the cyclone eye and the atmospheric pressure drop are the major parameters considered to classify the cyclones. To estimate the category of cyclonic disturbance two important aspects are considered as: (i) satellite cloud images (expressed by ‘T’ numbers) are used by taking into account of meteorological conditions of the region; (ii) the wind speed associated with the low pressure systems. As per the criteria adopted by the World Meteorological Organization (WMO), Indian Meteorological Department (IMD) classified the cyclone over North Indian Ocean (NIO) into 7 categories (Table 4.1). The pressure deficient, wind speed, sea condition and wave heights of different low pressure systems as per Regional Specialized Meteorological Centre (RSMC) are depicted in the Table 4.1.

Furthermore, the cyclones are classified into 5 categories based on expected damage in relation with wind speed (Table 4.2). Storm associated with heavy rainfall and storm induced surge are eventually prime elements to cause damage to property and loss of lives. The damage produced by winds are widespread in nature. However sometimes the extent

of windblown is more than extent of rainfall region and storm surge induced inundation. Storm associated with rainfall is another major source of damage during cyclones in the form of unexpected flood in the region. The cyclones are even more dangerous causing heavy damage to infrastructure facilities when storm surge associated with heavy rainfall. Post cyclone relief operations are also interrupted and difficult to carry out in the effected region due to torrential rains.

Table 4.1 Classification of cyclones as per RSMC, New Delhi, India

Type of disturbance	Wind speed	Sea Condition	Wave Height (m)	Satellite 'T' No.
Low Pressure Area (L)	< 31 km/h (< 17 kn)	Calm to Slight	< 1.25	1.0
Depression (D)	31-49 km/h (17-27 kn)	Moderate to Rough	> 1.25 - < 4.0	1.5
Deep Depression (DD)	50-61 km/h (28-33 kn)	Very Rough	> 4.0 - < 6.0	2.0
Cyclonic Storm (CS)	62-88 km/h (34-47 kn)	High	> 6.0 - < 9.0	2.5-3.0
Severe Cyclonic Storm (SCS)	89-117 km/h (48-63 kn)	Very High	> 1.25 - < 4.0	3.5
Very Severe Cyclone Storm (VSCS)	118-221 km/h (64-119 kn)	Phenomenal	> 14	4.0-6.0
Super Cyclone (SuCS)	> 222 km/h (> 120 kn)	Phenomenal	> 14	6.5 and above

Table 4.2 Set of limiting values of wind speed based on the expected damage

Cyclone Category	Wind Speed (kmph)	Damage Capacity
1	120-150	Minimum
2	151-180	Moderate
3	181-210	Extensive
4	211-250	Extreme
5	251 and above	Catastrophic

Table 4.3 Storm intensity, expected damage and suggested actions for various types of disturbances

Intensity	Damage expected	Action Suggested
Deep Depression	Minimal damage	Instructed fishermen not to go for fishing
Cyclonic Storm	Damage to thatched houses and slight damage to power transmission and communication systems	Fishing operations are completely postponed
Severe Cyclonic Storm	Severe damage to thatched houses and Slight damage due to uprooting of large trees to power transmission and communication systems. Escape routes are subjected to flooding.	Fishing operations are completely postponed, Coastal inhabitants to be moved to safer places. Public are advised to remain indoors in affected areas
Very Severe Cyclonic Storm	Severe damage to thatched huts and partial trouble of power transmission and communication systems. Rail and road traffic slightly effected and flying debris would cause potential threat. Escape routes are subjected to flooding.	Fishing operations are completely postponed. Public are instructed to evacuate from coastal regions and advised to remain indoors in affected areas. Careful instructions are given to both rail and road traffic.
Very Severe Cyclonic Storm	Severe damage to thatched huts and structural damage to old constructions and severe damage to power transmission and communication systems. Heavy distraction of rail and road traffic due to widespread flooding in coastal regions. Flying debris would cause potential threat.	Fishing operations are completely postponed. Coastal regions are completely under evacuation. Road and rail traffic should be diverted or cancelled the trips. Public are advised to remain indoors in affected areas
Super Cyclone	Residential and industrial structures are under severe damage. Complete shutdown of power & communication systems. Heavy distraction of rail and road traffic due to widespread flooding in coastal regions. Flying debris would cause potential threat.	Fishing operations are completely postponed. Evacuation of people staying in coastal area on large scale. Road and rail traffic should be diverted or cancelled the trips. Public are advised to remain indoors in affected areas.

In addition to the above, on infrastructure front, extreme rainfall destroys the water distribution system which become critical to renovate after cyclone period. Storm surge is one of the major cause for destruction during cyclones. The potential storm surge depends on a number of different factors like forward speed of cyclone eye, size and extent of wind and pressure fields, approach angle to the coast, central and neutral pressures, shape and coastline features, width and slope of continental slope and landfall location. The IMD suggested relationship among storm intensity, expected damage and suggested actions for various types of disturbances are given in Table 4.3.

4.1.1. Naming of cyclones

Tropical cyclones are named to provide quick communication between forecasters and public regarding predictions and warnings. Cyclonic storms are active for a week or even more and simultaneous occurrence of cyclones in same region, names can reduce the confusion about what storm is being described. The cyclone names over North Indian Ocean are not in alphabetical order. However, the cyclones are named in sequence suggested by country which contributed the name in alphabetical order (Table 4.4). Unless the wind speed reaches 34 kn (i.e. 62 km/h), the cyclones are not given any names. Since September 2004 onwards the tropical cyclones are given with names over north Indian Ocean.

Importance for naming tropical cyclones

- Identification of cyclones is easier when cyclones occur in sequence.
- Helps the public to get fully aware of its development
- Easier for local and international media to report on tropical cyclones.
- To avoid confusion in the public if more number of cyclones occurred the same region.
- Public remembered for quite long-time as unforgettable event based on its consequences.

- Warning messages reach very rapidly to the general public in case of emergency.

Cyclones are the natural hazards that affect Indian coastline every year causing extensive damage to infrastructure, property and loss of lives. Hazards associated with tropical cyclones can often last a week or even longer with high wind speed with associated rainfall and storm surge. Out of these, the storm surge associated with cyclone has greatest effect on coastal community. Storm surge inundates low lying coastal regions causing heavy floods, breaching of embankments and erosion of beaches, damage to flora and fauna and decreasing soil fertility. On top of that flooding due to storm surges pollute drinking water resources and lead water borne diseases to the local public.

India has a coastline of about 7516 km of which 5400 km is along mainland and has exposure to 7% of the global tropical cyclones. The complete Indian coastline is effected by cyclonic storms with varying frequency and intensity. Majority of cyclones have their origin over the Bay of Bengal and strike the East coast of India. An average 5 to 6 tropical cyclones hit the Indian coastline per year, out of which 2 or 3 could be severe (Singh et al. 2001). The frequency of cyclones is more in Bay of Bengal than the Arabian Sea and the ratio is approximately 4:1 (Dube et al. 1997). There are eight maritime states viz. Gujarat, Maharashtra, Karnataka and Kerala on West coast and Tamil Nadu, Andhra Pradesh, Odisha and West Bengal on East coast of India that have deeply suffered from tropical cyclones.

Even though the total Indian coastline affected by cyclones, majorly four states viz., Tamil Nadu, Andhra Pradesh, Odisha and West Bengal and Pondicherry (Union Territory) on the East coast of India and Gujarat on the West coast of India are more prone to cyclone hazards. For the cyclone in India, Indian Meteorological Department (IMD) is the nodal government agency which provides weather services.

Table 4.4 Naming of cyclones over North Indian Ocean (2004-2017)

Contributed By	Names							
	1	2	3	4	5	6	7	8
Bangladesh	Onil (2004)	Ogni (2006)	Nisha (2008)	Giri (2010)	Helen (2013)	Chapala (2015)	Ockhi (2017)	Fani
India	Agni (2004)	Akash (2007)	Bijli (2009)	Jal (2010)	Lehar (2013)	Megh (2015)	Sagar	Vayu
Maldives	Hibaru (2005)	Gonu (2007)	Aila (2009)	Keila (2011)	Madi (2013)	Roanu (2016)	Mekunu	Hikaa
Myanmar	Pyarr (2005)	Yemyin (2007)	Phyan (2009)	Thane (2011)	Nanauk (2014)	Kyant (2016)	Daye	Kyarr
Oman	Baaz (2005)	Sidr (2007)	Ward (2009)	Murjan (2012)	Hudhud (2014)	Nada (2016)	Luban	Maha
Pakistan	Fanoos (2005)	Nargis (2008)	Laila (2010)	Nilam (2012)	Nilofar (2014)	Vardah (2016)	Titli	Bulbul
Sri Lanka	Mala (2006)	Rashmi (2008)	Band (2010)	Viyaru (2013)	Ashobaa (2015)	Marutha (2017)	Gigum	Soba
Thailand	Mukda (2006)	Khai Muk (2008)	Phet (2010)	Phailin (2013)	Komen (2015)	Mora (2017)	Phethai	Amphan

4.2. CYCLONE INDUCED MORPHOLOGY STUDIES

4.2.1. Introduction

The study of morphodynamics at the tidal inlet is crucial because there needs to be an understanding of the behaviour of the sediment movement to maintain the stability of the inlet. It is almost impossible to keep the hydro and morphological parameters under observation all the time especially during heavy winds or during the action of cyclones. The most conventional and best way to monitor the changes in the morphology of the tidal inlet is to observe satellite images. But during cyclone, the cloud covers the vision of the satellite image which is evident in the snapshots obtained from the imageries. The images from Google Earth® are available in public domain and are only available prior to and post monsoon but not during the monsoon. It is also a fact that surveying for field measurements during cyclones is impractical as the atmospheric conditions are severely dynamic and unstable. Hence, numerical modelling for morphology changes during the cyclone seems most practical and safest way of studying morphological changes at the tidal inlet. However, the modelling of storm surges in complex terrain requires true representation of coastal geometry as well as detailed onshore topography and bathymetry which are to be obtained from reliable sources.

Morphology changes can occur due to sediment variations in the vicinity on the coast and nearshore regions. Erosion or accretion either progressive or intermittent depends on the sediment transport gradients of the region. The extreme weather events like storms/cyclones make a huge impact on the coastal sediment transport, which can be studied through sediment transport variations due to such catastrophic events. This study deals with the morphology changes in the alongshore and nearshore regions along the east coast of India due to a very severe cyclone.

The study of cyclone induced morphology changes near tidal inlet is a challenging task particularly during cyclones. To study this objective, a case study of cyclone Phailin has been taken which had occurred in the year 2013 and had a landfall point at Gopalpur in Odisha. The reasons to taken up this study area is: (1) the measured data of wind and wave are available for the validation of the numerical model during the cyclone Phailin, (2) the landfall point is closer to the coast where a tidal inlet was found and (3) observations show that there is a breach on the berm after the cyclone, which is a morphology change and before cyclone Phailin the breach was not there.

4.2.2. The Cyclone Phailin

On 6th October 2013, the Phailin formed in the South China Sea. On 7th October it was identified as low pressure region over north Andaman Sea. On 9th October morning it further intensified as Deep Depression (DD) and later on the same day in the evening further intensified into Cyclonic Storm (CS) and was named as Phailin which was contributed from the Thailand. On 10th October it further intensified into a Severe Cyclonic Storm (SCS) by moving north-westwards over Bay of Bengal (BoB) and on the same day forenoon intensified into a Very Severe Cyclonic Storm (VSCS) over eastern Bay of Bengal. The VSCS Phailin crossed the coastal states of Odisha & adjoining north Andhra Pradesh coast near Gopalpur (Odisha) on 12th October 2013 around 2230 hrs IST. Near the landfall location the Phailin has a sustained wind speed of 200-210 km/h and gust of 220 km/h (IMD, 2013). The observed track of a Very Severe Cyclonic Storm, Phailin is shown in the Figure 4.1.

At the time of landfall, i.e., on 12th October, estimated central pressure was 940 hPa with pressure drop of 66 hPa at the centre of cyclone eye compared to surroundings. Due to this, the Phailin caused severe rainfall over coastal Odisha state. Hence the water rushed in the form of floods in almost all coastal districts of Odisha state and strong winds leading to devastating structural damage. There was about storm surge of 2-2.5m triggering extensive

coastal inundation over the coastal Odisha state. Maximum 24 hour cumulative rainfall of 38 cm has been reported over Banki in Cuttack district of Odisha. Based on post-cyclone survey report, maximum of storm surge of 2-2.5 meters above the astronomical tide in the low lying areas of Ganjam district of Odisha and the in-land inundation of saline water extended up to about 1 km from the coast. The numerical weather prediction (NWP) and dynamical statistical models provided good guidance with respect to its genesis, track and intensity. IMD accurately predicted the genesis, intensity, track and point & time of landfall and also the adverse weather like heavy rainfall, gale wind and storm surge 4 to 5 days in advance.

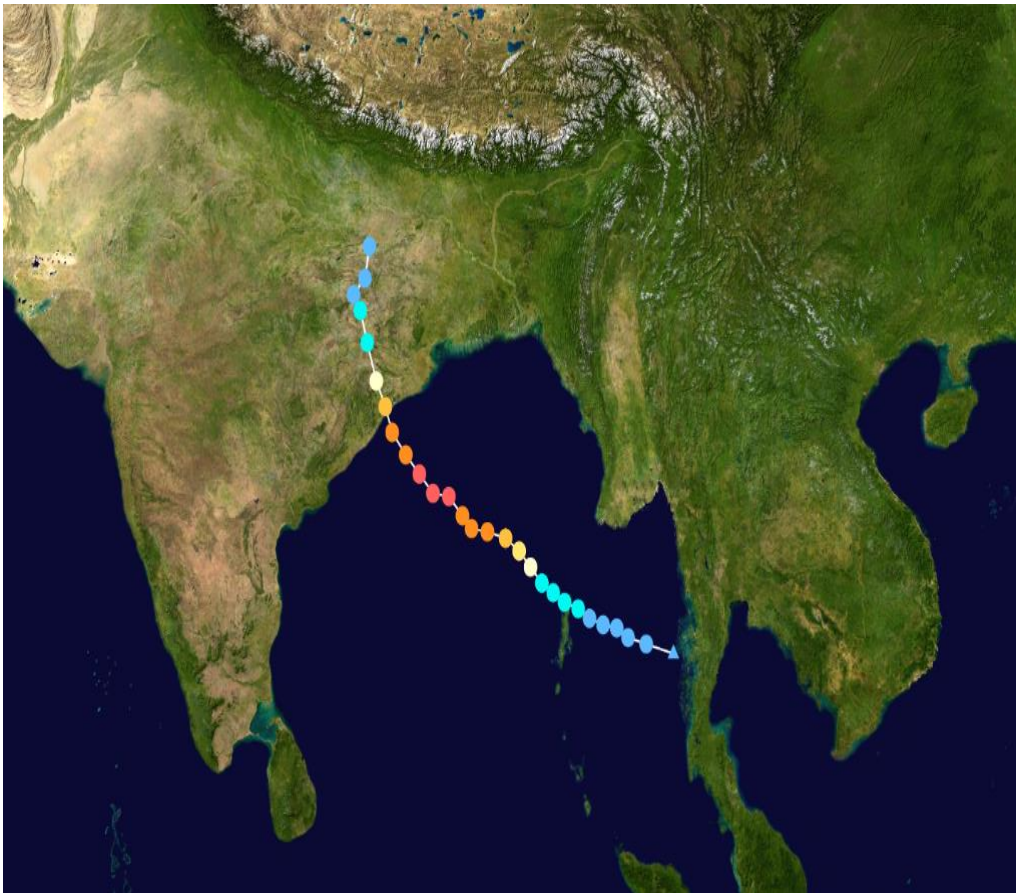


Figure 4.1 Observed track of VSCS, Phailin during 8th -14th October 2013 (Source: IMD)

4.3. STUDY AREA

The Khalakata tidal inlet (19.85° , 86.05°) has been considered to study the morphology changes in the coastline in the vicinity of the inlet for the Phailin cyclone. The inlet location is about 140 km from the landfall location of VSCS Phailin. The inlet is having a sand spit of length 2.8 km and an average width of 100 m. The tides in this region are semi-diurnal with a spring tidal range of about 1.2 m. The oceanographic climate in this region is generally divided into north-east monsoon (October-January), south-west monsoon (June-September) and fair weather season (February-May). The significant wave heights are comparatively higher during the northeast monsoon, predominantly from the NE and during southwest as well as fair weather period the waves are from east and south east direction. The longshore sediment transport is predominantly towards north with a reversal during the NE monsoon period. The study region abuts the Bay of Bengal which is prone to cyclones every year with an average of about 4 cyclones occurring yearly.

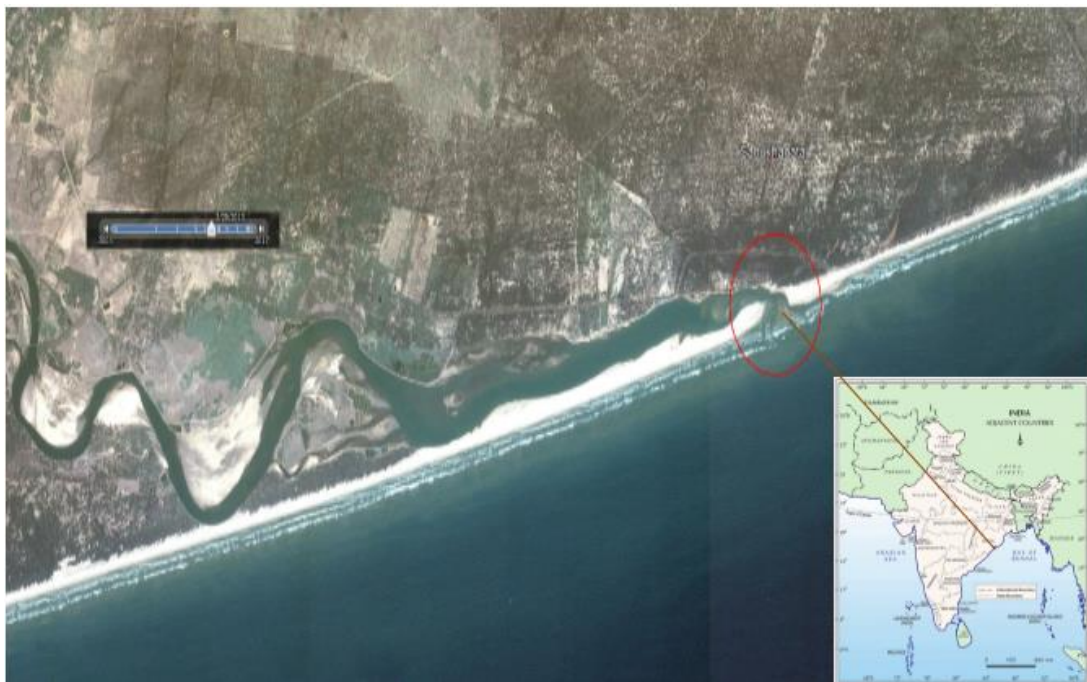


Figure 4.2(a) Study area [Google Earth image as on 25-03-2013 (i.e. before Phailin cyclone)]



Figure 4.2(b) Study area [Google Earth image as on 14-01-2014 (i.e. after Phailin cyclone)]

4.4. DISCRIPTION OF NUMERICAL MODELS

MIKE by DHI, a state of the art numerical modelling software suite is used to simulate the coupled hydrodynamics and morphology of the region. The coupled model consists of modules for hydrodynamics, waves, mud transport and sediment transport. All these modules take feedback from each other as well as provide inputs to each other. For example, the hydrodynamic model or flow model provides flow conditions to the wave model which uses it to include the wave current interaction, and provides the modified wave condition to the flow model. The modified wave conditions taken into the flow model then provides the modified flow conditions which are used in the morphology model and the mud transport model. The sediment and mud transport models also utilise the wave parameters from the wave model. In this manner, the coupled model provides output of modified flow, wave and changes in the bed morphology in the study region.

The numerical models used in this study are described in this section. Parametric wind model has been used to generate the wind during the cyclone. The coupled modelling comprising of flow model, wave model and sediment transport model is used to study the hydrodynamics and morphology impact in the region after the cyclone Phailin.

4.4.1. Parametric wind models

The MIKE 21 model allows for automatic generation of wind and pressure fields of cyclones using a parameterised description of the cyclone shape with a predefined track. Space and time varying wind and pressure fields have been generated from the parameterised data sets and incorporated as boundary conditions for the hydrodynamic and wave modelling simulations. Input parameters required for wind and pressure fields' generation using different parametric models are given in Table 4.5. There are four types of parametric models for the automatic generation of wind and pressure fields and are described as follows:

4.4.1.1. Young and Sobey model

According to Young and Sobey (1981) the rotational wind gradient speed (V_g) at a distance 'r' from the centre of cyclone, is given by:

$$V_g(r) = V_{max} \left(\frac{r}{R_{mw}} \right)^7 \exp \left[7 \left(1 - \frac{r}{R_{mw}} \right) \right] \quad \text{for } r < R_{mw} \quad 4.1(a)$$

$$V_g(r) = V_{max} \exp \left[(0.0025R_{mw} + 0.05) \left(1 - \frac{r}{R_{mw}} \right) \right] \quad \text{for } r \geq R_{mw} \quad 4.1(b)$$

where R_{mw} is the radius of maximum wind speed and V_{max} is the maximum wind speed. Young and Sobey were given the pressure 'p' following the Shore Protection Manual (SPM 1984) as:

$$p(r) = p_c + (p_n - p_c) \exp \left(-\frac{R_{mw}}{r} \right) \quad (4.2)$$

where p_c is the central pressure and p_n is the neutral pressure.

4.4.1.2. Holland single vortex model

Holland make use of the parameters p_c and p_n that are already introduced in Young and Sobey model and the pressure 'p' is given as:

$$p(r) = p_c + (p_n - p_c) \exp\left(-\frac{R_{mw}}{r}\right)^B \quad (4.3)$$

where B is a shape parameter ($1 < B < 2.5$)

The wind gradient speed, $V_g(r)$ is then given as:

$$V_g(r) = \sqrt{(p_{nn} - p_c) \frac{B}{\rho_A} \left(\frac{R_{mw}}{r}\right)^B \exp\left(-\frac{R_{mw}}{r}\right)^B + \left(\frac{r * f}{2}\right)^2} - \frac{r|f|}{2} \quad (4.4)$$

where, ρ_A is the air density and f is the coriolis parameter

By neglecting the coriolis parameter (f), the Eq. 4.4 becomes

$$V_{max} = \sqrt{(p_{nn} - p_c) \frac{B}{\rho_A * e}} \quad (4.5)$$

The Eq. 4.5 can also be used to determine the parameter B when the maximum wind speed is known and is given by:

$$B = \frac{\rho_A * e * V_{max}^2}{(p_n - p_c)} \quad (4.6)$$

Alternatively, Harper et al. (2001) and Phadke et al. (2003) and Harper and Holland (1999) suggested that standard B values might be obtained by:

$$B = 2.0 - (p_c - 900)/160 \quad (4.7)$$

where, p_c is central pressure in hPa

4.4.1.3. Holland Double Vortex model

Holland (1980) had introduced Holland Double Vortex model based on the parametric model by following the works of Cardone et al. (1994, 1996). Based on this model, the pressure ‘ p ’ is given as:

$$p(r) = p_c + \Delta p_1 \exp\left(-\frac{R_{mw1}}{r}\right)^{B_1} + \Delta p_2 \exp\left(\frac{R_{mw2}}{r}\right)^{B_2} \quad (4.8)$$

where $\Delta p_1 + \Delta p_2 = p_n - p_c = \Delta p$

The wind gradient speed, $V_g(r)$ is then given as:

$$V_g(r) = \sqrt{\frac{\left(\frac{R_{mw1}}{r}\right)^{B_1} \frac{B_1 \Delta p_1}{\rho_A} \exp\left(-\frac{R_{mw1}}{r}\right)^{B_1} + \left(\frac{R_{mw2}}{r}\right)^{B_2} \frac{B_2 \Delta p_2}{\rho_A} \exp\left(\frac{R_{mw2}}{r}\right)^{B_2} + \left(\frac{r * f}{2}\right)^2}{-\frac{r|f|}{2}}} \quad (4.9)$$

4.4.1.4. Rankine vortex model

The modified Rankine vortex model uses the following velocity distribution:

$$V_g(r) = \begin{cases} V_{max} \cdot \left(\frac{r}{R_{mw}}\right) & \text{for } 0 \leq r < R_{mw} \\ V_{max} \cdot \left(\frac{r}{R_{mw}}\right)^X & \text{for } r > R_{mw} \end{cases} \quad (4.10)$$

The shape parameter X is used to adjust the wind speed distribution in the radial direction. Typical values of X are in the range of 0.4 to 0.6.

4.4.1.5. Wind Correction

In order to obtain surface winds, a boundary layer wind speed correction can be applied to the gradient wind. The near-surface wind, V_{10} , is usually obtained by the following relation (Harper et al., 2001):

$$V_{10}(r) = K_m \cdot V_g(r) \quad (4.11)$$

As mentioned by Harper et al, (2001) different values for the parameter K_m are available in the literature. These values can be entered in the Cyclone Wind Generation Tool using a constant type of geostrophic correction.

A speed-dependent formulation for K_m is also proposed by Harper et al. (2001) and seems widely used in Australia. This has been implemented in the Cyclone Wind Generation Tool as the ‘Harper et al.’ geostrophic correction type where the K_m factor is computed as:

$$K_m = \begin{cases} 0.81 & \text{for } V_g < 6 \text{ m/s} \\ 0.81 - 2.96 \times 10^{-3} (V_g - 6) & \text{for } 6 \leq V_g < 19.5 \\ 0.77 - 4.31 \times 10^{-3} (V_g - 19.5) & \text{for } 19.5 \leq V_g < 45 \\ 0.66 & \text{for } V_g > 45 \text{ m/s} \end{cases} \quad (4.12)$$

Table 4.5 Input parameters required (green blocks) for wind and pressure fields’ generation using different parametric models

Parametric Models	Time	Long	Lat	R_{max}	V_{max}	P_c	P_n	B	D_{P2}	B_2	R_{max2}	X
Young and Sobey	Green	Green	Green	Green	Green	Green	Green	Red	Red	Red	Red	Red
Holland-single vertex	Green	Green	Green	Green	Red	Green	Green	Red	Red	Red	Red	Red
Holland-double vertex	Green	Green	Green	Green R_{max1}	Red	Green	Green	Green B_1	Green	Green	Green	Red
Rankine	Green	Green	Green	Green	Green	Red	Green	Red	Red	Red	Red	Green

4.4.2. Coupled modelling

The MIKE 21 coupled model FM is used in this study which dynamically couples the flow, sediment transport and wave calculations. Full feedback of bed level changes on flow and wave calculations is included in this formulation. The coupled model FM is mostly used for investigating the morphological evolution of the near shore bathymetry due to the impact of engineering works (coastal structures, dredging works etc.) and also to study the morphological evolution of tidal inlets. It is most suitable for medium-term morphological investigations (several weeks to months) over a limited coastal area. The computational effort can become quite large for long-term simulations, or for larger areas. The different models used in the coupled model are briefly described below.

4.4.2.1. Hydrodynamic model

The Hydrodynamic Module is the basic computational component of the entire MIKE21 Flow Model FM modelling system. The MIKE 21 Flow Model FM is a modelling system based on a flexible mesh approach providing the hydrodynamic basis for the Mud Transport Module and Sand Transport Module as well as providing input for water level changes for the spectral wave model.

The modelling system is based on the numerical solution of the two-dimensional shallow water equations i.e., depth-integrated incompressible Reynolds Averaged Navier-Stokes equations. Thus, the model consists of continuity, momentum, temperature, salinity and density equations. In the horizontal domain both Cartesian and spherical coordinates can be used. The governing equations for 3D model are presented using Cartesian coordinates are given below.

The local continuity equation

$$\frac{\partial u}{\partial x} + \frac{\partial v}{\partial y} + \frac{\partial w}{\partial z} = S \quad (4.13)$$

The horizontal momentum equation for the x- component

$$\begin{aligned} \frac{\partial u}{\partial t} + \frac{\partial u^2}{\partial x} + \frac{\partial uv}{\partial y} + \frac{\partial wu}{\partial z} = fv - g \frac{\partial \eta}{\partial x} - \\ \frac{1}{\rho_0} \frac{\partial p_a}{\partial x} - \frac{g}{\rho_0} \int_z^\eta \frac{\partial p}{\partial x} dz + F_u + \frac{\partial}{\partial z} \left(v_t \frac{\partial u}{\partial z} \right) + u_s S \end{aligned} \quad (4.14)$$

The horizontal momentum equation for the y- component

$$\begin{aligned} \frac{\partial v}{\partial t} + \frac{\partial v^2}{\partial y} + \frac{\partial uv}{\partial x} + \frac{\partial wv}{\partial z} = -fu - g \frac{\partial \eta}{\partial y} - \\ \frac{1}{\rho_0} \frac{\partial p_a}{\partial y} - \frac{g}{\rho_0} \int_z^\eta \frac{\partial p}{\partial y} dz + F_v + \frac{\partial}{\partial z} \left(v_t \frac{\partial v}{\partial z} \right) + v_s S \end{aligned} \quad (4.15)$$

The general transport-diffusion equations for the calculations of transports of Temperature (T) and Salinity (s) are given as:

$$\frac{\partial T}{\partial t} + \frac{\partial uT}{\partial x} + \frac{\partial vT}{\partial y} + \frac{\partial wT}{\partial z} = F_T + \frac{\partial}{\partial z} \left(D_v \frac{\partial T}{\partial z} \right) + \hat{H} + T_s S \quad (4.16)$$

$$\frac{\partial s}{\partial t} + \frac{\partial us}{\partial x} + \frac{\partial vs}{\partial y} + \frac{\partial ws}{\partial z} = F_s + \frac{\partial}{\partial z} \left(D_v \frac{\partial s}{\partial z} \right) + s_s S \quad (4.17)$$

The horizontal diffusion terms are defined as:

$$(F_T, F_s) = \left[\frac{\partial}{\partial x} \left(D_h \frac{\partial}{\partial x} \right) + \frac{\partial}{\partial y} \left(D_h \frac{\partial}{\partial y} \right) \right] (T, s) \quad (4.18)$$

The equations for two-dimensional flow are obtained by integrating of the equations over depth.

The spatial discretization of the basic equations is performed using a cell-centred finite volume method wherein the spatial domain is discretized by subdivision of the continuum

into non-overlapping element/cells. An unstructured grid comprising of triangles or quadrilateral element is used in the horizontal plane. An approximate Riemann solver is used for computation of the convective fluxes, which makes it possible for MIKE21 FM model to handle discontinuous solutions. For the time integration an explicit scheme is used. Coriolis term, eddy viscosity using Smagoransky formulation and bed friction are included in the model.

The application areas are: (i) to evaluate the hydrographic parameters for the design, construction and operation of structures and plants; (ii) to carry out the environmental impact assessment studies for various existing or proposed structures and plants; (iii) to study the effect of coastal flooding and cyclone induced storm surge on coastal environs; (iv) to hindcast or forecast the weather systems for the study of coastline features; (v) to study various coastal protection infrastructures etc.

The input parameters required are: (i) model domain and amount of computational time; (ii) factors related to calibration such as bed resistance, wind friction factors and moment dispersion coefficients; (iii) initial conditions such as water levels and velocity components; and (iv) boundary conditions (i.e. what are the open and closed boundaries in the domain, water levels at different boundaries and discharge at boundaries if any) along with tide, wind speed and direction and wave radiation stresses.

At each mesh element and at each time step the output parameters are: (i) water depth and surface elevation; (ii) flux densities; (iii) velocities; (iv) temperatures and salinities; (v) current speed and velocities; (vi) wind velocities; (vii) Courant/CFL number; (viii) eddy viscosity etc.

4.4.2.2. Wave model

MIKE 21 SW, a state-of-the-art numerical tool for prediction and analysis of wave climates in offshore and coastal areas is used for simulating the waves in the study region. MIKE 21 SW includes a new 3rd generation spectral wind-wave model based on unstructured meshes. The model simulates the growth, decay and transformation of wind-generated waves in offshore and coastal areas. MIKE 21 SW includes two different formulations viz., Directional decoupled parametric formulation and fully spectral formulation. In this study the fully spectral formulation has been used (Eq. 3.18). The fully spectral formulation is based on the wave action conservation equation, where the directional-frequency wave action spectrum is the dependent variable.

$$N(\sigma, \theta) = \frac{E}{\sigma} \quad (4.19)$$

where $N(\sigma, \theta)$ is wave action density spectrum, E is wave energy density spectrum and σ is angular frequency.

MIKE 21 SW includes the following physical phenomena: (i) wave growth by action of wind, (ii) non-linear wave-wave interaction, (iii) dissipation due to white-capping, (iv) dissipation due to bottom friction, (v) dissipation due to depth-induced wave breaking, (vi) refraction and shoaling due to depth variations, (vii) wave-current interaction, (viii) effect of time-varying water depth and flooding and drying.

The discretization of the governing equation in geographical and spectral space is performed using cell-centered finite volume method similar to the hydrodynamic model. In the geographical domain, an unstructured mesh technique is used. The time integration is performed using a fractional step approach where a multi-sequence explicit method is applied for the propagation of wave action. MIKE 21 SW is also used in connection with the calculation of the sediment transport, which for a large part is determined by wave conditions and associated wave-induced currents. MIKE 21 SW can be used to calculate

the wave conditions and associated radiation stresses. Subsequently the wave-induced flow is calculated using MIKE 21 Flow Model FM.

The various application areas of MIKE21 Spectral Wave model are: (i) used to assess wave climates both coastal and offshore regions; (ii) used for the design of offshore, coastal and port structures where wave related information play a significant role to the safety and economic design of the above structures; (iii) used particularly for the regions where simultaneous wave prediction and analysis on regional scale and local scale are required. Coarse spatial and temporal resolution is used for the regional part of the mesh and a high resolution boundary and depth-adaptive mesh is used for the shallow waters; (iv) MIKE 21 SW is also used in the calculation of the sediment transport rates, which for a large part is determined by wave conditions and associated wave-induced currents. The wave-induced current is generated by the gradients in radiation stresses. MIKE 21 SW can be used to calculate the wave conditions and associated radiation stresses.

The input parameters required for the wave model are: (i) model domain and amount of computational time; (ii) equations namely discretization and solution technique, formulation type, frequency and directional discretization; (iii) forcing parameters such as water levels, currents and wind data etc.; (iv) source function parameters such as non-linear energy transfer, wave breaking, bottom friction and white capping; (v) initial conditions and (vi) boundary conditions (i.e. closed or opened boundaries).

The output parameters from the wave model are significant wave height, maximum wave height, peak wave period, mean wave period, mean wave direction, wave velocity components, wave radiation stresses, etc., amongst other parameters.

4.4.2.3. Non-cohesive Sediment transport model

The Sand Transport module calculates the resulting transport of non-cohesive materials based on the flow conditions found in the hydrodynamic calculations and, if included, wave conditions from wave calculations. A mean sediment grain size can be given as input to the model over the entire domain or varying in the domain. In this study the wave and current formulation of sediment transport is considered with the flow model providing the currents and the wave information obtained from the wave model. The modelling system is based on the numerical solution of the two/three dimensional incompressible Reynolds averaged Navier-Stokes equations subject to the assumptions of Boussinesq and of hydrostatic pressure. Thus the model consists of continuity, momentum, temperature, salinity and density equations and it is closed by a turbulent closure scheme. The density does not depend on the pressure, but only on the temperature and the salinity. For the 3D model, the free surface is taken into account using a sigma coordinate transformation approach. The Sand Transport Module can calculate the transport of a scalar quantity. The conservation equation for a scalar quantity is given as:

$$\frac{\partial C}{\partial t} + \frac{\partial uC}{\partial x} + \frac{\partial vC}{\partial y} + \frac{\partial wC}{\partial z} = F_C + \frac{\partial}{\partial z} \left(D_v \frac{\partial C}{\partial z} \right) - k_p C + C_s S \quad (4.20)$$

The horizontal diffusion term is defined as:

$$(F_C) = \left[\frac{\partial}{\partial x} \left(D_h \frac{\partial}{\partial x} \right) + \frac{\partial}{\partial y} \left(D_h \frac{\partial}{\partial y} \right) \right] C \quad (4.21)$$

For 2D calculations, the conservation equation is integrated over the depth and is given as:

$$\frac{\partial h\bar{C}}{\partial t} + \frac{\partial h\bar{u}\bar{C}}{\partial x} + \frac{\partial h\bar{v}\bar{C}}{\partial y} = hF_C - hk_p\bar{C} + hC_s S \quad (4.22)$$

where t is time; x, y, z are Cartesian coordinates; D_v is vertical turbulent diffusion coefficient; S is magnitude of discharge due to point sources; F_C is horizontal diffusion term and D_h is horizontal diffusion coefficient; h is depth; \bar{u}, \bar{v} are depth averaged velocity components; C is concentration of scalar quantity; k_p is linear decay rate of scalar quantity and C_s is concentration of scalar quantity in source.

The application areas are:(i) used to study the field engineering problems like sediment transport rates for non-cohesive sediments; (ii) to study wide range of hydraulic and other related phenomena; (iii) used to study various coastal and marine applications where sediment transport is main influencing parameter; and (iv) used to study water quality studies, flushing studies and tracer simulations tec.

The input parameters required for the wave model besides the input for hydrodynamic model alone are component type, decay information, dispersion coefficient, initial conditions and boundary conditions. The output parameters from the transport model are sediment transport rates, bed level changes, amongst other parameters.

4.5. METHODOLOGY

The extraction of cyclone data, preparation of bathymetry and model parameters are discussed in the following sections.

4.5.1. Cyclone wind data

Cyclone track data for the very severe cyclonic storm Phailin is obtained from the Joint Typhoon Warning Centre (JTWC) site (http://metoc.ndbc.noaa.gov/jtwc/best_tracks) is used to estimate the storm induced parameters. The model domain covering both the entire Bay of Bengal and Arabian Sea, was schematised on a rectangular uniform grid with spacing of 9.72km is given as input for the generation of cyclone induced wind and pressure fields (Figure 4.3).

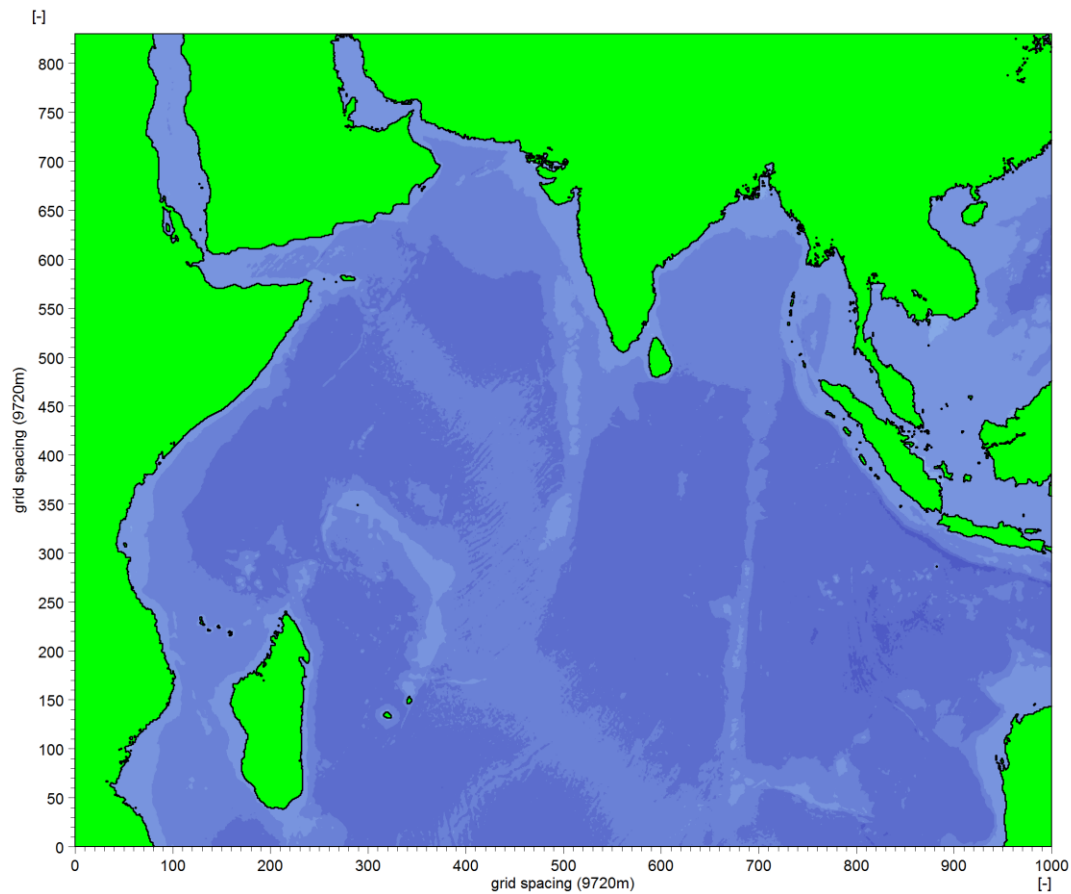


Figure 4.3 Bathymetry and mesh adopted for generation of cyclone induced parameters

The basic input data viz., central pressure (P_c), neutral pressure (P_n), maximum sustained wind speeds (V_{max}), radius of maximum winds (R_{max}) obtained from the above mentioned database (Table 4.6) are used in Rankine vortex parametric wind model (Depperman, 1947) to obtain the wind field (Figure 4.4) and pressure fields (Figure 4.5) over the study region. The cyclone wind fields from the model are compared with available measured winds off Gopalpur during Phailin cyclone. The cyclonic modelled winds over the study region are used to obtain the hydrodynamics of the region over which the sediment transport modelling is carried out.

Table 4.6 Basic input data for the cyclone Phailin (Start date 07-10-2013 00:00:00UTC)

Time (h)	Long (Deg.)	Lat (Deg.)	R _{mw} (km)	V _{max} (m/s)	P _c (hPa)	P _n (hPa)	X
0	99.10	11.6	30	10.28	1002.2	1004	0.5
6	98.40	11.6	30	12.86	1002.2	1004	0.5
12	97.50	11.6	30	12.86	1002.2	1004	0.5
18	96.60	11.7	30	12.86	1002.2	1004	0.5
24	95.70	11.9	30	12.86	1002.2	1004	0.5
30	94.80	12.3	30	15.43	1002.2	1004	0.5
36	94.10	12.7	30	15.43	1002.2	1004	0.5
42	93.40	13.2	30	18.00	1002.2	1004	0.5
48	93.00	13.4	30	20.00	1002.2	1004	0.5
54	92.26	13.75	30	25.20	997.2	1004	0.5
60	91.6	14.08	30	30.35	990.6	1004	0.5
66	90.98	14.48	30	40.94	976.1	1004	0.5
72	90.83	14.85	30	46.29	968.1	1004	0.5
78	90.22	15.39	30	57.82	948.9	1004	0.5
84	89.42	15.59	30	69.34	928	1004	0.5
90	88.8	15.72	30	70.68	924.6	1004	0.5
96	88.31	16.14	30	69.34	927.8	1004	0.5
102	87.62	16.73	30	62.86	935.8	1004	0.5
108	87.02	16.79	30	68.00	926.8	1004	0.5
114	86.53	17.45	30	69.34	924.9	1004	0.5
120	85.85	17.95	30	66.66	929.2	1004	0.5
126	85.01	18.7	30	59.15	942.5	1004	0.5
132	84.96	19.28	30	48.76	959.1	1004	0.5
138	84.91	19.24	30	48.76	959.1	1004	0.5
144	84.00	21.20	30	18.00	968.2	1004	0.5
150	83.80	22.50	30	18.00	994	1004	0.5
156	83.50	22.70	30	15.43	996	1004	0.5
162	84.10	24.00	30	12.86	1002	1004	0.5
168	84.20	24.50	30	12.86	1004	1004	0.5

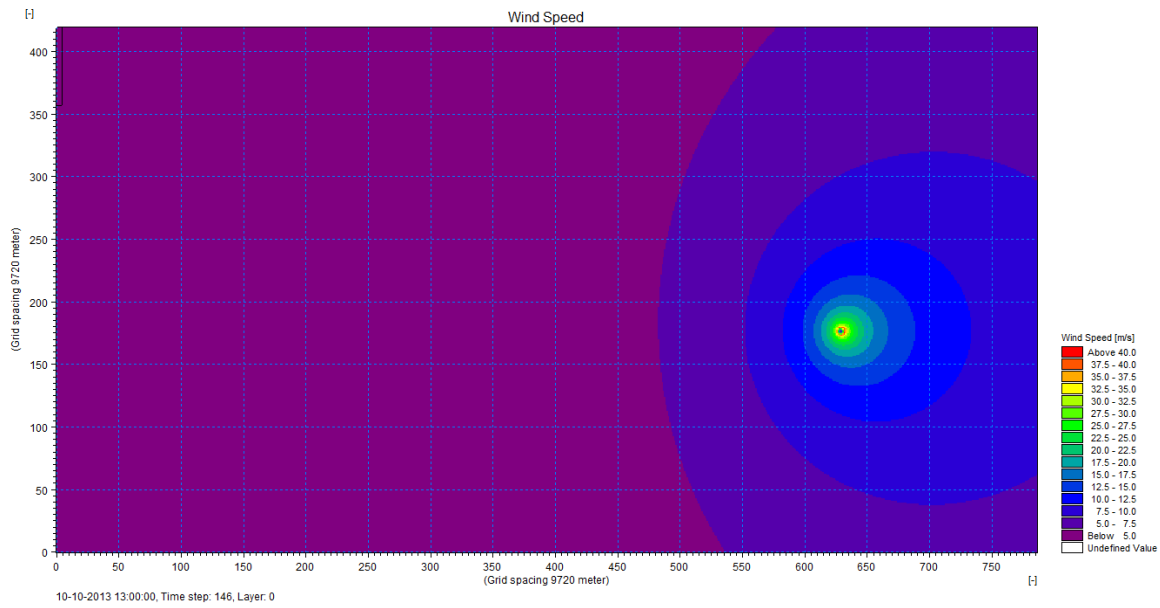


Figure 4.4 Wind fields of the Phailin cyclone

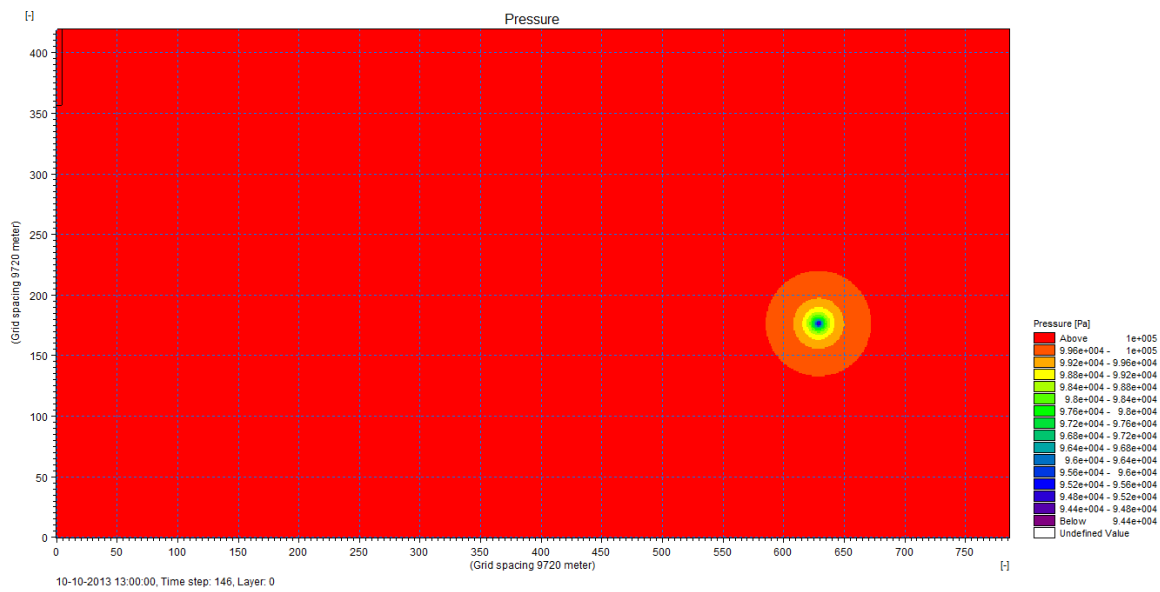


Figure 4.5 Pressure fields of the Phailin cyclone

4.5.2. Model domain and mesh generation

The inputs considered to the numerical model are bathymetry, coastline, tides, winds and waves. In order to obtain reliable results from the model, reliable input data is required. The coastline from the available Google® imageries before the cyclone was considered as input to the numerical model. The shoreline was digitized and used in preparation of the bathymetry of the study region. The bathymetry used in the model is taken from the NHO charts primarily meant for navigational purposes which cover specific areas of interest to shipping routes.

In this study, the appropriate selection of area to be modelled (i.e. model domain) is shown in Figure 4.6. At the points of interest very fine mesh has been considered (Figure 4.7). The water levels at the north, south and east open boundaries of the model were specified based on the tidal elevations predicted using MIKE21 FM tidal prediction module. The rest of the domain was interpolated by means of MIKE21FM interpolation tool. A constant water level and zero velocity were used as initial conditions at all grid points. The tidal level at the open boundaries was used as the boundary condition and the flow direction at the open boundary was considered to be perpendicular to the boundary.

4.5.3. Model parameters

The MIKE 21 coupled model FM is used in this study which dynamically couples the flow, sediment transport and wave calculations. There are two obvious choices to run the MIKE21 coupled model: (i) include Spectra Waves in module selection along with Hydrodynamics and Sediment Transport, (ii) run Spectral Wave model separately and then feed the output to MIKE21 coupled model by selecting only Hydrodynamics and Sediment Transport modules. In the present study later one was chosen to avoid model blowup during the simulation.

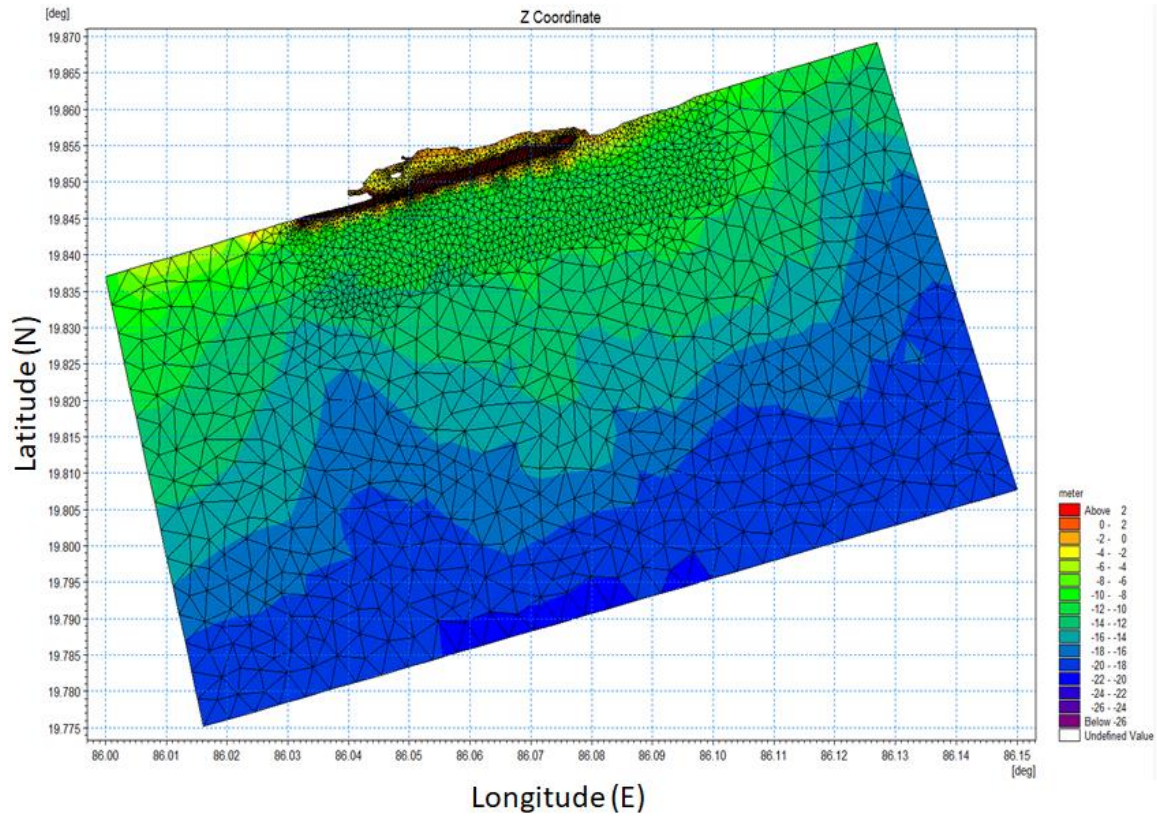


Figure 4.6 Model domain and mesh used in the study

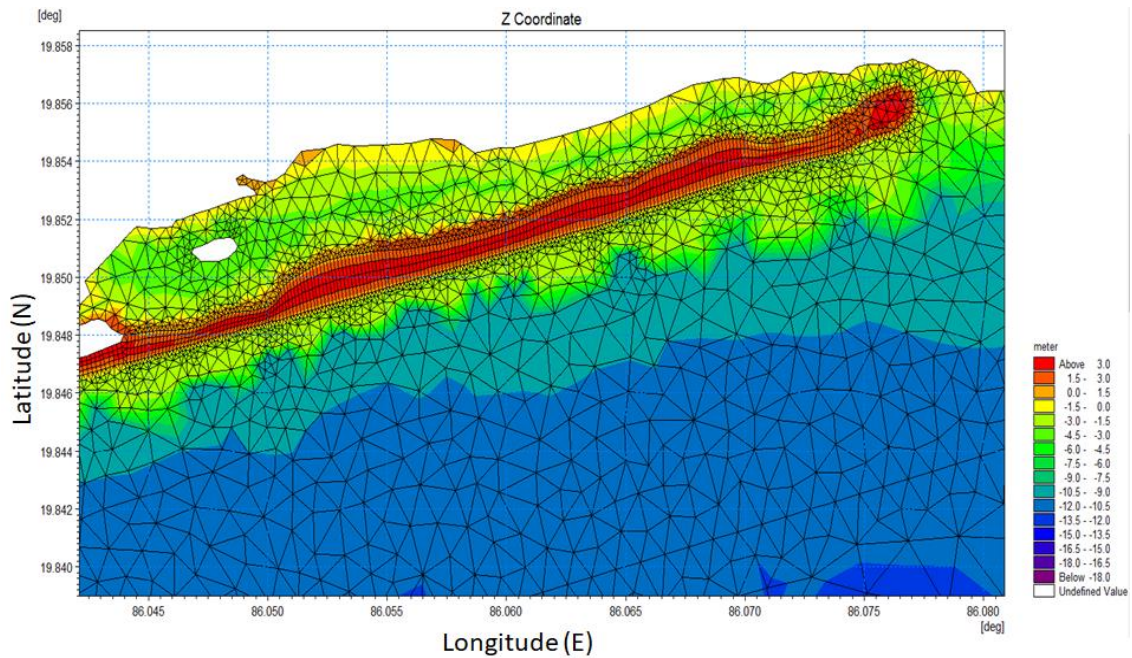


Figure 4.7 Model domain showing the mesh and bathymetry contours at points of interest

4.5.3.1. MIKE21 Spectral Waves FM model parameters

MIKE21 Spectral Waves FM model has been simulated for the considered study area (Figure 4.6) for a period of 195 hrs from 07-10-2013 06:00:00 to 14-10-2013 09:00:00 with a time step of 5min. The model uses fully spectral formulation which is based on wave action conservation equation with in-stationary time formulation mode. The model uses lower order fast algorithm discretization technique which is performed using a cell centered finite volume method with unstructured mesh. Model considered no variations in water levels and currents as initial conditions at all grid points. Cyclone induced winds has been given as input for the model. Wave breaking, bottom friction and white capping are also included in the model. North and south boundaries are given as lateral boundaries and wave parameter are given at east boundary. The boundaries 5 and 6 are considered as closed boundaries (Figure 4.8). The output parameters viz. significant wave heights, mean wave period and direction and radiation stresses are extracted at 10m water depths with a time step of 5min.

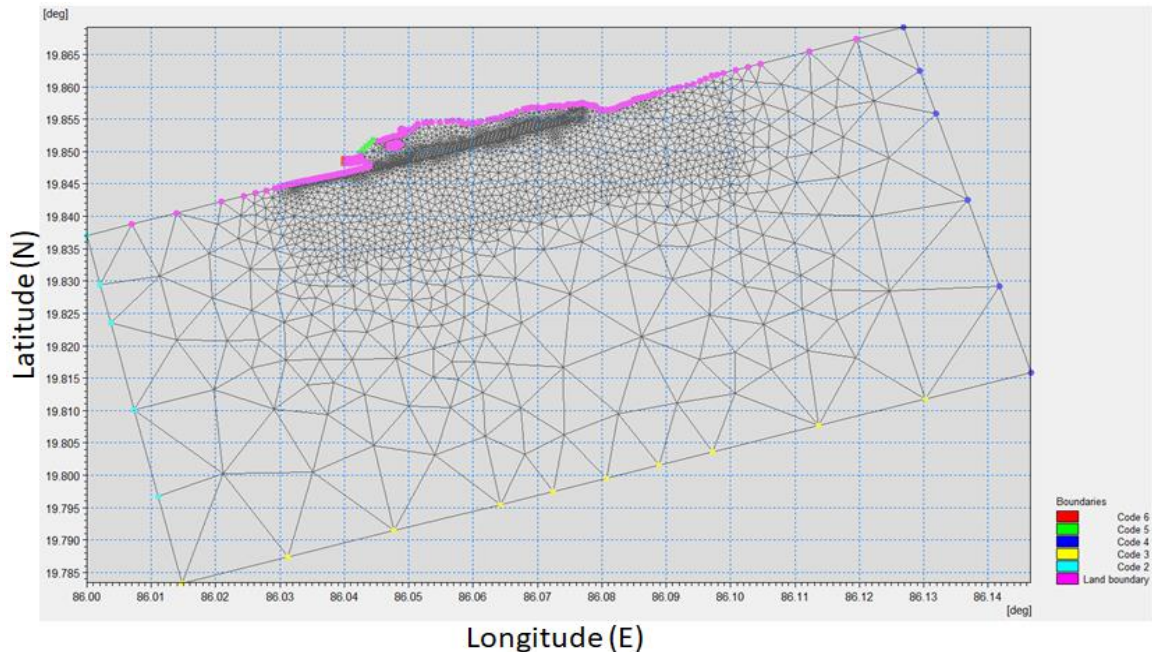


Figure4.8 Boundary conditions of the SW model

4.5.3.2. MIKE21 Coupled Model FM model parameters

The MIKE21 2D Hydrodynamics model has been run for the reduced model domain (Figure 4.7) with domain specification with 2.6m as maximum depth of cut-off. The hydrodynamic model was also simulated for the same period as mentioned in spectral wave model. The hydrodynamic modelling system is based on the numerical solution of the two-dimensional shallow water equations i.e., depth-integrated incompressible Reynolds Averaged Navier-Stokes equations. Thus, the model consists of continuity, momentum, temperature, salinity and density equations. Cyclone generated wind forcing is given as varying in time and constant in domain. Coriolis forcing, eddy viscosity using Smagoransky formulation and bed friction in the form of Manning number with a constant value of $32 m^{1/3}/s$ are also included in the model. Wave radiation stresses are included in the model in the form of varying in time and constant in domain.

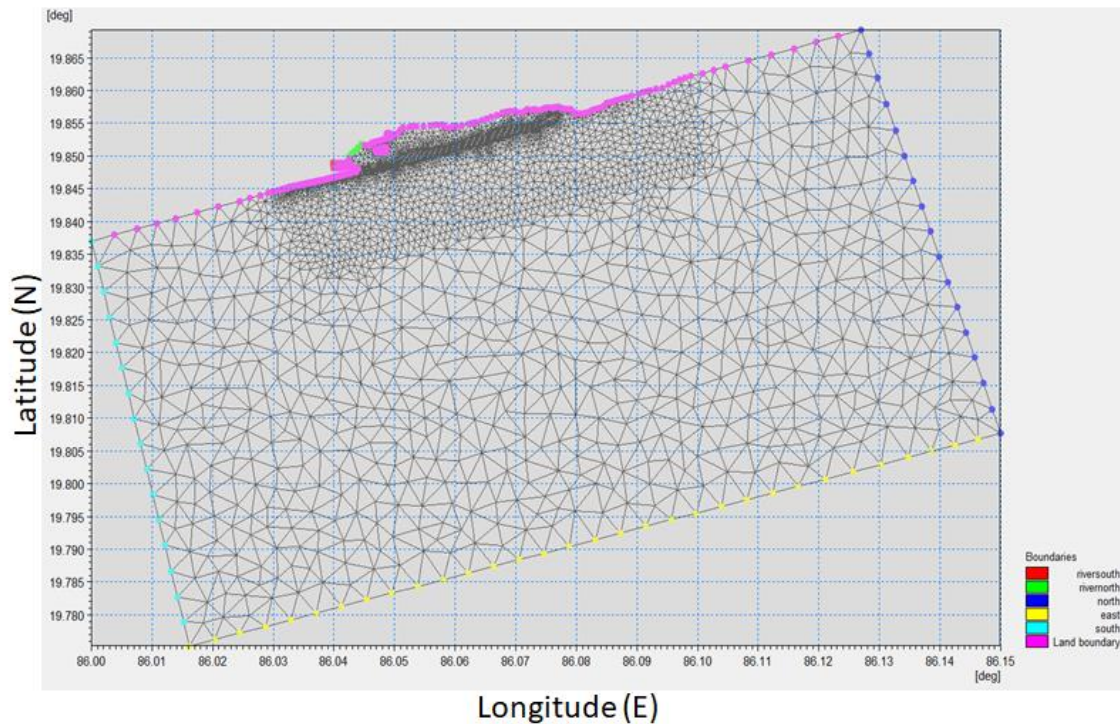


Figure 4.9 Boundary conditions of the Coupled Model FM

South and river north boundaries are given with specific discharges of $2 \text{ m}^3/\text{s}$ and $1 \text{ m}^3/\text{s}$ respectively whereas south and river north boundaries are also given with specific discharges under weak formulation (Figure 4.9). The output parameters in hydrodynamic model viz. surface elevation, U and V velocities, current speed and direction along with Courant–Friedrichs–Lewy (CFL) number are extracted with a time step of 5min.

MIKE21 ST module uses the wave and current formulation of sediment transport with the flow model providing the currents and the wave information obtained from the wave model. The modelling system is based on the numerical solution of the two/three dimensional incompressible Reynolds averaged Navier-Stokes equations subject to the assumptions of Boussinesq and of hydrostatic pressure. Thus the model consists of continuity, momentum, temperature, salinity and density equations and it is closed by a turbulent closure scheme. Sediment properties like porosity (0.4), grain diameter (0.2mm) and gradient coefficient (1.1) are considered in the model. Wave field obtained from the SW model is given as forcing function in the model domain. Regarding the morphology parameters, no slope failure condition, and zero sediment flux gradient at all the boundaries have been given. The output parameters in transport model are sediment transport rates and bed level changes and are extracted at every 5min interval.

4.6. RESULTS AND DISCUSSION

4.6.1. Cyclone winds

The cyclone winds are generated using parametric model and is compared with the available measured winds off Gopalpur during the cyclone Phailin (Jaya Kumar and Mani Murali, 2014). The model winds were compared for about a period of 24 hrs (i.e. from 11-10-13 23:00 UTC to 12-10-2013 23:00 UTC). The modelled winds showed good comparison with measured winds. The measurements of wind gusts made using automatic weather data measurement system on the Gopalpur coast (Desai et al, 2010) are compared

with the modelled wind speed and both were in close agreement. The comparison plot between measured (blue line) and modelled (black line) cyclone winds for the Phailin cyclone is showed in the Figure 4.10. The measured wind speeds could not obtain after 23hrs IST from 12th Oct 2013 for this location due to failure of the instrument. The cyclone wind model results comprising of wind speed (m/s), wind direction (degree) and atmospheric pressure (hPa) were used as input to the MIKE21 spectral wave model.

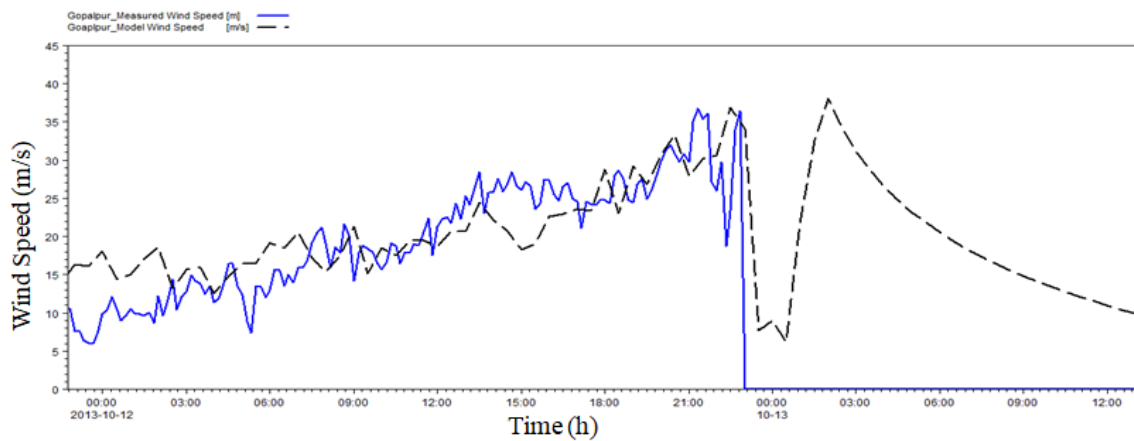


Figure 4.10 Comparison of measured and modelled cyclone winds at Gopalpur (19.3081⁰N, 84.9614⁰E) for cyclone Phailin

4.6.2. Storm waves

The storm winds generated are used as input in the MIKE21-spectral wind wave model to generate storm induced waves. The waves were simulated from 07-10-2013 06:00:00 to 14-10-2013 09:00:00 with time step interval of 5min (i.e. from starting of the cyclone to till its dissipation). Simulations were carried out in order to generate different wave parameters such as significant wave height, wave period, and wave direction. The variation in significant wave height at different locations namely breaching point, in between breaching point and offshore, offshore, two points on the berm and inlet location (Figure 4.11) has been shown in Figure A4.1(d) at different time steps.

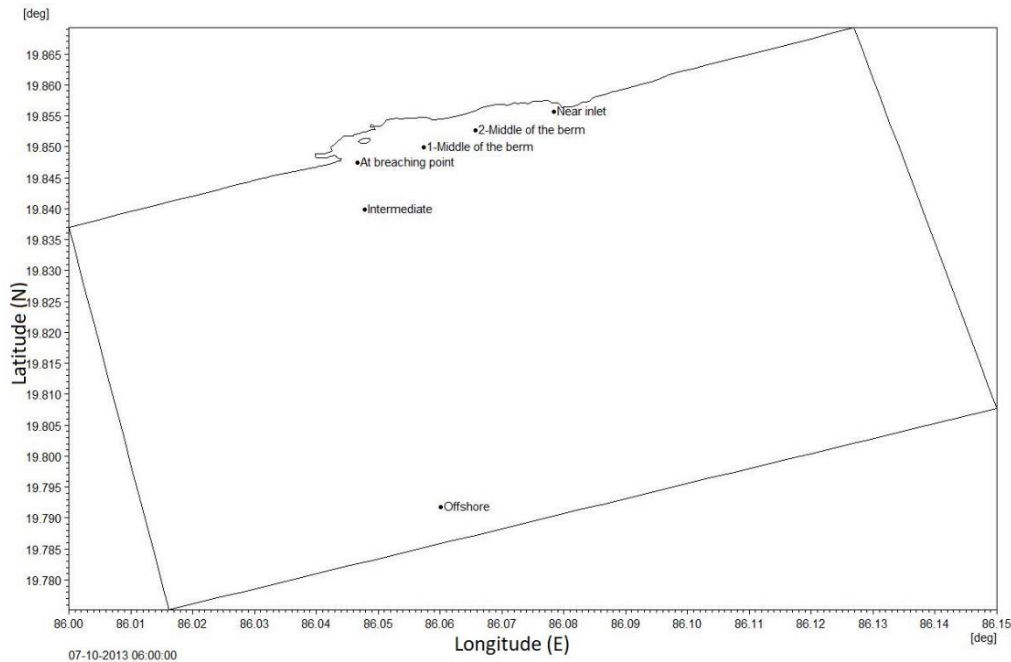


Figure 4.11 Points of interest in the study

The wave from the MIKE21 spectral wave model are observed to match well with the measurements obtained from wave rider buoy, as reported in Nair et al. 2014, recorded at Gopalpur, the landfall point of the Phailin cyclone. The wave height comparison of the Phailin cyclone wind wave model for Gopalpur and Paradip locations and measured wave heights at Gopalpur are represented in the Figure 4.12 (Jaya Kumar and Mani Murali, 2014). At initial time steps, the wave model gave lower wave heights but the cyclone reaches nearby landfall point wave heights match well with the measured data before the buoy cut loose from its mooring. The significant wave heights at the points of interest (Figure A4.1 (d)) are not varying much till the cyclone reaches nearby the landfall point on the Odisha coast. From 11th Oct 2013 18:00:00, the significant wave heights at the four points of interest (i.e. at breaching point, 1-middle of the berm, 2-middle of the berm and inlets location in Figure A4.9(d) to Figure A4.17(d) show the considerable difference (>2m at all points) for a period of 2 days. Similarly the wave period also suddenly raised at the time the cyclone made a landfall on the Gopalpur coast but the values are constant for entire berm length of 2.8km. However, the wave direction is constant from the north during this

cyclone. Over a period of 24hrs (12-10-2013 12:00:00 to 13-10-2013 12:00:00) there is a continuous waves forcing of magnitude more than 3.2m all along the berm.

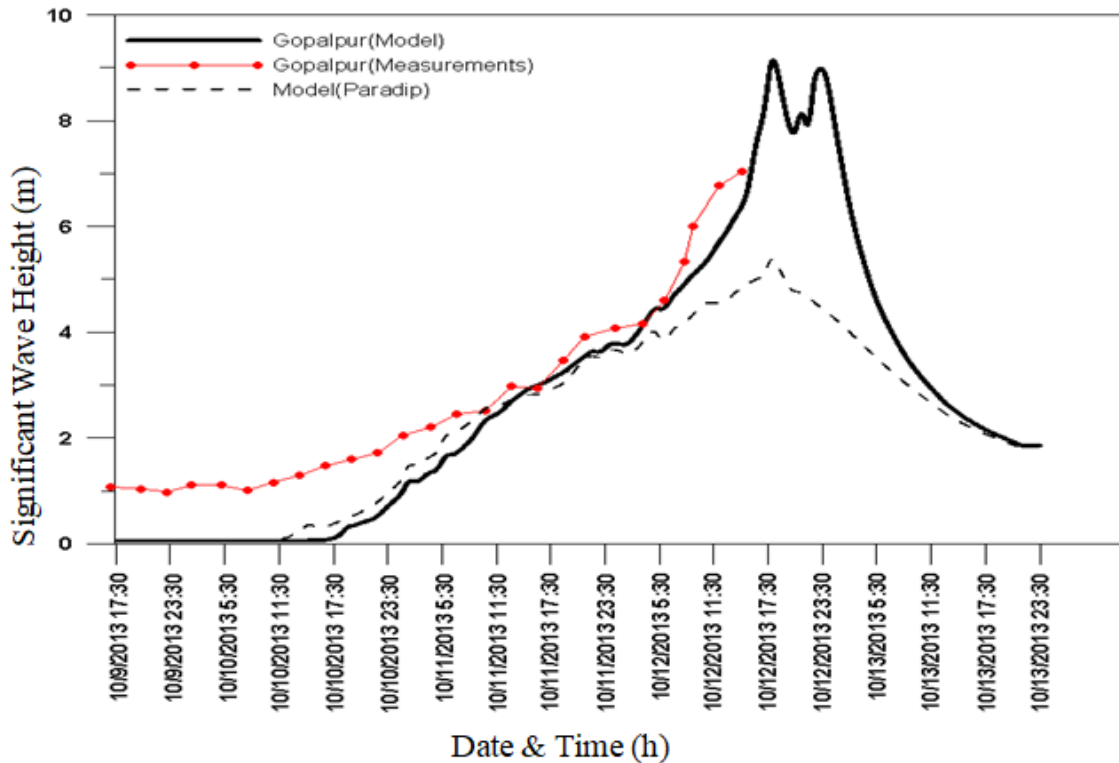


Figure 4.12 Wave heights obtained from Phailin Cyclone wind wave model for Gopalpur (solid line) and Paradip (dash line) compared with measured wave heights at Gopalpur (dot-dash line).

4.6.3. Surface elevation and storm surge near Khalakata Inlet

The surface elevations were extracted from MIKE21 Hydrodynamic module at three points of interest viz. tidal inlet, middle of the berm and breaching point at 10m water depth by giving the locations as point series. From the Figure A4.1 (f), it is understood that the surface elevation at 10m water depth is same through the entire berm length of 2.8km except offshore location. To evaluate the surge, the surface elevations were also extracted at the same locations in the absence of cyclone winds and waves. Then the storm surge

values were obtained by subtracting the surface elevation values without cyclone winds and waves from the surface elevation values with cyclone winds and waves. The storm surge values at breaching point is showed in Figure A4.1 (e).The numerical model is well validated with measured data of waves and surge.

4.6.4. Bed level Changes

To study the bed level changes line series files are extracted near the points of interest with hundred points on line. Breaching was observed from satellite images after the Phailin cyclone at this location and hence the study of bed level changes has been taken in this location. In addition, bed level changes near the inlet location has been studied. Since the measured topographic data at the berm is not available, the simulations were carried out by assuming the berm height of 3m near the breaching point.

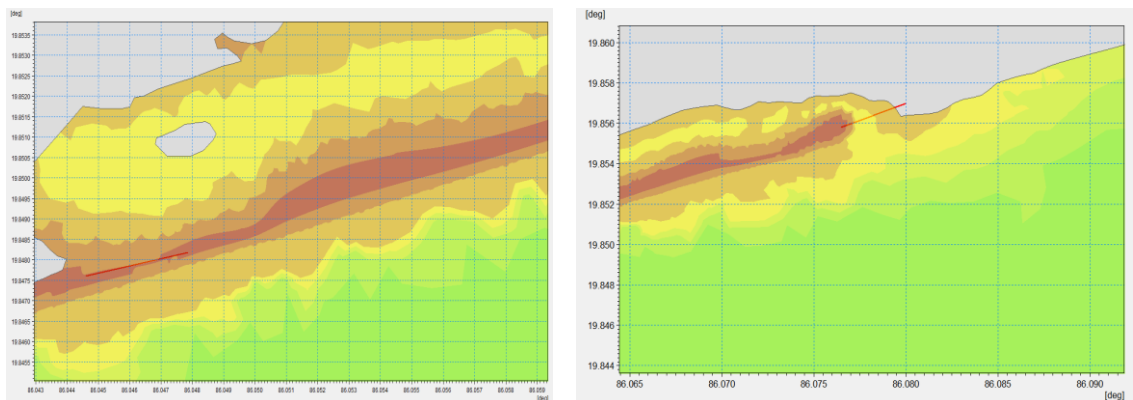


Figure 4.13 Locations considered to study Bed level changes along the berm at (a) breach location and (b) inlet location

Various simulations have been performed by changing the berm topography using datum shift approach till the breaching appeared. The breaching of the berm started when the

height is 2.45m. However, the width of the breach after the cyclone cleared did not match with the satellite images for the berm height of 2.45m. Therefore further reduction in the berm height was carried out till the breach width from the model matched with the breach width observed in the satellite image. For the berm height of 2m the breach width was observed to be in good comparison with that of observed information.

4.6.4.1. Bed level changes along the berm

To study the bed level changes along the entire model domain in nearshore region, four transects are considered at water depth less than 10m as shown in the Figure 4.14. The bed level changes observed at the four transects is given in Figure 4.15.

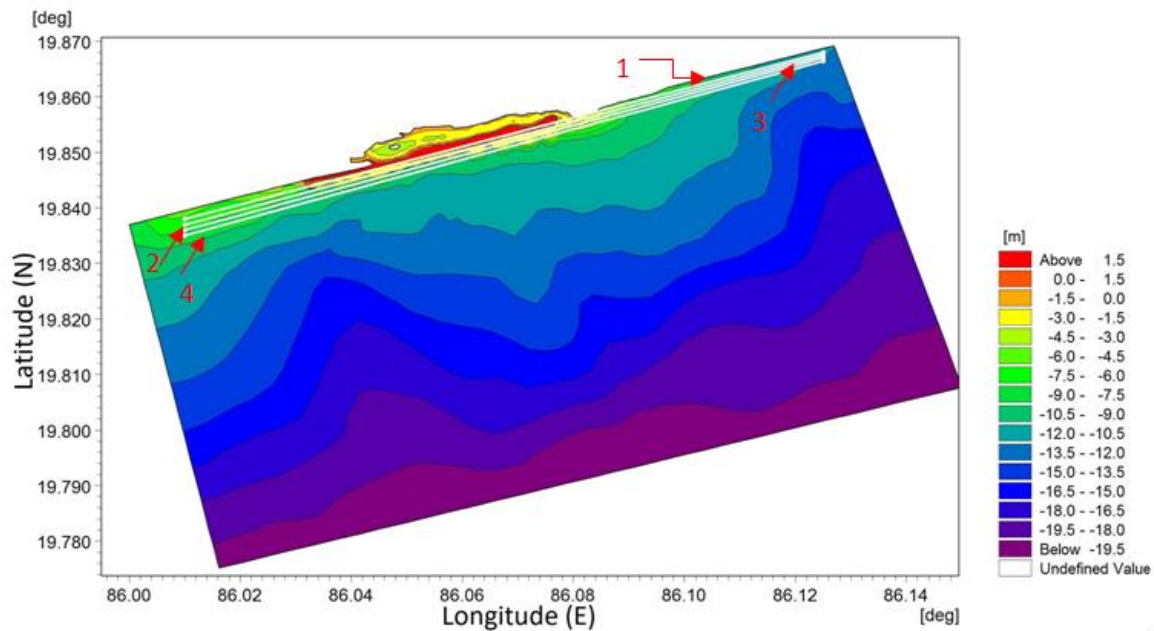


Figure 4.14 Locations and transects considered for study of bed level changes alongshore close to the berm.

The variation in the bed level along the transect results in the thickening of the lines as seen in Figure 4.15. It has been observed from the Figure 4.15 that the bed level changes mostly

occur at water depths less than 6m. In addition to that the changes in bed levels are observed at only two transects (Figure 4.15)

In addition to the above four points two more transects of length 400m and 350m are considered on the berm at breaching point and inlet location respectively as shown in Figure 4.13. The red line in the Figure 4.13 is the length of the berm considered to study the bed level changes. The bed level changes at breaching location have been observed from 9th October 2013 18:00:00. Before that there is no much change in the bed levels. The bed level changes for breached location is presented in Figure 4.16. The maximum bed level change observed is 3.8m near the breaching location. Similar to breaching location, in case near inlet also the bed level changes are observed from 9th October 2013 18:00:00 (Figure 4.17).

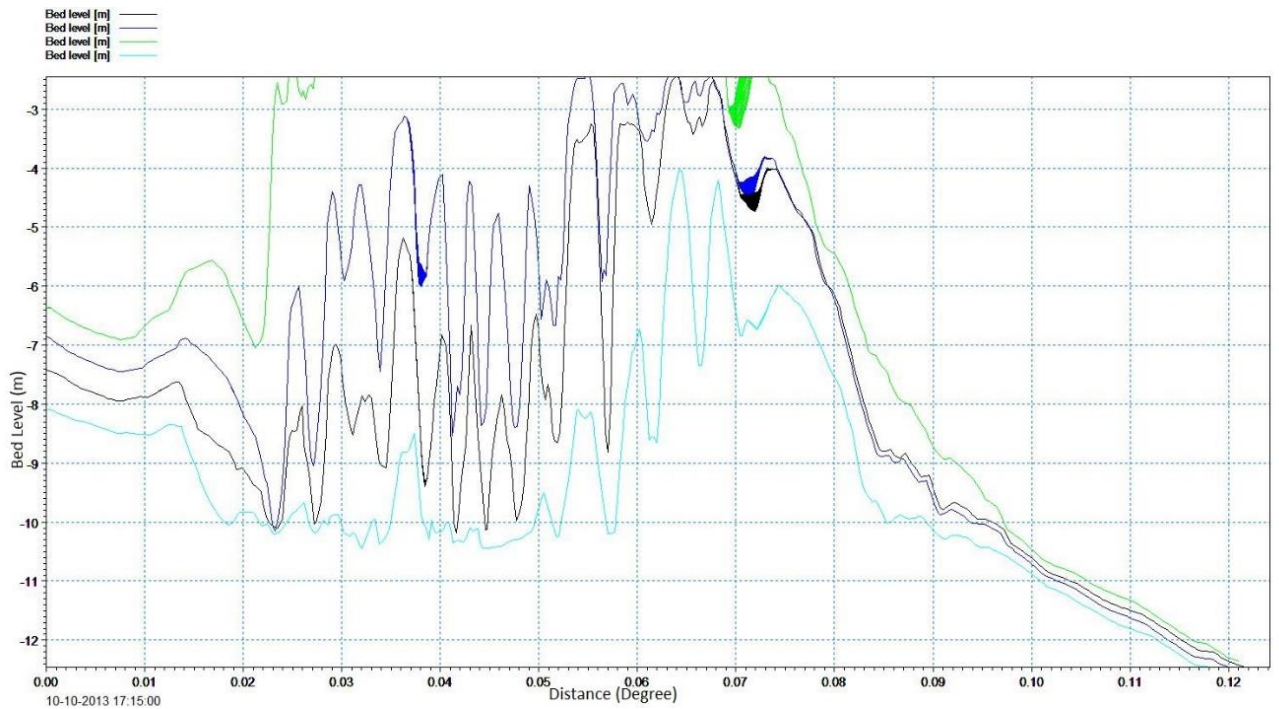


Figure 4.15 Bed level changes along the berm at 4 transect lines

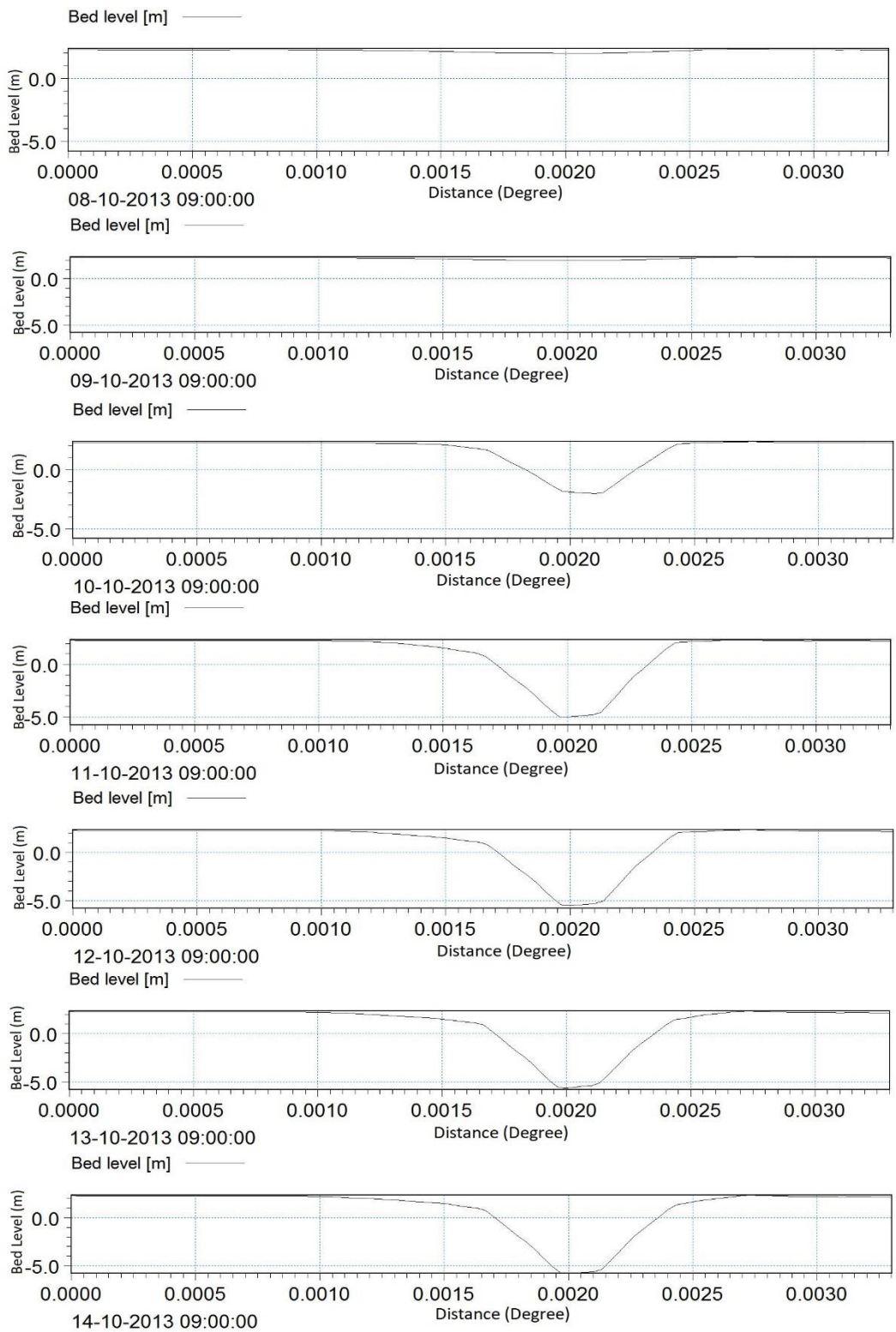


Figure 4.16 Bed level changes at 2.2m berm height of the berm near breaching point

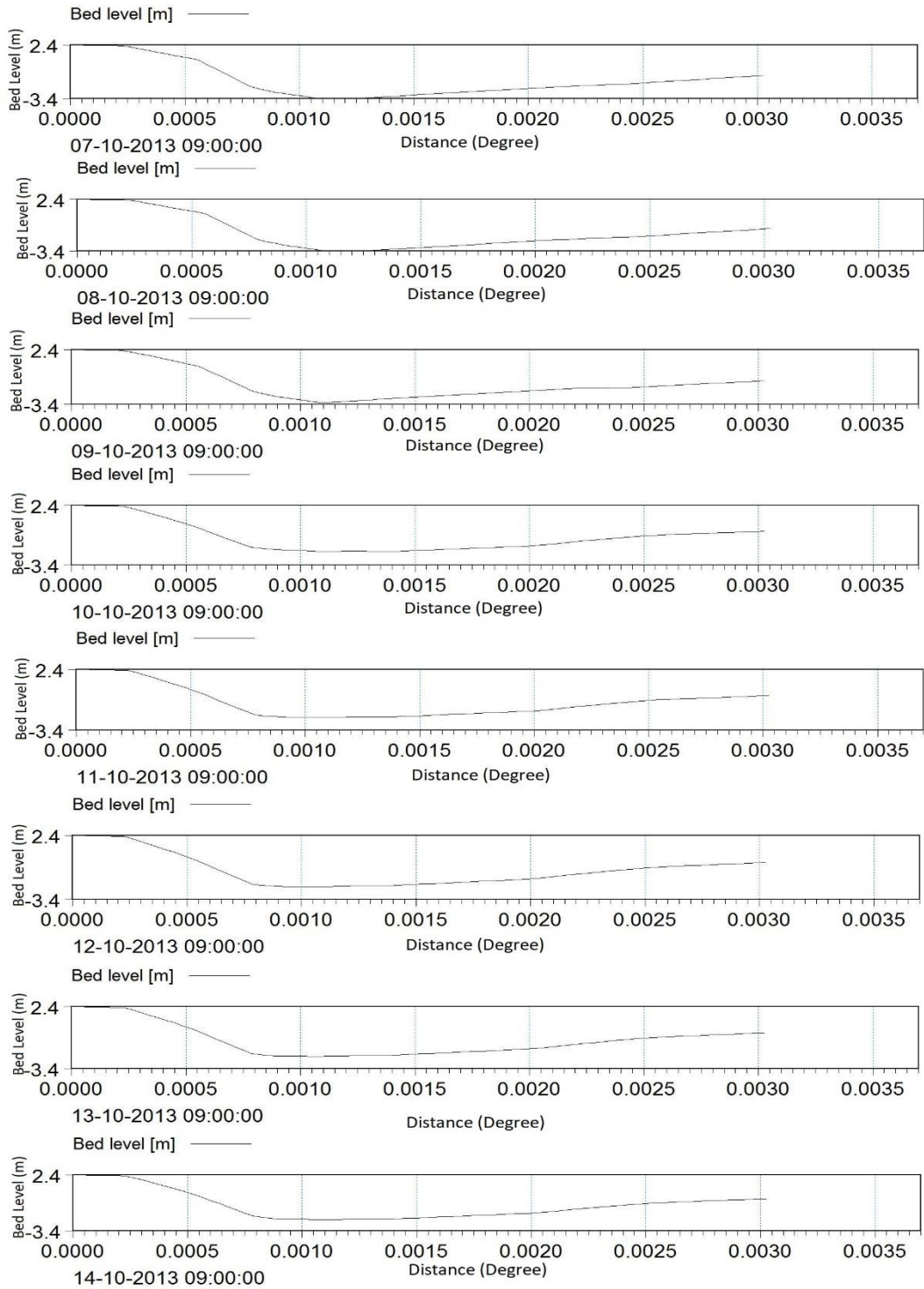


Figure 4.17 Bed level changes at 2.2m berm height of the berm near inlet location

4.6.4.2. Bed level changes across the berm

To study the bed level changes across the berm four locations are considered (breaching point, two locations on the berm and inlet location) as shown in the Figure 4.18. At all the locations time series data is extracted with 500 points on the line. The bed level changes at breaching location for transect A-A at all time steps is presented in the Figure 4.19.

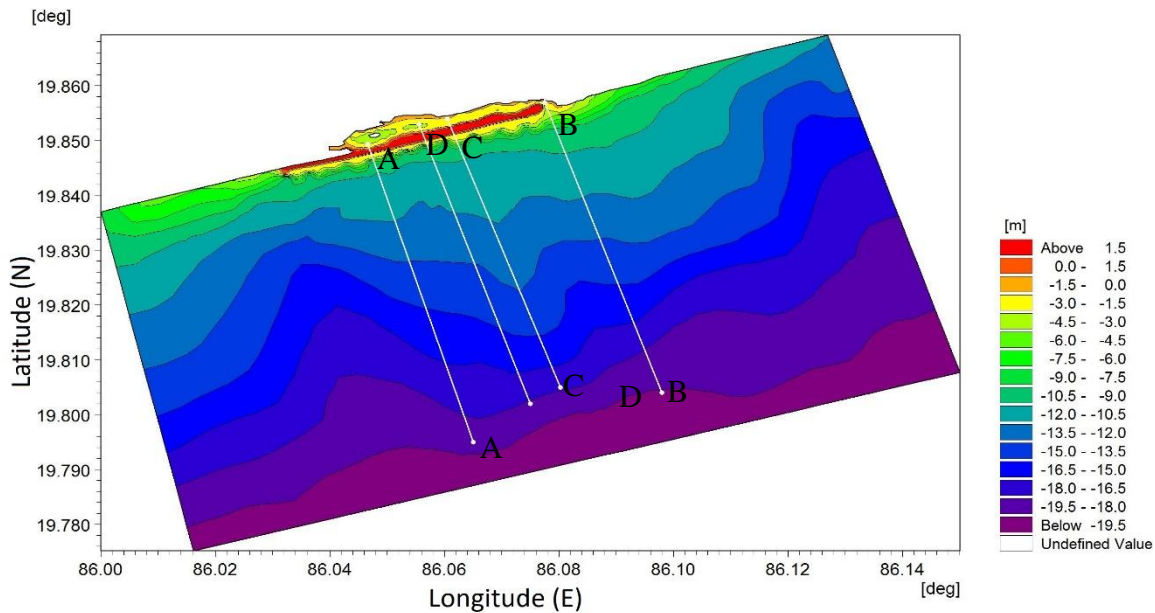


Figure 4.18 Locations considered for study of bed level changes across the berm

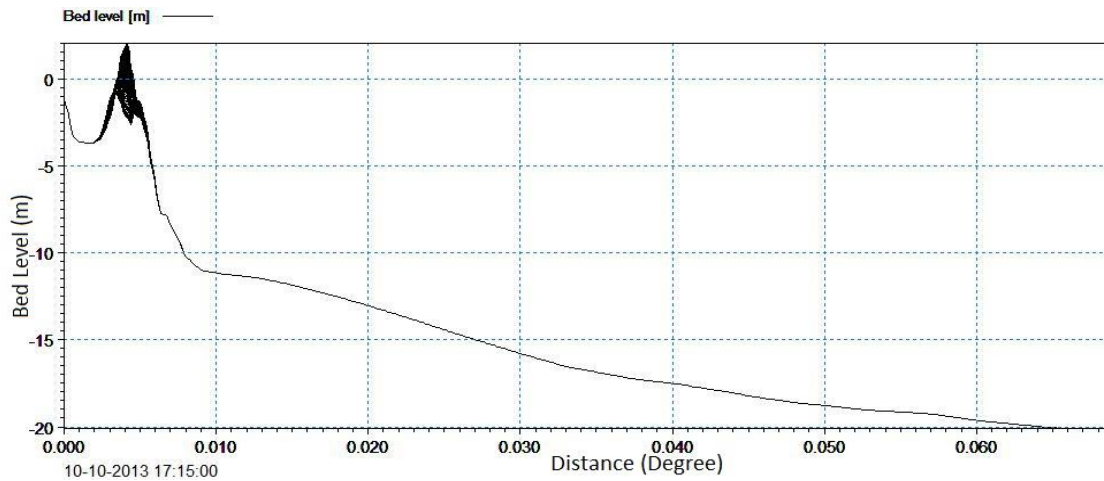


Figure 4.19 Bed level changes across the berm at breaching location

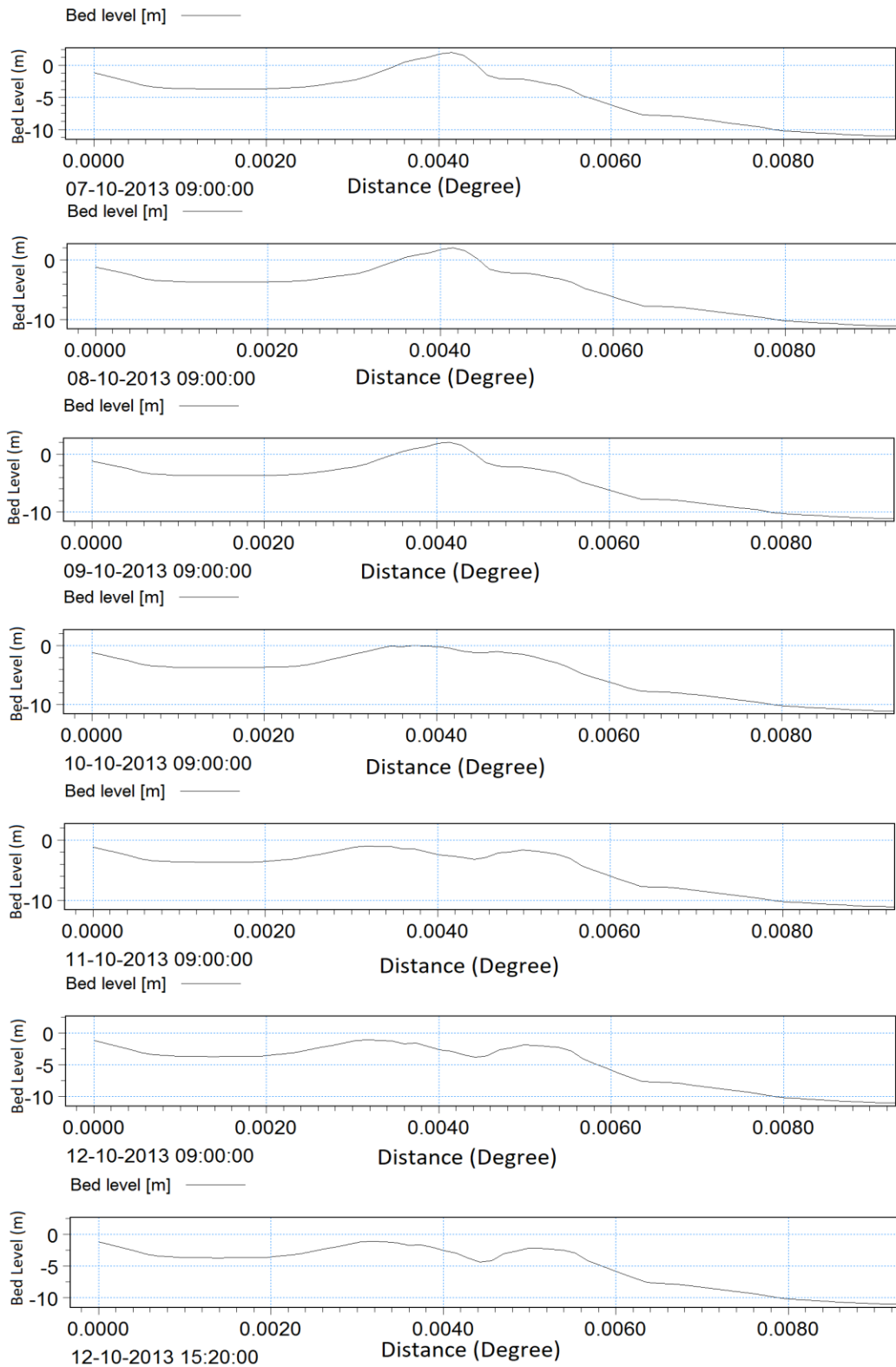


Figure 4.20 Bed level changes across the berm at breach location at different time steps

From the Figure 4.19, it is understood that the bed level changes near the breaching location has been observed. To study the bed level changes in detail near the breach, the time series plot has been drawn at different intervals as shown in Figure 4.20. The bed level does not change much till 9th October 2013 12:00:00. The maximum bed level change observed during the last time step (i.e. 12th Oct. 2013 15:20:00) is 4.5m. The transect C-C and transect D-D are observed to have no change in bed levels during the whole cyclone period (Figure 4.21(a)& 4.21(b)).

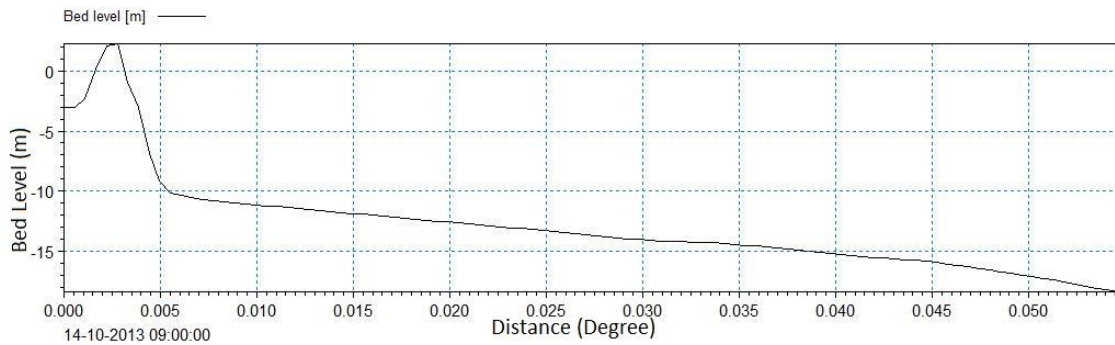


Figure 4.21(a) Bed level changes across the berm at Transect D-D

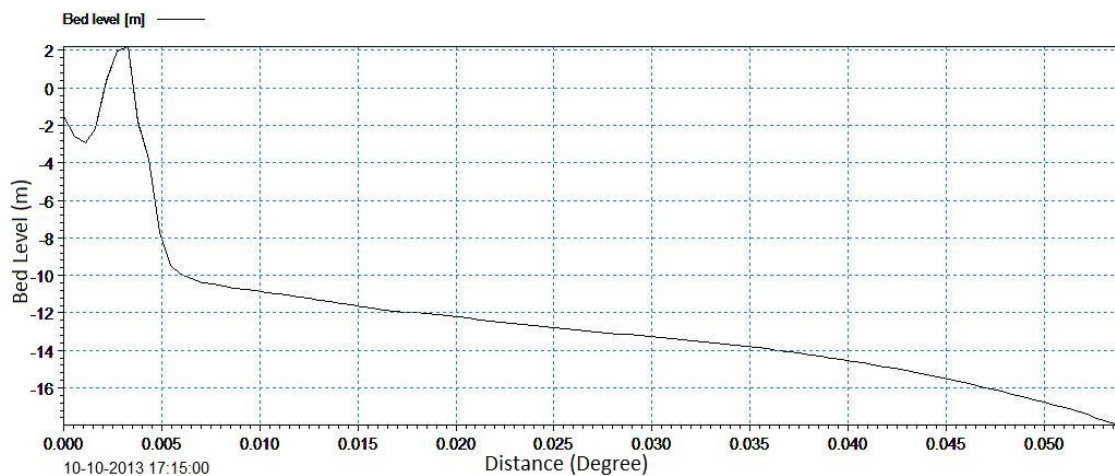


Figure 4.21(b) Bed level changes across the berm at Transect C-C

The bed level changes across the berm at tidal inlet location during the considered simulation period for the cyclone Phailin is given in Figure 4.22. The bed level changes are observed at inlet location for a length of about 250m. The bed level change at different

time steps is presented in Figure 4.23. The maximum bed level change of 1.7m has been observed at inlet location.

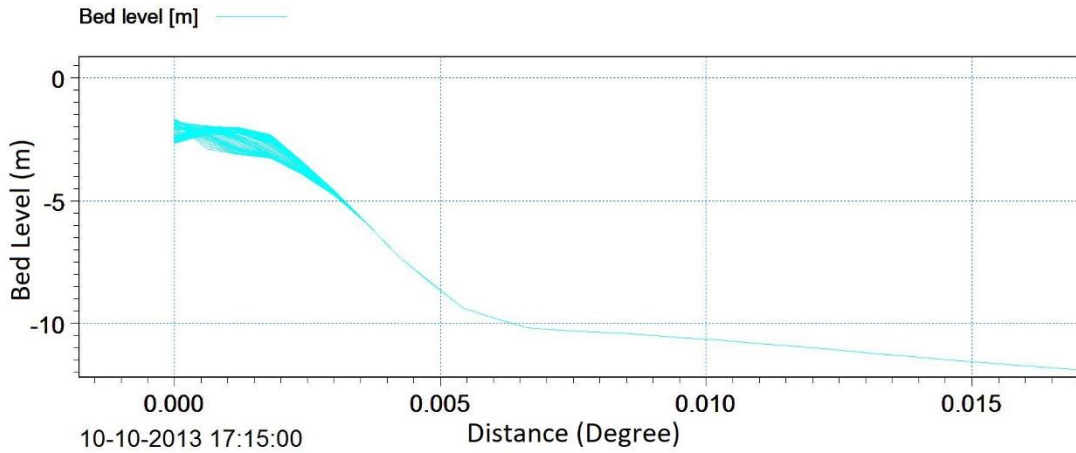


Figure 4.22 Bed level changes across the berm at inlet location

4.6.5. Flow pattern at points of interest

The flow pattern changes are studied by observing the significant wave height, surge and tidal elevations and flow speeds at breaching location and at the tidal inlet location. The flow patterns for different time steps at 6 hrs interval starting from 09th October 2016 19:00:00 are also presented. The bed morphology changes give the expected change in bed levels in the study region.

A total of 18 times steps at 6 hrs interval in the study region are considered for comparing the changes in hydrodynamics, i.e., flow speed and water levels. The graphical plots representing the flow speeds, significant wave height, surge and water level variation, at each time step for entire model domain and points of interest (i.e. at breaching and inlet locations) are shown in Figure A4.1 to Figure A4.18.

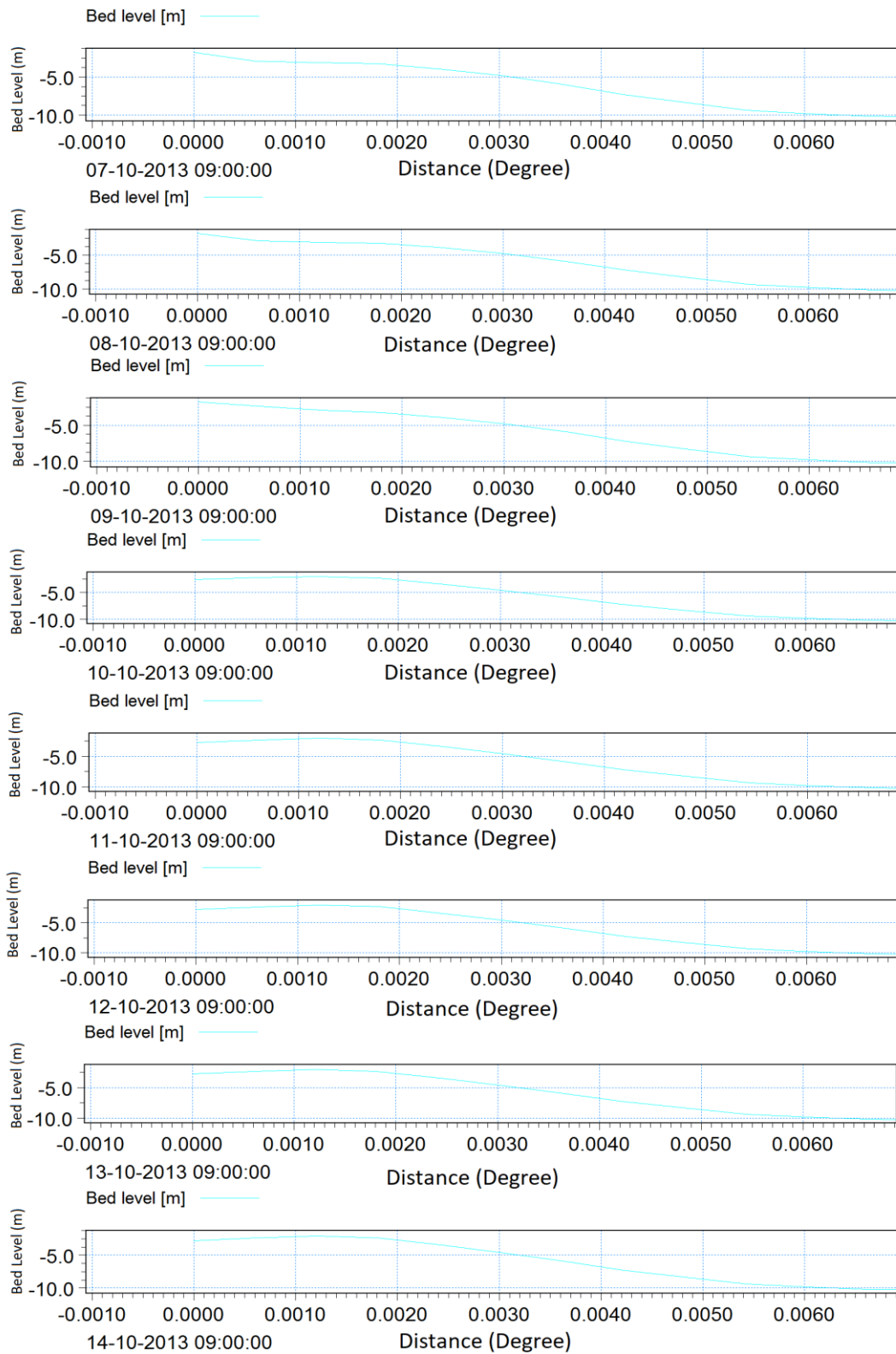


Figure 4.23 Bed level changes across the berm at inlet location at different time steps

The flow speed is 0.2 m/s at water depth of 3m whereas at breached location the flow speed reaches up to 0.6m/s and the flow direction is northeast on 9th October 2013 18:00:00 (Figure A4.1b). The flow speed at same time step at inlet location is observed to be 0.8m/s at a water depth of 3m whereas, at inlet the flow speed is up to 1.4m/s (Figure A4.1c) in the same direction.

On 9th October at 22:00:00 there is a surge of about 30cm at the breach location whereas at the other location it is not observed. However, it occurs before the cyclone landfall hit the coast. The flow speed is 0.4m/s at water depth of 3m whereas at breached location the flow speed goes up to 1.6m/s and the flow direction is northeast on 10th October 2013 00:00:00 (Figure A4.2b). The flow speed at same time step at inlet location is observed to be 1m/s at a water depth of 3m whereas at inlet gorge the flow goes upto 1.6m/s (Figure A4.1c) in the same direction. The flow speeds at time step 3 (i.e. at 10th October 2013 06:00:00) were marginally decreased of the order of 0.2m/s at both the locations whereas the flow direction remain unchanged (Figure A4.3b and Figure A4.3c).

On 10th October 09:00:00 there is a surge of about 70cm at breach location has been observed. However, this is observed 12.5 hrs before cyclone landfall point. This may be the probable reason for the increase of the breach width and also observed that from this time step the breach width is in increasing order in each time step. The flow speeds at breaching location remain unchanged between time steps 4 to 6 (i.e. from 10th October 12:00:00, 10th October 18:00:00 and 11th October 00:00:00), whereas, the flow speeds at inlet location was 0.8m/s, 1m/s and 0.6m/s at respective time steps. The flow direction remains unchanged at all 3 time steps (Figure A4.4 to Figure A4.6).

At all other remaining time steps the flow speeds and flow direction at inlet location are marginal changed. However, the flow direction from time step 13th October onwards slightly oriented towards north. Whereas at the breaching location the flow speeds are varying between 1.6m/s to 0.8m/s at different time steps (Figure A4.7 to Figure A4.18).

Model simulations has been run for different berm heights near breaching location till the breached width matches with data from Google earth images. The modelled data give breached location width as 143.6m for a berm height of 2.2m. However, the breached width of the inlet at 3 different transects from Google earth image is given in Figure 4.24(a).

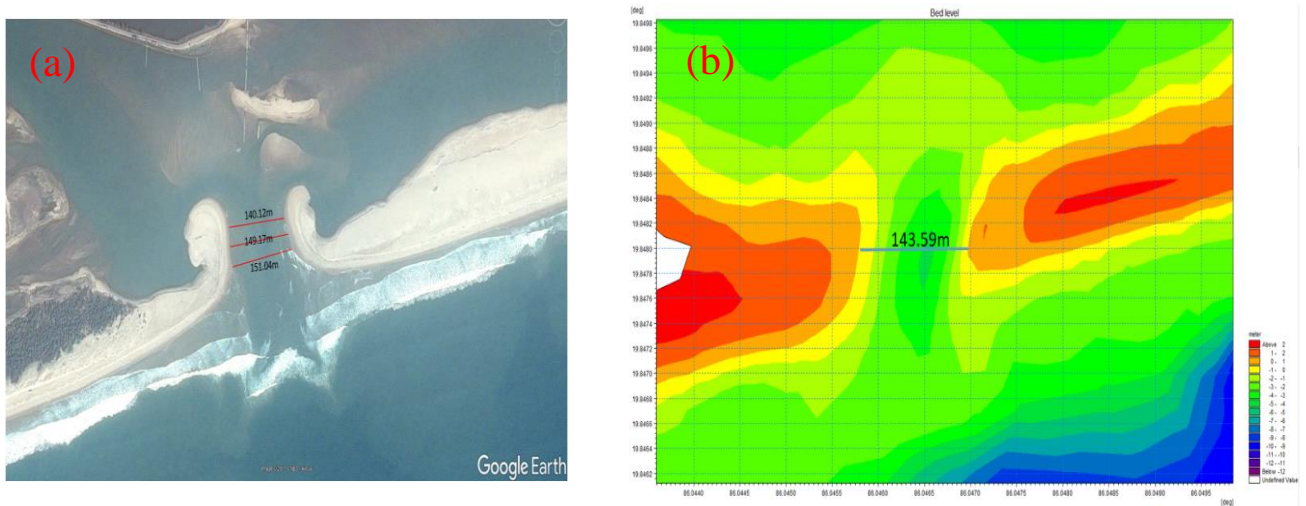


Figure 4.24 Width of the berm at breach location after the cyclone Phailin (a) Google earth image and (b) MIKE modelled data

4.6.6. Berm breaching process

In order to further understand the primary forcing parameters for the berm to breach, numerical model simulations were carried out with the following boundary conditions for the berm height of 2.2 m, viz., (i) simulation with tide only, (ii) simulation with wave only, (iii) simulation with wind only, (iv) simulation with tide and wave, (v) simulation with tide and wind, and (vi) simulation with wind and wave. The bed level changes obtained from the above five simulations are shown in Figures 4.25 to 4.30.

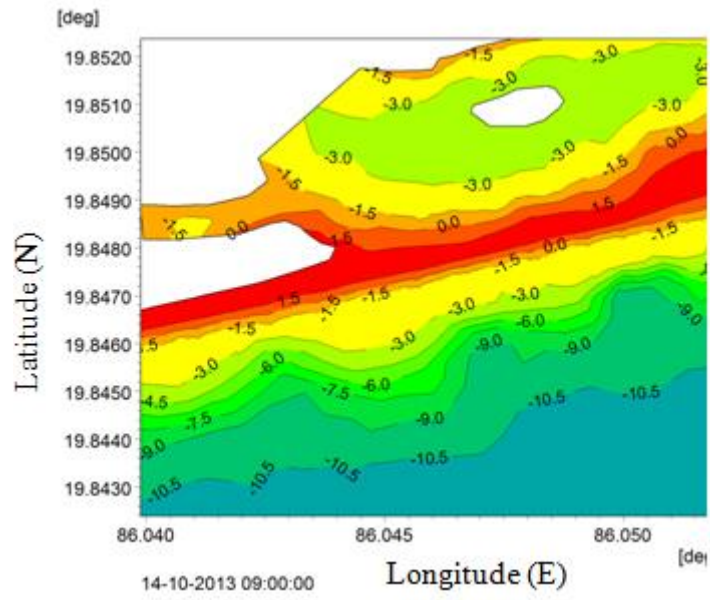


Figure 4.25 Bed level at the end of simulation for Wind only case

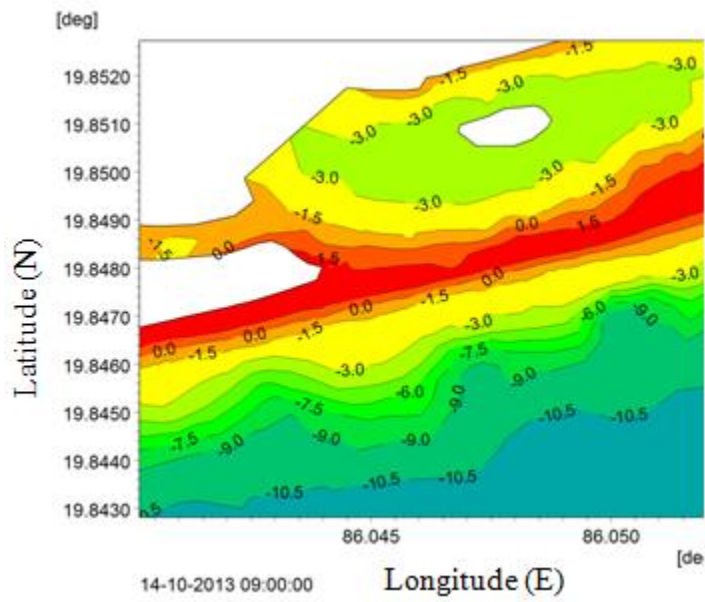


Figure 4.26 Bed level at the end of simulation for wave only case

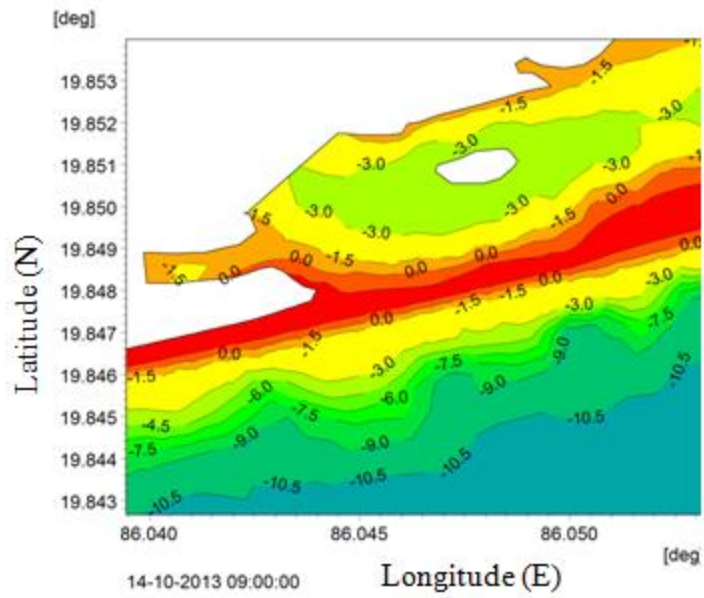


Figure 4.27 Bed level at the end of simulation for Tide only case

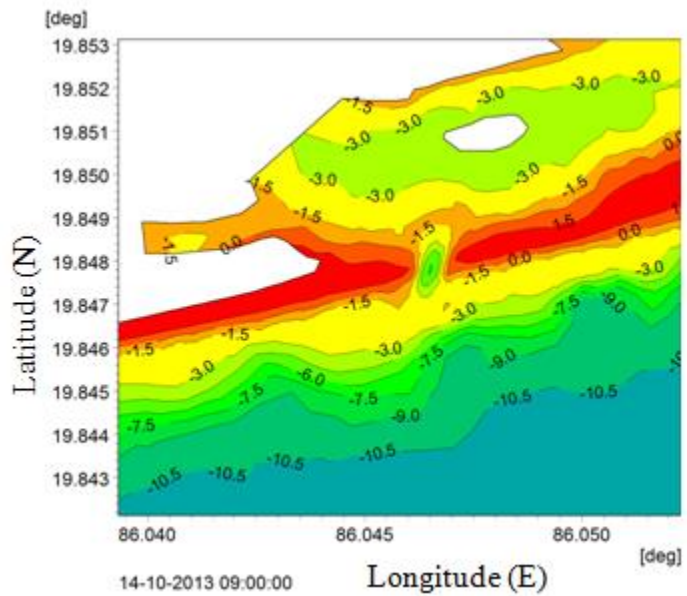


Figure 4.28 Bed level at the end of simulation for Tide+Wind case

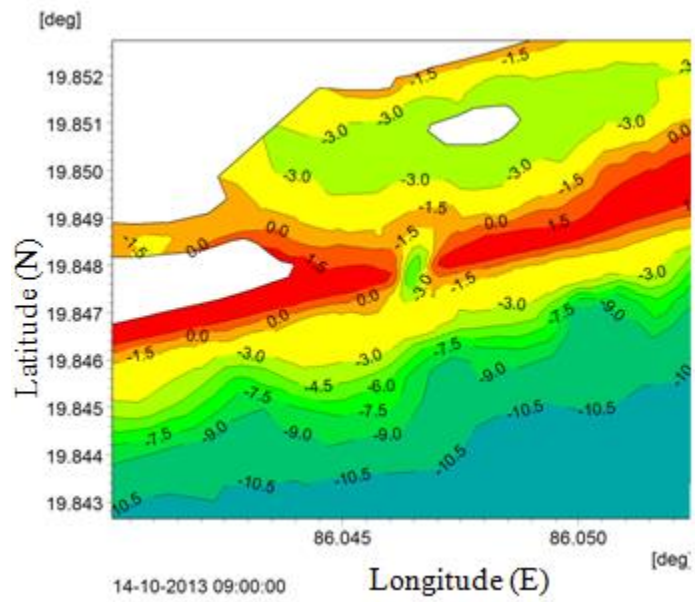


Figure 4.29 Bed level at the end of simulation for Tide+Wave case

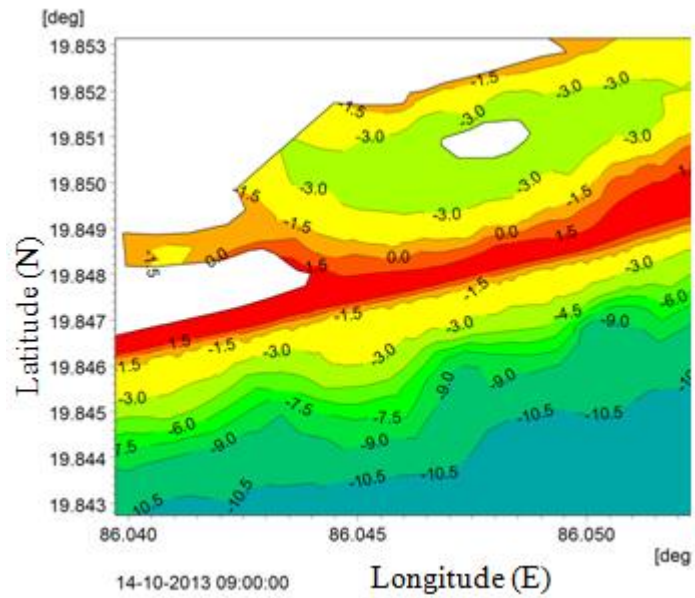


Figure 4.30 Bed level at the end of simulation for Wave+Wind casess

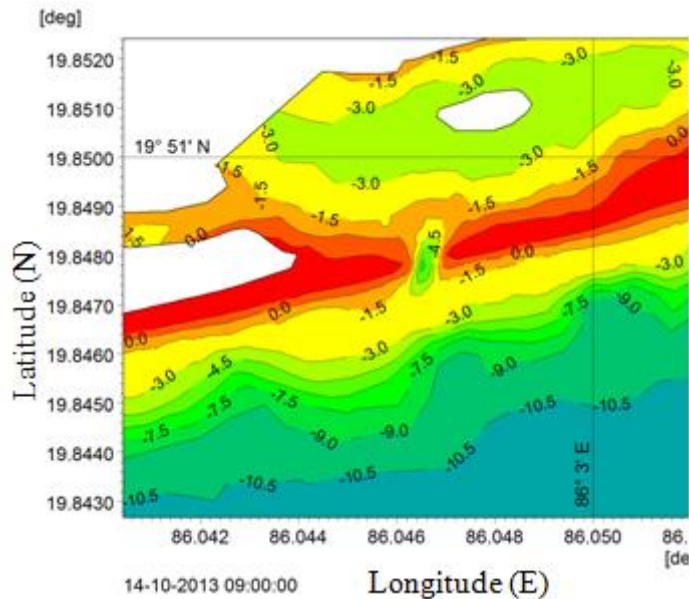


Figure 4.31 Bed level at the end of simulation for Tide +Wind+ Wave case

The study results showed that the stand alone condition of wind or wave or tide do not cause berm breaching (Figure 4.25 to Figure 4.27). The combined case of Tide with wind and wave (Figure 4.28 and 4.29) show breaching of berm, whereas, the case of wind and wave combination does not breach the berm (Figure 4.30). And the combined case of Tide, wind and wave results in berm breaching with a breach depth of more than 4.5m after the end of simulation. The tide and wave combination resulted in stronger breach compared to tide and wind case, this is observed from the deepening and width of the breach. From this exercise of numerical model simulations, it is clear that tide levels or surge along with the wave played a major role in berm breaching.

4.7. SUMMARY

The cyclone induced hydrodynamics, sediment transport and morphology changes have been studied using MIKE 21 numerical model at Khalakata tidal inlet in Odisha coastline. The numerical models (MIKE 21 Spectral Wave model and MIKE 21 Coupled Model used in the study provided reliable estimates of waves, surface elevation and storm surges. Most

of the hydrodynamic and sediment transport activity limited to the nearshore region (<20m). The breaching of the berm was observed when the berm height is a minimum of 2.45m along the centre line of breach location, but the width of the breach for this berm height is only 34m. Since the width of breach is less compared to measured data from Google earth[®] images further simulations were carried out till the breach width matches with the Google earth images. It was observed that when the berm height is 2.2m, the width of breach gave good agreement with Google earth[®] images. However, the breach is observed to occur before the cyclone landfall point due to over wash from increased water levels due to tide, wave and wind. The forcing from the waves, tide and wind individually did not result in the breach. However, the combination of tide with both wind and wave resulted in breaching.

CHAPTER-V

SUMMARY & CONCLUSIONS

The thesis presents the classification of Indian coastal tidal inlets in terms of hydrodynamic and morphodynamic parameters under the three main forcing functions viz. tide, waves and river flow. In this study, an example of extreme event (Cyclone Phailin, Odisha) is studied for the post event morphological changes in the vicinity of the tidal inlets. Also, the study includes the use of non-parametric hydrological models for the discharge estimation in the ungauged tidal inlets that is used for the further inlet classification. The study will help the research community to understand the behavior and categorization of tidal inlets system along the shoreline for India as well as worldwide by using the three subjected input parameters. The main conclusions of this research is summarized in the subsequent sections.

5.1 CLASSIFICATION OF INDIAN TIDAL INLETS

A total of 471 tidal inlets are classified along the nine maritime states of India viz. Gujarat (42), Maharashtra (65), Goa (11), Karnataka (27) and Kerala (68) on west coast of India and Tamil Nadu (121), Andhra Pradesh (106), Odisha (23) and West Bengal (8) on east coast of India. The tidal range classification shows that 40 inlets are macrotidal, 82 inlets are mesotidal and 91 inlets are microtidal along west coast of India. The Gujarat coast experience macro-, meso- and micro tidal environment due to its unique configuration and behavior of the inlets in northern and southern parts of Gujarat. The northern part of Maharashtra inlets shows macrotidal environment with tidal range more than 4m, whereas, the central and southern parts of Maharashtra show mesotidal environment with the tidal range in between 3.74m to 2.07m. The Goa coast inlets and inlets along Uttar Kannada district of Karnataka show mesotidal environment whereas the inlets along Udupi and

Dakshina Kannada districts along with the Kerala state show microtidal environment. The microtidal environment is the main reason for migration and dynamic behavior of inlets along Kerala and southern and central Karnataka. Among 258 inlets along the east coast of India, only 21 inlets exhibit mesotidal and remaining all inlets exhibit microtidal environment. No inlet falls under the category of macrotidal along the entire east coast. Moreover, the complete Tamil Nadu and Andhra Pradesh coasts and south of Odisha coast are completely under microtidal environment.

Wave exposure regime classification shows that the entire west coast of India falls under highly exposed wave energy environment with minimum wave energy of $28.47 \text{ m}^2\text{s}^2$ at Bhatthaiya inlet along Gujarat coast and maximum of $112.70 \text{ m}^2\text{s}^2$ at Paravur lake inlet along Kerala coast respectively. However, the east coast of India 108 inlets falls under the category of moderately exposed and 105 inlets are highly exposed wave energy environments with minimum wave energy of $3.56 \text{ m}^2\text{s}^2$ at Pudhuvalasai inlet and maximum of $122.24 \text{ m}^2\text{s}^2$ at Kadiyapattanam inlet along Tamil Nadu coast. None of inlets along east and west coast of India fall under mildly exposed wave energy environment.

Hydrodynamic classification shows that 284, 232, 288, 307 inlets fall under mixed energy classification followed by 130, 202, 89, 95 wave-dominated inlets and 54, 35, 93, 67 tide dominated inlets for annual, south west, north east and fair weather seasons respectively. However, only four in Annual, two in South West Monsoon (SWM), one in North East Monsoon (NEM) and two in Fair Weather (FW) season fell into the subclass of formation of barrier at inlet entrance. For, the SWM, almost 45% (202 inlets) fall under Wave Dominated (WD) subclass. However approximately 20% of the inlets in NEM (89 inlets) and FW season (95 inlets) fall under WD subclass, whereas around 28% of inlets (130 inlets) fall under same category for annual season.

Mixed Energy (Wave Dominated) inlets are near to 40% for all the seasons viz. Annual (209), SWM (170), NEM (170) and FW (181) seasons. This shows that mixed energy wave dominance is there irrespective of temporal variations for tidal range at all inlets. However,

Mixed Energy (Tide Dominance) is observed near about 15% of the inlets for both annual (75) and SWM (62) season and 25% for NEM (118) and FW (126) seasons respectively. The subclass Tide Dominated (Low) is observed at only 5% of the inlets for all three seasons including annual, whereas Tide Dominated (High) subclass is not consistent (7% - Annual, 2% - SWM, 14% - NEM and 10% - FW). Barrier formation is observed only at 4 out of 471 inlets for annual variations in wave height. This is because of river discharge and factors influencing the shape of inlets (i.e. bay area, tidal prism, tidal period etc.) are not included in the classification.

Geomorphological classification shows that 78 inlets are Tide Dominated (TD), 88 being Wave Dominated (WD), 15 being Mixed Energy (ME), and 31 being Intermittently Closed and Opened Lakes and Lagoons (ICOLLs) along the west coast of India. However, along the west coast of India, 18 inlets are Tide Dominated (TD), 158 being Wave Dominated (WD), 37 being Mixed Energy (ME), and 44 being Intermittently Closed and Opened Lakes and Lagoons (ICOLLs). Seasonal closure of tidal inlets is observed in about 14% and 17% of the inlets along the west and east coasts because of high wave activity during summer season. Most of the inlets along Gujarat and Maharashtra coastline are tide dominated because of submerged coast. On the other hand, most of the inlets along the east coast of India are wave dominated because of high wave activity in relative comparison with tide. Mixed energy inlets are also more along the Tamil Nadu and Andhra Pradesh coasts. Few inlets along Kerala, Tamil Nadu and Andhra Pradesh coastlines are ICOLLs, this is because of the river discharge and tidal forcing are not significant enough to keep the entrance open all the time.

The non-dimensional classification has been done only for 75 inlets due to non-availability of river discharge at rest of the inlets. The non-dimensional classification without wave period shows that 32 inlets fall under Tide Dominated, 2 inlets being Tide Dominated-Bays, 2 inlets being River Dominated, 11 inlets being Wave Dominated followed by 28 inlets Wave Dominated ICOLLs. The non-dimensional classification with wave period shows that 27 inlets fall under Tide Dominated, 7 inlets being River Dominated, 11 inlets

being Wave Dominated followed by 30 inlets Wave Dominated ICOLLS. The non-dimensional classification with mean wave period at 75 tidal inlets along the Indian coastline sets the new states of limits (Figure 3.24) as: (1) Wave Dominated (ICOLLS) with $\frac{Q_f}{(g^{1.75}H^{1.25}T^{2.5})} \leq 0.0001$ and $\frac{\hat{Q}_{Tide}}{(g^{1.75}H^{1.25}T^{2.5})} < 0.045$, (2) Wave Dominated (WD) with $\frac{Q_f}{(g^{1.75}H^{1.25}T^{2.5})} > 0.0001$ and $\frac{\hat{Q}_{Tide}}{(g^{1.75}H^{1.25}T^{2.5})} < 0.045$, (3) Tide Dominated (TD) with $\frac{Q_f}{(g^{1.75}H^{1.25}T^{2.5})} > 0.0001$ and $\frac{\hat{Q}_{Tide}}{(g^{1.75}H^{1.25}T^{2.5})} > 0.045$, (4) River Dominated (RD) with $\frac{Q_f}{(g^{1.75}H^{1.25}T^{2.5})} \leq 0.0001$ and $\frac{\hat{Q}_{Tide}}{(g^{1.75}H^{1.25}T^{2.5})} > 0.045$. The new set of limits reduces the discrepancies that are there in non-dimensional classification without wave period under consideration introduced by Vu (2013). The improved classification system will show the better prediction of long-term morphological changes in the vicinity of the tidal inlets worldwide.

5.2 ESTIMATION OF FLOOD DISCHARGE AT TIDAL INLETS

Many Indian catchments are devoid of rain gauge stations. Even though those are installed and operating by Central Water Commission, India, most of the them are near about 1km away from the basin/catchment outlet (hereafter basin outlet is tidal inlet entrance and vice versa). This is one of major reasons for estimation of the river discharge at the ungauged basins using Synthetic Unit Hydrograph (SUH) methods.

Based on the total discharge values at ungauged catchments along coastal Karnataka and Kerala states, it is be observed that the Unit Hydrographs (UHs) generated through SUH methods have been found useful and effective along Konkan and Malabar coasts. The statistical evaluation of the UH ordinates obtained from the nine methods indicated that there are considerable differences in the methods except for Transmutation approach, two parameter Gamma distribution method and Hybrid model which have relatively close values regarding peak discharge ordinates (q_p), time to peak (t_p) and total discharge values (Q_f).

Even though the traditional methods (CWC methods, Snyder method and Soil Conservation Service method) are used widely in practical engineering problems, the manual fitting with limited characteristics points needs a high degree of subjectivity and trial and error whereas the probability distribution functions (pdfs) based SUH methods (Gray method, Croley method, Transmutation approach, two parameter Gamma method) and conceptual based SUH method (Hybrid model) gives the complete shape of UH and also satisfies the prerequisite for UH criterion. Adopting various methods available in the literature, and validating them with available measurements, unreported discharge estimates along the Karnataka and Kerala Coasts hitherto are provided in this study. The computed flood discharges could be used as prime input parameter to determine the type of dominance (i.e. wave-dominated, tide-dominated or river dominated) along the coastal tidal inlets, which seldom are available along the Indian coastline.

5.3 CYCLONE INDUCED MORPHOLOGY CHANGES IN THE VICINITY OF INLET

The cyclone induced hydrodynamics, sediment transport and morphology changes have been studied using MIKE 21 coupled model at Khalakata tidal inlet in Odisha coastline. The numerical models (MIKE 21 Spectral Wave model and MIKE 21 Coupled Model used in the study provided reliable estimates of waves, surface elevation and storm surges. Most of the hydrodynamic and sediment transport activity limited to the nearshore region (<20m). The breaching of the berm was observed when the berm height is 2.45m along the center line of breach location, but the width of the opening across the berm have been observed as only 34m. Hence further simulations were carried out till the breach width matches with the satellite images. It was observed that when the berm height is 2.2m, the width of breach (143.6m) gave good agreement with Google earth images (149.17m). The forcing functions influencing the berm breach were observed to be tide including surge, wave and wind while individually these three forcing parameters did not breach the

berm. Combination of tide with wave is observed to be more effective in breaching than tide with wind.

5.4 LIMITATIONS OF THE STUDY

- Synthetic unit hydrograph methods are used to estimate the flood discharge at the tidal inlet entrances
- Tidal inlets having throat width less than 5m is not considered for the classification of inlets
- Google earth images are used to identify the tidal inlets whose throat width is greater than 5m
- Geomorphological classification of all the tidal inlets has been done based on visual examination of the google earth images
- Longshore Sediment Transport Rate (LSTR) is not included in the classification of tidal inlets
- Measurements have not done before and after Phailin cyclone to observe the actual morphological changes in the vicinity of the tidal inlet

5.5 RESEARCH FINDINGS

- The non-dimensional method including wave period for classification of coastal systems can be applied worldwide with the three major forcing functions viz. tide, waves and river flow where one of the forcings is relatively constant.
- A non-dimensional UH is implemented for entire Konkan and Malabar Coast, India using non-dimensional method developed by the Central Water Commission (CWC-India)
- The morphological changes for microtidal wave dominated tidal inlet is being well predicted by MIKE 21 coupled model that has been validated with the measured wave and surge data. Therefore, MIKE 21 coupled model can be used to find out

the morphological changes around the coastal systems for microtidal wave dominated inlets.

- The breaching of the berm is observed to occur before the cyclone landfall point due to over wash from water flowing speeds. The combination of tide with both wind and wave resulted in breaching in comparison with individual forcing from the waves, tide or wind.

5.6 MATTERS OF FURTHER RESEARCH

- A quantitative measure efficiency of different Synthetic Unit Hydrograph methods like Nash and Sutcliffe (NS) efficiency shall give a better insight into the analysis. However, NS efficiency need the measured rainfall runoff data at the outlet of the catchments. Therefore, if the measured data is available then the comparison of total discharge values can represent more accurate results.
- The work of Bruun and Gerritson (1960) and Brunn et al. (1978) related whether an inlet would remain open or close. If the inlet stayed open, how sediment bypassing around an inlet would occur, to the tidal prism divided by the total gross transport delivered to the inlet in a given year. Bruun et al.'s relationships have the advantage that they incorporate sediment sources to the inlet. The Longshore Sediment Transport Rate (LSTR) is not included in the present study. For better results, LSTR has to be estimated at each tidal inlet and included as one of the significant drivers in shaping the inlet.
- With reference to the geomorphological classification, the inlets are visually examined and the dominance of wave, tide or river is decided. The visual examination of the tidal inlet may not be correct all the time. As on now, the tidal inlets are classified from the available satellite images. It would be more specific, if the images of the tidal inlets are obtained in all the seasons. This seasonal geomorphological classification, on comparing with other methods gives better idea about the character of the tidal inlets seasonally.

- The river discharge data (Q_f) is to be obtained from a reliable source or manually gathered or estimated using the various available synthetic methods at the respective tidal inlets along the Indian coastline. This would complete the dimensionless classification for all the identified inlets. Measurements should be done prior and post cyclone periods to get better understanding how the morphology is changing in the vicinity of the tidal inlets and also to validate the numerical model.
- Only one cyclone is considered for morphology studies in vicinity of tidal inlets due to limited availability of measured data. Studies using more cyclones would provide further knowledge on the morphodynamics of tidal inlets due to cyclones.
- The numerical model simulations to understand berm breach need further investigation in terms of berm slope stability, water table changes, morphology changes weeks before and months after the cyclone duration are needed.

APPENDICES

Appendix - I

Table A1.1 Historical cyclonic disturbances formed over NIO & its characteristics and effects on Indian coastline

S.No.	Year	Month	Date	Type & Origin	Name & Origin	Sustained Wind speed (km/h)	Central Pressure (hPa)	Storm Surge (m)	T-No.	Damage over India	Landfall point
1	2001	May	21-28	VSCS	India cyclone & AS	215	932	-	6	No damage was reported	Dissipated over sea off Saurashtra coast
2	2001	Sep	24-27	CS	- & AS	65	1000	-	2.5	No damage was reported	Dissipated over north-west Arabian sea near Oman coast
3	2001	Oct	8-10	CS	- & AS	65	998	-	2.5	No damage was reported	Dissipated over east central Arabian Sea
4	2001	Oct	14-17	CS	- & BoB	65	998	-	2.5	No. of deaths:108 Houses damaged-fully/partially:55747 Damage to crops: 125000 hectors	Crossed south Andhra Pradesh coast near Nellore
5	2002	May	6-10	CS	Oman cyclone & AS	65	994	wave ht. up to 4m	2.5	No damage was reported	South of Salalah Port, Oman

6	2002	Nov	10-12	SCS	WB cyclone & BoB	100	990	-	3.5	No. of deaths:20 Heavy rainfall in Odisha coast	Near Sagar Island, South of Kolkata, West Bengal
7	2002	Nov	23-28	CS	- & BoB	65	1000	-	2.5	No damage was reported	Central Bay of Bengal
8	2002	Dec	21-25	CS	- & BoB	65	1000	-	2.5	No damage was reported	Southeast Bay of Bengal
9	2003	May	10-19	VSCS	Sri Lanka cyclone & BoB	140	980	-	4.5	No damage was reported	North of Kyaukpyu, Myanmar coast
10	2003	Nov	12-15	SCS	- & AS	100	990	-	3.5	No damage was reported	Off Somalia coast
11	2003	Dec	11-16	SCS	- & BoB	100	990	-	3.5	No. of deaths:81 Houses damaged-fully:1637 Houses damaged-partially:7453 Agricultural area affected: 61898 hec.	Near Machilipatnam, Andhra Pradesh
12	2004	May	5-10	SCS	- & AS	100	984	-	3.5	No. of deaths:9 Houses damaged-fully/partially:45	Off Gujarat coast

13	2004	May	16-19	VSCS	Myanmar cyclone & AS	165	952	-	5.0	No damage was reported	Near Sittwe, along northwestern Myanmar
14	2004	Sep-Oct	30-3	SCS	Onil & AS	100	990	-	3.5	No damage was reported	Near Porbandar, Gujarat coast
15	2004	Nov-Dec	29-2	SCS	Agni & AS	120	994	-	3.5	No damage was reported	South of Sri Lanka
16	2005	Jan	13-17	CS	Hibaru & BoB	65	1000	-	2.5	No damage was reported	Southwest Bay of Bengal
17	2005	Sep	17-21	CS	Pyarr & South China Sea	65	988	-	2.5	No. of deaths:1 Houses damaged-fully/partially:12041 Crop loss: 482188 h Affected state: Andhra Pradesh, Odisha	Northeast of Kalingapatnam, Andhra Pradesh
18	2005	Nov - Dec	28-2	CS	Baaz & BoB	85	998	-	3.0	No. of depths:11 Heavy rainfall: Tamil Nadu, Andhra Pradesh	North of Pondicherry, East of India
19	2005	Dec	6-10	CS	Fanoos & BoB	85	998	-	3.0	No damage was reported	Near Vedaranyam, eastern Tamil Nadu coast
20	2006	Apr	24-30	ESCS	Mala & BoB	185	954	-	5.5	No damage was reported	Rakhine state, Myanmar coast

21	2006	Sep	21-24	SCS	Mukda & AS	100	988	-	3.5	No damage was reported	Weakened over the east-central Arabian sea
22	2006	Oct	29-30	CS	Ogni & BoB	65	1002	-	2.5	No. of deaths:24 Houses damaged-fully:26853 Houses damaged-partially:73218 Affected state: Andhra Pradesh	Close to Bapatla, Andhra Pradesh coast
23	2007	May	13-15	CS	Akash & BoB	85	990	-	3.0	No damage was reported	Close to the south of Cox's Bazar, south Bangladesh coast
24	2007	Jun	1-7	SCS	Gonu & AS	235	920	-	6.5	No damage was reported	Oman coast
25	2007	Jun	21-26	CS	Yemyin & BoB	65	986	-	2.5	No. of deaths:140	Near Kakinada, Andhra Pradesh coast
26	2007	Nov	11-16	ESCS	Sidr & BoB	215	944	Tidal wave of about 6m	6.0	No. of deaths:1 Villages affected: 46 Crop damaged: thousands of hectors	Along Bangladesh coast
27	2008	Apr-May	27-3	ESCS	Nargis & BoB	165	962	3-5	5.0	No. of deaths:84000 Houses damaged-745764 Affected population: 11 million	Southwest coast of Myanmar

28	2008	Oct	25-27	CS	Rashmi & BoB	85	984	1.8	3.0	No. of deaths:13 Heavy rains in Shillong	West of Khepupara, Bangladesh coast
29	2008	Nov	13-16	CS	Khai Muk & BoB	65	996	-	2.5	No Significant damage was reported	North of Kavali, south Andhra Pradesh coast
30	2008	Nov	25-29	CS	Nisha & BoB	85	996	-	3.0	No. of deaths:100 Crop damaged: 11.63 lakh hectares Affected state: Tamil Nadu and Andhra Pradesh	Near Karaikal, Puducherry coast
31	2009	Apr	14-17	CS	Bijli & BoB	75	996	-	2.5	No damage was reported	Near south of Chittagaon, Bangladesh coast
32	2009	May	23-26	SCS	Aila & BoB	110	968	3	3.5	No. of deaths:100 Houses damaged-fully:61000 Houses damaged-partially:132000 Affected state: West Bengal, Odisha and Meghalaya	Near East of Sagar Island, West Bengal coast
33	2009	Nov	9-12	CS	Phyan & BoB	85	988	-	3.0	No. of deaths:7 Houses damaged:1000 Fishermen missing:44 Affected state: Goa and Konkan region	Between Alibag and Mumbai, along Maharashtra coast

34	2009	Dec	10-15	CS	Ward	85	996	-	3.0	No damage was reported	North-east Sri Lanka coast
35	2010	May	17-21	SCS	Laila & BoB	100	986	2-3	3.5	No. of deaths:06 Substantial damage to agriculture, horticulture, and roads and buildings in Andhra Pradesh	Near Bapatla, Guntur District, Andhra Pradesh
36	2010	May	19-23	CS	Bandu & AS	75	994	-	2.5	No damage was reported	Weakened and dissipated over the Gulf of Aden
37	2010	May-Jun	31-7	VSCS	Phet & AS	155	970	-	4.5	No. of deaths:05 Heavy rains in Gujarat, Saurashtra, Rajasthan	South of Karachi, Pakistan coast
38	2010	Oct	20-23	VSCS	Giri & BoB	195	950	3.7	5.5	No. of deaths:157 Heavy damage to agriculture, horticulture, and roads and buildings in Andhra Pradesh	At Kyaukphyu, Arakan, Myanmar
39	2010	Nov	4-8	SCS	Jal & Indian Ocean	110	988	-	3.5	No. of deaths:16 Hundreds of houses were damaged in Andhra Pradesh & Tamil Nadu Heavy rainfall in TN, Puducherry, Andhra Pradesh & Karnataka	At Chennai, Tamil Nadu coast
40	2011	Oct - Nov	29-4	CS	Keila & AS	65	996	-	2.5	No damage was reported	Close to Salalah, Oman coastline

41	2011	Dec	25-31	VSCS	Thane & BoB	140	969	1	4.5	No. of deaths:46 Heavy rainfall along Tamil Nadu, Puducherry, Andhra Pradesh and Kerala	North Tamil Nadu coast between Cuddalore and Pondicherry
42	2012	Oct	22-26	CS	Murjan & AS	75	998	-	2.5	No damage was reported	Along the coast of Somalia
43	2012	Oct - Nov	28-1	CS	Nilam & BoB	85	987	-	3.0	No damage was reported	Near Mahabalipuram, Tamil Nadu
44	2013	May	10-17	CS	Viyaru & BoB	85	990	1	3.0	No damage was reported	Near Chittagong, Bangladesh
45	2013	Oct	8-14	ESCS	Phailin & BoB	215	940	2-2.5	6.0	No. of deaths:01 Houses effected-fully: 419052 Affected states: Andhra Pradesh, Odisha	Near Gopalpur, Odisha coast
46	2013	Nov	19-23	SCS	Helen & BoB	100	990	-	3.5	No. of deaths:11 Considerable damage to Krishna, east & west Godavari districts	South of Machilipatnam, Andhra Pradesh
47	2013	Nov	23-28	VSCS	Lehar & BoB	140	980	-	4.0	No damage was reported	Near Machilipatnam, Andhra Pradesh
48	2013	Dec	6-13	VSCS	Madi & BoB	120	986	-	4.0	No damage was reported	Near Tondi, Tamil Nadu coast

49	2014	Jun	10-14	CS	Nanauk & AS	85	986	-	3.0	No damage was reported	Dissipated over the Arabian Sea
50	2014	Oct	7-14	ESCS	Hudhud & BoB	185	950	1.4	5.0	No. of deaths:46 Houses effected-fully:41269 Heavy damage to Andhra coast	Near Visakhapatnam, Andhra Pradesh
51	2014	Oct	25-31	ESCS	Nilofar & AS	205	950	-	5.5	No damage was reported	Weakened over the Arabian Sea
52	2015	Jun	7-12	CS	Ashobaa & AS	85	990	-	3.0	No damage was reported	Off Oman coast
53	2015	Jul - Aug	26-2	CS	Komen & BoB	75	986	1-2	2.5	No. of deaths:83 Houses damaged-fully:107808 Houses damaged-partially:368238	Near Chittagong, Bangladesh
54	2015	Oct-Nov	28-4	ESCS	Chapala & AS	215	940	-	6.0	No damage was reported	Mountainous terrain of mainland Yemen
55	2015	Nov	5-10	ESCS	Megh & AS	175	964	-	5.0	No damage was reported	Coast of Yemen
56	2016	May	17-22	CS	Roanu & BoB	85	983	1.5	3.0	No. of deaths: Nil Torrential rainfall: Tamil Nadu, Andhra Pradesh, Kerala and Odisha	Near Chittagong, Bangladesh

57	2016	Oct	21-27	CS	Kyant & BoB	75	996	-	2.5	No damage reported	Off the coast of southern Andhra Pradesh
58	2016	Nov - Dec	29-2	CS	Nada & BoB	75	1000	-	2.5	No damage reported	Over southern Karnataka
59	2016	Dec	6-13	VSCS	Vardah & BoB	130	975	1	4.0	No. of deaths:24 Infrastructure damage: 22573cr Crop damage: 34206 hectares	Close to Chennai coast
60	2017	Apr	15-17	CS	Maarutha & BoB	75	996	-	2.5	No damage was reported	Near Sandoway in Myanmar
61	2017	May	28-31	SCS	Mora & BoB	110	978	-	3.5	No. of deaths: Nil Houses damaged: 20	Near Chittagong, Southern coast of Bangladesh
62	2017	Nov - Dec	29-6	VSCS	Ockhi & BoB	155	976	-	-	No. of deaths:218 Houses damaged-fully:1687 Houses damaged-partially:2817	Off the coast of Gujarat

Note: CS-Cyclonic Storm; SCS-Severe Cyclonic Storm; VSCS-Very Severe Cyclonic Storm; ESCS-Extremely Severe Cyclonic Storm; AS- Arabian Sea; BoB-Bay of Benga

Appendix - II

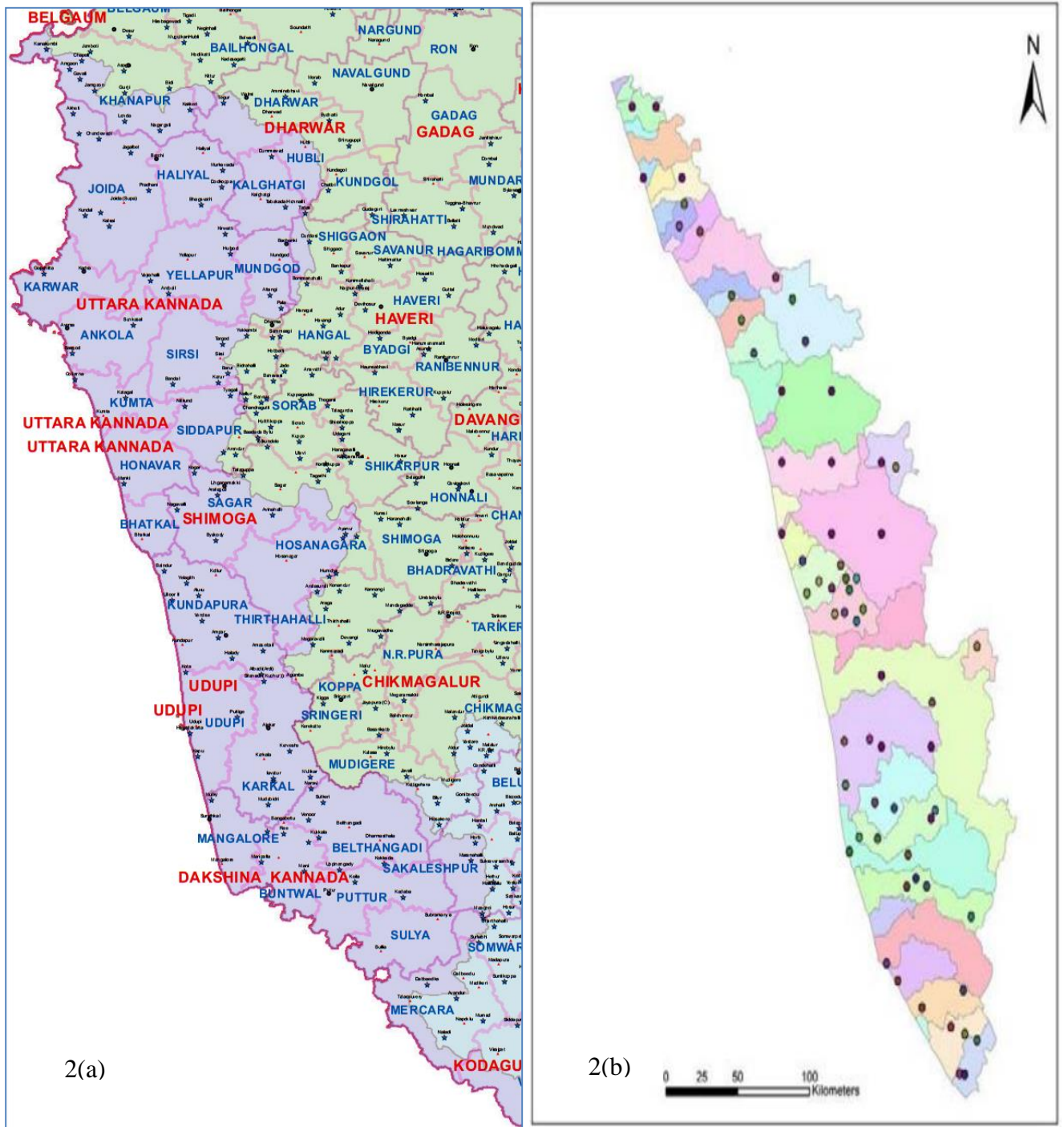


Figure A2.1 (a) Rain Gauge network (* symbol) along the Dakshina Kannada, Udupi and Uttara Kannada districts of Karnataka state (b) Location of rain gauge stations (● symbol) in watersheds of Kerala

Table A2.1 Physical and UH parameters studied to establish relationships in CWC sub-zone 5(a) and 5 (b).

S. No.	Independent variables	Constant	Dependant variables	Exponent
1	$\frac{LL_c}{\sqrt{S}}$	1.378	q_p	-0.238
2	$\frac{L_c}{\sqrt{S}}$	1.006	q_p	-0.473
3	$\frac{L_c}{S}$	0.686	q_p	-0.426
4	$\frac{L}{S}$	0.918	q_p	-0.431
5	t_p	1.137	q_p	-0.746
6	q_p	1.561	t_p	-1.081

Table A2.2 List of railway bridge/M.O.T. catchments, availability of gauge, discharge and rainfall data

S. No.	Name of stream	Railway bridge No.	Subzone	No. of rain gauges	Data availability	No. of years
1	Amlika	MOT-6	5(a)	8	1980-86	7
2	Pinjal	MOT-4	5(a)	5	1981-86	6
3	Kapri	MOT-5	5(a)	4	1983-86	4
4	Chimoni Puzha	104	5(b)	5	1961-64	4
5	Swarna	MOT-8	5(b)	2	1980-88	9
6	Amba	MOT-2	5(a)	2	1980-86	7
7	Kal	MOT-1	5(a)	2	1980-86	7
8	Kodavadi Pallam	273	5(b)	6	1961-66	6
9	Velliar	117	5(b)	5	1961-64	4
10	Ithikara	MOT-11	5(b)	2	1980-86	7
11	Anjarakandi Puzha	MOT-9	5(b)	1	1980-86	7
12	Bennehole	MOT-7	5(b)	1	1980-85	6
13	Achipatti	260	5(b)	1	1969-72	4

Table A2.3 Location and Basin characteristics of 13 catchments of CWC report (CWC, 1992)

S.No.	Location		Bridge No.	Area (sq km)	L (km)	Lc (km)	S (m/km)
	Longitude (E)	Latitude (N)					
1	73 ⁰ 20'10"	20 ⁰ 51'30"	MOT-6	988.00	82.05	48.27	4.74
2	73 ⁰ 04'45"	19 ⁰ 40'10"	MOT-4	610.00	68.38	37.00	3.47
3	73 ⁰ 30'30"	20 ⁰ 49'00"	MOT-5	480.00	71.44	37.81	4.61
4	73 ⁰ 30'08"	20 ⁰ 47'30"	104	388.50	50.36	29.77	0.89
5	74 ⁰ 58'50"	13 ⁰ 17'35"	MOT-8	327.00	33.63	12.06	7.03
6	73 ⁰ 12'00"	18 ⁰ 32'00"	MOT-2	310.00	34.75	14.48	3.10
7	73 ⁰ 17'00"	18 ⁰ 14'00"	MOT-1	256.00	38.29	20.92	5.05
8	77 ⁰ 01'10"	10 ⁰ 45'45"	273	200.21	24.94	12.87	5.58
9	76 ⁰ 16'22"	11 ⁰ 03'40"	117	189.07	25.74	10.46	0.88
10	76 ⁰ 52'00"	8 ⁰ 53'25"	MOT-11	177.00	30.59	13.68	2.32
11	75⁰34'40"	11⁰52'25"	MOT-9	176.00	38.48	20.29	4.21
12	74 ⁰ 36'30"	14 ⁰ 31'30"	MOT-7	62.00	12.55	11.26	8.21
13	77 ⁰ 01'00"	10 ⁰ 49'10"	260	48.02	12.87	7.24	7.62

Table A2.4 Representative 1-hour unit hydrograph parameters for subzone 5(a) and 5(b)

S.No	Bridge No	q _p (Cumecs /sq km)	t _p (h)	T _B (h)	T _m (h)	W ₅₀ (h)	W ₇₅ (h)	W _{R50} (h)	W _{R75} (h)	Q _p (m ³ /s)
1	MOT-6	0.60	2.50	15.00	3.00	3.70	1.77	0.90	0.57	592.80
2	MOT-4	0.40	4.50	15.00	5.00	6.40	2.90	1.90	0.90	244.00
3	MOT-5	0.36	3.50	22.00	4.00	6.60	3.50	1.40	0.90	172.80
4	104	0.08	28.50	100.00	29.00	28.25	14.75	11.25	6.50	31.08
5	MOT-8	0.32	5.50	20.00	6.00	7.85	4.00	3.00	1.75	104.64
6	MOT-2	0.43	1.50	15.00	2.00	2.30	1.04	0.77	0.40	133.30
7	MOT-1	0.45	4.50	17.00	5.00	5.35	2.23	1.65	0.68	116.55
8	273	0.63	4.50	16.00	5.00	3.40	2.10	1.00	0.70	126.13
9	117	0.34	6.50	24.00	7.00	6.60	3.50	2.80	1.70	64.28
10	MOT-11	0.12	13.50	70.00	14.00	19.60	8.90	4.40	2.20	21.24
11	MOT-9	0.35	4.50	22.00	5.00	5.98	3.02	1.83	1.04	62.13
12	MOT-7	0.88	1.50	13.00	2.00	2.00	1.23	0.75	0.50	54.56
13	260	0.63	3.50	15.00	4.00	3.30	1.70	0.90	0.50	30.25

Table A2.5 Ordinates of Unit Hydrograph at Bridge Site No. 8 (MOT-8)

Time (t_i) (h)	UH ordinate (Q_i) (cumecs)	t_i / T_m	$(Q_i * T_m) / V$
0	0.00	0	0
1	17.44	0.17	0.12
2	34.88	0.33	0.23
3	52.32	0.50	0.35
4	73.25	0.67	0.48
5	89.69	0.83	0.59
6	104.64	1.00	0.69
7	93.01	1.17	0.61
8	81.39	1.33	0.54
9	70.93	1.50	0.47
10	60.87	1.67	0.40
11	51.46	1.83	0.34
12	45.74	2.00	0.30
13	40.03	2.17	0.26
14	34.31	2.33	0.23
15	28.59	2.50	0.19
16	22.87	2.67	0.15
17	17.15	2.83	0.11
18	11.44	3.00	0.08
19	5.72	3.17	0.04
20	0.00	3.33	0.00

Note: In the Table 5, $T_m = 6$ h and $V = 2.78XA = 2.78 \times 327 = 908.3 \text{ m}^3$

Table A2.6 Ordinates of average dimensionless UGs at 13 CWC bridge catchments

t_i/T_m	$(Q_i \cdot T_m)/V$												
	MOT-6	MOT-4	MOT-5	104	MOT-8	MOT-2	MOT-1	273	117	MOT-11	MOT-9	MOT-7	260
0.00	0.00	0.00	0.00	0.00	0.00	0.00	0.00	0.00	0.00	0.00	0.00	0.00	0.00
0.20	0.07	0.12	0.12	0.14	0.14	0.12	0.12	0.14	0.14	0.09	0.11	0.10	0.12
0.40	0.14	0.23	0.24	0.27	0.28	0.24	0.24	0.28	0.29	0.18	0.22	0.20	0.23
0.60	0.21	0.35	0.35	0.41	0.41	0.35	0.36	0.43	0.44	0.26	0.33	0.33	0.35
0.80	0.31	0.52	0.51	0.65	0.59	0.54	0.54	0.57	0.67	0.41	0.53	0.48	0.53
1.00	0.53	0.72	0.79	0.84	0.70	0.91	0.81	1.13	0.86	0.60	0.71	0.63	0.91
1.20	0.45	0.63	0.65	0.69	0.60	0.81	0.68	0.93	0.69	0.54	0.62	0.54	0.76
1.40	1.21	0.54	0.54	0.55	0.51	0.64	0.57	0.68	0.54	0.48	0.53	0.44	0.60
1.60	1.30	0.47	0.47	0.41	0.43	0.54	0.47	0.53	0.42	0.42	0.44	0.37	0.49
1.80	1.35	0.40	0.43	0.37	0.35	0.42	0.39	0.46	0.37	0.37	0.36	0.33	0.41
2.00	1.38	0.33	0.40	0.32	0.30	0.35	0.34	0.40	0.32	0.32	0.33	0.29	0.37
2.20	1.03	0.26	0.28	0.28	0.26	0.59	0.29	0.33	0.28	0.29	0.31	0.28	0.33
2.40	0.73	0.20	0.27	0.24	0.21	0.58	0.24	0.26	0.23	0.27	0.29	0.27	0.28
2.60	0.74	0.13	0.21	0.19	0.17	0.12	0.20	0.20	0.19	0.24	0.26	0.25	0.24
2.80	0.75	0.07	0.18	0.15	0.12	0.09	0.15	0.13	0.14	0.23	0.24	0.24	0.20
3.00	0.76	0.00	0.13	0.10	0.08	0.05	0.10	0.07	0.10	0.21	0.22	0.23	0.16
3.20	0.77		0.09	0.05	0.03	0.18	0.05	0.00	0.05	0.19	0.19	0.21	0.12
3.40	0.78		0.03	0.01	0.00	0.16	0.00		0.01	0.16	0.17	0.20	0.07
3.60	0.78		0.01	0.00		0.14			0.00	0.14	0.15	0.19	0.03
3.80	0.79		0.00			0.12				0.12	0.13	0.18	0.00
4.00	0.79					0.10				0.10	0.11	0.16	
4.20	0.79					0.07				0.08	0.09	0.15	
4.40	0.79					0.07				0.06	0.07	0.14	
4.60	0.79					0.02				0.04	0.05	0.12	
4.80	0.79					0.02				0.02	0.02	0.10	
5.00	0.00					0.00				0.00	0.00	0.00	

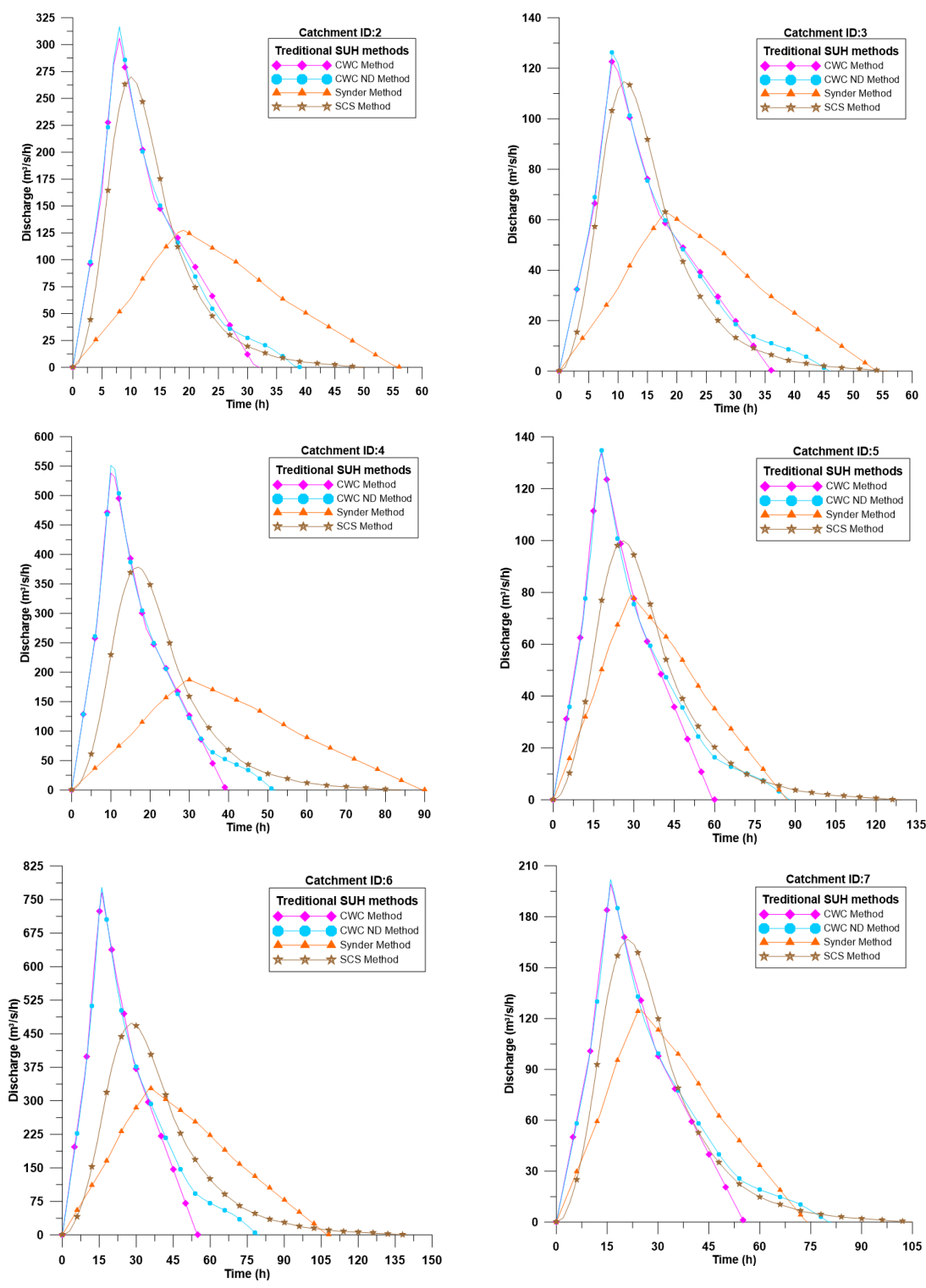


Figure A2.2 SUH of 1-hour duration during using Traditional SUH methods at Catchments IDs 2, 3, 4, 5, 6 and 7

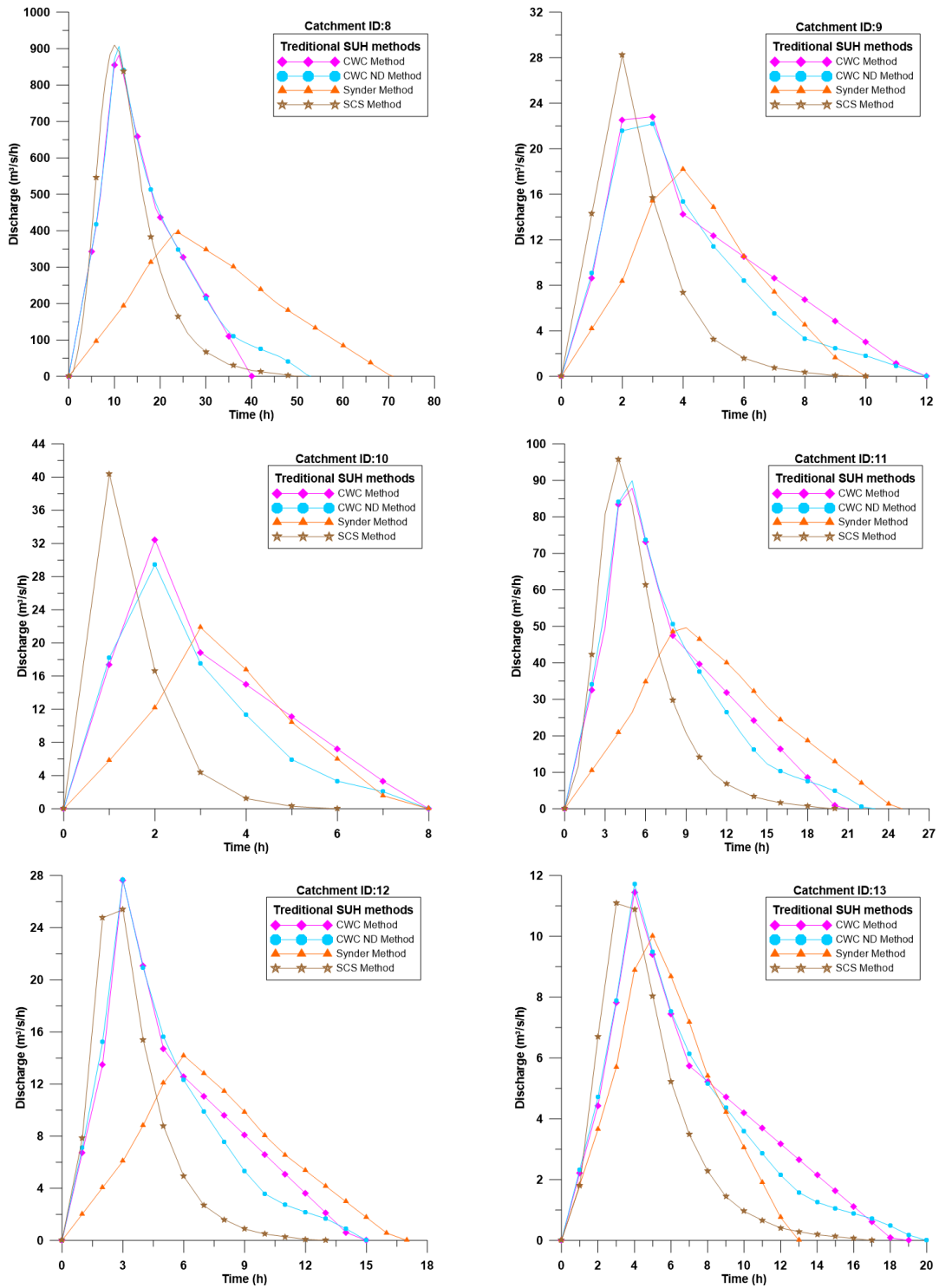


Figure A2.3 SUH of 1-hour duration during using Traditional SUH methods at Catchments IDs 8, 9, 10, 11, 12 and 13

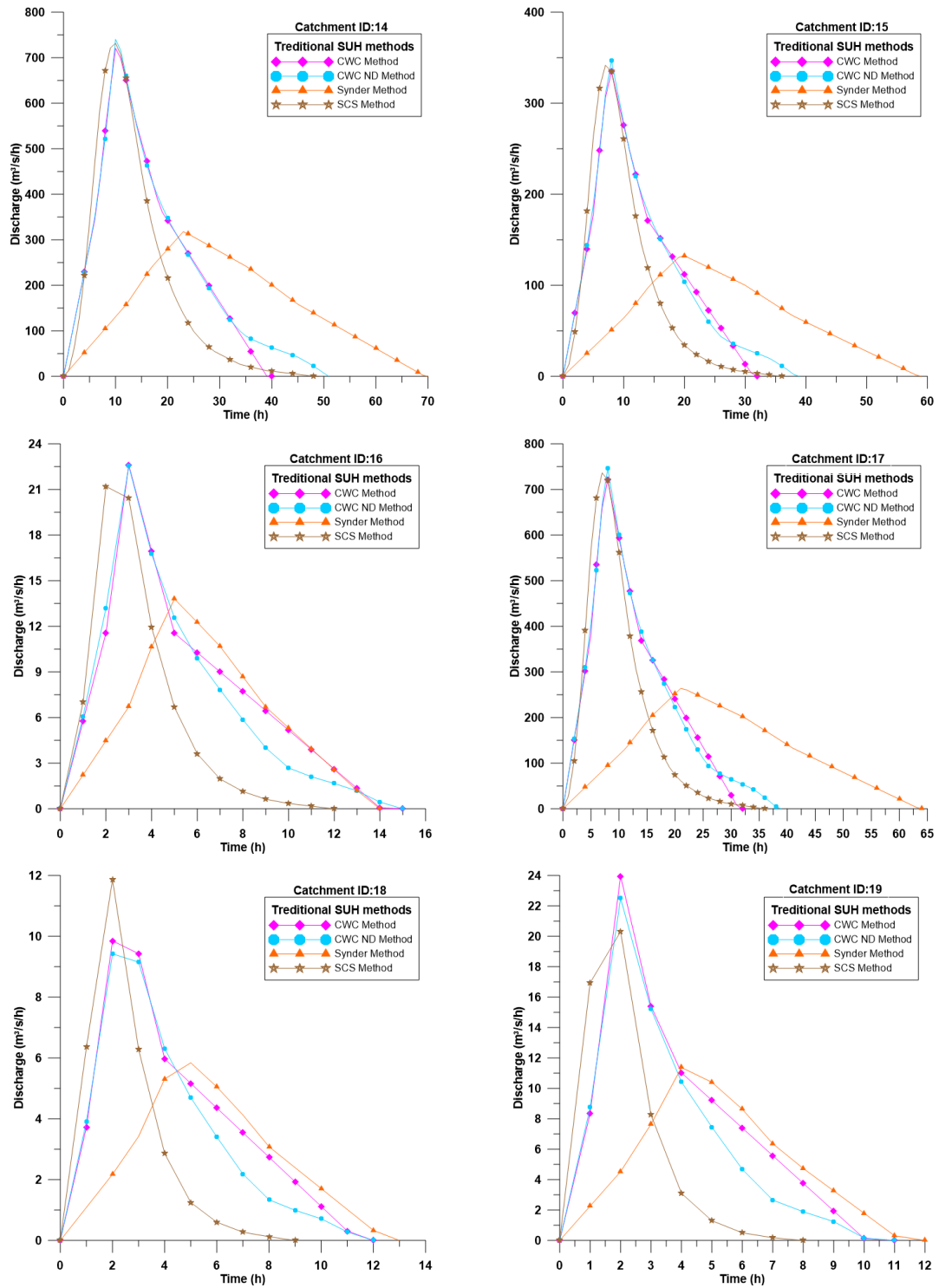


Figure A2.4 SUH of 1-hour duration during using Traditional SUH methods at Catchments IDs 14, 15, 16, 17, 18 and 19

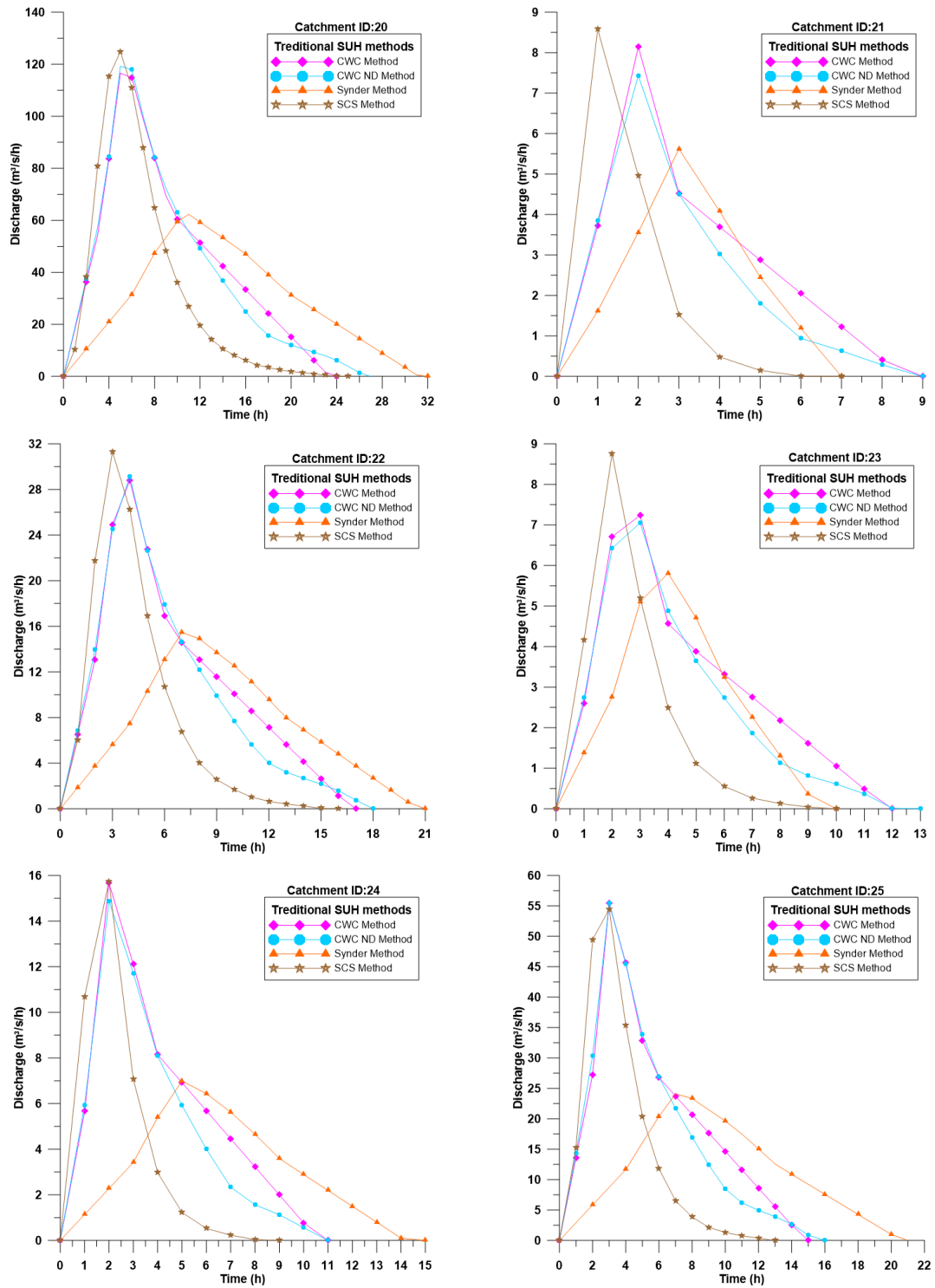


Figure A2.5 SUH of 1-hour duration during using Traditional SUH methods at Catchments IDs 20,21, 22, 23, 24 and 25

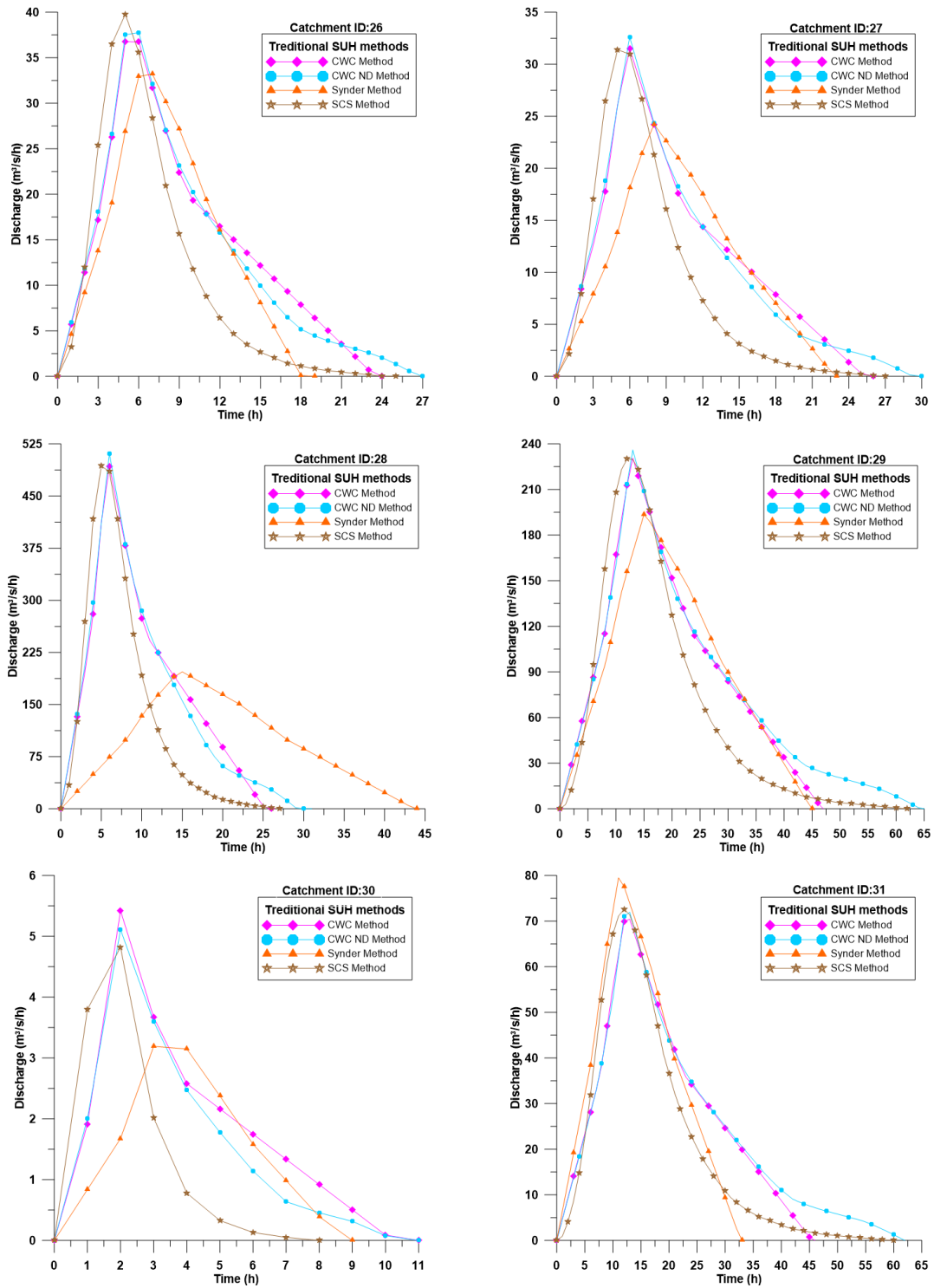


Figure A2.6 SUH of 1-hour duration during using Traditional SUH methods at Catchments IDs 26, 27, 28, 29,30 and 31

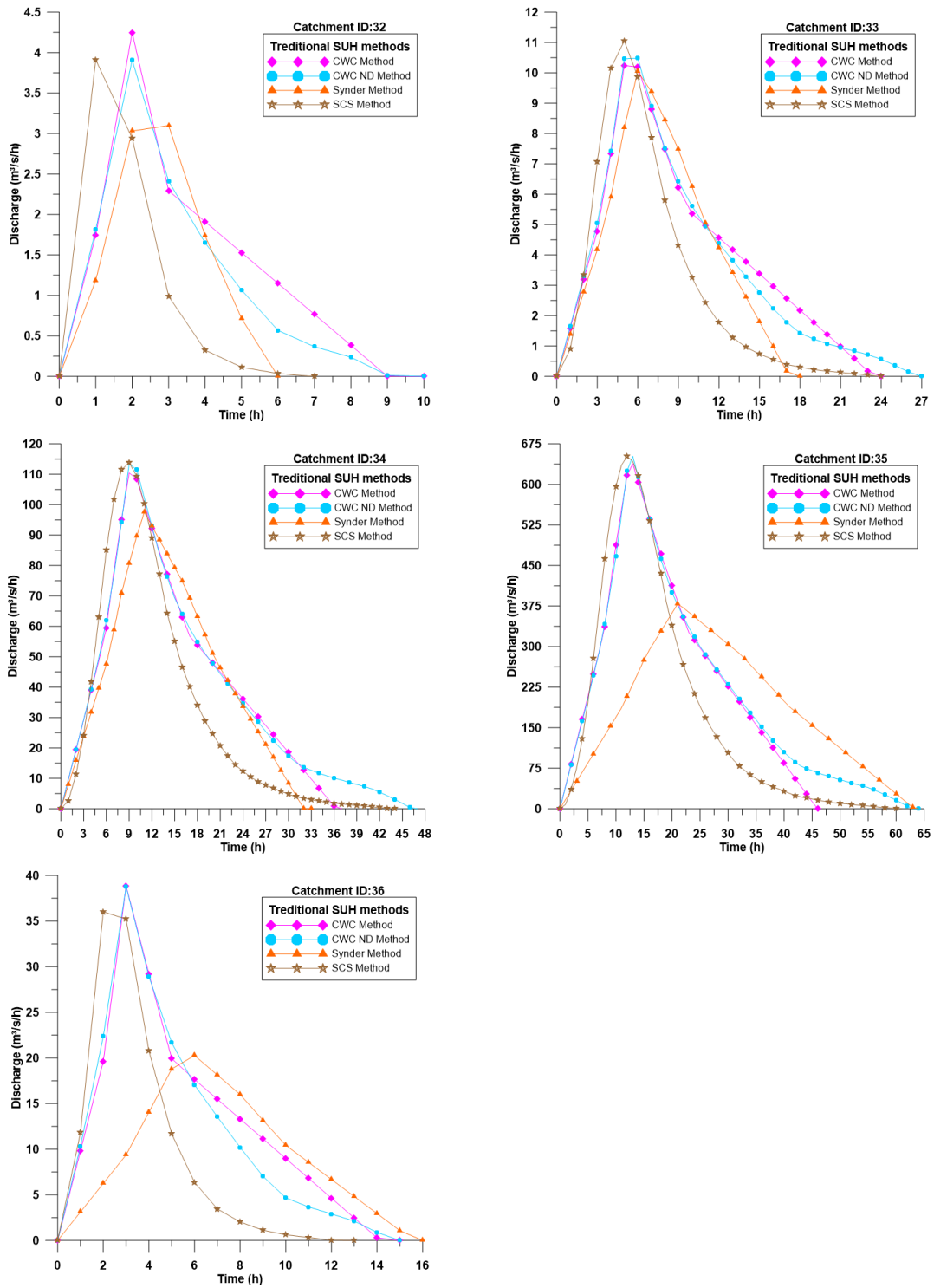


Figure A2.7 SUH of 1-hour duration during using Traditional SUH methods at Catchments IDs 32, 33, 34, 35 and 36

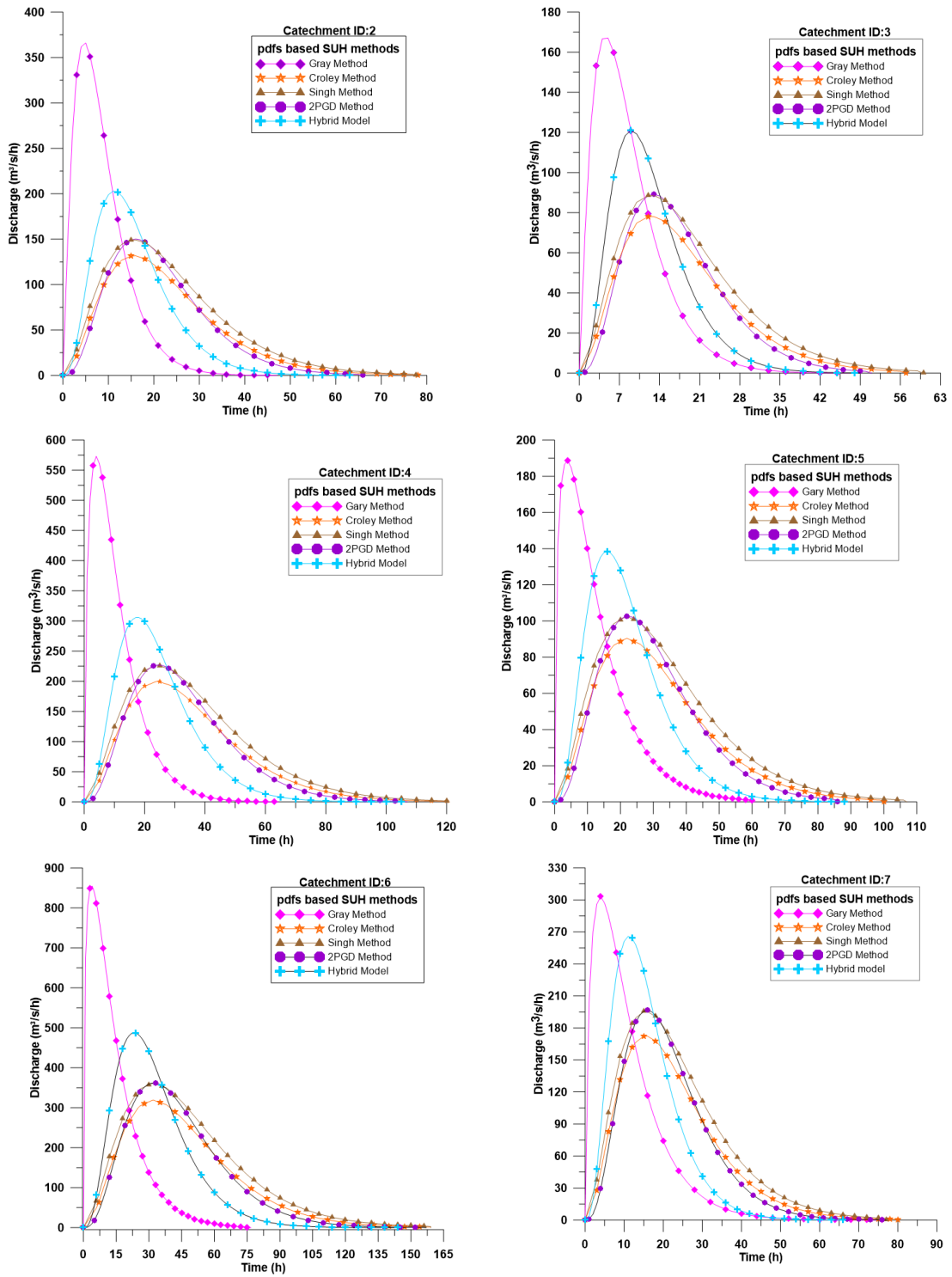


Figure A2.8 SUH of 1-hour duration during using pdfs based SUH methods at Catchments IDs 2, 3, 4, 5, 6 and 7

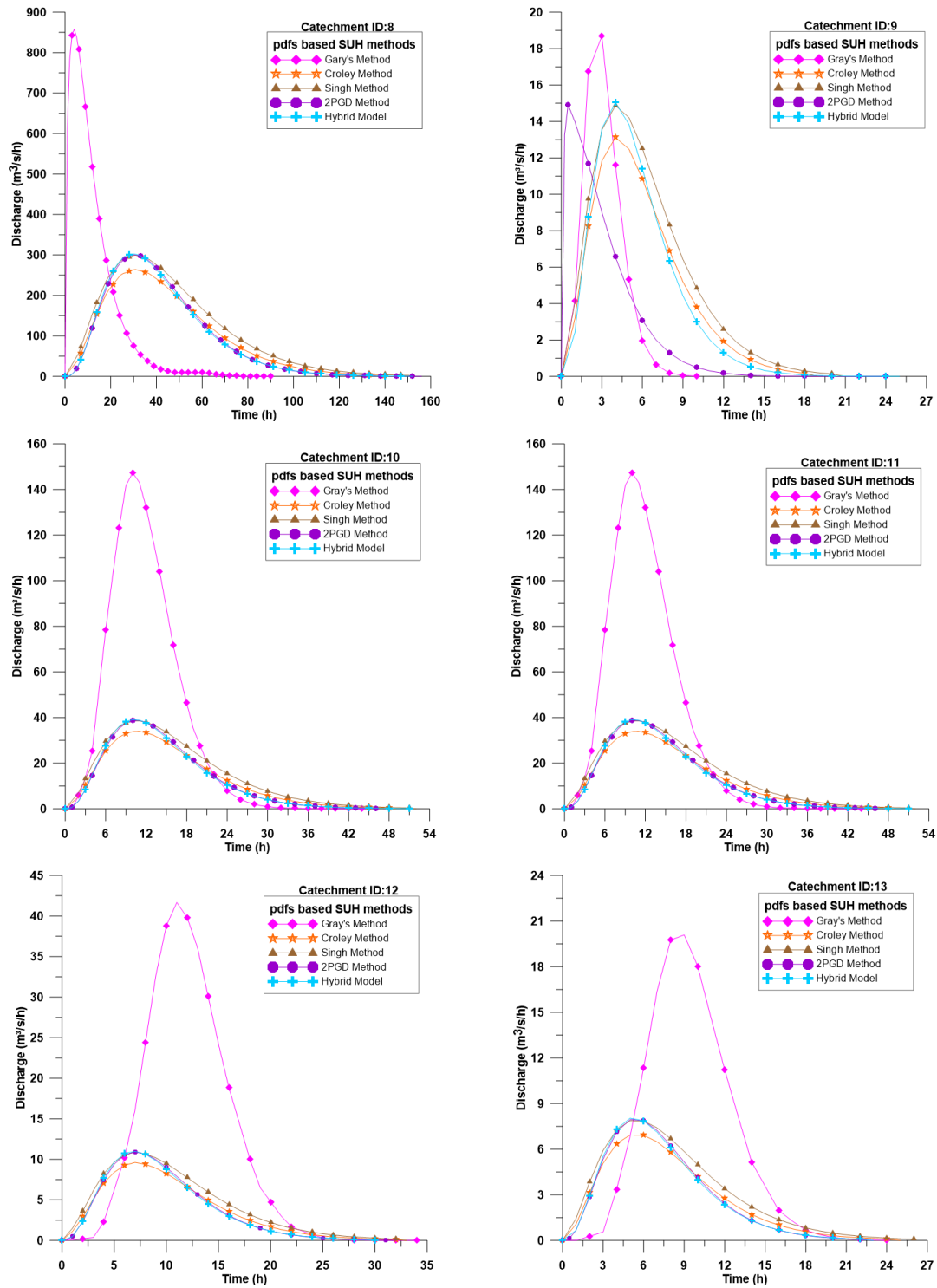


Figure A2.9 SUH of 1-hour duration during using pdfs based SUH methods at Catchments IDs 8, 9, 10, 11, 12 and 13

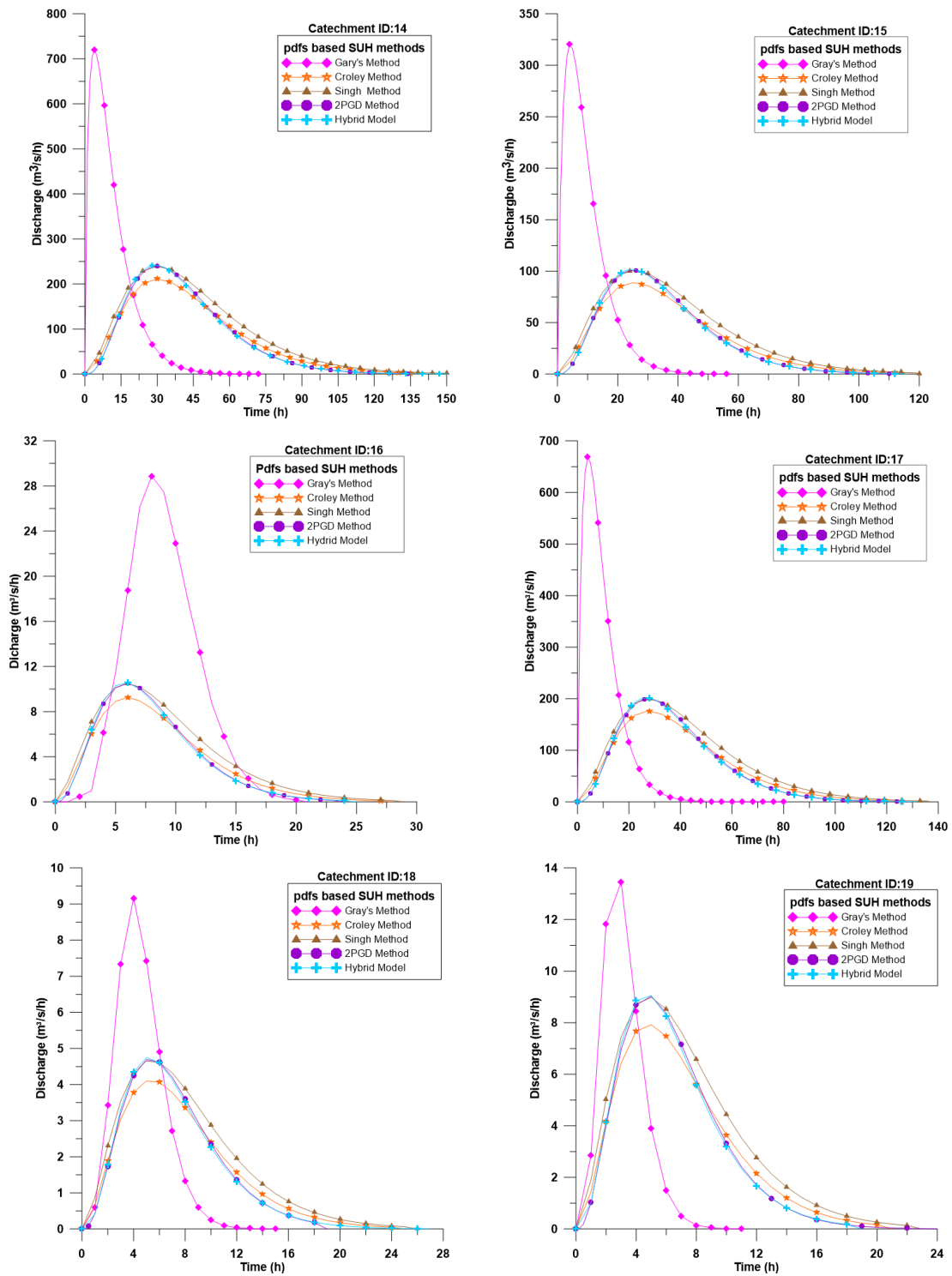


Figure A2.10 SUH of 1-hour duration during using pdfs based SUH methods at Catchments IDs 14, 15, 16, 17, 18 and 19

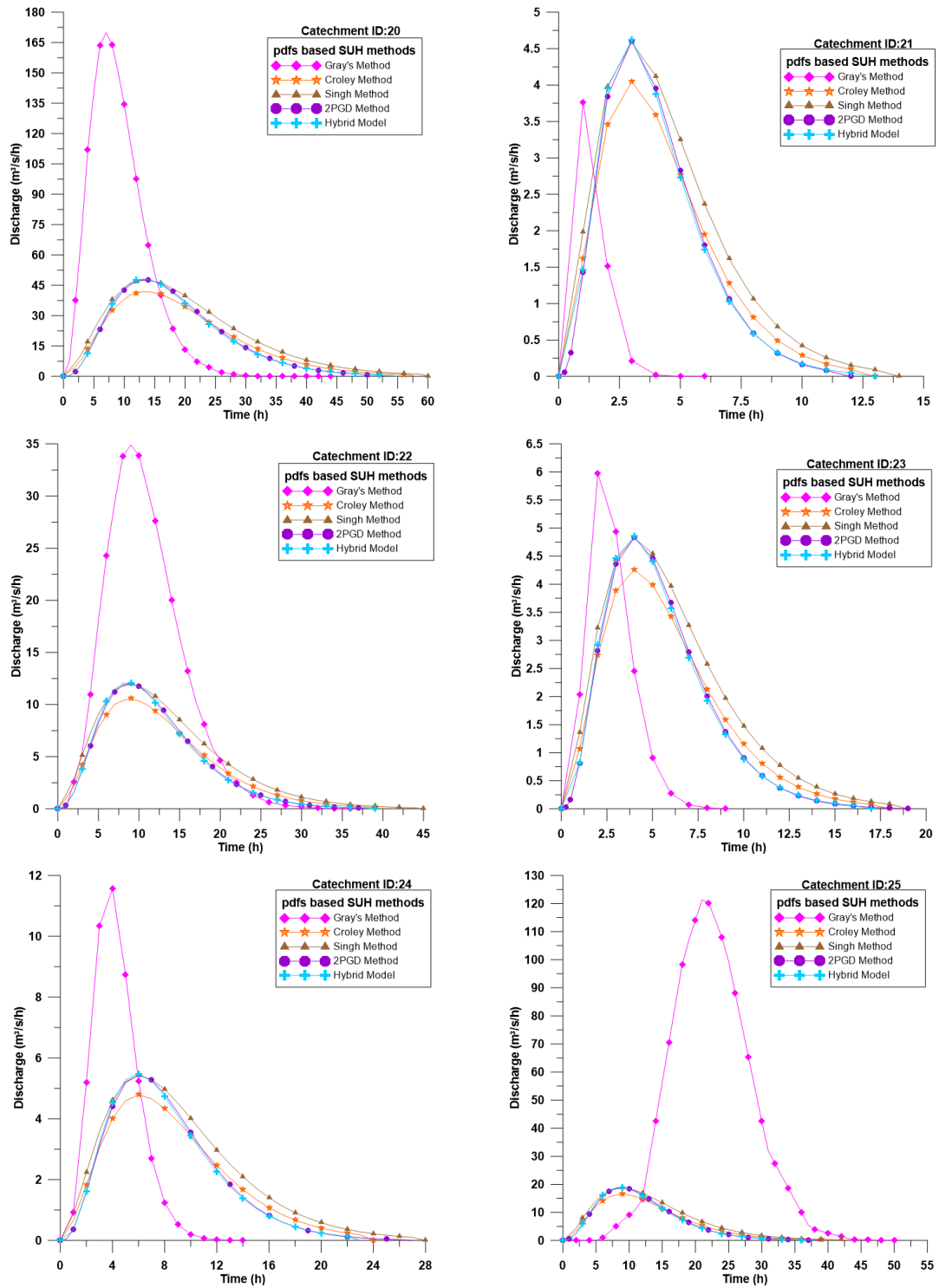


Figure A2.11 SUH of 1-hour duration during using pdfs based SUH methods at Catchments IDs 20, 21, 22, 23, 24 and 25

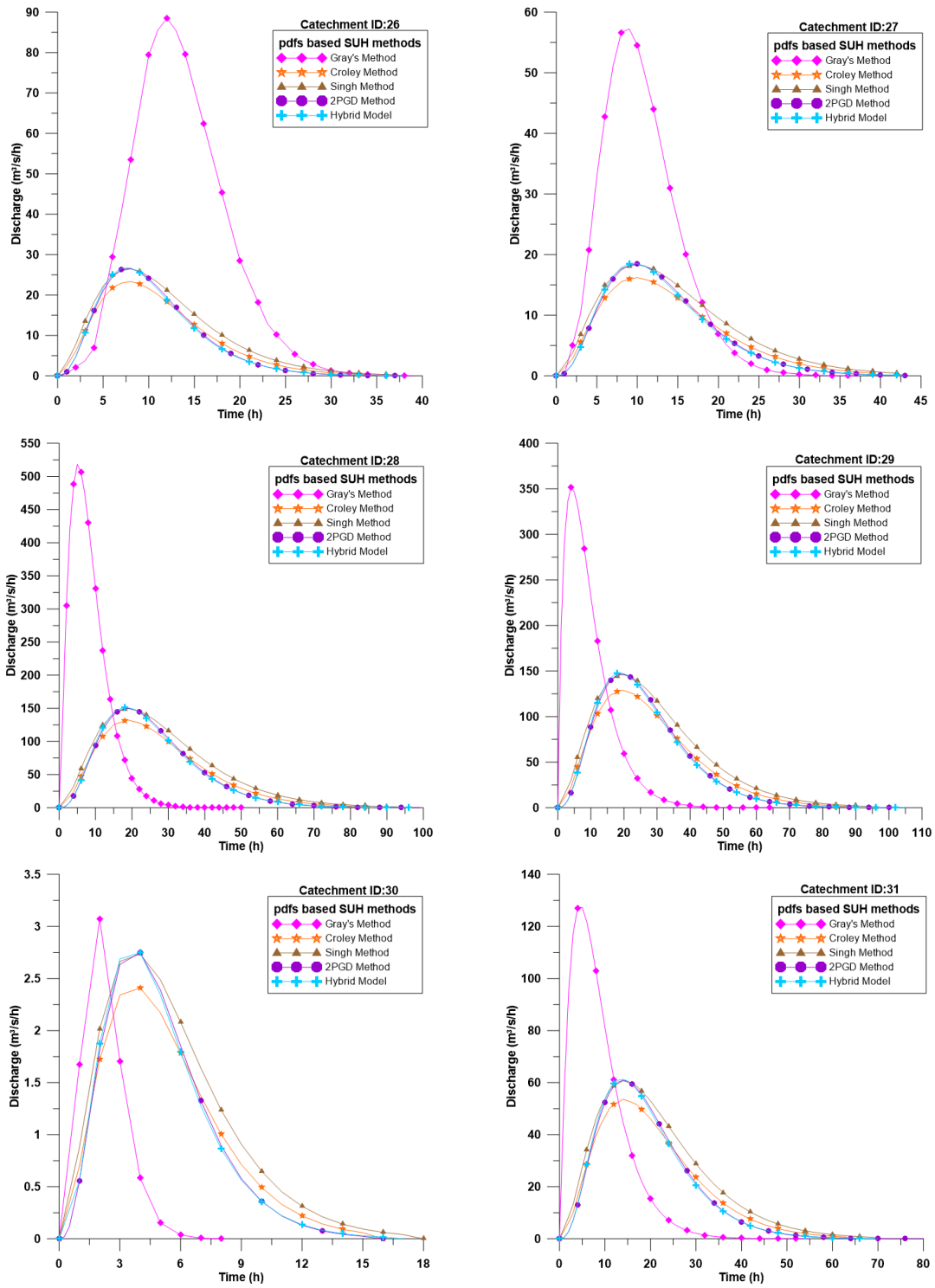


Figure A2.12 SUH of 1-hour duration during using pdfs based SUH methods at Catchments IDs 26, 27, 28, 29, 30 and 31

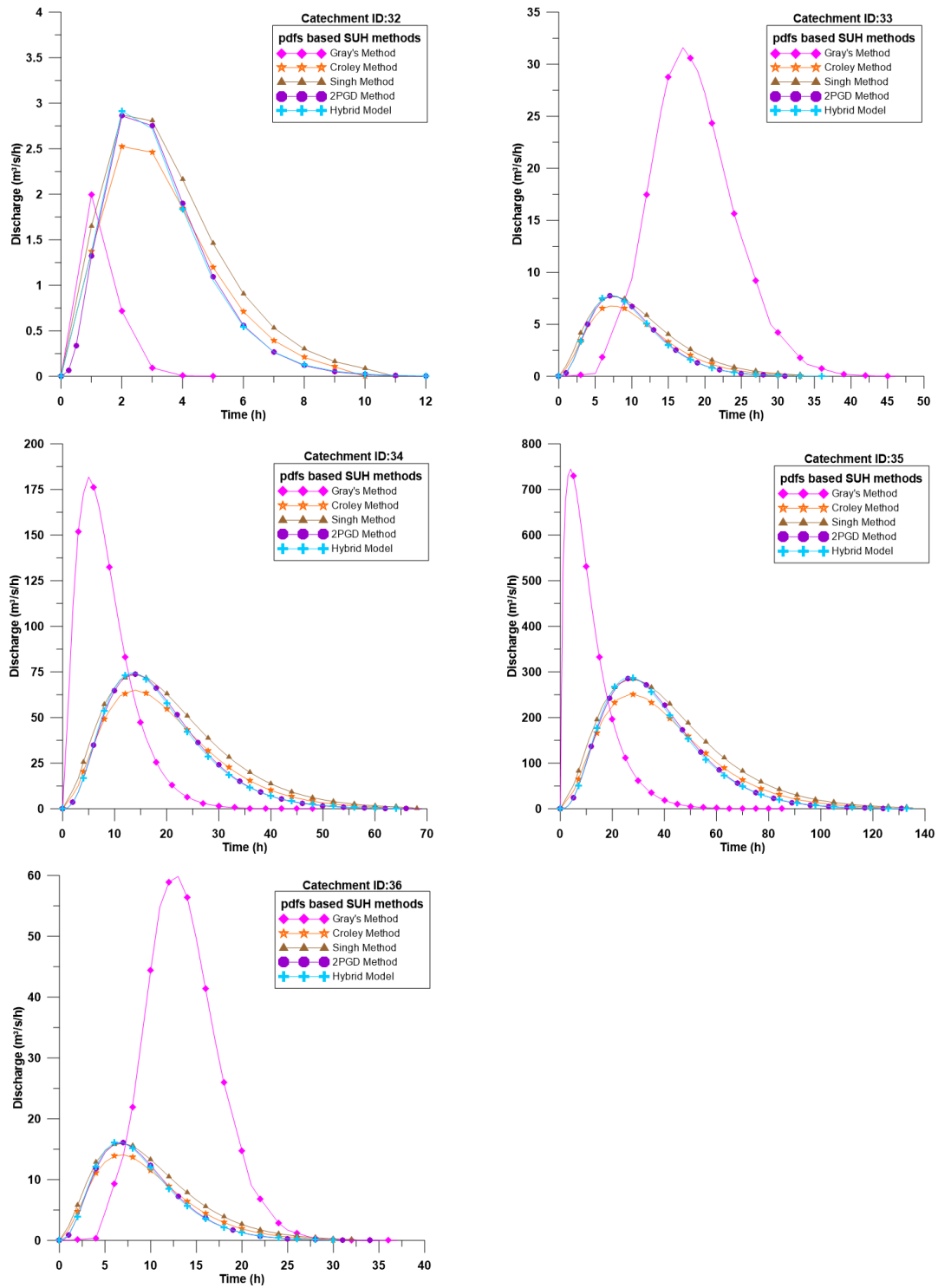


Figure A2.13 SUH of 1-hour duration during using pdfs based SUH methods at Catchments IDs 32, 33, 34, 35, and 36

Appendix – III

Table A3.1 Classification of tidal inlets based on tidal range and wave exposure condition

Inlet No.	R _{to} (m)	H _{s,avg} (m)	T _{mean} (s)	H ² *T ² (m ² s ²)	Based on the tidal range		Based on wave exposure
					Devies (1964)	Hayes (1975)	
Gujarat coast							
1	4.51	No data available		-	Macrotidal	Low-macrotidal	-
2	4.28			-	Macrotidal	Low-macrotidal	-
3	4.25			-	Macrotidal	Low-macrotidal	-
4	3.34	1.40	6.51	83.57	Mesotidal	High-mesotidal	High
5	3.18	1.42	6.53	85.69	Mesotidal	High-mesotidal	High
6	3.09	1.43	6.54	87.74	Mesotidal	High-mesotidal	High
7	3.03	1.43	6.54	87.88	Mesotidal	High-mesotidal	High
8	2.62	1.43	6.63	89.63	Mesotidal	High-mesotidal	High
9	2.55	1.43	6.64	89.42	Mesotidal	High-mesotidal	High
10	2.43	1.40	6.56	83.90	Mesotidal	High-mesotidal	High
11	2.21	1.36	6.53	78.98	Mesotidal	High-mesotidal	High
12	2.15	1.37	6.57	80.53	Mesotidal	High-mesotidal	High
13	2.09	1.38	6.67	84.47	Mesotidal	High-mesotidal	High
14	1.96	1.41	6.89	94.55	Microtidal	low-mesotidal	High
15	1.86	1.41	6.95	95.64	Microtidal	low-mesotidal	High
16	1.86	1.40	6.96	94.66	Microtidal	low-mesotidal	High
17	1.38	1.34	6.84	83.40	Microtidal	low-mesotidal	High
18	2.17	1.27	6.75	73.49	Mesotidal	High-mesotidal	High
19	2.31	1.22	6.74	67.59	Mesotidal	High-mesotidal	High
20	2.38	1.20	6.78	66.55	Mesotidal	High-mesotidal	High
21	2.38	1.21	6.78	66.73	Mesotidal	High-mesotidal	High
22	2.65	1.17	6.86	64.17	Mesotidal	High-mesotidal	High
23	3.07	1.11	7.01	60.99	Mesotidal	High-mesotidal	High
24	3.43	1.06	6.92	53.83	Mesotidal	High-mesotidal	High
25	6.37	0.86	6.22	28.80	Macrotidal	Macrotidal	High
26	6.19	0.93	5.80	29.00	Macrotidal	Macrotidal	High
27	5.96	0.93	5.75	28.88	Macrotidal	Macrotidal	High
28	6.11	0.93	5.73	28.53	Macrotidal	Macrotidal	High
29	5.45	0.94	5.75	28.99	Macrotidal	Macrotidal	High
30	5.75	0.94	5.72	28.98	Macrotidal	Macrotidal	High

31	5.61	0.94	5.74	29.05	Macrotidal	Macrotidal	High
32	5.51	0.94	5.76	29.32	Macrotidal	Macrotidal	High
33	5.44	0.94	5.79	29.73	Macrotidal	Macrotidal	High
34	5.42	0.93	5.72	28.47	Macrotidal	Macrotidal	High
35	5.41	0.94	5.79	29.73	Macrotidal	Macrotidal	High
36	5.4	0.96	5.92	32.08	Macrotidal	Macrotidal	High
37	5.4	0.97	5.95	33.31	Macrotidal	Macrotidal	High
38	5.4	0.97	5.94	33.20	Macrotidal	Macrotidal	High
39	5.36	0.97	5.90	32.52	Macrotidal	Macrotidal	High
40	4.66	1.00	6.05	36.96	Macrotidal	Low-macrotidal	High
41	4.45	1.03	6.19	40.81	Macrotidal	Low-macrotidal	High
42	5.1	1.04	6.21	41.78	Macrotidal	Macrotidal	High
Maharashtra coast							
43	5.14	1.06	6.27	43.75	Macrotidal	Macrotidal	High
44	5.09	1.06	6.27	43.79	Macrotidal	Macrotidal	High
45	4.96	1.08	6.29	46.34	Macrotidal	Low-macrotidal	High
46	4.84	1.09	6.01	43.18	Macrotidal	Low-macrotidal	High
47	4.76	1.10	6.00	43.64	Macrotidal	Low-macrotidal	High
48	4.74	1.10	5.83	41.11	Macrotidal	Low-macrotidal	High
49	4.72	1.10	5.90	42.42	Macrotidal	Low-macrotidal	High
50	4.65	1.09	5.56	36.65	Macrotidal	Low-macrotidal	High
51	4.66	1.10	5.75	39.73	Macrotidal	Low-macrotidal	High
52	4.65	1.10	5.76	39.97	Macrotidal	Low-macrotidal	High
53	4.62	1.11	5.87	42.46	Macrotidal	Low-macrotidal	High
54	4.59	1.11	5.88	42.78	Macrotidal	Low-macrotidal	High
55	4.58	1.12	5.87	43.00	Macrotidal	Low-macrotidal	High
56	4.25	1.19	6.21	54.69	Macrotidal	Low-macrotidal	High
57	4.25	1.19	6.21	54.69	Macrotidal	Low-macrotidal	High
58	4.23	1.20	6.32	57.45	Macrotidal	Low-macrotidal	High
59	3.7	1.21	6.38	59.41	Mesotidal	Low-macrotidal	High
60	4.14	1.21	6.35	58.83	Macrotidal	Low-macrotidal	High
61	4.1	1.22	6.29	59.06	Macrotidal	Low-macrotidal	High
62	4.02	1.22	6.20	57.43	Macrotidal	Low-macrotidal	High
63	3.74	1.22	6.19	57.40	Mesotidal	Low-macrotidal	High
64	3.69	1.22	6.25	58.29	Mesotidal	Low-macrotidal	High
65	3.87	1.22	6.20	57.68	Mesotidal	Low-macrotidal	High
66	3.72	1.20	6.05	52.62	Mesotidal	Low-macrotidal	High

67	3.67	1.20	6.11	53.48	Mesotidal	Low-macrotidal	High
68	3.61	1.20	6.09	53.10	Mesotidal	Low-macrotidal	High
69	3.53	1.21	6.24	57.05	Mesotidal	Low-macrotidal	High
70	3.5	1.21	6.21	56.36	Mesotidal	High-mesotidal	High
71	3.41	1.21	6.24	57.12	Mesotidal	High-mesotidal	High
72	3.35	1.21	6.27	57.45	Mesotidal	High-mesotidal	High
73	3.28	1.21	6.40	60.50	Mesotidal	High-mesotidal	High
74	3.22	1.21	6.41	60.32	Mesotidal	High-mesotidal	High
75	3.19	1.21	6.45	61.08	Mesotidal	High-mesotidal	High
76	3.13	1.21	6.45	61.02	Mesotidal	High-mesotidal	High
77	2.87	1.22	6.67	66.30	Mesotidal	High-mesotidal	High
78	2.81	1.22	6.73	67.61	Mesotidal	High-mesotidal	High
79	2.76	1.22	6.74	67.46	Mesotidal	High-mesotidal	High
80	2.71	1.22	6.76	67.68	Mesotidal	High-mesotidal	High
81	2.67	1.22	6.77	68.40	Mesotidal	High-mesotidal	High
82	2.62	1.22	6.78	68.20	Mesotidal	High-mesotidal	High
83	2.6	1.22	6.78	68.89	Mesotidal	High-mesotidal	High
84	2.57	1.23	6.78	69.41	Mesotidal	High-mesotidal	High
85	2.55	1.23	6.79	69.91	Mesotidal	High-mesotidal	High
86	2.55	1.23	6.78	69.72	Mesotidal	High-mesotidal	High
87	2.51	1.24	6.79	71.14	Mesotidal	High-mesotidal	High
88	2.46	1.25	6.80	72.33	Mesotidal	High-mesotidal	High
89	2.42	1.25	6.79	72.54	Mesotidal	High-mesotidal	High
90	2.37	1.26	6.80	72.80	Mesotidal	High-mesotidal	High
91	2.3	1.26	6.81	73.12	Mesotidal	High-mesotidal	High
92	2.26	1.27	6.85	75.24	Mesotidal	High-mesotidal	High
93	2.24	1.27	6.88	76.16	Mesotidal	High-mesotidal	High
94	2.22	1.27	6.90	77.01	Mesotidal	High-mesotidal	High
95	2.19	1.27	6.92	77.88	Mesotidal	High-mesotidal	High
96	2.16	1.28	6.95	79.61	Mesotidal	High-mesotidal	High
97	2.13	1.30	6.98	81.95	Mesotidal	High-mesotidal	High
98	2.13	1.30	6.98	82.53	Mesotidal	High-mesotidal	High
99	2.11	1.31	7.00	84.18	Mesotidal	High-mesotidal	High
100	2.11	1.31	7.00	84.29	Mesotidal	High-mesotidal	High
101	2.1	1.29	7.00	81.84	Mesotidal	High-mesotidal	High
102	2.1	1.29	7.00	82.05	Mesotidal	High-mesotidal	High

103	2.1	1.29	7.00	81.28	Mesotidal	High-mesotidal	High
104	2.09	1.29	7.00	81.20	Mesotidal	High-mesotidal	High
105	2.09	1.29	7.00	81.02	Mesotidal	High-mesotidal	High
106	2.08	1.28	6.99	80.33	Mesotidal	High-mesotidal	High
107	2.07	1.28	6.98	79.68	Mesotidal	High-mesotidal	High
Goa coast							
108	2.07	1.27	6.93	77.54	Mesotidal	High-mesotidal	High
109	2.06	1.26	6.87	74.90	Mesotidal	High-mesotidal	High
110	2.06	1.26	6.85	74.59	Mesotidal	High-mesotidal	High
111	2.05	1.26	6.85	74.59	Mesotidal	High-mesotidal	High
112	2.05	1.27	6.84	75.17	Mesotidal	High-mesotidal	High
113	2.04	1.26	6.83	74.49	Mesotidal	High-mesotidal	High
114	2.04	1.27	6.87	76.57	Mesotidal	High-mesotidal	High
115	2.03	1.27	6.88	76.74	Mesotidal	High-mesotidal	High
116	2.03	1.27	6.89	77.01	Mesotidal	High-mesotidal	High
117	2.03	1.27	6.88	76.76	Mesotidal	High-mesotidal	High
118	2.03	1.28	6.91	78.23	Mesotidal	High-mesotidal	High
Karnataka coast							
119	2.03	1.28	6.93	79.10	Mesotidal	High-mesotidal	High
120	2.02	1.24	6.85	72.33	Mesotidal	High-mesotidal	High
121	2.02	1.23	6.82	70.75	Mesotidal	High-mesotidal	High
122	2.03	1.24	6.83	71.27	Mesotidal	High-mesotidal	High
123	2.02	1.23	6.83	71.02	Mesotidal	High-mesotidal	High
124	2.02	1.23	6.82	70.83	Mesotidal	High-mesotidal	High
125	2.02	1.23	6.83	70.50	Mesotidal	High-mesotidal	High
126	2.01	1.22	6.81	69.30	Mesotidal	High-mesotidal	High
127	2	1.22	6.81	68.58	Microtidal	low-mesotidal	High
128	1.98	1.23	6.85	71.18	Microtidal	low-mesotidal	High
129	1.96	1.23	6.86	71.42	Microtidal	low-mesotidal	High
130	1.92	1.23	6.83	71.12	Microtidal	low-mesotidal	High
131	1.9	1.22	6.79	69.04	Microtidal	low-mesotidal	High
132	1.89	1.25	6.93	75.37	Microtidal	low-mesotidal	High
133	1.89	1.22	6.78	68.11	Microtidal	low-mesotidal	High
134	1.88	1.22	6.78	68.09	Microtidal	low-mesotidal	High
135	1.85	1.20	6.73	65.63	Microtidal	low-mesotidal	High

136	1.84	1.21	6.75	66.69	Microtidal	low-mesotidal	High
137	1.77	1.22	6.81	69.45	Microtidal	low-mesotidal	High
138	1.68	1.25	6.94	75.34	Microtidal	low-mesotidal	High
139	1.62	1.27	7.01	79.10	Microtidal	low-mesotidal	High
140	1.58	1.26	6.98	77.66	Microtidal	low-mesotidal	High
141	1.55	1.25	6.93	74.95	Microtidal	low-mesotidal	High
142	1.55	1.25	6.94	75.40	Microtidal	low-mesotidal	High
143	1.52	1.25	6.92	74.56	Microtidal	low-mesotidal	High
144	1.5	1.24	6.90	73.80	Microtidal	low-mesotidal	High
145	1.48	1.25	6.95	75.95	Microtidal	low-mesotidal	High
Kerala state							
146	1.47	1.26	7.01	78.42	Microtidal	low-mesotidal	High
147	1.45	1.28	7.06	81.09	Microtidal	low-mesotidal	High
148	1.45	1.28	7.07	81.29	Microtidal	low-mesotidal	High
149	1.44	1.28	7.09	82.30	Microtidal	low-mesotidal	High
150	1.43	1.28	7.13	83.72	Microtidal	low-mesotidal	High
151	1.43	1.29	7.15	84.53	Microtidal	low-mesotidal	High
152	1.42	1.29	7.17	84.85	Microtidal	low-mesotidal	High
153	1.42	1.29	7.18	85.39	Microtidal	low-mesotidal	High
154	1.41	1.28	7.21	85.16	Microtidal	low-mesotidal	High
155	1.4	1.29	7.23	87.47	Microtidal	low-mesotidal	High
156	1.36	1.29	7.26	87.70	Microtidal	low-mesotidal	High
157	1.36	1.28	7.25	86.70	Microtidal	low-mesotidal	High
158	1.34	1.26	7.18	82.21	Microtidal	low-mesotidal	High
159	1.33	1.25	7.14	79.17	Microtidal	low-mesotidal	High
160	1.33	1.25	7.15	79.83	Microtidal	low-mesotidal	High
161	1.33	1.24	7.13	77.82	Microtidal	low-mesotidal	High
162	1.32	1.22	7.09	74.95	Microtidal	low-mesotidal	High
163	1.32	1.18	7.06	69.97	Microtidal	low-mesotidal	High
164	1.31	1.21	7.07	73.05	Microtidal	low-mesotidal	High
165	1.31	1.21	7.07	72.64	Microtidal	low-mesotidal	High
166	1.3	1.19	7.05	70.62	Microtidal	low-mesotidal	High
167	1.29	1.18	7.04	68.75	Microtidal	low-mesotidal	High
168	1.28	1.18	7.03	68.25	Microtidal	low-mesotidal	High
169	1.27	1.17	7.01	67.05	Microtidal	low-mesotidal	High
170	1.25	1.18	7.04	69.14	Microtidal	low-mesotidal	High
171	1.24	1.18	7.05	69.53	Microtidal	low-mesotidal	High

172	1.23	1.18	7.04	69.19	Microtidal	low-mesotidal	High
173	1.22	1.18	7.03	68.72	Microtidal	low-mesotidal	High
174	1.19	1.20	7.06	71.46	Microtidal	low-mesotidal	High
175	1.18	1.20	7.08	72.08	Microtidal	low-mesotidal	High
176	1.17	1.21	7.14	74.49	Microtidal	low-mesotidal	High
177	1.17	1.21	7.14	74.72	Microtidal	low-mesotidal	High
178	1.16	1.22	7.18	76.40	Microtidal	low-mesotidal	High
179	1.14	1.21	7.11	73.68	Microtidal	low-mesotidal	High
180	1.14	1.21	7.09	73.31	Microtidal	low-mesotidal	High
181	1.14	1.20	7.08	72.59	Microtidal	low-mesotidal	High
182	1.13	1.20	7.07	72.42	Microtidal	low-mesotidal	High
183	1.13	1.20	7.06	72.17	Microtidal	low-mesotidal	High
184	1.13	1.20	7.05	71.24	Microtidal	low-mesotidal	High
185	1.13	1.19	7.04	70.53	Microtidal	low-mesotidal	High
186	1.13	1.19	6.98	69.29	Microtidal	low-mesotidal	High
187	1.11	1.21	6.98	71.39	Microtidal	low-mesotidal	High
188	1.05	1.24	7.11	77.32	Microtidal	low-mesotidal	High
189	1.04	1.25	7.18	80.89	Microtidal	low-mesotidal	High
190	1.04	1.25	7.19	81.13	Microtidal	low-mesotidal	High
191	1.04	1.26	7.22	82.85	Microtidal	low-mesotidal	High
192	1.03	1.26	7.24	83.11	Microtidal	low-mesotidal	High
193	1.03	1.26	7.25	83.59	Microtidal	low-mesotidal	High
194	1.03	1.26	7.25	83.66	Microtidal	low-mesotidal	High
195	1.03	1.26	7.26	83.71	Microtidal	low-mesotidal	High
196	1.03	1.26	7.27	84.06	Microtidal	low-mesotidal	High
197	1.03	1.26	7.27	84.03	Microtidal	low-mesotidal	High
198	1.03	1.26	7.29	84.79	Microtidal	low-mesotidal	High
199	1.03	1.26	7.30	85.09	Microtidal	low-mesotidal	High
200	1.03	1.26	7.31	85.43	Microtidal	low-mesotidal	High
201	1.03	1.27	7.05	80.61	Microtidal	low-mesotidal	High
202	1.03	1.28	7.33	87.69	Microtidal	low-mesotidal	High
203	1	1.30	7.39	92.14	Microtidal	Microtidal	High
204	0.97	1.33	7.50	99.06	Microtidal	Microtidal	High
205	0.95	1.36	7.59	105.93	Microtidal	Microtidal	High
206	0.94	1.36	7.60	107.44	Microtidal	Microtidal	High
207	0.92	1.35	7.86	112.70	Microtidal	Microtidal	High
208	0.92	1.34	7.57	102.90	Microtidal	Microtidal	High

209	0.91	1.32	7.51	98.71	Microtidal	Microtidal	High
210	0.9	1.35	7.56	103.58	Microtidal	Microtidal	High
211	0.89	1.37	7.60	108.24	Microtidal	Microtidal	High
212	0.88	1.36	7.56	105.23	Microtidal	Microtidal	High
213	0.88	1.35	7.53	102.79	Microtidal	Microtidal	High
Tamil Nadu coast							
214	0.863	1.39	7.63	111.80	Microtidal	Microtidal	High
215	0.852	1.43	7.69	120.82	Microtidal	Microtidal	High
216	0.85	1.44	7.70	122.24	Microtidal	Microtidal	High
217	0.849	1.40	7.72	117.58	Microtidal	Microtidal	High
218	1.149	1.39	7.67	113.33	Microtidal	low-mesotidal	High
219	0.848	1.39	7.65	112.29	Microtidal	Microtidal	High
220	0.848	1.17	7.91	86.30	Microtidal	Microtidal	High
221	0.845	1.20	7.32	77.18	Microtidal	Microtidal	High
222	0.841	1.19	6.73	64.24	Microtidal	Microtidal	High
223	0.842	1.08	6.66	51.81	Microtidal	Microtidal	High
224	0.842	1.06	6.63	49.49	Microtidal	Microtidal	High
225	0.842	1.05	6.54	46.97	Microtidal	Microtidal	High
226	0.841	1.02	6.09	38.57	Microtidal	Microtidal	High
227	0.851	0.88	6.20	29.47	Microtidal	Microtidal	High
228	0.854	0.87	6.04	27.28	Microtidal	Microtidal	Moderate
229	0.854	0.88	6.13	28.89	Microtidal	Microtidal	High
230	0.861	0.87	6.04	27.80	Microtidal	Microtidal	Moderate
231	0.864	0.88	6.03	27.88	Microtidal	Microtidal	Moderate
232	0.882	0.88	5.91	26.98	Microtidal	Microtidal	Moderate
233	0.908	0.91	6.18	31.86	Microtidal	Microtidal	High
234	0.96	0.95	6.04	33.14	Microtidal	Microtidal	High
235	1.033	1.03	6.11	39.35	Microtidal	low-mesotidal	High
236	1.051	1.03	5.85	36.40	Microtidal	low-mesotidal	High
237	1.082	1.00	5.92	35.37	Microtidal	low-mesotidal	High
238	1.154	0.52	3.79	3.90	Microtidal	low-mesotidal	Moderate
239	1.194	0.50	3.74	3.56	Microtidal	low-mesotidal	Moderate
240	1.316	0.53	3.82	4.13	Microtidal	low-mesotidal	Moderate
241	1.386	0.50	3.80	3.56	Microtidal	low-mesotidal	Moderate
242	1.407	0.57	3.94	4.99	Microtidal	low-mesotidal	Moderate
243	1.407	0.57	3.94	4.99	Microtidal	low-mesotidal	Moderate
244	1.441	0.57	4.01	5.22	Microtidal	low-mesotidal	Moderate

245	1.44	0.57	4.03	5.35	Microtidal	low-mesotidal	Moderate
246	1.431	0.58	4.04	5.40	Microtidal	low-mesotidal	Moderate
247	1.416	0.59	4.09	5.77	Microtidal	low-mesotidal	Moderate
248	1.402	0.59	4.13	5.91	Microtidal	low-mesotidal	Moderate
249	1.402	0.59	4.13	5.89	Microtidal	low-mesotidal	Moderate
250	1.392	0.60	4.18	6.19	Microtidal	low-mesotidal	Moderate
251	1.395	0.60	4.20	6.38	Microtidal	low-mesotidal	Moderate
252	1.382	0.60	4.24	6.52	Microtidal	low-mesotidal	Moderate
253	1.635	0.61	4.26	6.65	Microtidal	low-mesotidal	Moderate
254	1.376	0.62	4.27	6.99	Microtidal	low-mesotidal	Moderate
255	1.355	0.63	4.30	7.28	Microtidal	low-mesotidal	Moderate
256	0.869	0.65	4.37	8.18	Microtidal	Microtidal	Moderate
257	0.997	0.62	4.42	7.47	Microtidal	Microtidal	Moderate
258	1.279	0.59	4.39	6.74	Microtidal	low-mesotidal	Moderate
259	1.43	0.62	4.43	7.49	Microtidal	low-mesotidal	Moderate
260	1.267	0.62	4.43	7.45	Microtidal	low-mesotidal	Moderate
261	1.337	0.61	4.43	7.41	Microtidal	low-mesotidal	Moderate
262	1.386	0.61	4.43	7.41	Microtidal	low-mesotidal	Moderate
263	1.489	0.61	4.43	7.41	Microtidal	low-mesotidal	Moderate
264	1.266	0.62	4.43	7.48	Microtidal	low-mesotidal	Moderate
265	1.715	0.62	4.44	7.51	Microtidal	low-mesotidal	Moderate
266	1.363	0.62	4.44	7.51	Microtidal	low-mesotidal	Moderate
267	1.403	0.60	4.44	7.13	Microtidal	low-mesotidal	Moderate
268	1.74	0.60	4.44	7.13	Microtidal	low-mesotidal	Moderate
269	1.487	0.60	4.44	7.13	Microtidal	low-mesotidal	Moderate
270	1.487	0.61	4.44	7.31	Microtidal	low-mesotidal	Moderate
271	1.215	0.61	4.44	7.28	Microtidal	low-mesotidal	Moderate
272	1.624	0.61	4.44	7.28	Microtidal	low-mesotidal	Moderate
273	1.105	0.60	4.44	7.06	Microtidal	low-mesotidal	Moderate
274	1.105	0.60	4.44	7.06	Microtidal	low-mesotidal	Moderate
275	1.105	0.60	4.44	7.06	Microtidal	low-mesotidal	Moderate
276	1.105	0.61	4.45	7.26	Microtidal	low-mesotidal	Moderate
277	1.105	0.62	4.46	7.54	Microtidal	low-mesotidal	Moderate
278	1.105	0.66	4.54	9.02	Microtidal	low-mesotidal	Moderate
279	1.105	0.66	4.54	9.02	Microtidal	low-mesotidal	Moderate
280	1.105	0.66	4.54	9.02	Microtidal	low-mesotidal	Moderate
281	1.105	0.66	4.54	9.02	Microtidal	low-mesotidal	Moderate

282	1.105	0.66	4.54	9.02	Microtidal	low-mesotidal	Moderate
283	1.013	0.66	4.54	9.02	Microtidal	low-mesotidal	Moderate
284	1.109	0.66	4.54	9.02	Microtidal	low-mesotidal	Moderate
285	1.078	0.66	4.54	9.02	Microtidal	low-mesotidal	Moderate
286	0.868	0.66	4.53	8.87	Microtidal	Microtidal	Moderate
287	0.984	0.74	4.58	11.41	Microtidal	Microtidal	Moderate
288	0.751	0.84	4.79	16.06	Microtidal	Microtidal	Moderate
289	0.894	0.83	4.80	15.98	Microtidal	Microtidal	Moderate
290	0.927	0.83	4.82	16.12	Microtidal	Microtidal	Moderate
291	0.922	0.82	4.83	15.67	Microtidal	Microtidal	Moderate
292	0.861	0.82	4.87	15.92	Microtidal	Microtidal	Moderate
293	0.87	0.82	4.88	15.97	Microtidal	Microtidal	Moderate
294	0.88	0.81	4.88	15.81	Microtidal	Microtidal	Moderate
295	0.895	0.81	4.89	15.74	Microtidal	Microtidal	Moderate
296	0.929	0.81	4.89	15.83	Microtidal	Microtidal	Moderate
297	0.951	0.81	4.89	15.83	Microtidal	Microtidal	Moderate
298	0.994	0.81	4.89	15.88	Microtidal	Microtidal	Moderate
299	0.987	0.81	4.89	15.55	Microtidal	Microtidal	Moderate
300	0.973	0.81	4.89	15.81	Microtidal	Microtidal	Moderate
301	0.959	0.83	4.94	16.79	Microtidal	Microtidal	Moderate
302	0.87	0.81	4.89	15.84	Microtidal	Microtidal	Moderate
303	0.868	0.82	4.92	16.30	Microtidal	Microtidal	Moderate
304	0.87	0.83	4.94	16.82	Microtidal	Microtidal	Moderate
305	0.872	0.83	4.94	16.79	Microtidal	Microtidal	Moderate
306	0.881	0.83	4.95	17.00	Microtidal	Microtidal	Moderate
307	0.886	0.84	4.98	17.46	Microtidal	Microtidal	Moderate
308	0.887	0.84	4.99	17.53	Microtidal	Microtidal	Moderate
309	0.895	0.84	5.00	17.80	Microtidal	Microtidal	Moderate
310	0.906	0.85	5.08	18.86	Microtidal	Microtidal	Moderate
311	0.906	0.86	5.13	19.38	Microtidal	Microtidal	Moderate
312	0.906	0.87	5.18	20.30	Microtidal	Microtidal	Moderate
313	0.902	0.88	5.26	21.47	Microtidal	Microtidal	Moderate
314	0.902	0.88	5.27	21.24	Microtidal	Microtidal	Moderate
315	0.902	0.87	5.26	20.96	Microtidal	Microtidal	Moderate
316	0.902	0.87	5.26	20.98	Microtidal	Microtidal	Moderate
317	0.944	0.89	5.32	22.67	Microtidal	Microtidal	Moderate
318	0.902	0.90	5.34	23.13	Microtidal	Microtidal	Moderate

319	0.96	0.91	5.35	23.43	Microtidal	Microtidal	Moderate
320	0.944	0.91	5.36	23.68	Microtidal	Microtidal	Moderate
321	0.944	0.93	5.40	25.25	Microtidal	Microtidal	Moderate
322	0.96	0.93	5.42	25.52	Microtidal	Microtidal	Moderate
323	0.974	0.94	5.43	25.97	Microtidal	Microtidal	Moderate
324	0.995	0.95	5.46	26.90	Microtidal	Microtidal	Moderate
325	1.043	1.01	5.63	32.03	Microtidal	low-mesotidal	High
326	1.085	1.01	5.65	32.86	Microtidal	low-mesotidal	High
327	1.072	1.04	5.69	34.69	Microtidal	low-mesotidal	High
328	1.058	1.04	5.69	35.15	Microtidal	low-mesotidal	High
329	1.115	1.04	5.70	35.46	Microtidal	low-mesotidal	High
330	1.239	1.06	5.71	36.32	Microtidal	low-mesotidal	High
331	1.239	1.05	5.71	35.83	Microtidal	low-mesotidal	High
332	1.217	1.04	5.71	35.16	Microtidal	low-mesotidal	High
333	1.217	1.04	5.71	35.18	Microtidal	low-mesotidal	High
334	1.217	1.05	5.83	37.64	Microtidal	low-mesotidal	High
Andhra Pradesh coast							
335	1.22	0.95	5.79	30.26	Microtidal	low-mesotidal	High
336	1.22	0.96	5.79	30.93	Microtidal	low-mesotidal	High
337	1.22	0.96	5.78	31.04	Microtidal	low-mesotidal	High
338	1.22	0.96	5.77	30.42	Microtidal	low-mesotidal	High
339	1.19	0.93	5.75	28.84	Microtidal	low-mesotidal	High
340	1.19	0.92	5.73	27.67	Microtidal	low-mesotidal	Moderate
341	1.19	0.91	5.71	26.99	Microtidal	low-mesotidal	Moderate
342	1.18	0.91	5.71	26.76	Microtidal	low-mesotidal	Moderate
343	1.2	0.90	5.70	26.35	Microtidal	low-mesotidal	Moderate
344	1.2	0.90	5.69	26.24	Microtidal	low-mesotidal	Moderate
345	1.2	0.91	5.69	26.55	Microtidal	low-mesotidal	Moderate
346	1.2	0.93	5.71	28.37	Microtidal	low-mesotidal	High
347	1.19	0.94	5.71	28.64	Microtidal	low-mesotidal	High
348	0.8	0.95	5.74	29.80	Microtidal	Microtidal	High
349	1.2	0.96	5.77	30.51	Microtidal	low-mesotidal	High
350	1.2	0.96	5.79	31.07	Microtidal	low-mesotidal	High
351	1.21	0.96	5.77	30.54	Microtidal	low-mesotidal	High
352	1.2	0.94	5.76	29.48	Microtidal	low-mesotidal	High
353	1.2	0.92	5.71	27.34	Microtidal	low-mesotidal	Moderate
354	1.2	0.90	5.68	26.38	Microtidal	low-mesotidal	Moderate

355	1.22	0.86	5.66	23.51	Microtidal	low-mesotidal	Moderate
356	1.22	0.86	5.67	23.60	Microtidal	low-mesotidal	Moderate
357	1.25	0.86	5.76	24.56	Microtidal	low-mesotidal	Moderate
358	1.26	0.85	5.77	23.90	Microtidal	low-mesotidal	Moderate
359	1.27	0.85	5.78	23.96	Microtidal	low-mesotidal	Moderate
360	1.27	0.85	5.78	23.84	Microtidal	low-mesotidal	Moderate
361	1.27	0.85	5.77	23.82	Microtidal	low-mesotidal	Moderate
362	1.31	0.91	6.00	29.95	Microtidal	low-mesotidal	High
363	0.83	0.91	6.07	30.58	Microtidal	Microtidal	High
364	1.3	0.90	6.15	30.78	Microtidal	low-mesotidal	High
365	1.31	0.90	6.17	30.49	Microtidal	low-mesotidal	High
366	1.31	0.89	6.18	30.29	Microtidal	low-mesotidal	High
367	1.3	0.87	6.17	28.91	Microtidal	low-mesotidal	High
368	1.3	0.87	6.18	29.01	Microtidal	low-mesotidal	High
369	1.3	0.87	6.18	29.25	Microtidal	low-mesotidal	High
370	1.31	0.89	6.16	30.30	Microtidal	low-mesotidal	High
371	1.3	0.89	6.15	30.03	Microtidal	low-mesotidal	High
372	1.3	0.90	6.11	30.23	Microtidal	low-mesotidal	High
373	1.3	0.89	5.96	28.30	Microtidal	low-mesotidal	High
374	1.29	0.90	5.89	27.95	Microtidal	low-mesotidal	High
375	1.29	0.95	6.02	32.75	Microtidal	low-mesotidal	High
376	1.29	0.96	6.03	33.41	Microtidal	low-mesotidal	High
377	1.28	1.06	5.99	39.99	Microtidal	low-mesotidal	High
378	1.28	1.08	6.07	43.28	Microtidal	low-mesotidal	High
379	1.27	1.09	6.13	44.93	Microtidal	low-mesotidal	High
380	1.26	1.09	6.00	42.67	Microtidal	low-mesotidal	High
381	1.26	1.09	6.00	42.67	Microtidal	low-mesotidal	High
382	1.27	1.08	5.97	41.66	Microtidal	low-mesotidal	High
383	1.26	1.03	5.73	34.82	Microtidal	low-mesotidal	High
384	1.26	1.01	5.71	33.44	Microtidal	low-mesotidal	High
385	1.26	0.99	5.69	31.93	Microtidal	low-mesotidal	High
386	1.25	0.97	5.85	31.90	Microtidal	low-mesotidal	High
387	1.26	0.94	5.98	31.26	Microtidal	low-mesotidal	High
388	1.26	0.93	5.99	31.12	Microtidal	low-mesotidal	High
389	1.26	0.93	5.99	31.11	Microtidal	low-mesotidal	High
390	1.26	0.95	6.12	34.09	Microtidal	low-mesotidal	High
391	1.27	1.01	6.15	38.70	Microtidal	low-mesotidal	High

392	1.27	1.03	6.01	38.29	Microtidal	low-mesotidal	High
393	1.3	1.13	6.07	46.92	Microtidal	low-mesotidal	High
394	1.32	1.15	6.14	49.67	Microtidal	low-mesotidal	High
395	1.33	1.16	6.22	51.91	Microtidal	low-mesotidal	High
396	1.35	1.17	6.22	53.09	Microtidal	low-mesotidal	High
397	1.4	1.22	6.29	58.53	Microtidal	low-mesotidal	High
398	1.42	1.01	6.09	38.05	Microtidal	low-mesotidal	High
399	1.46	0.97	5.06	24.12	Microtidal	low-mesotidal	Moderate
400	1.46	0.97	5.06	24.10	Microtidal	low-mesotidal	Moderate
401	1.46	1.02	5.36	30.00	Microtidal	low-mesotidal	High
402	1.46	1.03	5.46	31.42	Microtidal	low-mesotidal	High
403	1.47	1.11	6.13	46.13	Microtidal	low-mesotidal	High
404	1.47	1.12	6.16	47.41	Microtidal	low-mesotidal	High
405	1.47	1.13	6.17	48.16	Microtidal	low-mesotidal	High
406	1.48	1.13	6.17	48.94	Microtidal	low-mesotidal	High
407	1.49	1.16	6.19	51.40	Microtidal	low-mesotidal	High
408	1.51	1.18	6.21	53.59	Microtidal	low-mesotidal	High
409	1.51	1.18	6.22	53.73	Microtidal	low-mesotidal	High
410	1.51	1.19	6.22	54.41	Microtidal	low-mesotidal	High
411	1.52	1.19	6.23	55.05	Microtidal	low-mesotidal	High
412	1.53	1.20	6.23	55.73	Microtidal	low-mesotidal	High
413	1.56	1.19	6.21	54.82	Microtidal	low-mesotidal	High
414	1.57	1.18	6.22	54.14	Microtidal	low-mesotidal	High
415	1.59	1.18	6.23	53.92	Microtidal	low-mesotidal	High
416	1.59	1.17	6.24	53.42	Microtidal	low-mesotidal	High
417	1.61	1.14	6.25	50.74	Microtidal	low-mesotidal	High
418	1.63	1.13	6.24	49.88	Microtidal	low-mesotidal	High
419	1.64	1.13	6.24	49.51	Microtidal	low-mesotidal	High
420	1.65	1.13	6.25	49.80	Microtidal	low-mesotidal	High
421	1.65	1.13	6.25	50.22	Microtidal	low-mesotidal	High
422	1.65	1.14	6.25	50.38	Microtidal	low-mesotidal	High
423	1.67	1.14	6.25	50.89	Microtidal	low-mesotidal	High
424	1.67	1.14	6.26	51.07	Microtidal	low-mesotidal	High
425	1.67	1.15	6.26	51.59	Microtidal	low-mesotidal	High
426	1.69	1.17	6.26	53.77	Microtidal	low-mesotidal	High
427	1.72	1.20	6.28	56.70	Microtidal	low-mesotidal	High
428	1.74	1.21	6.30	58.51	Microtidal	low-mesotidal	High

429	1.75	1.21	6.34	59.06	Microtidal	low-mesotidal	High
430	1.76	1.20	6.32	57.39	Microtidal	low-mesotidal	High
431	1.78	1.17	6.27	53.54	Microtidal	low-mesotidal	High
432	1.78	1.17	6.28	53.76	Microtidal	low-mesotidal	High
433	1.8	1.17	6.32	55.02	Microtidal	low-mesotidal	High
434	1.82	1.15	6.30	52.83	Microtidal	low-mesotidal	High
435	1.82	1.15	6.31	52.86	Microtidal	low-mesotidal	High
436	1.83	1.12	6.24	49.21	Microtidal	low-mesotidal	High
437	1.84	1.11	6.21	47.65	Microtidal	low-mesotidal	High
438	0.97	1.12	6.17	47.73	Microtidal	Microtidal	High
439	1.86	1.13	6.20	49.13	Microtidal	low-mesotidal	High
440	1.86	1.14	5.73	42.75	Microtidal	low-mesotidal	High
Odisha coast							
441	1.92	1.17	6.31	54.19	Microtidal	low-mesotidal	High
442	1.92	1.18	6.33	55.54	Microtidal	low-mesotidal	High
443	1.93	1.19	6.37	57.47	Microtidal	low-mesotidal	High
444	1.95	1.19	6.39	58.08	Microtidal	low-mesotidal	High
445	1.92	1.19	6.40	57.93	Microtidal	low-mesotidal	High
446	1.97	1.18	6.51	58.94	Microtidal	low-mesotidal	High
447	2.01	1.17	6.56	58.83	Mesotidal	High-mesotidal	High
448	2.03	1.18	6.59	60.81	Mesotidal	High-mesotidal	High
449	2.05	1.19	6.58	61.42	Mesotidal	High-mesotidal	High
450	2.06	1.21	6.55	62.35	Mesotidal	High-mesotidal	High
451	2.07	1.22	6.57	63.76	Mesotidal	High-mesotidal	High
452	2.05	1.19	6.56	60.75	Mesotidal	High-mesotidal	High
453	2.1	1.17	6.51	57.89	Mesotidal	High-mesotidal	High
454	2.16	1.18	6.56	60.33	Mesotidal	High-mesotidal	High
455	2.28	1.14	6.62	56.95	Mesotidal	High-mesotidal	High
456	2.36	1.14	6.61	56.52	Mesotidal	High-mesotidal	High
457	2.33	1.12	6.61	54.97	Mesotidal	High-mesotidal	High
458	2.41	1.15	6.56	56.64	Mesotidal	High-mesotidal	High
459	2.89	1.04	6.61	47.42	Mesotidal	High-mesotidal	High
460	3.95	0.87	6.17	28.81	Mesotidal	Low-macrotidal	High
461	4.05	0.87	6.17	28.81	Macrotidal	Low-macrotidal	High
462	3.98	0.90	6.12	30.40	Mesotidal	Low-macrotidal	High
463	3.8	0.94	6.12	33.16	Mesotidal	Low-macrotidal	High

West Bengal coast							
464	3.41	1.01	6.42	41.97	Mesotidal	High-mesotidal	High
465	1.69	1.00	6.39	40.82	Microtidal	low-mesotidal	High
466	1.78	1.00	6.39	40.82	Microtidal	low-mesotidal	High
467	1.7	1.00	6.39	40.82	Microtidal	low-mesotidal	High
468	1.73	1.00	6.39	40.82	Microtidal	low-mesotidal	High
469	2.36	1.00	6.39	40.82	Mesotidal	High-mesotidal	High
470	2.84	1.00	6.39	40.82	Mesotidal	High-mesotidal	High
471	3.3	1.00	6.39	40.82	Mesotidal	High-mesotidal	High

Table A3.2 Geomorphological classification of tidal inlets along Indian coast

Inlet No.	Inlet Name	Longitude (E)	Latitude (N)	Geomorphological Classification
Gujarat coast				
1	Gandhiya	69°31'00.26"	22°22'24.74"	TD
2	Kalawad	69°29'22.81"	22°20'15.65"	TD
3	Panero	69°27'27.42"	22°19'58.58"	TD
4	Mithapur	68°58'39.24"	22°24'12.82"	TD
5	Makanpur	68°57'34.30"	22°21'11.88"	ICOLL
6	Dwaraka	68°57'33.43"	22°15'20.92"	TD
7	Hari kund	68°57'55.39"	22°14'07.26"	TD
8	Goji	69°11'44.70"	21°58'58.62"	ICOLL
9	Navadra	69°14'42.80"	21°56'02.00"	ICOLL
10	Miyani	69°22'14.90"	21°49'52.61"	ICOLL
11	Porbandar	69°35'28.17"	21°38'20.22"	Mixed Energy
12	Tukada	69°42'21.71"	21°32'12.73"	ICOLL
13	Chikasa	69°46'35.66"	21°27'37.87"	WD
14	Shil	70°01'47.76"	21°10'38.96"	ICOLL
15	Ravon	70°20'45.12"	20°54'58.10"	TD
16	Prabhas	70°24'39.02"	20°52'51.13"	TD
17	Mul Dwarka	70°40'22.49"	20°45'42.59"	TD
18	Sarkhadi	70°52'16.25"	20°42'32.80"	TD
19	Diu	70°59'13.56"	20°43'11.68"	TD
20	Bandar	71°04'33.79"	20°44'35.99"	TD
21	Rajput	71°05'07.98"	20°45'22.00"	WD
22	Rajpara	71°12'14.39"	20°47'52.91"	TD
23	Jafrabad	71°22'18.34"	20°52'03.14"	TD
24	Chanch	71°32'18.40"	20°57'08.10"	TD

25	Tena river	72°36'29.15"	21°13'40.12"	TD
26	Mindhola river	72°41'24.75"	21°03'59.65"	TD (H)
27	Puma river	72°46'42.98"	20°54'32.08"	TD (H)
28	Kavai creek	72°50'02.88"	20°48'16.88"	TD (H)
29	Ambika river	72°51'06.84"	20°45'09.94"	TD (H)
30	Auranga river	72°53'19.71"	20°37'59.02"	TD (H)
31	Umarsadi	72°53'19.62"	20°31'57.29"	Mixed Energy
32	Kolak river	72°51'27.38"	20°28'01.27"	Mixed Energy
33	Daman	72°49'50.96"	20°24'41.47"	Mixed Energy
34	Bhathaiya	72°49'35.44"	20°23'06.00"	TD
35	Kalu river	72°49'16.63"	20°22'05.88"	TD
36	Kalai	72°48'41.14"	20°21'17.96"	TD
37	Kalgam 1	72°46'31.09"	20°19'27.77"	TD
38	Kalgam 2	72°46'36.88"	20°20'02.08"	TD
39	Maroli	72°46'23.57"	20°18'08.68"	TD
40	Varoli river	72°45'08.94"	20°15'40.21"	TD
41	Nargol	72°44'51.00"	20°12'09.18"	TD
42	Deheri	72°44'31.92"	20°09'54.97"	TD
Maharashtra coast				
43	Zai	72°44'18.81"	20°07'42.89"	TD
44	Gholvad	72°43'34.53"	20°04'55.60"	TD
45	Dahanu	72°43'33.52"	19°58'09.91"	TD
46	Navapur	72°41'47.30"	19°47'32.14"	WD
47	Dudh river	72°43'07.00"	19°43'47.60"	WD
48	Darapada	72°43'44.81"	19°37'13.80"	TD
49	Kelwa	72°45'35.45"	19°35'53.92"	TD
50	Bhadve	72°47'40.71"	19°29'35.95"	TD
51	Rajodi	72°45'41.27"	19°25'01.74"	TD
52	Bhuigaon Kh.	72°46'03.57"	19°23'34.91"	TD
53	Vasai	72°48'12.01"	19°19'01.34"	TD
54	Malad	72°48'01.66"	19°11'52.98"	TD
55	Versova	72°50'02.88"	19°08'40.27"	TD
56	Revas	72°53'00.05"	18°53'43.55"	TD
57	Mandve	72°57'33.40"	18°50'09.28"	TD
58	Awass	72°51'52.17"	18°46'10.60"	TD
59	Surekhar	72°52'01.58"	18°45'27.00"	WD
60	Navgaon	72°51'48.01"	18°42'04.28"	WD
61	Navapada	72°52'00.98"	18°40'07.18"	WD
62	Akshi	72°53'19.62"	18°38'18.24"	TD
63	Bagmala	72°55'29.89"	18°34'42.10"	TD
64	Revdanda	72°55'58.00"	18°32'18.35"	TD
65	Wandeli	72°54'37.73"	18°30'12.20"	WD

66	Surulpeth	72°55'46.98"	18°22'23.88"	TD
67	Eakdara	72°58'23.06"	18°19'12.47"	TD
68	Rajapuri	72°58'48.79"	18°16'53.15"	TD
69	Velas Agar	72°59'18.88"	18°11'44.52"	TD
70	Diveagar	73°00'00.61"	18°09'32.72"	TD
71	Walavati kh.	73°01'00.09"	18°04'20.10"	TD
72	Shrivardhan	73°02'31.35"	18°01'34.86"	TD
73	Bankot	73°02'59.86"	17°58'59.52"	TD
74	Sakhari	73°04'08.17"	17°55'54.52"	TD
75	Koliwada	73°05'27.49"	17°53'25.37"	TD
76	Jaikar	73°10'06.76"	17°50'30.62"	TD
77	Dabhol	73°10'36.96"	17°34'47.14"	TD
78	Mouje	73°11'51.31"	17°30'54.72"	WD
79	Palshet	73°13'15.74"	17°26'15.97"	TD
80	Muslondi	73°13'37.22"	17°21'16.13"	TD
81	Jaigad	73°14'24.96"	17°17'32.78"	TD
82	Bhandrawada	73°15'42.85"	17°11'58.02"	TD
83	Bhandarpule	73°16'29.11"	17°09'30.49"	WD
84	Kajitbhati	73°17'17.98"	17°06'00.40"	WD
85	Sadye	73°17'33.98"	17°04'40.84"	TD
86	Sadamirya	73°17'03.86"	17°02'17.30"	TD
87	Karle	73°18'02.16"	16°59'09.17"	TD
88	Bhatiwadi	73°18'59.66"	16°53'27.60"	TD
89	Khsheli	73°19'38.43"	16°48'23.26"	TD
90	Wadativre	73°21'26.23"	16°41'13.74"	TD
91	Vijayadurg	73°19'47.99"	16°34'14.38"	TD
92	Phanase	73°22'21.04"	16°26'36.31"	WD
93	Padavne	73°23'10.95"	16°23'34.26"	WD
94	Taramumbari	73°24'40.81"	16°21'36.50"	TD
95	Morve	73°26'03.17"	16°16'28.34"	WD
96	Pirawadi	73°27'46.55"	16°12'04.03"	TD
97	Sariekot	73°27'56.98"	16°05'16.91"	WD
98	Malvan	73°29'26.36"	16°04'15.67"	TD
99	Kalethar	73°30'13.56"	16°00'36.72"	TD
100	Bhogwa	73°32'02.41"	15°58'01.20"	WD
101	Shriramwadi	73°34'03.09"	15°56'17.45"	TD
102	Khalchiwadi	73°35'11.19"	15°55'08.80"	TD
103	Kelus 1	73°35'48.19"	15°54'37.76"	TD
104	Kelus 2	73°36'40.63"	15°53'42.32"	ICOLL
105	Dabholi	73°39'12.07"	15°51'56.74"	WD
106	Tank	73°39'49.45"	15°47'37.82"	WD
107	Khalchikar	73°41'23.10"	15°45'12.49"	TD

Goa coast				
108	Tiracol	73°44'10.86"	15°43'16.82"	TD
109	Siolim	73°44'53.07"	15°36'38.81"	TD
110	Baga	73°47'24.54"	15°33'46.08"	WD
111	Mandovi	73°48'56.41"	15°29'08.81"	TD
112	Zuari	73°57'03.30"	15°25'36.88"	TD
113	Mobor	73°58'47.73"	15°08'30.41"	WD
114	Cola	74°00'56.30"	15°03'15.66"	WD
115	Anjadip	74°02'07.85"	15°00'48.28"	WD
116	Canacona 2	74°02'19.25"	14°59'36.53"	WD
117	Canacona 1	74°02'59.10"	14°59'02.65"	WD
118	Mashem	74°07'19.97"	14°57'27.72"	WD
Karnataka coast				
119	Karwar	74°09'31.59"	14°50'29.72"	TD
120	Chendia	74°13'41.79"	14°45'08.89"	WD
121	Todur	74°15'51.25"	14°44'41.14"	WD
122	Belekeri	74°16'45.48"	14°42'42.52"	Mixed Energy
123	Ankola	74°17'02.63"	14°39'41.98"	WD
124	Belambar	74°17'32.99"	14°38'49.38"	WD
125	Manjaguni	74°21'28.42"	14°36'00.86"	TD
126	Tadadi Port	74°23'34.51"	14°31'11.78"	Mixed Energy
127	Alvekodi 2	74°25'27.75"	14°25'03.94"	Mixed Energy
128	Karki	74°28'11.32"	14°17'56.65"	WD
129	Nakhuda	74°30'05.06"	14°11'20.62"	Mixed Energy
130	Alvekodi 1	74°31'04.58"	14°01'36.62"	WD
131	Jali	74°32'05.18"	13°59'05.53"	Mixed Energy
132	Mavakurve	74°33'59.88"	13°58'01.81"	WD
133	Hadin	74°35'08.18"	13°56'59.86"	WD
134	Alivey Gadde	74°36'25.66"	13°55'20.78"	Mixed Energy
135	Paduvari	74°37'27.52"	13°52'05.52"	Mixed Energy
136	Koderi	74°40'11.33"	13°47'38.69"	Mixed Energy
137	Gangoli	74°41'43.50"	13°38'02.83"	TD
138	Kundapura	74°44'11.12"	13°27'00.94"	TD
139	Malpe	74°41'44.20"	13°20'50.24"	WD
140	Kaup	74°46'01.08"	13°13'26.04"	WD
141	Nadsal	74°46'36.57"	13°06'42.77"	WD
142	Hejamadi	74°48'22.09"	13°04'31.04"	WD
143	NMPT	74°49'40.85"	12°55'37.45"	WD
144	Netravati & Gurupur	74°51'49.84"	12°50'43.55"	TD
145	Kanwatheertha	74°53'15.69"	12°45'38.70"	WD
Kerala coast				
146	Hosabettu	74°55'13.85"	12°42'28.76"	WD

147	Bandiyod	74°55'54.92"	12°37'55.99"	WD
148	Shiriya	74°57'30.22"	12°36'25.02"	WD
149	Puthur	74°59'15.77"	12°32'28.03"	WD
150	Thalangara	75°00'16.70"	12°28'30.68"	Mixed Energy
151	chembirika	75°00'48.79"	12°26'26.99"	WD
152	Thekkekara	75°01'40.95"	12°25'15.06"	ICOLL
153	Tharavadu	75°03'41.29"	12°23'56.69"	ICOLL
154	Kadapuram	75°07'12.98"	12°20'39.37"	WD
155	Kaithakkad	75°13'37.10"	12°11'59.86"	WD
156	Madayi	75°17'46.82"	12°01'18.30"	WD
157	Azhikkal	75°24'16.63"	11°56'37.00"	Mixed Energy
158	Thottada	75°25'56.01"	11°50'17.81"	WD
159	Nadal	75°27'18.12"	11°48'30.71"	WD
160	Dharmadom	75°28'17.94"	11°46'42.28"	WD
161	Koduvalli	75°31'53.97"	11°45'55.98"	WD
162	Mahe	75°32'36.54"	11°42'13.75"	WD
163	Olavilam	75°32'51.21"	11°40'46.16"	ICOLL
164	Chombala	75°33'31.73"	11°40'14.70"	WD
165	Madappally	75°35'22.90"	11°38'49.13"	ICOLL
166	iringal	75°37'50.48"	11°34'06.64"	WD
167	Nandi	75°42'07.03"	11°28'06.82"	WD
168	Puthiyapurayil	75°44'08.04"	11°25'02.50"	ICOLL
169	Elathur	75°46'46.46"	11°20'46.21"	WD
170	Thekepuram	75°48'13.03"	11°13'39.50"	WD
171	Beypore	75°49'32.80"	11°09'42.91"	WD
172	Kudalundi	75°51'26.16"	11°07'27.70"	WD
173	Chiramangalam	75°54'42.27"	11°01'11.50"	WD
174	Malappuram	75°56'10.66"	10°47'13.70"	Mixed Energy
175	Veliancode	75°58'48.42"	10°43'56.06"	WD
176	Nallamkallu 2	75°58'56.33"	10°37'57.94"	ICOLL
177	Nallamkallu 1	76°02'18.55"	10°37'39.72"	ICOLL
178	Chettuva	76°04'56.79"	10°30'30.17"	WD
179	Nattika	76°05'54.13"	10°25'09.77"	ICOLL
180	Muriyamthodu	76°06'34.72"	10°22'45.08"	WD
181	Palapetty	76°06'44.76"	10°20'59.10"	WD
182	Chamakkala	76°07'24.18"	10°20'34.04"	ICOLL
183	Vazhiyambalam	76°07'39.62"	10°18'41.40"	ICOLL
184	Perinjanam	76°08'12.04"	10°17'54.49"	ICOLL
185	Ambalanada	76°09'51.08"	10°15'47.63"	ICOLL
186	Munambam	76°14'03.21"	10°10'41.70"	WD
187	Kochi inlet	76°17'04.09"	9°58'10.93"	WD
188	Andhakaranazhy	76°17'31.71"	9°44'57.35"	WD

189	Arthunkal	76°17'35.82"	9°39'45.00"	ICOLL
190	Kackary	76°17'46.46"	9°39'04.59"	ICOLL
191	Perunermangalm	76°17'55.12"	9°37'23.30"	WD
192	Janakshemam	76°18'01.46"	9°36'06.25"	ICOLL
193	Valavanadu 2	76°18'04.11"	9°35'18.41"	ICOLL
194	Valavanadu 1	76°18'09.90"	9°34'58.61"	ICOLL
195	Pollethai	76°18'19.63"	9°34'20.14"	ICOLL
196	Kattoor	76°18'28.43"	9°33'25.21"	ICOLL
197	Omanapuzha	76°18'45.79"	9°32'37.53"	WD
198	Poomkavu	76°18'52.78"	9°31'04.68"	ICOLL
199	Padinjare	76°19'26.59"	9°30'25.27"	ICOLL
200	Eravukadu	76°19'34.26"	9°27'51.94"	WD
201	Punnapra 2	76°19'55.53"	9°27'25.22"	ICOLL
202	Punnapra 1	76°22'59.14"	9°26'06.78"	ICOLL
203	Thottapally lake	76°27'46.41"	9°18'42.42"	WD
204	Azheekkal	76°31'10.27"	9°08'12.89"	WD
205	Kandathil	76°32'18.94"	9°01'04.13"	ICOLL
206	Neendakara	76°38'55.56"	8°56'03.60"	WD
207	Paravur lake	76°40'33.49"	8°48'44.33"	WD
208	Kappil	76°47'11.70"	8°46'38.49"	WD
209	Madanvila	76°53'10.64"	8°38'00.09"	WD
210	Veli	76°57'29.16"	8°30'30.05"	WD
211	Pachalloor	77°01'43.04"	8°25'29.72"	WD
212	Kochupally	77°04'45.62"	8°20'45.56"	WD
213	Paruthiyoor	77°09'59.76"	8°18'20.74"	WD
Tamil Nadu coast				
214	Erayumanthurai	77°14'45.45"	8°14'29.52"	WD
215	Sambasivapuram	77°18'10.77"	8°10'25.43"	TD
216	Kadiyapattanam	77°22'24.04"	8°08'20.76"	WD
217	Rajakamangalam Thurai	77°29'08.11"	8°06'54.58"	ICOLL
218	Manakudi	77°31'00.99"	8°05'15.47"	WD
219	Kovalam	77°38'23.23"	8°04'57.83"	WD
220	SRNP	77°48'03.67"	8°09'27.19"	ICOLL
221	Thottavilai	78°03'32.06"	8°14'21.69"	ICOLL
222	Manapad	78°07'22.98"	8°22'48.48"	WD
223	Govindamal colony	78°07'35.97"	8°30'12.50"	TD
224	Veerapandianpattinam	78°07'35.12"	8°31'20.70"	ICOLL
225	Mangaladevi	78°12'22.66"	8°33'07.26"	ICOLL
226	Punnaikayal	78°07'46.10"	8°38'27.51"	WD (H)
227	Veppalodai	78°14'42.40"	8°57'17.82"	WD
228	Sippikulam	78°16'04.43"	8°59'19.60"	ICOLL
229	Vaippar	78°17'57.81"	9°00'14.43"	WD

230	Velayudhapuram 2	78°18'56.38"	9°01'27.78"	WD
231	Velayudhapuram 1	78°22'06.31"	9°02'16.25"	ICOLL
232	Vembar	78°29'08.59"	9°04'47.97"	ICOLL
233	Mookaiyur	78°38'51.98"	9°07'42.92"	WD
234	Valinokkam	78°49'58.85"	9°11'03.77"	WD
235	Sethu karai	78°54'55.95"	9°14'40.49"	WD
236	Muthariyarnagar	78°55'16.55"	9°15'27.09"	ICOLL
237	Mandapam	79°08'46.08"	9°17'10.54"	WD
238	Atrangarai	79°01'34.80"	9°20'42.44"	WD
239	Pudhuvalasai	78°57'54.56"	9°23'32.78"	ICOLL
240	Thiruppalaikudi	78°57'05.81"	9°31'45.98"	Mixed Energy
241	Karankadu	78°58'14.97"	9°38'43.48"	WD
242	Alikkudi	78°58'22.51"	9°39'30.79"	WD
243	Pudupattinam	78°59'59.52"	9°40'15.22"	Mixed Energy
244	Velangudi	79°01'51.35"	9°44'53.87"	WD
245	Muthuramalingapattinam	79°02'56.41"	9°45'13.72"	WD
246	odavayal	79°04'40.94"	9°46'08.24"	Mixed Energy
247	Kaliyanagari	79°05'54.97"	9°48'01.60"	WD
248	S.P.Pattinam 2	79°06'22.15"	9°50'01.48"	Mixed Energy
249	S.P.Pattinam 1	79°07'23.50"	9°50'15.95"	Mixed Energy
250	Muthukuda	79°07'45.21"	9°51'38.29"	Mixed Energy
251	Arsanagaripattinam	79°07'25.48"	9°53'02.44"	Mixed Energy
252	Embakkottai	79°09'05.77"	9°54'40.59"	Mixed Energy
253	Gopalapattinam	79°09'43.35"	9°55'04.82"	Mixed Energy
254	Sannathi	79°11'51.10"	9°56'16.23"	Mixed Energy
255	Kottaippattannam	79°13'34.38"	9°58'16.40"	WD
256	Tandalai	79°13'40.52"	10°00'25.38"	WD
257	Manamelkudi 2	79°16'02.79"	10°02'41.10"	Mixed Energy
258	Manamelkudi 1	79°15'11.75"	10°03'09.14"	TD
259	Mumpalai 5	79°15'13.89"	10°03'24.41"	TD
260	Mumpalai 4	79°15'22.66"	10°03'43.49"	TD
261	Mumpalai 3	79°14'53.26"	10°04'18.44"	TD
262	Mumpalai 2	79°14'29.67"	10°04'24.28"	TD
263	Mumpalai 1	79°14'16.79"	10°04'24.13"	TD
264	Kandanivayal	79°14'15.08"	10°04'55.45"	TD
265	Subramanyapuram	79°13'42.31"	10°06'19.94"	Mixed Energy
266	Ravuttanvayal	79°13'42.00"	10°06'32.40"	WD
267	Sembiyan 3	79°13'48.01"	10°07'59.66"	TD
268	Sembiyan 2	79°13'46.05"	10°08'06.07"	TD
269	Sembiyan 1	79°13'43.06"	10°08'10.64"	TD
270	Manthirippattinam 2	79°13'56.48"	10°08'32.32"	Mixed Energy
271	Tiruvathevan 3	79°14'23.42"	10°09'14.22"	Mixed Energy

272	Tiruvathevan 2	79°14'28.12"	10°09'25.34"	Mixed Energy
273	Tiruvathevan 1	79°14'22.27"	10°09'57.20"	TD
274	Palliya kulam	79°14'19.90"	10°10'12.50"	TD
275	Manthiripattinam 1	79°14'42.56"	10°10'24.56"	Mixed Energy
276	Perumagalur	79°15'10.46"	10°11'12.37"	WD
277	Adaikkathevan	79°16'32.57"	10°12'14.54"	Mixed Energy
278	Villunivayal	79°17'05.02"	10°13'01.99"	WD (H)
279	Ravuthanvayal	79°16'03.09"	10°13'40.22"	TD
280	Marakkavalasai	79°16'46.63"	10°14'32.71"	WD
281	Nayagathivayal	79°17'32.70"	10°15'01.58"	Mixed Energy
282	Manora	79°18'25.85"	10°15'29.74"	Mixed Energy
283	Sarabendrarajanpattinam	79°19'22.36"	10°15'56.66"	WD
284	Kallivayal	79°22'02.80"	10°16'50.09"	WD
285	Keezhathottam	79°31'13.21"	10°17'40.96"	WD
286	Thuraikkadu	79°44'21.93"	10°18'45.00"	Mixed Energy
287	Kodiyakadu	79°45'40.93"	10°16'40.33"	WD
288	Kodikkarai	79°50'10.80"	10°16'33.46"	WD
289	Vedaranyam	80°00'44.46"	10°20'04.06"	WD
290	Madavilagam	79°52'43.26"	10°22'30.40"	WD
291	Thopputhurai	79°52'15.25"	10°24'12.20"	WD
292	Naluvethapathi	79°52'00.91"	10°29'31.52"	WD
293	Vanvanmahadevi	79°51'42.19"	10°31'26.87"	WD
294	Vettaikarairuppu	79°51'37.09"	10°33'27.11"	WD
295	pudupalli	79°51'27.44"	10°34'35.33"	WD
296	Vizhunthamavadi	79°51'24.50"	10°35'37.18"	WD
297	Tirupoondi	79°51'19.66"	10°38'00.67"	ICOLL
298	Velankanni	79°51'12.59"	10°40'40.76"	WD
299	Nagapattinam	79°51'06.94"	10°45'51.95"	WD
300	Thethinagar	79°51'05.00"	10°49'34.43"	WD
301	keezhaiyur 2	79°51'07.36"	10°50'39.23"	WD
302	Keezhaiyur 1	79°51'10.39"	10°53'16.12"	WD
303	Bharathi nagar	79°51'12.90"	10°54'49.43"	WD
304	Akkampettai	79°51'12.61"	10°57'45.54"	WD
305	Chandrapady	79°51'13.56"	10°59'42.07"	ICOLL
306	Kittiyandiyur	79°51'20.24"	11°01'13.62"	WD
307	Veepanchery	79°51'26.83"	11°05'19.90"	WD
308	Vanagiri	79°51'27.05"	11°06'38.56"	WD
309	Pompuhar	79°51'29.31"	11°08'08.77"	WD
310	Thirumullaivasal	79°50'58.76"	11°14'40.63"	WD
311	Chinnakottaimedu	79°50'31.36"	11°18'09.29"	ICOLL
312	Pazhaiyar	79°49'56.10"	11°21'31.50"	WD
313	Chinna vaaikaal	79°48'20.90"	11°27'25.78"	WD (H)

314	Ariyakoshti	79°46'48.83"	11°30'10.19"	WD (H)
315	Pudukuppam	79°46'34.96"	11°31'49.33"	WD
316	Samiyaar	79°45'52.18"	11°32'25.80"	ICOLL
317	Cuddalore	79°47'09.08"	11°42'24.08"	WD (Jetti)
318	Devanampattinam	79°47'21.48"	11°44'16.26"	WD
319	Pudukuppam	79°47'36.99"	11°45'16.02"	ICOLL
320	Subauppalavadi	79°47'53.21"	11°46'19.96"	WD
321	Aladimedu	79°49'20.75"	11°49'59.41"	WD
322	C veerampattinam	79°49'44.04"	11°52'39.54"	WD
323	Puducherry	79°49'50.89"	11°54'22.36"	WD (Jetti)
324	Muthaialpet	79°50'45.15"	11°57'47.45"	ICOLL
325	Vembalur	80°02'54.61"	12°15'49.43"	WD
326	Odiyur	80°02'57.24"	12°19'23.34"	WD
327	KPK	80°08'26.14"	12°26'14.78"	WD
328	Sudurangapattinam	80°09'15.82"	12°27'57.17"	WD
329	Kalpakkam	80°10'14.06"	12°30'33.84"	ICOLL
330	Kokkilamedu	80°11'31.23"	12°34'34.00"	WD
331	Padur	80°14'56.52"	12°48'12.49"	WD
332	Srinivasapuram	80°17'21.52"	13°00'49.43"	WD
333	Sathya Nagar	80°18'37.21"	13°04'01.42"	WD (Jetti)
334	Athipatti	80°20'19.79"	13°14'01.72"	WD
Andhra Pradesh coast				
335	Karimanal	80°18'58.11"	13°27'59.83"	WD
336	Shar	80°15'04.34"	13°45'57.13"	ICOLL
337	Chinnathota	80°14'54.28"	13°49'04.26"	WD
338	Nalagamula	80°13'44.53"	13°51'35.89"	ICOLL
339	Konduru	80°09'15.61"	14°01'45.12"	WD
340	Swanamukhi River	80°09'02.09"	14°04'29.03"	WD
341	Kothapatnam	80°07'47.80"	14°07'32.16"	WD
342	Srinivasa	80°07'37.31"	14°09'11.30"	ICOLL
343	Gunnampadia 2	80°07'40.83"	14°11'21.95"	ICOLL
344	Gunnampadia 1	80°07'45.06"	14°12'18.68"	ICOLL
345	Gopalapuram 2	80°08'07.21"	14°13'12.14"	ICOLL
346	Gopalapuram 1	80°08'15.43"	14°14'42.97"	WD
347	Nelaturu	80°09'26.20"	14°19'09.88"	WD
348	Pathapalem	80°10'37.10"	14°22'22.87"	WD
349	Koruturu	80°10'59.90"	14°28'26.58"	ICOLL
350	Ramudupalem	80°11'04.38"	14°31'58.26"	WD
351	Utukuru	80°12'51.64"	14°35'24.43"	Mixed Energy
352	Ramathirtham	80°09'43.47"	14°38'37.61"	ICOLL
353	Isakapalle	80°07'36.58"	14°44'23.28"	WD
354	Juvvaladinne	80°06'01.91"	14°49'08.44"	WD

355	Ramayapatnam 2	80°04'57.49"	15°02'44.09"	ICOLL
356	Ramayapatnam 1	80°02'56.41"	15°04'11.35"	WD
357	Karedu	80°05'11.59"	15°11'19.72"	WD
358	Pakala	80°05'22.53"	15°16'56.64"	ICOLL
359	Anantavaram 2	80°06'16.17"	15°18'47.12"	WD
360	Anantavaram 1	80°06'46.04"	15°19'23.45"	WD
361	Peddapattapalam	80°06'55.49"	15°21'10.58"	ICOLL
362	Motumala	80°13'27.95"	15°30'05.83"	WD
363	Chintayigari palem	80°14'20.39"	15°32'41.39"	WD
364	Kanuparthi	80°14'30.17"	15°36'09.79"	WD
365	Peddaganjam	80°15'48.42"	15°38'00.38"	WD
366	Pallepalem	80°16'37.29"	15°39'22.25"	WD
367	Pullaripalem 3	80°18'42.28"	15°43'07.86"	ICOLL
368	Pullaripalem 2	80°19'15.33"	15°43'27.37"	ICOLL
369	Pullaripalem 1	80°19'51.67"	15°43'43.90"	ICOLL
370	Katari palem	80°22'58.52"	15°44'42.18"	WD
371	Krupa nagar	80°26'00.35"	15°46'35.94"	WD
372	Pandurangapuram	80°32'40.18"	15°48'22.46"	WD
373	East Gollapallem	80°38'19.72"	15°51'13.72"	WD
374	Gokarnamatam	80°41'51.21"	15°52'35.29"	WD
375	Dindiadavala	80°46'02.41"	15°52'52.03"	WD
376	Haripuram	80°49'54.57"	15°51'45.61"	WD
377	LVD	80°55'48.36"	15°42'42.08"	Mixed Energy
378	Elachetladibba	81°04'00.91"	15°43'24.53"	Mixed Energy
379	RKP	81°06'09.92"	15°54'34.96"	WD
380	Ramakrishnapuram 2	81°06'13.53"	15°56'47.11"	ICOLL
381	Ramakrishnapuram 1	81°07'50.47"	15°56'52.91"	ICOLL
382	Palakayatippa	81°10'24.88"	15°58'25.50"	Mixed Energy
383	Machilipatnam	81°11'10.10"	16°04'46.67"	WD
384	polatitippa	81°12'05.76"	16°06'13.64"	Mixed Energy
385	Chlilkalapudi	81°12'24.18"	16°08'38.65"	WD
386	Kara agramam	81°14'13.68"	16°10'46.49"	Mixed Energy
387	Gokavaram	81°14'54.15"	16°14'21.34"	WD
388	Tallapalem	81°15'58.00"	16°15'19.48"	WD
389	Kanuru	81°23'46.99"	16°16'43.68"	Mixed Energy
390	Kruthivennu	81°29'23.23"	16°20'37.93"	WD
391	Peda Gollapalem	81°32'39.44"	16°21'19.62"	WD
392	Chinna Gollapalem	81°43'06.80"	16°20'55.90"	WD
393	Marritippa	81°57'10.98"	16°19'09.08"	WD
394	Odalaravu	82°02'01.04"	16°24'20.81"	Mixed Energy
395	Komaragiri patanam	82°08'38.60"	16°26'27.49"	Mixed Energy
396	Gachakayala pora	82°16'51.49"	16°29'55.72"	WD

397	Kothapalem	82°20'22.34"	16°35'42.11"	Mixed Energy
398	Gadimoga	82°20'58.07"	16°43'58.91"	WD
399	Sasikanth Nagar	82°18'07.94"	16°59'09.56"	Mixed Energy
400	Nemam	82°18'49.23"	17°02'17.02"	WD
401	Mulapeta 2	82°21'44.42"	17°05'21.55"	WD
402	Mulapeta 1	82°36'02.01"	17°06'04.68"	WD
403	Pentakota	82°42'11.08"	17°17'28.00"	WD
404	Rajanagaram	82°36'40.49"	17°17'07.19"	WD
405	Boyapadu	82°44'37.68"	17°20'35.05"	ICOLL
406	Dhandawaka	82°52'12.09"	17°21'47.66"	ICOLL
407	Bangarammapalem	82°59'37.95"	17°25'05.41"	WD
408	Pudimadaka	83°00'27.91"	17°28'32.66"	WD
409	Chippada	83°03'31.61"	17°29'59.42"	ICOLL
410	Dosuru	83°05'31.40"	17°31'23.52"	ICOLL
411	Cheepurupalle	83°10'13.77"	17°32'19.03"	WD
412	Peddapalem	83°17'33.97"	17°34'05.48"	WD
413	Vishaka Port	83°20'35.91"	17°41'17.41"	WD
414	MVP sector	83°21'44.28"	17°44'01.72"	WD
415	Musalayyapalem	83°23'20.98"	17°45'47.52"	Mixed Energy
416	Pedda Rushikonda	83°27'19.63"	17°47'25.58"	WD
417	Kummaripalem	83°33'05.72"	17°54'01.94"	WD
418	Kancheru	83°34'14.44"	17°58'34.36"	WD
419	Konada	83°36'25.93"	18°00'47.02"	Mixed Energy
420	Kollaya valasa 2	83°36'45.31"	18°02'22.63"	ICOLL
421	Kollaya valasa 1	83°37'33.68"	18°02'35.16"	ICOLL
422	Pathiwada	83°39'25.24"	18°03'03.17"	WD
423	Chintapalli	83°40'46.92"	18°04'23.20"	WD
424	NJR puram	83°42'19.66"	18°05'19.07"	WD
425	Tekkai	83°48'24.23"	18°06'16.96"	ICOLL
426	Kuppili	83°56'45.45"	18°09'17.17"	WD
427	Bontala koduru	84°00'28.91"	18°12'48.10"	WD
428	Vastavalasa	84°05'19.85"	18°14'49.52"	WD
429	seepanapeta	84°08'11.50"	18°17'21.41"	WD
430	Kalingapatanam	84°12'59.53"	18°20'41.14"	Mixed Energy
431	Siddibeharakothuru	84°14'12.08"	18°26'22.85"	WD
432	Malagam	84°21'22.45"	18°27'30.60"	ICOLL
433	Devunalthada	84°27'17.06"	18°33'50.33"	WD
434	Vajrapukothuru	84°30'42.22"	18°41'42.58"	WD
435	Metturu	84°34'33.78"	18°45'27.65"	ICOLL
436	Pithali	84°35'23.30"	18°50'48.19"	ICOLL
437	Uppalam	84°41'03.22"	18°52'18.52"	WD
438	Borivenka	84°42'28.98"	18°58'14.70"	WD

439	Pukkalapalyam	84°44'42.58"	19°00'03.78"	ICOLL
440	Donkuru	84°47'16.76"	19°03'02.52"	WD
Odisha coast				
441	Sonpur	84°48'14.39"	19°06'59.72"	WD
442	Alladpur	84°50'10.08"	19°08'49.02"	WD
443	Dhepanuapada	84°55'03.26"	19°11'15.61"	WD
444	Venketraipur	85°04'14.92"	19°15'53.75"	WD
445	Pallibandha	85°31'23.98"	19°22'23.92"	WD
446	Anandapur	85°47'11.82"	19°40'24.92"	WD (H)
447	Baliapanda	85°54'58.26"	19°46'56.96"	WD
448	Bhimapur	86°02'49.31"	19°49'09.48"	WD
449	Khalakata	86°13'44.43"	19°50'55.03"	WD
450	Tandahar	86°22'13.36"	19°54'11.05"	WD
451	Dhanuhar Belari	86°25'40.67"	19°57'38.63"	WD (H)
452	Saharabedi	86°33'53.54"	20°02'47.51"	WD
453	Nuagan	86°42'30.41"	20°12'29.02"	WD
454	Kaudia	86°43'31.01"	20°17'36.17"	WD
455	Baligarh	86°44'24.47"	20°23'40.31"	RD
456	Banapada	86°45'22.12"	20°28'14.99"	WD
457	Joginatha	86°51'13.05"	20°30'25.24"	TD
458	Krishnapriyapur	86°57'38.81"	20°35'14.82"	WD
459	Amarnagar	87°03'38.89"	20°46'43.97"	Mixed Energy
460	Pirikhi	87°07'19.40"	21°28'29.46"	WD
461	Huladigudi	87°12'26.38"	21°30'54.72"	Mixed Energy
462	Jambhirei	87°22'05.64"	21°32'49.38"	TD
463	Chandrabali	87°32'50.10"	21°33'58.93"	WD (H)
West Bengal coast				
464	Begundiha	87°38'27.31"	21°38'01.57"	WD
465	Tajpur	87°45'32.41"	21°38'55.14"	WD
466	Serpujalpai	87°53'22.42"	21°41'41.39"	Mixed Energy
467	Nijkashba	88°00'05.27"	21°47'31.88"	WD
468	Gagra char	88°01'00.28"	21°54'19.98"	WD
469	Jadu bari chak	88°03'09.51"	21°56'30.91"	WD
470	Haldia	88°11'45.07"	22°01'00.95"	WD
471	Durgachak	88°11'45.07"	22°02'19.32"	TD

Table A3.3 Hydrodynamic classification based on Hayes (1979) for all seasons along the Indian coast

No.	Name	Tidal Range (m)	H (m)	H _{SW} (m)	H _{NE} (m)	H _{FW} (m)	HYDRODYNAMIC CLASSIFICATION			
							Annual	SW Monsoon	NE Monsoon	Fair Weather
Gujarat coast										
1	Gandhiya	4.51	DATA NOT AVAILABLE							
2	Kalawad	4.28								
3	Panero	4.25								
4	Mithapur	3.34	1.40	2.18	0.77	1.26	ME (TD)	ME (TD)	TD (High)	ME (TD)
5	Makanpur	3.18	1.42	2.20	0.79	1.26	ME (TD)	ME (WD)	TD (low)	ME (TD)
6	Dwaraka	3.09	1.43	2.22	0.82	1.25	ME (TD)	ME (WD)	TD (low)	ME (TD)
7	Hari kund	3.03	1.43	2.23	0.82	1.25	ME (TD)	ME (WD)	TD (low)	ME (TD)
8	Goji	2.62	1.43	2.24	0.84	1.21	ME (TD)	ME (WD)	TD (low)	ME (TD)
9	Navadra	2.55	1.43	2.24	0.84	1.20	ME (TD)	ME (WD)	TD (low)	ME (TD)
10	Miyani	2.43	1.40	2.19	0.83	1.17	ME (TD)	ME (WD)	ME (TD)	ME (TD)
11	Porbandar	2.21	1.36	2.14	0.82	1.12	ME (TD)	ME (WD)	ME (TD)	ME (TD)
12	Tukada	2.15	1.37	2.15	0.82	1.12	ME (TD)	ME (WD)	ME (TD)	ME (TD)
13	Chikasa	2.09	1.38	2.18	0.84	1.12	ME (TD)	ME (WD)	ME (TD)	ME (TD)
14	Shil	1.96	1.41	2.28	0.85	1.10	ME (TD)	WD	ME (TD)	ME (WD)
15	Ravon	1.86	1.41	2.30	0.85	1.07	ME (TD)	WD	ME (TD)	ME (WD)
16	Prabhas	1.86	1.40	2.29	0.84	1.06	ME (TD)	WD	ME (TD)	ME (WD)
17	Mul Dwarka	1.38	1.34	2.18	0.81	1.01	ME (TD)	WD	ME (WD)	ME (WD)
18	Sarkhadi	2.17	1.27	2.10	0.76	0.95	ME (TD)	ME (WD)	ME (TD)	ME (TD)
19	Diu	2.31	1.22	2.03	0.72	0.91	ME (TD)	ME (WD)	TD (low)	ME (TD)
20	Bandar	2.38	1.20	2.01	0.70	0.90	ME (TD)	ME (WD)	TD (low)	ME (TD)
21	Rajput	2.38	1.21	2.01	0.71	0.90	ME (TD)	ME (WD)	TD (low)	ME (TD)
22	Rajpara	2.65	1.17	1.96	0.68	0.87	ME (TD)	ME (WD)	TD (low)	TD (Low)

23	Jafrabad	3.07	1.11	1.86	0.65	0.83	ME (TD)	ME (TD)	TD (High)	TD (Low)
24	Chanch	3.43	1.06	1.77	0.61	0.79	TD (Low)	ME (TD)	TD (High)	TD (Low)
25	Tena river	6.37	0.86	1.47	0.44	0.68	TD (High)	TD (High)	TD (High)	TD (High)
26	Mindhola river	6.19	0.93	1.63	0.44	0.72	TD (High)	TD (High)	TD (High)	TD (High)
27	Puma river	5.96	0.93	1.65	0.44	0.72	TD (High)	TD (High)	TD (High)	TD (High)
28	Kavai creek	6.11	0.93	1.65	0.43	0.71	TD (High)	TD (High)	TD (High)	TD (High)
29	Ambika river	5.45	0.94	1.66	0.43	0.71	TD (High)	TD (High)	TD (High)	TD (High)
30	Auranga river	5.75	0.94	1.68	0.43	0.71	TD (High)	TD (High)	TD (High)	TD (High)
31	Umarsadi	5.61	0.94	1.67	0.43	0.71	TD (High)	TD (High)	TD (High)	TD (High)
32	Kolak river	5.51	0.94	1.67	0.43	0.71	TD (High)	TD (High)	TD (High)	TD (High)
33	Daman	5.44	0.94	1.66	0.45	0.72	TD (High)	TD (High)	TD (High)	TD (High)
34	Bhathaiya	5.42	0.93	1.65	0.44	0.71	TD (High)	TD (High)	TD (High)	TD (High)
35	Kalu river	5.41	0.94	1.66	0.45	0.72	TD (High)	TD (High)	TD (High)	TD (High)
36	Kalai	5.40	0.96	1.69	0.46	0.73	TD (High)	TD (Low)	TD (High)	TD (High)
37	Kalgam 1	5.40	0.97	1.71	0.47	0.74	TD (High)	TD (Low)	TD (High)	TD (High)
38	Kalgam 2	5.40	0.97	1.70	0.47	0.74	TD (High)	TD (Low)	TD (High)	TD (High)
39	Maroli	5.36	0.97	1.70	0.47	0.73	TD (High)	TD (Low)	TD (High)	TD (High)
40	Varoli river	4.66	1.00	1.76	0.50	0.76	TD (High)	TD (Low)	TD (High)	TD (High)
41	Nargol	4.45	1.03	1.80	0.52	0.78	TD (High)	TD (Low)	TD (High)	TD (High)
42	Deheri	5.10	1.04	1.81	0.52	0.78	TD (High)	TD (Low)	TD (High)	TD (High)
Maharashtra coast										
43	Zai	5.14	1.06	1.84	0.53	0.79	TD (High)	TD (Low)	TD (High)	TD (High)
44	Gholvad	5.09	1.06	1.84	0.53	0.79	TD (High)	TD (Low)	TD (High)	TD (High)
45	Dahanu	4.96	1.08	1.88	0.55	0.81	TD (High)	TD (Low)	TD (High)	TD (High)
46	Navapur	4.84	1.09	1.88	0.57	0.83	TD (High)	TD (Low)	TD (High)	TD (High)
47	Dudh river	4.76	1.10	1.88	0.58	0.84	TD (High)	TD (Low)	TD (High)	TD (High)
48	Darapada	4.74	1.10	1.85	0.59	0.85	TD (High)	TD (Low)	TD (High)	TD (High)

49	Kelwa	4.72	1.10	1.87	0.59	0.85	TD (High)	TD (Low)	TD (High)	TD (High)
50	Bhadve	4.65	1.09	1.80	0.61	0.86	TD (High)	TD (Low)	TD (High)	TD (High)
51	Rajodi	4.66	1.10	1.81	0.61	0.87	TD (High)	TD (Low)	TD (High)	TD (High)
52	Bhuigaon Kh.	4.65	1.10	1.82	0.61	0.87	TD (High)	TD (Low)	TD (High)	TD (High)
53	Vasai	4.62	1.11	1.83	0.62	0.88	TD (High)	TD (Low)	TD (High)	TD (High)
54	Malad	4.59	1.11	1.84	0.62	0.87	TD (High)	TD (Low)	TD (High)	TD (High)
55	Versova	4.58	1.12	1.86	0.62	0.87	TD (High)	TD (Low)	TD (High)	TD (High)
56	Revas	4.25	1.19	2.04	0.64	0.89	TD (Low)	ME (TD)	TD (High)	TD (High)
57	Mandve	4.25	1.19	2.04	0.64	0.89	TD (Low)	ME (TD)	TD (High)	TD (High)
58	Awass	4.23	1.20	2.06	0.65	0.89	TD (Low)	ME (TD)	TD (High)	TD (High)
59	Surekhar	3.70	1.21	2.08	0.65	0.89	TD (Low)	ME (TD)	TD (High)	TD (High)
60	Navgaon	4.14	1.21	2.08	0.65	0.89	TD (Low)	ME (TD)	TD (High)	TD (High)
61	Navapada	4.10	1.22	2.10	0.66	0.91	TD (Low)	ME (TD)	TD (High)	TD (High)
62	Akshi	4.02	1.22	2.10	0.66	0.91	TD (Low)	ME (TD)	TD (High)	TD (High)
63	Bagmala	3.74	1.22	2.10	0.67	0.91	TD (Low)	ME (TD)	TD (High)	TD (High)
64	Revdanda	3.69	1.22	2.10	0.66	0.91	TD (Low)	ME (TD)	TD (High)	TD (Low)
65	Wandeli	3.87	1.22	2.10	0.67	0.91	TD (Low)	ME (TD)	TD (High)	TD (High)
66	Surulpeth	3.72	1.20	2.05	0.65	0.90	TD (Low)	ME (TD)	TD (High)	TD (High)
67	Eakdara	3.67	1.20	2.04	0.65	0.89	TD (Low)	ME (TD)	TD (High)	TD (Low)
68	Rajapuri	3.61	1.20	2.04	0.65	0.89	TD (Low)	ME (TD)	TD (High)	TD (Low)
69	Velas Agar	3.53	1.21	2.07	0.66	0.90	TD (Low)	ME (TD)	TD (High)	TD (Low)
70	Diveagar	3.50	1.21	2.06	0.66	0.90	TD (Low)	ME (TD)	TD (High)	TD (Low)
71	Walavati kh.	3.41	1.21	2.07	0.66	0.90	TD (Low)	ME (TD)	TD (High)	TD (Low)
72	Shrivardhan	3.35	1.21	2.06	0.66	0.90	ME (TD)	ME (TD)	TD (High)	TD (Low)
73	Bankot	3.28	1.21	2.07	0.67	0.90	ME (TD)	ME (TD)	TD (High)	TD (Low)
74	Sakhari	3.22	1.21	2.06	0.67	0.90	ME (TD)	ME (TD)	TD (High)	TD (Low)
75	Koliwada	3.19	1.21	2.06	0.67	0.90	ME (TD)	ME (WD)	TD (High)	TD (Low)

76	Jaikar	3.13	1.21	2.06	0.67	0.90	ME (TD)	ME (WD)	TD (High)	TD (Low)
77	Dabhol	2.87	1.22	2.07	0.68	0.91	ME (TD)	ME (WD)	TD (Low)	TD (Low)
78	Mouje	2.81	1.22	2.07	0.68	0.91	ME (TD)	ME (WD)	TD (Low)	TD (Low)
79	Palshet	2.76	1.22	2.07	0.68	0.91	ME (TD)	ME (WD)	TD (Low)	TD (Low)
80	Musloni	2.71	1.22	2.07	0.67	0.90	ME (TD)	ME (WD)	TD (Low)	ME (TD)
81	Jaigad	2.67	1.22	2.08	0.68	0.91	ME (TD)	ME (WD)	TD (Low)	ME (TD)
82	Bhandrawada	2.62	1.22	2.08	0.67	0.90	ME (TD)	ME (WD)	TD (Low)	ME (TD)
83	Bhandarpule	2.60	1.22	2.09	0.68	0.90	ME (TD)	ME (WD)	TD (Low)	ME (TD)
84	Kajitbhati	2.57	1.23	2.10	0.68	0.90	ME (TD)	ME (WD)	TD (Low)	ME (TD)
85	Sadye	2.55	1.23	2.11	0.68	0.91	ME (TD)	ME (WD)	TD (Low)	ME (TD)
86	Sadamirya	2.55	1.23	2.10	0.68	0.90	ME (TD)	ME (WD)	TD (Low)	ME (TD)
87	Karle	2.51	1.24	2.12	0.69	0.91	ME (TD)	ME (WD)	TD (Low)	ME (TD)
88	Bhatiwadi	2.46	1.25	2.13	0.70	0.92	ME (TD)	ME (WD)	TD (Low)	ME (TD)
89	Khsheli	2.42	1.25	2.13	0.71	0.92	ME (TD)	ME (WD)	TD (Low)	ME (TD)
90	Wadativare	2.37	1.26	2.12	0.71	0.92	ME (TD)	ME (WD)	TD (Low)	ME (TD)
91	Vijayadurg	2.30	1.26	2.12	0.72	0.93	ME (TD)	ME (WD)	TD (Low)	ME (TD)
92	Phanase	2.26	1.27	2.13	0.73	0.93	ME (TD)	ME (WD)	ME (TD)	ME (TD)
93	Padavne	2.24	1.27	2.14	0.73	0.94	ME (TD)	ME (WD)	ME (TD)	ME (TD)
94	Taramumbari	2.22	1.27	2.14	0.74	0.94	ME (WD)	ME (WD)	ME (TD)	ME (TD)
95	Morve	2.19	1.27	2.14	0.74	0.94	ME (WD)	ME (WD)	ME (TD)	ME (TD)
96	Pirawadi	2.16	1.28	2.16	0.75	0.95	ME (WD)	ME (WD)	ME (TD)	ME (TD)
97	Sariekot	2.13	1.30	2.18	0.75	0.95	ME (WD)	ME (WD)	ME (TD)	ME (TD)
98	Malvan	2.13	1.30	2.19	0.76	0.96	ME (WD)	ME (WD)	ME (TD)	ME (TD)
99	Kalethar	2.11	1.31	2.20	0.77	0.96	ME (WD)	ME (WD)	ME (TD)	ME (TD)
100	Bhogwa	2.11	1.31	2.21	0.77	0.96	ME (WD)	ME (WD)	ME (TD)	ME (TD)
101	Shriramwadi	2.10	1.29	2.18	0.75	0.95	ME (WD)	ME (WD)	ME (TD)	ME (TD)
102	Khalchiwadi	2.10	1.29	2.18	0.75	0.95	ME (WD)	ME (WD)	ME (TD)	ME (TD)

103	Kelus 1	2.10	1.29	2.17	0.75	0.94	ME (WD)	ME (WD)	ME (TD)	ME (TD)
104	Kelus 2	2.09	1.29	2.17	0.75	0.94	ME (WD)	ME (WD)	ME (TD)	ME (TD)
105	Dabholi	2.09	1.29	2.17	0.74	0.94	ME (WD)	ME (WD)	ME (TD)	ME (TD)
106	Tank	2.08	1.28	2.17	0.74	0.94	ME (WD)	ME (WD)	ME (TD)	ME (TD)
107	Khalchikar	2.07	1.28	2.16	0.74	0.94	ME (WD)	ME (WD)	ME (TD)	ME (TD)
Goa coast										
108	Tiracol	2.07	1.27	2.14	0.74	0.93	ME (WD)	ME (WD)	ME (TD)	ME (TD)
109	Siolim	2.06	1.26	2.12	0.73	0.93	ME (WD)	ME (WD)	ME (TD)	ME (TD)
110	Baga	2.06	1.26	2.12	0.73	0.93	ME (WD)	ME (WD)	ME (TD)	ME (TD)
111	Mandovi river	2.05	1.26	2.12	0.73	0.93	ME (WD)	ME (WD)	ME (TD)	ME (TD)
112	Zuari estuary	2.05	1.27	2.11	0.75	0.93	ME (WD)	ME (WD)	ME (TD)	ME (TD)
113	Mobor	2.04	1.26	2.11	0.75	0.93	ME (WD)	ME (WD)	ME (TD)	ME (TD)
114	Cola	2.04	1.27	2.12	0.76	0.94	ME (WD)	ME (WD)	ME (TD)	ME (TD)
115	Anjadip	2.03	1.27	2.12	0.76	0.93	ME (WD)	ME (WD)	ME (TD)	ME (TD)
116	Canacona 2	2.03	1.27	2.13	0.76	0.93	ME (WD)	ME (WD)	ME (TD)	ME (TD)
117	Canacona 1	2.03	1.27	2.12	0.76	0.93	ME (WD)	ME (WD)	ME (TD)	ME (TD)
118	Mashem	2.03	1.28	2.14	0.76	0.94	ME (WD)	ME (WD)	ME (TD)	ME (TD)
Karnataka coast										
119	Karwar	2.03	1.28	2.15	0.76	0.94	ME (WD)	ME (WD)	ME (TD)	ME (TD)
120	Chendia	2.02	1.24	2.09	0.73	0.91	ME (WD)	ME (WD)	ME (TD)	ME (TD)
121	Todur	2.02	1.23	2.07	0.73	0.90	ME (WD)	ME (WD)	ME (TD)	ME (TD)
122	Belekeri	2.03	1.24	2.07	0.73	0.90	ME (WD)	ME (WD)	ME (TD)	ME (TD)
123	Ankola	2.02	1.23	2.07	0.73	0.90	ME (WD)	ME (WD)	ME (TD)	ME (TD)
124	Belambar	2.02	1.23	2.07	0.73	0.90	ME (WD)	ME (WD)	ME (TD)	ME (TD)
125	Manjaguni	2.02	1.23	2.07	0.72	0.90	ME (WD)	ME (WD)	ME (TD)	ME (TD)
126	Tadadi Port	2.01	1.22	2.05	0.72	0.90	ME (WD)	ME (WD)	ME (TD)	ME (TD)
127	Alvekodi 2	2.00	1.22	2.04	0.72	0.89	ME (WD)	ME (WD)	ME (TD)	ME (TD)

128	Karki	1.98	1.23	2.06	0.73	0.91	ME (WD)	ME (WD)	ME (TD)	ME (TD)
129	Nakhuda	1.96	1.23	2.05	0.73	0.91	ME (WD)	ME (WD)	ME (TD)	ME (TD)
130	Alvekodi 1	1.92	1.23	2.06	0.73	0.91	ME (WD)	ME (WD)	ME (TD)	ME (TD)
131	Jali	1.90	1.22	2.05	0.72	0.90	ME (WD)	ME (WD)	ME (TD)	ME (TD)
132	Mavakurve	1.89	1.25	2.10	0.74	0.92	ME (WD)	WD	ME (TD)	ME (TD)
133	Hadin	1.89	1.22	2.04	0.72	0.90	ME (WD)	WD	ME (TD)	ME (TD)
134	Alivey Gadde	1.88	1.22	2.04	0.72	0.90	ME (WD)	WD	ME (TD)	ME (TD)
135	Paduvari	1.85	1.20	2.01	0.71	0.89	ME (WD)	WD	ME (TD)	ME (TD)
136	Koderi	1.84	1.21	2.03	0.71	0.89	ME (WD)	WD	ME (TD)	ME (TD)
137	Gangoli	1.77	1.22	2.04	0.72	0.90	ME (WD)	WD	ME (TD)	ME (TD)
138	Kundapura	1.68	1.25	2.08	0.75	0.92	ME (WD)	WD	ME (TD)	ME (WD)
139	Malpe	1.62	1.27	2.10	0.77	0.94	ME (WD)	WD	ME (TD)	ME (WD)
140	Kaup	1.58	1.26	2.08	0.77	0.94	ME (WD)	WD	ME (TD)	ME (WD)
141	Nadsal	1.55	1.25	2.04	0.76	0.94	ME (WD)	WD	ME (TD)	ME (WD)
142	Hejamadi	1.55	1.25	2.05	0.76	0.94	ME (WD)	WD	ME (TD)	ME (WD)
143	NMPT	1.52	1.25	2.03	0.77	0.94	ME (WD)	WD	ME (TD)	ME (WD)
144	Netravati & Gurupur	1.50	1.24	2.02	0.77	0.94	ME (WD)	WD	ME (TD)	ME (WD)
145	Kanwatheertha	1.48	1.25	2.03	0.78	0.95	ME (WD)	WD	ME (TD)	ME (WD)
Kerala coast										
146	Hosabettu	1.47	1.26	2.05	0.78	0.96	ME (WD)	WD	ME (WD)	ME (WD)
147	Bandiyod	1.45	1.28	2.06	0.80	0.96	ME (WD)	WD	ME (WD)	ME (WD)
148	Shiriya	1.45	1.28	2.06	0.80	0.97	ME (WD)	WD	ME (WD)	ME (WD)
149	Puthur	1.44	1.28	2.07	0.80	0.97	ME (WD)	WD	ME (WD)	ME (WD)
150	Thalangara	1.43	1.28	2.07	0.80	0.97	ME (WD)	WD	ME (WD)	ME (WD)
151	chembirika	1.43	1.29	2.07	0.81	0.97	ME (WD)	WD	ME (WD)	ME (WD)
152	Thekkekara	1.42	1.29	2.07	0.81	0.97	ME (WD)	WD	ME (WD)	ME (WD)
153	Tharavadu	1.42	1.29	2.08	0.81	0.98	ME (WD)	WD	ME (WD)	ME (WD)

154	Kadapuram	1.41	1.28	2.06	0.80	0.97	WD	WD	ME (WD)	ME (WD)
155	Kaithakkad	1.40	1.29	2.08	0.82	0.98	WD	WD	ME (WD)	ME (WD)
156	Madayi	1.36	1.29	2.08	0.81	0.97	WD	WD	ME (WD)	ME (WD)
157	Azhikkal	1.36	1.28	2.07	0.81	0.97	WD	WD	ME (WD)	ME (WD)
158	Thottada	1.34	1.26	2.04	0.80	0.95	WD	WD	ME (WD)	ME (WD)
159	Nadal	1.33	1.25	2.01	0.79	0.94	WD	WD	ME (WD)	ME (WD)
160	Dharmadom	1.33	1.25	2.02	0.79	0.94	WD	WD	ME (WD)	ME (WD)
161	Koduvalli	1.33	1.24	2.00	0.78	0.93	WD	WD	ME (WD)	ME (WD)
162	Mahe	1.32	1.22	1.97	0.77	0.92	WD	WD	ME (WD)	ME (WD)
163	Olavilam	1.32	1.18	1.91	0.75	0.89	WD	WD	ME (WD)	ME (WD)
164	Chombala	1.31	1.21	1.95	0.76	0.91	WD	WD	ME (WD)	ME (WD)
165	Madappally	1.31	1.21	1.95	0.76	0.91	WD	WD	ME (WD)	ME (WD)
166	Iringal	1.30	1.19	1.92	0.76	0.90	WD	WD	ME (WD)	ME (WD)
167	Nandi	1.29	1.18	1.91	0.75	0.88	WD	WD	ME (WD)	ME (WD)
168	Puthiyapurayil	1.28	1.18	1.91	0.74	0.88	WD	WD	ME (WD)	ME (WD)
169	Elathur	1.27	1.17	1.89	0.74	0.87	WD	WD	ME (WD)	ME (WD)
170	Thekepuram	1.25	1.18	1.92	0.75	0.88	WD	WD	ME (WD)	ME (WD)
171	Beypore	1.24	1.18	1.92	0.75	0.88	WD	WD	ME (WD)	ME (WD)
172	Kudalundi	1.23	1.18	1.92	0.75	0.88	WD	WD	ME (WD)	ME (WD)
173	Chiramangalam	1.22	1.18	1.91	0.75	0.88	WD	WD	ME (WD)	ME (WD)
174	Malappuram	1.19	1.20	1.93	0.76	0.89	WD	WD	ME (WD)	ME (WD)
175	Veliancode	1.18	1.20	1.93	0.77	0.89	WD	WD	ME (WD)	ME (WD)
176	Nallamkallu 2	1.17	1.21	1.94	0.78	0.90	WD	WD	ME (WD)	ME (WD)
177	Nallamkallu 1	1.17	1.21	1.94	0.78	0.90	WD	WD	ME (WD)	ME (WD)
178	Chettuva	1.16	1.22	1.95	0.79	0.91	WD	WD	ME (WD)	ME (WD)
179	Nattika	1.14	1.21	1.93	0.79	0.90	WD	WD	ME (WD)	ME (WD)
180	Muriyamthodu	1.14	1.21	1.93	0.79	0.90	WD	WD	ME (WD)	ME (WD)

181	Palapetty	1.14	1.20	1.92	0.79	0.90	WD	WD	ME (WD)	ME (WD)
182	Chamakkala	1.13	1.20	1.92	0.79	0.90	WD	WD	ME (WD)	ME (WD)
183	Vazhiyambalam	1.13	1.20	1.92	0.79	0.90	WD	WD	ME (WD)	ME (WD)
184	Perinjanam	1.13	1.20	1.91	0.78	0.90	WD	WD	ME (WD)	ME (WD)
185	Ambalanada	1.13	1.19	1.91	0.78	0.89	WD	WD	ME (WD)	ME (WD)
186	Munambam	1.13	1.19	1.91	0.78	0.89	WD	WD	ME (WD)	ME (WD)
187	Kochi	1.11	1.21	1.93	0.80	0.90	WD	WD	ME (WD)	ME (WD)
188	Andhakaranazhy	1.05	1.24	1.95	0.83	0.93	WD	WD	ME (WD)	WD
189	Arthunkal	1.04	1.25	1.96	0.85	0.95	WD	WD	ME (WD)	WD
190	Kackary	1.04	1.25	1.96	0.85	0.95	WD	WD	ME (WD)	WD
191	Perunneermangalam	1.04	1.26	1.97	0.86	0.95	WD	WD	ME (WD)	WD
192	Janakshemam	1.03	1.26	1.96	0.86	0.95	WD	WD	ME (WD)	WD
193	Valavanadu 2	1.03	1.26	1.97	0.86	0.96	WD	WD	ME (WD)	WD
194	Valavanadu 1	1.03	1.26	1.96	0.86	0.96	WD	WD	ME (WD)	WD
195	Pollethai	1.03	1.26	1.96	0.86	0.96	WD	WD	WD	WD
196	Kattoor	1.03	1.26	1.96	0.86	0.96	WD	WD	WD	WD
197	Omanapuzha	1.03	1.26	1.96	0.86	0.96	WD	WD	WD	WD
198	Poomkavu	1.03	1.26	1.96	0.87	0.96	WD	WD	WD	WD
199	Padinjare	1.03	1.26	1.96	0.87	0.96	WD	WD	WD	WD
200	Eravukadu	1.03	1.26	1.96	0.87	0.96	WD	WD	WD	WD
201	Punnapra 2	1.03	1.27	1.97	0.88	0.97	WD	WD	WD	WD
202	Punnapra 1	1.03	1.28	1.97	0.88	0.97	WD	WD	WD	WD
203	Thottapally lake	1.00	1.30	1.99	0.90	0.99	WD	WD	WD	WD
204	Azheekkal	0.97	1.33	2.02	0.94	1.02	WD	WD	WD	WD
205	Kandathil	0.95	1.36	2.05	0.97	1.05	WD	WD	WD	WD
206	Neendakara	0.94	1.36	2.05	0.98	1.06	WD	WD	WD	WD
207	Paravur lake	0.92	1.35	2.00	0.98	1.06	WD	WD	WD	WD

208	Kappil	0.92	1.34	1.98	0.98	1.06	WD	WD	WD	WD
209	Madanvila	0.91	1.32	1.92	0.99	1.06	WD	WD	WD	WD
210	Veli	0.90	1.35	1.95	1.00	1.08	WD	WD	WD	WD
211	Pachalloor	0.89	1.37	1.99	1.02	1.09	WD	WD	WD	WD
212	Kochupally	0.88	1.36	1.97	1.01	1.09	WD	WD	WD	WD
213	Paruthiyoor	0.88	1.35	1.95	1.00	1.08	WD	WD	WD	WD
Tamil Nadu coast										
214	Erayumanthurai	0.863	1.39	2.01	1.03	1.11	WD	WD	WD	WD
215	Sambasivapuram	0.852	1.43	2.06	1.08	1.15	WD	WD	WD	WD
216	Kadiyapattanam	0.850	1.44	2.06	1.09	1.16	WD	WD	WD	WD
217	Rajakamangalam Thurai	0.849	1.40	1.98	1.09	1.15	WD	WD	WD	WD
218	Manakudi	1.149	1.39	1.91	1.10	1.15	WD	WD	WD	WD
219	Kovalam	0.848	1.39	1.90	1.10	1.15	WD	WD	WD	WD
220	SRNP	0.848	1.17	1.53	0.97	1.02	WD	WD	WD	WD
221	Thottavilai	0.845	1.20	1.54	1.01	1.05	WD	WD	WD	WD
222	Manapad	0.841	1.19	1.52	1.01	1.04	WD	WD	WD	WD
223	Govindamal colony	0.842	1.08	1.36	0.93	0.95	WD	WD	WD	WD
224	Veerapandianpattinam	0.842	1.06	1.33	0.91	0.93	WD	WD	WD	WD
225	Mangaladevi	0.842	1.05	1.31	0.91	0.93	WD	WD	WD	WD
226	Punnaikayal	0.841	1.02	1.26	0.89	0.90	WD	WD	WD	WD
227	Veppalodai	0.851	0.88	1.09	0.75	0.78	WD	WD	WD	WD
228	Sippikulam	0.854	0.87	1.07	0.75	0.78	WD	WD	WD	WD
229	Vaippar	0.854	0.88	1.09	0.75	0.79	WD	WD	WD	WD
230	Velayudhapuram 2	0.861	0.87	1.09	0.75	0.78	WD	WD	WD	WD
231	Velayudhapuram 1	0.864	0.88	1.09	0.75	0.79	WD	WD	WD	WD
232	Vembar	0.882	0.88	1.10	0.74	0.79	WD	WD	WD	WD

233	Mookaiyur	0.908	0.91	1.16	0.76	0.82	WD	WD	WD	WD
234	Valinokkam	0.960	0.95	1.21	0.80	0.85	WD	WD	WD	WD
235	Sethu karai	1.033	1.03	1.33	0.85	0.91	WD	WD	ME (WD)	WD
236	Muthariyarnagar	1.051	1.03	1.32	0.85	0.92	WD	WD	ME (WD)	WD
237	Mandapam	1.082	1.00	1.30	0.82	0.89	WD	WD	ME (WD)	ME (WD)
238	Atrangarai	1.154	0.52	0.56	0.53	0.47	ME (TD)	ME (TD)	ME (TD)	ME (TD)
239	Pudhuvalasai	1.194	0.50	0.53	0.52	0.46	ME (TD)	ME (TD)	ME (TD)	ME (TD)
240	Thiruppalaikudi	1.316	0.53	0.57	0.54	0.49	ME (TD)	ME (TD)	ME (TD)	ME (TD)
241	Karankadu	1.386	0.50	0.51	0.51	0.47	ME (TD)	ME (TD)	ME (TD)	ME (TD)
242	Alikkudi	1.407	0.57	0.61	0.57	0.53	ME (TD)	ME (TD)	ME (TD)	ME (TD)
243	Pudupattinam	1.407	0.57	0.61	0.57	0.53	ME (TD)	ME (TD)	ME (TD)	ME (TD)
244	Velangudi	1.441	0.57	0.60	0.57	0.53	ME (TD)	ME (TD)	ME (TD)	ME (TD)
245	Muthuramalinga pattinam	1.440	0.57	0.61	0.58	0.54	ME (TD)	ME (TD)	ME (TD)	ME (TD)
246	odavayal	1.431	0.58	0.61	0.58	0.54	ME (TD)	ME (TD)	ME (TD)	ME (TD)
247	Kaliyanagari	1.416	0.59	0.62	0.59	0.55	ME (TD)	ME (TD)	ME (TD)	ME (TD)
248	S.P.Pattinam 2	1.402	0.59	0.62	0.59	0.55	ME (TD)	ME (TD)	ME (TD)	ME (TD)
249	S.P.Pattinam 1	1.402	0.59	0.62	0.59	0.55	ME (TD)	ME (TD)	ME (TD)	ME (TD)
250	Muthukuda	1.392	0.60	0.63	0.60	0.56	ME (TD)	ME (TD)	ME (TD)	ME (TD)
251	Arsanagaripattinam	1.395	0.60	0.64	0.60	0.57	ME (TD)	ME (TD)	ME (TD)	ME (TD)
252	Embakkottai	1.382	0.60	0.64	0.60	0.57	ME (TD)	ME (TD)	ME (TD)	ME (TD)
253	Gopalapattinam	1.635	0.61	0.64	0.60	0.57	ME (TD)	ME (TD)	ME (TD)	ME (TD)
254	Sannathi	1.376	0.62	0.66	0.61	0.58	ME (TD)	ME (TD)	ME (TD)	ME (TD)
255	Kottaippattannam	1.355	0.63	0.67	0.62	0.59	ME (TD)	ME (WD)	ME (TD)	ME (TD)
256	Tandalai	0.869	0.65	0.70	0.64	0.62	ME (WD)	ME (WD)	ME (WD)	ME (WD)
257	Manamelkudi 2	0.997	0.62	0.66	0.60	0.60	ME (WD)	ME (WD)	ME (WD)	ME (WD)
258	Manamelkudi 1	1.279	0.59	0.63	0.57	0.57	ME (TD)	ME (TD)	ME (TD)	ME (TD)
259	Mumpalai 5	1.430	0.62	0.66	0.59	0.60	ME (TD)	ME (TD)	ME (TD)	ME (TD)

260	Mumpalai 4	1.267	0.62	0.66	0.59	0.60	ME (TD)	ME (WD)	ME (TD)	ME (TD)
261	Mumpalai 3	1.337	0.61	0.66	0.59	0.59	ME (TD)	ME (TD)	ME (TD)	ME (TD)
262	Mumpalai 2	1.386	0.61	0.66	0.59	0.59	ME (TD)	ME (TD)	ME (TD)	ME (TD)
263	Mumpalai 1	1.489	0.61	0.66	0.59	0.59	ME (TD)	ME (TD)	ME (TD)	ME (TD)
264	Kandanivayal	1.266	0.62	0.66	0.59	0.60	ME (TD)	ME (TD)	ME (TD)	ME (TD)
265	Subramanyapuram	1.715	0.62	0.66	0.59	0.60	ME (TD)	ME (TD)	ME (TD)	ME (TD)
266	Ravuttanvayal	1.363	0.62	0.66	0.59	0.60	ME (TD)	ME (TD)	ME (TD)	ME (TD)
267	Sembiyan 3	1.403	0.60	0.65	0.57	0.59	ME (TD)	ME (TD)	ME (TD)	ME (TD)
268	Sembiyan 2	1.740	0.60	0.65	0.57	0.59	ME (TD)	ME (TD)	ME (TD)	ME (TD)
269	Sembiyan 1	1.487	0.60	0.65	0.57	0.59	ME (TD)	ME (TD)	ME (TD)	ME (TD)
270	Manthirippattinam 2	1.487	0.61	0.66	0.58	0.59	ME (TD)	ME (TD)	ME (TD)	ME (TD)
271	Tiruvathevan 3	1.215	0.61	0.66	0.58	0.59	ME (TD)	ME (WD)	ME (TD)	ME (TD)
272	Tiruvathevan 2	1.624	0.61	0.66	0.58	0.59	ME (TD)	ME (TD)	ME (TD)	ME (TD)
273	Tiruvathevan 1	1.105	0.60	0.65	0.57	0.58	ME (WD)	ME (WD)	ME (WD)	ME (WD)
274	Palliya kulam	1.105	0.60	0.65	0.57	0.58	ME (WD)	ME (WD)	ME (WD)	ME (WD)
275	Manthiripattinam 1	1.105	0.60	0.65	0.57	0.58	ME (WD)	ME (WD)	ME (WD)	ME (WD)
276	Perumagalur	1.105	0.61	0.65	0.57	0.59	ME (WD)	ME (WD)	ME (WD)	ME (WD)
277	Adaikkathevan	1.105	0.62	0.67	0.58	0.60	ME (WD)	ME (WD)	ME (WD)	ME (WD)
278	Villunivayal	1.105	0.66	0.72	0.63	0.64	ME (WD)	ME (WD)	ME (WD)	ME (WD)
279	Ravuthanvayal	1.105	0.66	0.72	0.63	0.64	ME (WD)	ME (WD)	ME (WD)	ME (WD)
280	Marakkavalasai	1.105	0.66	0.72	0.63	0.64	ME (WD)	ME (WD)	ME (WD)	ME (WD)
281	Nayagathivayal	1.105	0.66	0.72	0.63	0.64	ME (WD)	ME (WD)	ME (WD)	ME (WD)
282	Manora	1.105	0.66	0.72	0.63	0.64	ME (WD)	ME (WD)	ME (WD)	ME (WD)
283	Sarabendrarajan pattinam	1.013	0.66	0.72	0.63	0.64	ME (WD)	ME (WD)	ME (WD)	ME (WD)
284	Kallivayal	1.109	0.66	0.72	0.63	0.64	ME (WD)	ME (WD)	ME (WD)	ME (WD)
285	Keezhathottam	1.078	0.66	0.72	0.63	0.64	ME (WD)	ME (WD)	ME (WD)	ME (WD)
286	Thuraikkadu	0.868	0.66	0.72	0.63	0.63	ME (WD)	ME (WD)	ME (WD)	ME (WD)

287	Kodiyakadu	0.984	0.74	0.80	0.72	0.69	ME (WD)	ME (WD)	ME (WD)	ME (WD)
288	Kodikkarai	0.751	0.84	0.89	0.84	0.78	WD	WD	WD	WD
289	Vedaranyam	0.894	0.83	0.88	0.83	0.78	WD	WD	WD	WD
290	Madavilagam	0.927	0.83	0.88	0.83	0.78	WD	WD	WD	WD
291	Thopputhurai	0.922	0.82	0.86	0.83	0.78	WD	WD	WD	WD
292	Naluvethapathi	0.861	0.82	0.84	0.84	0.78	WD	WD	WD	WD
293	Vanvanmahadevi	0.870	0.82	0.83	0.84	0.78	WD	WD	WD	WD
294	Vettaikarairuppu	0.880	0.81	0.82	0.84	0.78	WD	WD	WD	WD
295	pudupalli	0.895	0.81	0.82	0.84	0.77	WD	WD	WD	WD
296	Vizhunthamavadi	0.929	0.81	0.82	0.84	0.78	WD	WD	WD	WD
297	Tirupoondi	0.951	0.81	0.82	0.84	0.78	WD	WD	WD	ME (WD)
298	Velankanni	0.994	0.81	0.82	0.85	0.78	ME (WD)	ME (WD)	WD	ME (WD)
299	Nagapattinam	0.987	0.81	0.80	0.84	0.78	ME (WD)	ME (WD)	WD	ME (WD)
300	Thethinagar	0.973	0.81	0.80	0.85	0.78	ME (WD)	ME (WD)	WD	ME (WD)
301	keezhaiyur 2	0.959	0.83	0.82	0.86	0.80	WD	WD	WD	ME (WD)
302	Keezhaiyur 1	0.870	0.81	0.80	0.85	0.78	WD	WD	WD	WD
303	Bharathi nagar	0.868	0.82	0.81	0.86	0.79	WD	WD	WD	WD
304	Akkampettai	0.870	0.83	0.83	0.86	0.80	WD	WD	WD	WD
305	Chandirapady	0.872	0.83	0.82	0.86	0.80	WD	WD	WD	WD
306	Kittiyandiyur	0.881	0.83	0.83	0.87	0.80	WD	WD	WD	WD
307	Veepanchery	0.886	0.84	0.84	0.87	0.81	WD	WD	WD	WD
308	Vanagiri	0.887	0.84	0.84	0.88	0.81	WD	WD	WD	WD
309	Pompuhar	0.895	0.84	0.84	0.88	0.81	WD	WD	WD	WD
310	Thirumullaivasal	0.906	0.85	0.85	0.89	0.82	WD	WD	WD	WD
311	Chinnakottaimedu	0.906	0.86	0.85	0.89	0.83	WD	WD	WD	WD
312	Pazhaiyar	0.906	0.87	0.87	0.90	0.84	WD	WD	WD	WD
313	Chinna vaikaal	0.902	0.88	0.88	0.91	0.85	WD	WD	WD	WD

314	Ariyakoshti	0.902	0.88	0.87	0.90	0.85	WD	WD	WD	WD
315	Pudukuppam	0.902	0.87	0.86	0.90	0.85	WD	WD	WD	WD
316	Samiaar	0.902	0.87	0.86	0.90	0.85	WD	WD	WD	WD
317	Cuddalore	0.944	0.89	0.90	0.91	0.87	WD	WD	WD	WD
318	Devanampattinam	0.902	0.90	0.91	0.92	0.88	WD	WD	WD	WD
319	Pudukuppam	0.960	0.91	0.91	0.92	0.88	WD	WD	WD	WD
320	Subauppalavadi	0.944	0.91	0.92	0.92	0.88	WD	WD	WD	WD
321	Aladimedu	0.944	0.93	0.95	0.93	0.90	WD	WD	WD	WD
322	C veerampattinam	0.960	0.93	0.96	0.93	0.91	WD	WD	WD	WD
323	Puducherry	0.974	0.94	0.96	0.94	0.91	WD	WD	WD	WD
324	Muthaialpet	0.995	0.95	0.98	0.94	0.92	WD	WD	WD	WD
325	Vembalur	1.043	1.01	1.07	0.98	0.98	WD	WD	WD	WD
326	Odiyur	1.085	1.01	1.08	0.98	0.98	WD	WD	WD	WD
327	KPK	1.072	1.04	1.11	0.99	1.00	WD	WD	WD	WD
328	Sudurangapattinam	1.058	1.04	1.12	1.00	1.00	WD	WD	WD	WD
329	Kalpakkam	1.115	1.04	1.13	1.00	1.01	WD	WD	WD	WD
330	Kokkilamedu	1.239	1.06	1.14	1.01	1.01	ME (WD)	WD	ME (WD)	ME (WD)
331	Padur	1.239	1.05	1.13	1.00	1.01	ME (WD)	WD	ME (WD)	ME (WD)
332	Srinivasapuram	1.217	1.12	1.42	0.87	1.06	WD	WD	ME (WD)	WD
333	Sathya Nagar	1.217	1.13	1.44	0.88	1.07	WD	WD	ME (WD)	WD
334	Athipatti	1.217	1.14	1.46	0.88	1.08	WD	WD	ME (WD)	WD
Andhra Pradesh coast										
335	Karimanal	1.22	0.70	1.05	0.96	0.86	ME (WD)	ME (WD)	ME (WD)	ME (WD)
336	Shar	1.22	0.96	1.06	0.96	0.86	ME (WD)	ME (WD)	ME (WD)	ME (WD)
337	Chinnathota	1.22	0.96	1.06	0.97	0.86	ME (WD)	ME (WD)	ME (WD)	ME (WD)
338	Nalagamula	1.22	0.96	1.05	0.96	0.86	ME (WD)	ME (WD)	ME (WD)	ME (WD)
339	Konduru	1.19	0.93	1.02	0.94	0.85	ME (WD)	ME (WD)	ME (WD)	ME (WD)

340	Swanamukhi River	1.19	0.92	0.99	0.92	0.84	ME (WD)	ME (WD)	ME (WD)	ME (WD)
341	Kothapatnam	1.19	0.91	0.98	0.91	0.83	ME (WD)	ME (WD)	ME (WD)	ME (WD)
342	Srinivasa	1.18	0.91	0.98	0.91	0.83	ME (WD)	ME (WD)	ME (WD)	ME (WD)
343	Gunnampadia 2	1.20	0.90	0.97	0.90	0.83	ME (WD)	ME (WD)	ME (WD)	ME (WD)
344	Gunnampadia 1	1.20	0.90	0.97	0.90	0.83	ME (WD)	ME (WD)	ME (WD)	ME (WD)
345	Gopalapuram 2	1.20	0.91	0.98	0.91	0.83	ME (WD)	ME (WD)	ME (WD)	ME (WD)
346	Gopalapuram 1	1.20	0.93	1.02	0.94	0.84	ME (WD)	ME (WD)	ME (WD)	ME (WD)
347	Nelaturu	1.19	0.94	1.03	0.94	0.85	ME (WD)	ME (WD)	ME (WD)	ME (WD)
348	Pathapalem	0.80	0.95	1.05	0.95	0.85	WD	WD	WD	WD
349	Koruturu	1.20	0.96	1.05	0.96	0.86	ME (WD)	WD	ME (WD)	ME (WD)
350	Ramudupalem	1.20	0.96	1.06	0.97	0.86	ME (WD)	WD	ME (WD)	ME (WD)
351	Utukuru	1.21	0.96	1.05	0.96	0.86	ME (WD)	ME (WD)	ME (WD)	ME (WD)
352	Ramathirtham	1.20	0.94	1.03	0.95	0.85	ME (WD)	ME (WD)	ME (WD)	ME (WD)
353	Isakapalle	1.20	0.92	0.99	0.92	0.84	ME (WD)	ME (WD)	ME (WD)	ME (WD)
354	Juvvaladinne	1.20	0.90	0.98	0.91	0.83	ME (WD)	ME (WD)	ME (WD)	ME (WD)
355	Ramayapatnam 2	1.22	0.86	0.92	0.85	0.80	ME (WD)	ME (WD)	ME (WD)	ME (WD)
356	Ramayapatnam 1	1.22	0.86	0.92	0.85	0.80	ME (WD)	ME (WD)	ME (WD)	ME (WD)
357	Karedu	1.25	0.86	0.93	0.85	0.80	ME (WD)	ME (WD)	ME (WD)	ME (WD)
358	Pakala	1.26	0.85	0.92	0.83	0.79	ME (WD)	ME (WD)	ME (WD)	ME (WD)
359	Anantavaram 2	1.27	0.85	0.92	0.83	0.79	ME (WD)	ME (WD)	ME (WD)	ME (WD)
360	Anantavaram 1	1.27	0.85	0.92	0.83	0.78	ME (WD)	ME (WD)	ME (WD)	ME (WD)
361	Peddapattapalam	1.27	0.85	0.92	0.83	0.78	ME (WD)	ME (WD)	ME (WD)	ME (WD)
362	Motumala	1.31	0.91	1.03	0.90	0.81	ME (WD)	ME (WD)	ME (WD)	ME (WD)
363	Chintayigari palem	0.83	0.91	1.03	0.89	0.81	WD	WD	WD	WD
364	Kanuparthi	1.30	0.90	1.02	0.88	0.80	ME (WD)	ME (WD)	ME (WD)	ME (WD)
365	Peddaganjam	1.31	0.90	1.02	0.87	0.80	ME (WD)	ME (WD)	ME (WD)	ME (WD)
366	Pallepalem	1.31	0.89	1.02	0.86	0.79	ME (WD)	ME (WD)	ME (WD)	ME (WD)

367	Pullaripalem 3	1.30	0.87	1.00	0.84	0.77	ME (WD)	ME (WD)	ME (WD)	ME (WD)
368	Pullaripalem 2	1.30	0.87	1.00	0.84	0.78	ME (WD)	ME (WD)	ME (WD)	ME (WD)
369	Pullaripalem 1	1.30	0.87	1.01	0.84	0.78	ME (WD)	ME (WD)	ME (WD)	ME (WD)
370	Katari palem	1.31	0.89	1.04	0.86	0.78	ME (WD)	ME (WD)	ME (WD)	ME (WD)
371	Krupa nagar	1.30	0.89	1.05	0.85	0.77	ME (WD)	ME (WD)	ME (WD)	ME (WD)
372	Pandurangapuram	1.30	0.90	1.07	0.86	0.77	ME (WD)	ME (WD)	ME (WD)	ME (WD)
373	East Gollapallem	1.30	0.89	1.08	0.85	0.74	ME (WD)	ME (WD)	ME (WD)	ME (WD)
374	Gokarnamatam	1.29	0.90	1.09	0.86	0.73	ME (WD)	ME (WD)	ME (WD)	ME (WD)
375	Dindiadavala	1.29	0.95	1.16	0.91	0.78	ME (WD)	WD	ME (WD)	ME (WD)
376	Haripuram	1.29	0.96	1.17	0.92	0.78	ME (WD)	WD	ME (WD)	ME (WD)
377	LVD	1.28	1.06	1.29	1.02	0.85	ME (WD)	WD	ME (WD)	ME (WD)
378	Elachetladibba	1.28	1.08	1.33	1.04	0.88	ME (WD)	WD	ME (WD)	ME (WD)
379	RKP	1.27	1.09	1.34	1.05	0.89	ME (WD)	WD	ME (WD)	ME (WD)
380	Ramakrishna puram 2	1.26	1.09	1.32	1.06	0.88	ME (WD)	WD	ME (WD)	ME (WD)
381	Ramakrishna puram 1	1.26	1.09	1.32	1.06	0.88	ME (WD)	WD	ME (WD)	ME (WD)
382	Palakayatippa	1.27	1.08	1.31	1.05	0.88	ME (WD)	WD	ME (WD)	ME (WD)
383	Machilipatnam	1.26	1.03	1.23	1.01	0.84	ME (WD)	WD	ME (WD)	ME (WD)
384	polatitippa	1.26	1.01	1.21	1.00	0.83	ME (WD)	WD	ME (WD)	ME (WD)
385	Chlilikalapudi	1.26	0.99	1.18	0.98	0.82	ME (WD)	WD	ME (WD)	ME (WD)
386	Kara agraham	1.25	0.97	1.17	0.93	0.79	ME (WD)	WD	ME (WD)	ME (WD)
387	Gokavaram	1.26	0.94	1.14	0.89	0.78	ME (WD)	WD	ME (WD)	ME (WD)
388	Tallapalem	1.26	0.93	1.13	0.89	0.77	ME (WD)	WD	ME (WD)	ME (WD)
389	Kanuru	1.26	0.93	1.13	0.89	0.77	ME (WD)	WD	ME (WD)	ME (WD)
390	kruthivenu	1.26	0.95	1.18	0.89	0.78	ME (WD)	WD	ME (WD)	ME (WD)
391	Peda Gollapalem	1.27	1.01	1.28	0.94	0.81	ME (WD)	WD	ME (WD)	ME (WD)
392	Chinna Gollapalem	1.27	1.03	1.29	0.97	0.82	ME (WD)	WD	ME (WD)	ME (WD)

393	Marritippa	1.30	1.13	1.43	1.07	0.88	ME (WD)	WD	ME (WD)	ME (WD)
394	Odalaravu	1.32	1.15	1.48	1.06	0.90	ME (WD)	WD	ME (WD)	ME (WD)
395	Komaragiri patanam	1.33	1.16	1.48	1.09	0.90	ME (WD)	WD	ME (WD)	ME (WD)
396	Gachakayala pora	1.35	1.17	1.51	1.09	0.91	ME (WD)	WD	ME (WD)	ME (WD)
397	Kothapalem	1.40	1.22	1.58	1.13	0.94	ME (WD)	WD	ME (WD)	ME (WD)
398	Gadimoga	1.42	1.01	1.22	1.00	0.81	ME (WD)	ME (WD)	ME (WD)	ME (WD)
399	Sasikanth Nagar	1.46	0.97	1.15	0.99	0.78	ME (WD)	ME (WD)	ME (WD)	ME (WD)
400	Nemam	1.46	0.97	1.14	0.99	0.78	ME (WD)	ME (WD)	ME (WD)	ME (WD)
401	Mulapeta 2	1.46	1.02	1.24	1.01	0.81	ME (WD)	ME (WD)	ME (WD)	ME (WD)
402	Mulapeta 1	1.46	1.03	1.25	1.01	0.82	ME (WD)	ME (WD)	ME (WD)	ME (WD)
403	Pentakota	1.47	1.11	1.42	1.02	0.87	ME (WD)	WD	ME (WD)	ME (WD)
404	Rajanagaram	1.47	1.12	1.44	1.03	0.88	ME (WD)	WD	ME (WD)	ME (WD)
405	Boyapadu	1.47	1.13	1.46	1.03	0.88	ME (WD)	WD	ME (WD)	ME (WD)
406	Dhandawaka	1.48	1.13	1.47	1.04	0.88	ME (WD)	WD	ME (WD)	ME (WD)
407	Bangarammapalem	1.49	1.16	1.52	1.05	0.89	ME (WD)	WD	ME (WD)	ME (WD)
408	Pudimadaka	1.51	1.18	1.56	1.07	0.90	ME (WD)	WD	ME (WD)	ME (WD)
409	Chippada	1.51	1.18	1.56	1.07	0.90	ME (WD)	WD	ME (WD)	ME (WD)
410	Dosuru	1.51	1.19	1.57	1.07	0.91	ME (WD)	WD	ME (WD)	ME (WD)
411	Cheepurupalle	1.52	1.19	1.58	1.08	0.91	ME (WD)	WD	ME (WD)	ME (WD)
412	Peddapalem	1.53	1.20	1.60	1.08	0.91	ME (WD)	WD	ME (WD)	ME (WD)
413	Vishaka Port	1.56	1.19	1.59	1.07	0.91	ME (WD)	WD	ME (WD)	ME (WD)
414	MVP sector	1.57	1.18	1.58	1.07	0.90	ME (WD)	WD	ME (WD)	ME (WD)
415	Musalayyapalem	1.59	1.18	1.57	1.06	0.90	ME (WD)	WD	ME (WD)	ME (WD)
416	Pedda Rushikonda	1.59	1.17	1.56	1.06	0.89	ME (WD)	WD	ME (WD)	ME (WD)
417	Kummaripalem	1.61	1.14	1.52	1.03	0.87	ME (WD)	WD	ME (WD)	ME (WD)
418	Kancheru	1.63	1.13	1.50	1.02	0.87	ME (WD)	ME (WD)	ME (WD)	ME (WD)
419	Konada	1.64	1.13	1.50	1.02	0.87	ME (WD)	ME (WD)	ME (WD)	ME (WD)

420	Kollaya valasa 2	1.65	1.13	1.50	1.02	0.87	ME (WD)	ME (WD)	ME (WD)	ME (WD)
421	Kollaya valasa 1	1.65	1.13	1.51	1.02	0.87	ME (WD)	ME (WD)	ME (WD)	ME (WD)
422	Pathiwada	1.65	1.14	1.51	1.02	0.87	ME (WD)	ME (WD)	ME (WD)	ME (WD)
423	Chintapalli	1.67	1.14	1.52	1.02	0.87	ME (WD)	ME (WD)	ME (WD)	ME (WD)
424	NJR puram	1.67	1.14	1.52	1.03	0.87	ME (WD)	ME (WD)	ME (WD)	ME (WD)
425	Tekkai	1.67	1.15	1.53	1.03	0.88	ME (WD)	ME (WD)	ME (WD)	ME (WD)
426	Kuppili	1.69	1.17	1.58	1.04	0.89	ME (WD)	ME (WD)	ME (WD)	ME (WD)
427	Bontala koduru	1.72	1.20	1.63	1.06	0.90	ME (WD)	ME (WD)	ME (WD)	ME (WD)
428	Vastavalasa	1.74	1.21	1.66	1.07	0.91	ME (WD)	ME (WD)	ME (WD)	ME (WD)
429	Seepanapeta	1.75	1.21	1.65	1.07	0.91	ME (WD)	ME (WD)	ME (WD)	ME (WD)
430	Kalingapatanam	1.76	1.20	1.63	1.06	0.90	ME (WD)	ME (WD)	ME (WD)	ME (WD)
431	Siddibeharakothuru	1.78	1.17	1.58	1.03	0.88	ME (WD)	ME (WD)	ME (WD)	ME (WD)
432	Malagam	1.78	1.17	1.58	1.03	0.88	ME (WD)	ME (WD)	ME (WD)	ME (WD)
433	Devunalthada	1.80	1.17	1.60	1.04	0.88	ME (WD)	ME (WD)	ME (WD)	ME (WD)
434	Vajrapukothuru	1.82	1.15	1.56	1.02	0.87	ME (WD)	ME (WD)	ME (WD)	ME (WD)
435	Metturu	1.82	1.15	1.56	1.02	0.87	ME (WD)	ME (WD)	ME (WD)	ME (WD)
436	Pithali	1.83	1.12	1.52	0.99	0.85	ME (WD)	ME (WD)	ME (TD)	ME (WD)
437	Uppalam	1.84	1.11	1.50	0.99	0.85	ME (WD)	ME (WD)	ME (TD)	ME (WD)
438	Borivenka	0.97	1.12	1.52	0.98	0.85	WD	WD	WD	WD
439	Pukkalapalyam	1.86	1.13	1.54	0.99	0.86	ME (WD)	ME (WD)	ME (TD)	ME (WD)
440	Donkuru	1.86	1.14	1.56	1.00	0.86	ME (WD)	ME (WD)	ME (TD)	ME (WD)
Odisha coast										
441	Sonpur	1.92	1.13	1.55	0.90	1.19	ME(WD)	ME(WD)	ME (TD)	ME(WD)
442	Alladpur	1.92	1.13	1.56	0.89	1.19	ME(WD)	ME(WD)	ME (TD)	ME(WD)
443	Dhepanuapada	1.93	1.14	1.56	0.87	1.19	ME(WD)	ME(WD)	ME (TD)	ME(WD)
444	Venketraipur	1.95	1.14	1.56	0.84	1.18	ME(WD)	ME(WD)	ME (TD)	ME(WD)
445	Pallibandha	1.92	1.14	1.55	0.82	1.17	ME(WD)	ME(WD)	ME (TD)	ME(WD)

446	Anandapur	1.97	1.15	1.58	0.82	1.18	ME(WD)	ME(WD)	ME (TD)	ME(WD)
447	Baliapanda	2.01	1.16	1.59	0.82	1.19	ME(WD)	ME(WD)	ME (TD)	ME(WD)
448	Bhimapur	2.03	1.17	1.62	0.83	1.21	ME(WD)	ME(WD)	ME (TD)	ME(WD)
449	Khalakata	2.05	1.18	1.63	0.83	1.22	ME(WD)	ME(WD)	ME (TD)	ME(WD)
450	Tandahar	2.06	1.17	1.59	0.82	1.19	ME(WD)	ME(WD)	ME (TD)	ME(WD)
451	Dhanuhar Belari	2.07	1.15	1.56	0.80	1.17	ME (TD)	ME(WD)	ME (TD)	ME(WD)
452	Saharabedi	2.05	1.17	1.58	0.81	1.18	ME(WD)	ME(WD)	ME (TD)	ME (TD)
453	Nuagan	2.10	1.13	1.51	0.78	1.14	ME (TD)	ME(WD)	ME (TD)	ME (TD)
454	Kaudia	2.16	1.12	1.51	0.78	1.14	ME (TD)	ME(WD)	ME (TD)	ME (TD)
455	Baligarh	2.28	1.11	1.48	0.78	1.12	ME (TD)	ME(WD)	ME (TD)	ME (TD)
456	Banapada	2.36	1.13	1.53	0.79	1.15	ME (TD)	ME(WD)	ME (TD)	ME (TD)
457	joginatha	2.33	1.02	1.37	0.73	1.04	ME (TD)	ME (TD)	Barrier	ME (TD)
458	Krishnapriyapur	2.41	0.84	1.15	0.63	0.87	ME (TD)	ME (TD)	TD(Low)	ME (TD)
459	Amarnagar	2.89	0.84	1.15	0.63	0.87	Barrier	ME (TD)	TD(HIGH)	TD(Low)
460	Pirikhi	3.95	0.87	1.19	0.64	0.90	TD(HIGH)	TD(Low)	TD(HIGH)	TD(HIGH)
461	Huladigudi	4.05	0.92	1.25	0.66	0.94	TD(HIGH)	TD(Low)	TD(HIGH)	TD(HIGH)
462	Jambhirei	3.98	0.98	1.35	0.69	1.01	TD(HIGH)	Barrier	TD(HIGH)	TD(HIGH)
463	Chandrabali	3.80	0.97	1.34	0.69	1.00	TD(Low)	Barrier	TD(HIGH)	TD(Low)
West Bengal coast										
464	Begundiha	3.41	0.97	1.34	0.69	1.00	TD(Low)	ME (TD)	TD(HIGH)	TD(Low)
465	Tajpur	1.69	0.97	1.34	0.69	1.00	ME(WD)	ME(WD)	ME (TD)	ME(WD)
466	Serpujalpai	1.78	0.97	1.34	0.69	1.00	ME(WD)	ME(WD)	ME (TD)	ME(WD)
467	Nijkashba	1.70	0.97	1.34	0.69	1.00	ME(WD)	ME(WD)	ME (TD)	ME(WD)
468	Gagra char	1.73	0.97	1.34	0.69	1.00	ME(WD)	ME(WD)	ME (TD)	ME(WD)
469	Jadu bari chak	2.36	0.97	1.34	0.69	1.00	ME (TD)	ME (TD)	Barrier	ME (TD)
470	Haldia	2.84	0.97	1.34	0.69	1.00	ME (TD)	ME (TD)	TD(Low)	Barrier
471	Durgachak	3.30	0.97	1.34	0.69	1.00	Barrier	ME (TD)	TD(HIGH)	TD(Low)

Table A3.4 Classification of based on dimensionless parameters without wave period (Vu, 2013)

Inlet No	Inlet Name	Entrance location		A _b km ²	R _{to} m	P ML	H _s m	Q _{tide} m ³ /s	Q _f m ³ /s	$\sqrt{gH^5}$ m ³ /s	$\frac{Q_f}{\sqrt{gH^5}}$ -	$\frac{Q_{tide}}{\sqrt{gH^5}}$ -
		Lat	Long									
26	Mindhola river	72.69	21.07	2.37	6.19	14690.54	0.93	1032.2	0.59	2.6	0.23	397.19
27	Puma river	72.78	20.91	10.52	5.96	62643.79	0.93	4401.53	1.37	2.64	0.52	1667.62
33	Daman	72.83	20.41	1.15	5.44	6231.38	0.94	437.84	1.57	2.69	0.58	162.58
50	Bhadve	72.79	19.49	32.59	4.65	1.52E+05	1.09	10654.06	2.65	3.87	0.68	2750.58
57	Mandve	72.96	18.84	30.58	4.25	1.3E+05	1.19	9122.73	1.45	4.84	0.30	1884.08
64	Revdanda	72.93	18.54	11.96	3.69	44127	1.22	3100.49	0.108	5.17	0.02	599.73
87	Bhatiwadi	73.30	16.99	2.94	2.51	7374	1.24	518.12	1.213	5.38	0.23	96.26
108	Tiracol inlet	15.75	73.74	4.25	2.07	8800.55	1.27	618.35	5.21	5.71	0.91	108.34
109	Siolim inlet	15.72	73.75	9.08	2.06	18735.17	1.26	1316.39	18.66	5.58	3.34	235.88
110	Baga inlet	15.61	73.79	0.09	2.06	192.73	1.26	13.54	3.69	5.59	0.66	2.42
111	Mandovi river	15.56	73.82	57.65	2.05	1.18E+05	1.26	8289.84	113.52	5.59	20.31	1483.27
112	Zuari estuary	15.49	73.95	32.70	2.05	66921.98	1.27	4702.13	71.26	5.67	12.58	830.03
113	Mobor inlet	15.43	73.98	1.91	2.04	3896.89	1.26	273.81	22.02	5.62	3.92	48.70
114	Cola inlet	15.14	74.02	0.21	2.04	436.07	1.27	30.64	10.88	5.73	1.90	5.35
117	Canacona inlet 1	14.99	74.05	0.08	2.03	154.48	1.27	10.85	16.35	5.72	2.86	1.90
118	Mashem inlet	14.98	74.12	0.30	2.03	609.28	1.28	42.81	5.93	5.81	1.02	7.36
119	Karwar	14.84	74.16	12.38	2.03	25072.08	1.28	1761.64	3.92	5.84	0.67	301.86
120	Kelaginakeri	14.75	74.23	0.57	2.02	1152.70	1.24	80.99	0.03	5.39	0.005	15.03
121	Kantrivada Gudda	14.74	74.26	0.12	2.02	234.80	1.23	16.50	0.02	5.29	0.004	3.12
122	Belekeri	14.71	74.28	0.67	2.03	1357.58	1.24	95.39	0.17	5.32	0.033	17.94
123	Ankola	14.66	74.28	0.22	2.02	444.39	1.23	31.22	0.03	5.30	0.006	5.89
124	Belamber	14.65	74.29	0.28	2.02	555.32	1.23	39.02	0.02	5.29	0.003	7.38

125	Manjaguni	14.60	74.36	4.41	2.02	8919.67	1.23	626.72	3.07	5.26	0.585	119.23
126	Tadri	14.52	74.39	15.70	2.01	31620	1.22	2221.72	1.09	5.17	0.211	429.74
127	Alvekodi 2	14.42	74.42	0.34	2.00	680.21	1.22	47.79	0.03	5.12	0.005	9.34
128	Honaver	14.30	74.47	13.31	1.98	26362.37	1.23	1852.30	2.35	5.27	0.445	351.44
128_1	Manki	14.19	74.50	0.04	1.96	78.37	1.23	5.51	0.01	5.28	0.002	1.04
129	Navayatkeri	14.10	74.48	0.05	1.94	89.24	1.23	6.27	0.01	5.26	0.002	1.19
130	Alvekodi 1	14.03	74.52	1.55	1.92	2975.33	1.23	209.06	0.27	5.30	0.052	39.46
131	Jali	13.98	74.53	0.05	1.90	91.37	1.22	6.42	0.01	5.19	0.001	1.24
132	Mavakurve	13.97	74.57	0.27	1.89	501.98	1.25	35.27	0.05	5.50	0.008	6.41
133	Hadin	13.95	74.59	0.04	1.89	67.86	1.22	4.77	0.01	5.13	0.003	0.93
133_1	Gorta	13.92	74.58	0.04	1.88	78.96	1.22	5.55	0.01	5.15	0.003	1.08
134	Alvegadde	13.92	74.61	0.31	1.88	581.41	1.22	40.85	0.07	5.12	0.014	7.97
135	Paduvari	13.87	74.62	1.20	1.85	2224.67	1.20	156.31	0.09	4.98	0.018	31.42
136	Koderi	13.79	74.67	0.70	1.84	1284.51	1.21	90.25	0.08	5.03	0.015	17.93
137	Gangoli	13.63	74.70	21.00	1.77	37074.47	1.22	2604.96	1.21	5.18	0.233	502.53
138	Kundapura	13.45	74.74	15.40	1.68	25805.53	1.25	1813.17	0.00	5.48	0.001	330.60
138_1	Badanidiyoor	13.37	74.69	0.02	1.65	36.30	1.26	2.55	0.00	5.58	0.001	0.46
139	Malpe	13.35	74.70	5.40	1.62	8755.48	1.27	615.19	1.22	5.69	0.214	108.15
140	Kaup	13.22	74.77	0.02	1.58	37.99	1.26	2.67	0.37	5.62	0.065	0.48
141	Nadsal	13.11	74.78	0.28	1.55	435.20	1.25	30.58	0.00	5.46	0.001	5.60
142	Hejamadi	13.08	74.81	3.82	1.55	5905.89	1.25	414.96	0.02	5.49	0.004	75.57
144	Gurpur & Netravati	12.85	74.86	18.82	1.50	28152.29	1.24	1978.06	3.34	5.41	0.617	365.42
145	Kanwatheertha	12.76	74.89	0.20	1.48	295.03	1.25	20.73	0.05	5.51	0.008	3.76
150	Thalangara	75.00	12.48	4.61	1.43	6594.88	1.28	463.38	2.13	5.84	0.36	79.28
162	Mahe	11.70	75.53	1.17	1.32	1548.69	1.22	108.81	0.13	5.15	0.025	21.13
166	Iringal	11.56	75.59	3.43	1.3	4458.98	1.19	313.30	0.41	4.84	0.84	64.75
169	Elathur	11.35	75.73	7.33	1.27	9306.25	1.17	653.88	0.20	4.64	0.042	140.99

170	Thekupuram	11.23	75.78	0.36	1.25	451.71	1.18	31.73	0.96	4.74	0.203	6.70
171	Beypore	11.12	75.83	9.22	1.24	11428.47	1.18	802.99	0.39	4.74	0.083	169.50
174	Malappuram	10.79	75.19	13.37	1.19	15915.06	1.2	1118.23	2.02	4.94	0.409	226.33
178	Chettuva	10.51	76.04	8.35	1.16	9689.55	1.22	680.816	0.53	5.15	0.103	132.22
186	Munambam	76.23	10.18	10.76	1.13	12118	1.19	851.51	12.507	4.86	2.57	175.31
203	Thottapally lake	76.46	9.31	1.35	1	1349.26	1.33	94.8	4.27	6.35	0.67	14.93
206	Neendakara	76.65	8.93	51.39	0.94	48386	1.36	3399.8	1.04	6.8	0.15	499.84
214	Erayumanthurai	77.25	8.24	0.55	0.86	470.71	1.39	33.07	0.21	7.07	0.03	4.68
218	Manakudi	77.52	8.09	0.40	1.15	463.40	1.39	32.56	0.14	7.1	0.02	4.58
226	Punnaikayal	78.13	8.64	5.54	0.84	4656	1.02	327.14	0.34	3.29	0.10	99.40
229	Vaippar	78.30	9.00	0.50	0.85	423.15	0.88	29.73	0.02	2.28	0.01	13.07
301	Keezhaiyur 2	79.85	10.84	0.27	0.87	236	0.83	16.57	0.05	1.97	0.03	8.43
304	Akkampettai	79.85	10.96	0.02	0.87	134.37	0.83	0.94	0.04	1.97	0.02	0.48
312	Pazhaiyar	79.83	11.36	11.13	0.91	10087	0.87	708.76	7.35	2.21	3.32	320.53
314	Ariyakoshti	79.78	11.50	4.65	0.9	4193.64	0.88	294.66	5.53	2.28	2.43	129.50
320	Subauppalavadi	79.80	11.77	1.69	0.94	1596.89	0.91	112.2	0.2	2.47	0.08	45.35
322	C veerampattinam	79.83	11.88	2.72	0.96	2610	0.93	183.38	1.48	2.61	0.57	70.20
328	Sudurangapattinam	80.15	12.47	29.93	0.9	26935	1.04	1892.53	0.11	3.45	0.03	547.70
340	Swanamukhi river	80.15	14.07	1.42	1.19	1686.48	0.92	118.5	0.35	2.53	0.14	46.76
351	Utukuru	80.21	14.59	6.43	1.21	7748	0.96	544.4	0.4	2.81	0.14	193.83
363	Chintayigari palem	80.24	15.54	1.85	0.83	1532.23	0.91	107.66	0.55	2.48	0.22	43.35
377	LVD	80.93	15.71	42.38	1.28	54120	1.06	3802.62	5.1	3.59	1.42	1058.31
378	Elachetladibba	81.07	15.72	63.57	1.28	81180	1.08	5703.92	7.63	3.83	1.99	1488.79
427	Bontala koduru	84.01	18.21	1.58	1.72	2715.19	1.2	190.78	2.35	4.94	0.48	38.64
430	Kalingapatanam	84.22	18.34	2.32	1.77	4091	1.2	287.45	2.04	4.92	0.41	58.43
445	Pallibandha	85.52	19.37	0.41	1.9	784.84	1.19	55.15	1.34	4.83	0.28	11.41

Table A3.5 Classification of tidal inlets based on dimensionless parameters with the wave period

Inlet No	Inlet Name	Entrance location		H _s	T _m	Q _{tide}	Q _f	$\frac{Q_{tide}}{g^{1.75}H^{1.25}T^{2.5}}$	$\frac{Q_f}{g^{1.75}H^{1.25}T^{2.5}}$
		Lat	Long	m	s	m ³ /s	m ³ /s	[-]	[-]
26	Mindhola river	21.07	72.69	0.93	5.8	1032.20	0.59	0.2565	0.000147
27	Puma river	20.91	72.78	0.93	5.75	4401.53	1.37	1.1179	0.000349
33	Daman	20.41	72.83	0.94	5.79	437.84	1.57	0.1078	0.000387
50	Bhadve	19.49	72.79	1.09	5.56	10654.06	2.65	2.4134	0.000601
57	Mandve	18.84	72.96	1.19	6.21	9122.73	1.45	1.4046	0.000224
64	Revdanda	18.54	72.93	1.22	6.25	3100.49	1.31	0.4554	0.000192
87	Bhatiwadi	16.99	73.30	1.24	6.79	518.12	1.21	0.0606	0.000142
108	Tiracol inlet	15.75	73.74	1.27	6.93	618.35	5.21	0.0667	0.000562
109	Siolim inlet	15.72	73.75	1.26	6.87	1316.39	18.66	0.1467	0.002078
110	Baga inlet	15.61	73.79	1.26	6.85	13.54	3.69	0.0015	0.000414
111	Mandovi river	15.56	73.82	1.26	6.85	8289.84	113.52	0.9291	0.012723
112	Zuari estuary	15.49	73.95	1.27	6.84	4702.13	71.26	0.5254	0.007962
113	Mobor inlet	15.43	73.98	1.26	6.83	273.81	22.02	0.0308	0.002479
114	Cola inlet	15.14	74.02	1.27	6.88	30.64	10.88	0.0034	0.001190
117	Canacona inlet 1	14.99	74.05	1.27	6.88	10.85	16.35	0.0012	0.001789
118	Mashem inlet	14.98	74.12	1.28	6.91	42.81	5.93	0.0046	0.000639
119	Karwar	14.84	74.16	1.28	6.93	1761.64	3.92	0.1875	0.000417
120	Kelaginakeri	14.75	74.23	1.24	6.85	80.99	0.03	0.0093	0.000003
121	Kantrivada Gudda	14.74	74.26	1.23	6.82	16.50	0.02	0.0019	0.000003
122	Belekeri	14.71	74.28	1.24	6.83	95.39	0.17	0.0110	0.000020
123	Ankola	14.66	74.28	1.23	6.83	31.22	0.03	0.0036	0.000004
124	Belamber	14.65	74.29	1.23	6.82	39.02	0.02	0.0045	0.000002

125	Manjaguni	14.60	74.36	1.23	6.83	626.72	3.07	0.0731	0.000358
126	Tadri	14.52	74.39	1.22	6.81	2221.72	1.09	0.2625	0.000129
127	Alvekodi 2	14.42	74.42	1.22	6.81	47.79	0.03	0.0057	0.000003
128	Honaver	14.30	74.47	1.23	6.85	1852.30	2.35	0.2137	0.000271
128_1	Manki	14.19	74.50	1.23	6.86	5.51	0.01	0.0006	0.000001
129	Navayatkeri	14.10	74.48	1.23	6.85	6.27	0.01	0.0007	0.000001
130	Alvekodi 1	14.03	74.52	1.23	6.83	209.06	0.27	0.0242	0.000032
131	Jali	13.98	74.53	1.22	6.79	6.42	0.01	0.0008	0.000001
132	Mavakurve	13.97	74.57	1.25	6.93	35.27	0.05	0.0039	0.000005
133	Hadin	13.95	74.59	1.22	6.78	4.77	0.01	0.0006	0.000002
133_1	Gorta	13.92	74.58	1.22	6.78	5.55	0.01	0.0007	0.000002
134	Alvegadde	13.92	74.61	1.22	6.78	40.85	0.07	0.0049	0.000009
135	Paduvari	13.87	74.62	1.20	6.73	156.31	0.09	0.0194	0.000011
136	Koderi	13.79	74.67	1.21	6.75	90.25	0.08	0.0110	0.000009
137	Gangoli	13.63	74.70	1.22	6.81	2604.96	1.21	0.3074	0.000143
138	Kundapura	13.45	74.74	1.25	6.94	1813.17	0.00	0.1988	0.000001
138_1	Badanidiyoor	13.37	74.69	1.26	6.98	2.55	0.00	0.0003	0.000001
139	Malpe	13.35	74.70	1.27	7.01	615.19	1.22	0.0646	0.000128
140	Kaup	13.22	74.77	1.26	6.98	2.67	0.37	0.0003	0.000039
141	Nadsal	13.11	74.78	1.25	6.93	30.58	0.00	0.0034	0.000001
142	Hejamadi	13.08	74.81	1.25	6.94	414.96	0.02	0.0455	0.000003
144	Gurpur & Netravati	12.85	74.86	1.24	6.90	1978.06	3.34	0.2211	0.000373
145	Kanwatheertha	12.76	74.89	1.25	6.95	20.73	0.05	0.0023	0.000005
150	Thalangara	12.48	75.00	1.28	7.12	463.38	2.13	0.0463	0.000212
162	Mahe	11.70	75.53	1.22	7.09	108.82	0.13	0.0117	0.000014
166	Iringal	11.56	75.59	1.19	7.05	313.30	0.41	0.0351	0.000046
169	Elathur	11.35	75.73	1.17	7.01	653.88	0.20	0.0760	0.000023

170	Thekupuram	11.23	75.78	1.18	7.04	31.74	0.96	0.0036	0.000109
171	Beypore	11.12	75.83	1.18	7.05	803.00	0.39	0.0910	0.000044
174	Malappuram	10.79	75.19	1.2	7.06	1118.24	2.02	0.1236	0.000224
178	Chettuva	10.51	76.04	1.22	7.18	680.82	0.53	0.0707	0.000055
186	Munambam	10.18	76.23	1.19	6.98	851.51	12.51	0.0979	0.001438
203	Thottapally lake	9.31	76.46	1.33	7.39	94.80	4.27	0.0082	0.000370
206	Neendakara	8.93	76.65	1.36	7.6	3399.80	1.04	0.2673	0.000081
214	Erayumanthurai	8.24	77.25	1.39	7.63	33.07	0.21	0.0025	0.000016
218	Manakudi	8.09	77.52	1.39	7.67	32.56	0.14	0.0024	0.000011
226	Punnaikayal	8.64	78.13	1.02	6.09	327.14	0.34	0.0641	0.000067
229	Vaippar	9.00	78.30	0.88	6.13	29.73	0.02	0.0069	0.000005
301	Keezhaiyur	10.84	79.85	0.83	4.94	16.57	0.05	0.0071	0.000021
304	Akkampettai	10.96	79.85	0.83	4.94	0.94	0.04	0.0004	0.000017
312	Pazhaiyar	11.36	79.83	0.87	5.18	708.76	7.35	0.2540	0.002634
314	Ariyakoshti	11.50	79.78	0.88	5.27	294.66	5.53	0.0997	0.001871
320	Subauppalavadi	11.77	79.80	0.91	5.36	112.20	0.20	0.0349	0.000062
322	C veerampattinam	11.88	79.83	0.93	5.42	183.38	1.48	0.0540	0.000436
328	Sudurangapattinam	12.47	80.15	1.04	5.69	1892.53	0.11	0.4291	0.000025
340	Swanamukhi river	14.07	80.15	0.92	5.73	118.50	0.35	0.0308	0.000091
351	Utukuru	14.59	80.21	0.96	5.77	544.40	0.40	0.1317	0.000097
363	Chintayigari palem	15.54	80.24	0.91	6.07	107.66	0.55	0.0245	0.000125
377	LVD	15.71	80.93	1.06	5.99	3802.62	5.10	0.7404	0.000993
378	Elachetladibba	15.72	81.07	1.08	6.07	5703.92	7.63	1.0495	0.001404
427	Bontala Koduru	18.21	84.01	1.2	6.28	190.78	2.35	0.0283	0.000348
430	Kalingapatanam	18.34	84.22	1.2	6.32	287.45	2.04	0.0419	0.000297
445	Pallibandha	19.37	85.52	1.19	6.4	55.15	1.34	0.0079	0.000191

Appendix - IV

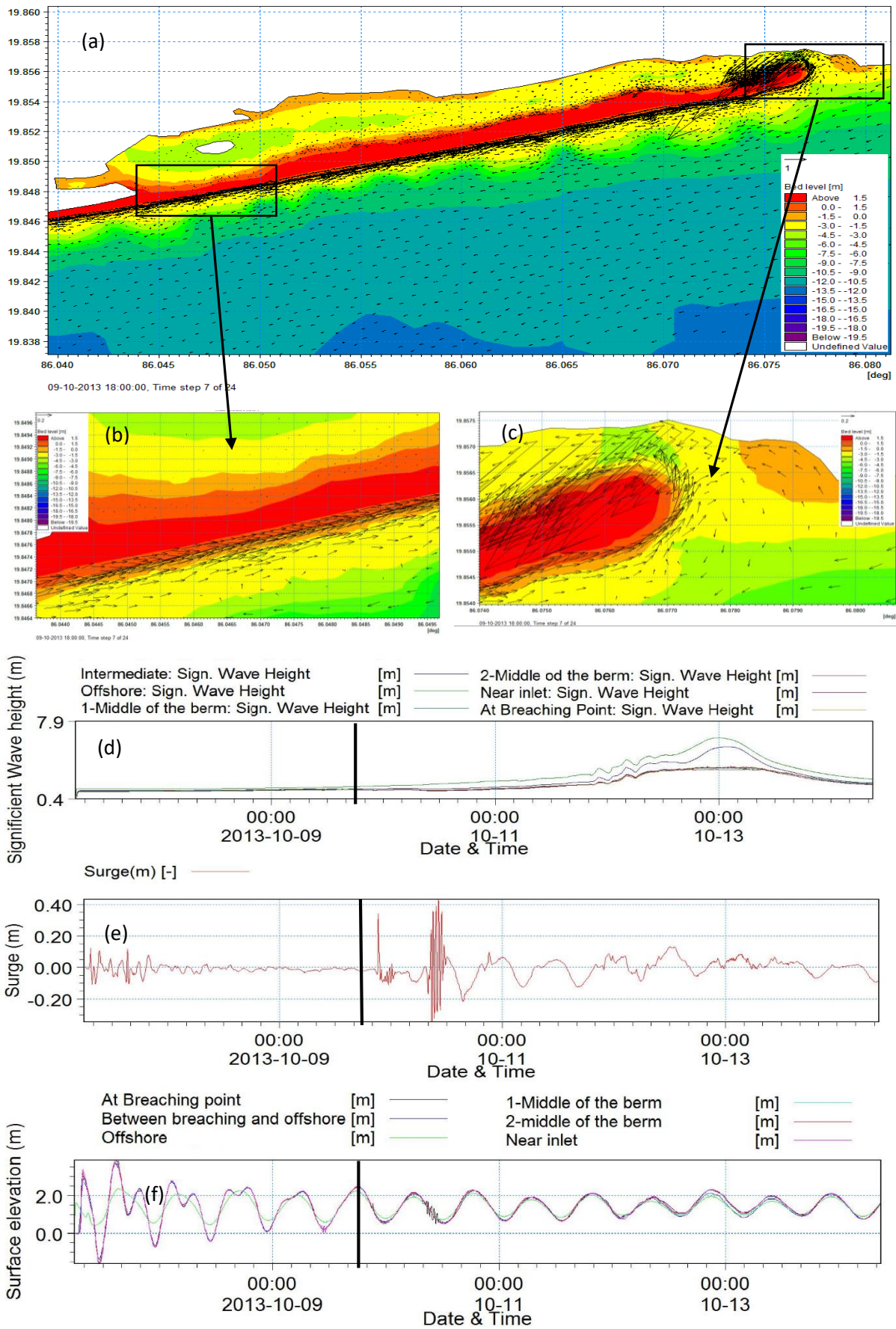


Figure A4.1 At 09-10-2013 18:00:00 time step the Figure shows vector plot (a) whole model domain, (b) near breach, (c) near inlet with time series plots of (d) significant Wave height, (e) surge and (f) surface elevation at various locations

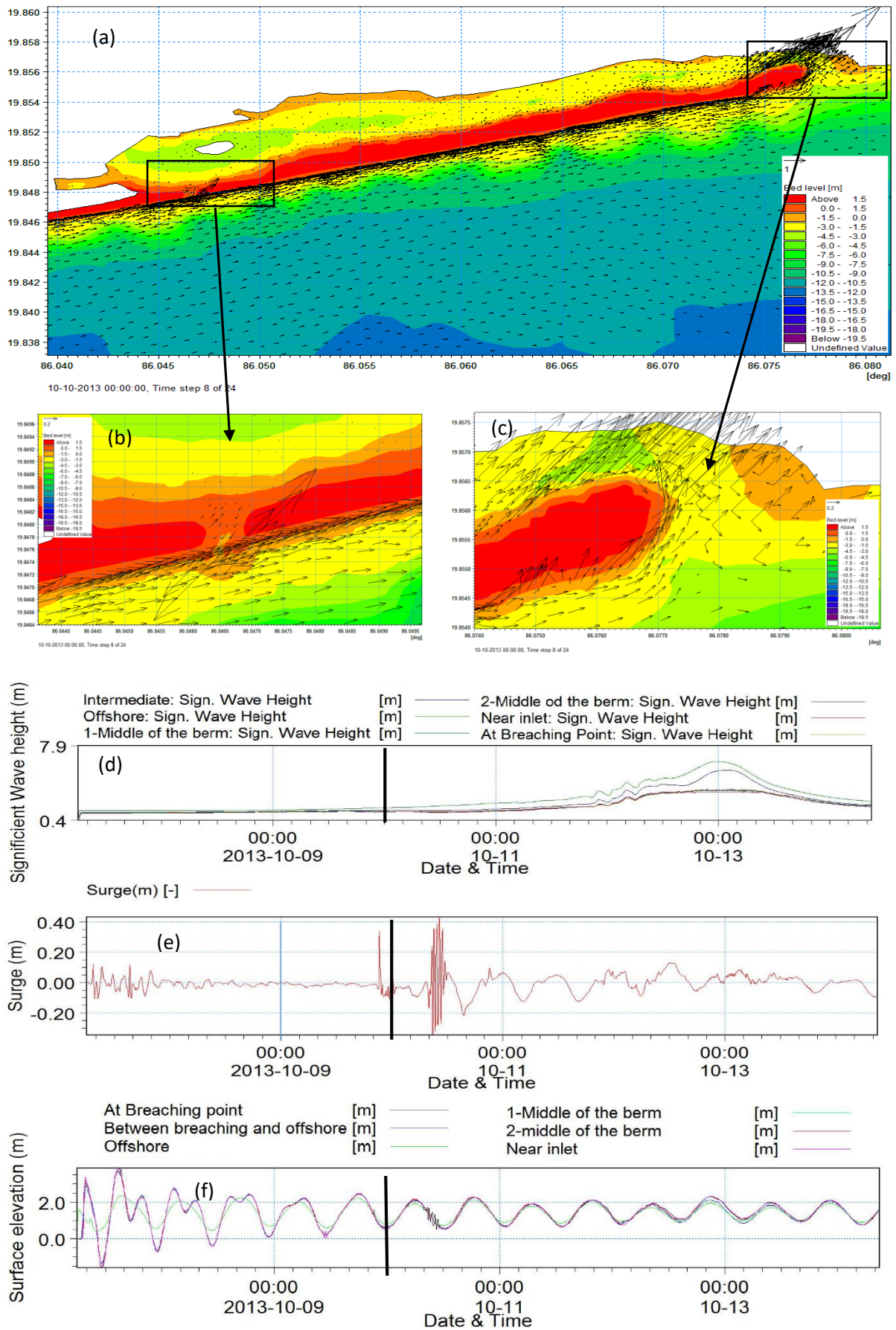


Figure A4.2 At 10-10-2013 00:00:00 time step the Figure shows vector plot (a) whole model domain, (b) near breach, (c) near inlet with time series plots of (d) significant Wave height, (e) surge and (f) surface elevation at various locations

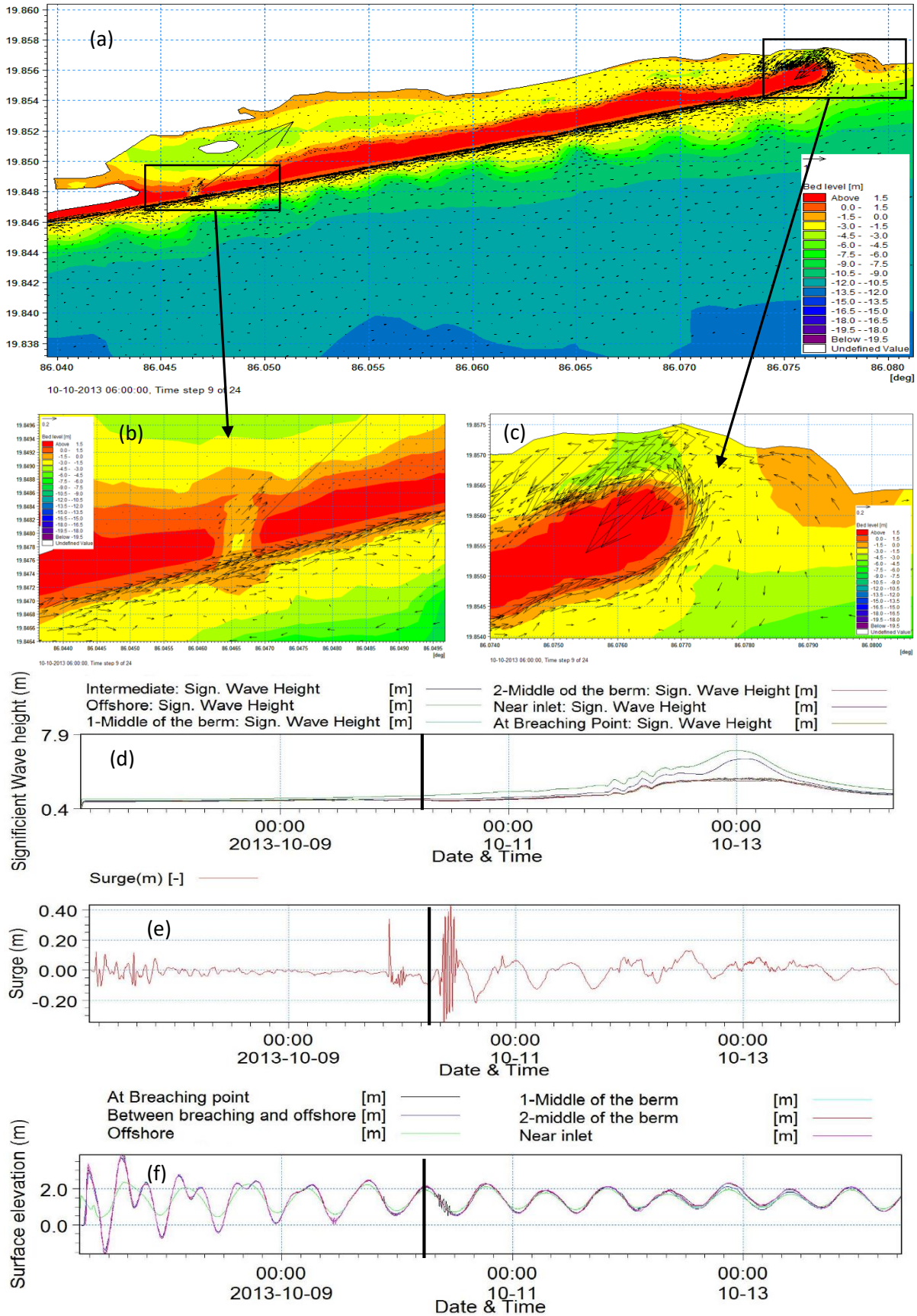


Figure A4.3 At 10-10-2013 06:00:00 time step the Figure shows vector plot (a) whole model domain, (b) near breach, (c) near inlet with time series plots of (d) significant Wave height, (e) surge and (f) surface elevation at various locations

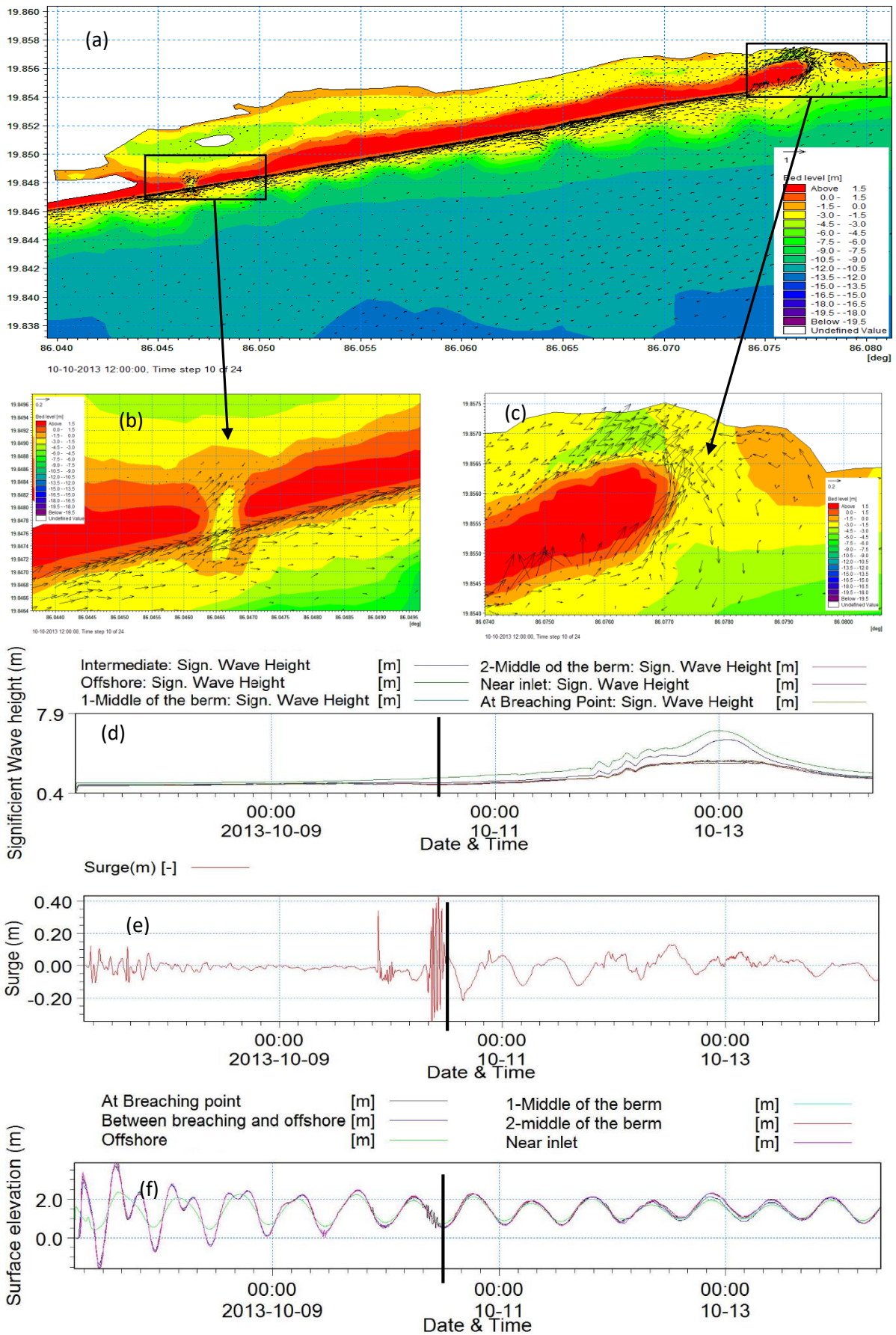


Figure A4.4 At 10-10-2013 12:00:00 time step the Figure shows vector plot (a) whole model domain, (b) near breach, (c) near inlet with time series plots of (d) significant Wave height, (e) surge and (f) surface elevation at various locations

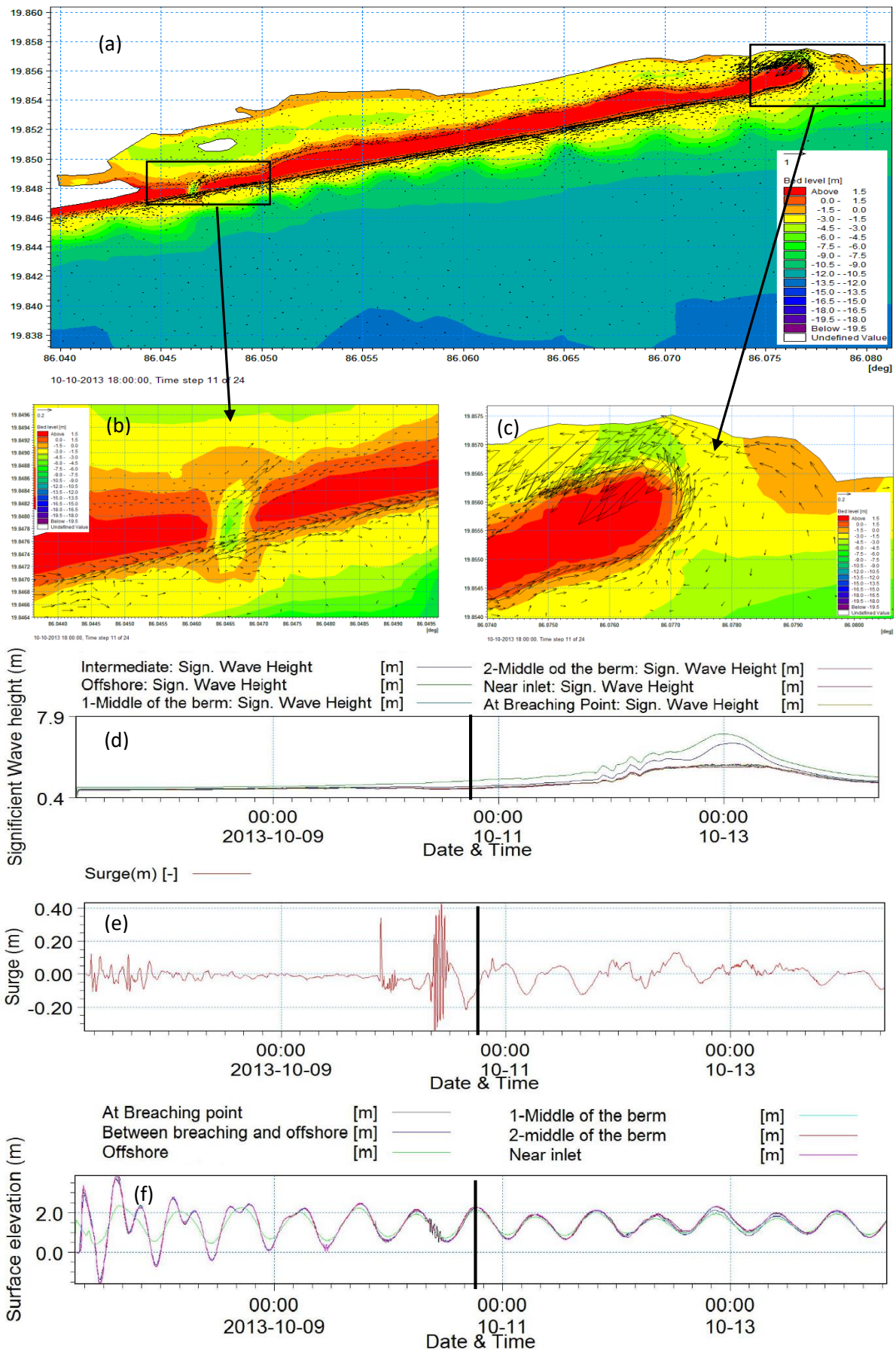


Figure A4.5 At 10-10-2013 18:00:00 time step the Figure shows vector plot (a) whole model domain, (b) near breach, (c) near inlet with time series plots of (d) significant Wave height, (e) surge and (f) surface elevation at various locations

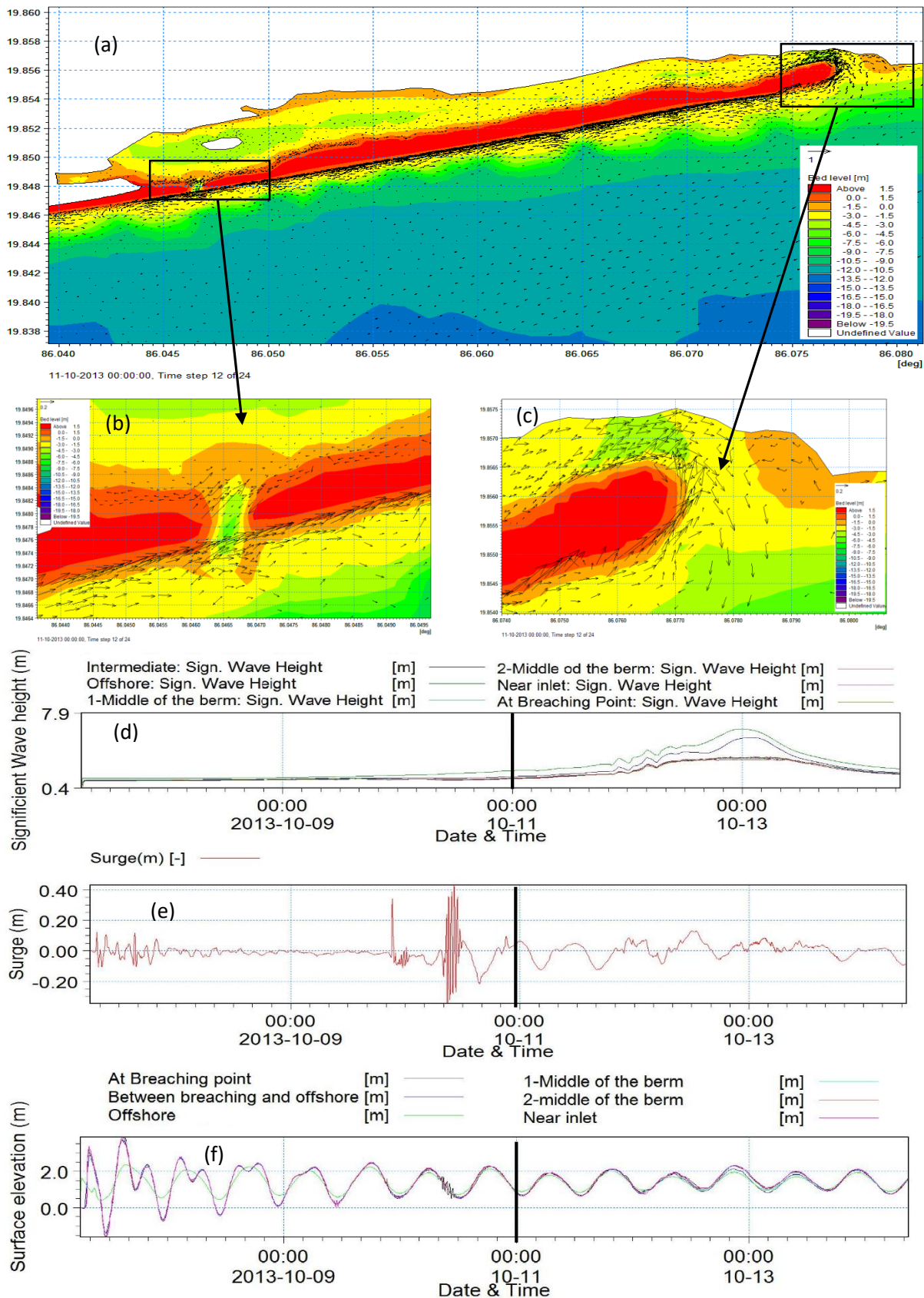


Figure A4.6 At 11-10-2013 00:00:00 time step the Figure shows vector plot (a) whole model domain, (b) near breach, (c) near inlet with time series plots of (d) significant Wave height, (e) surge and (f) surface elevation at various locations

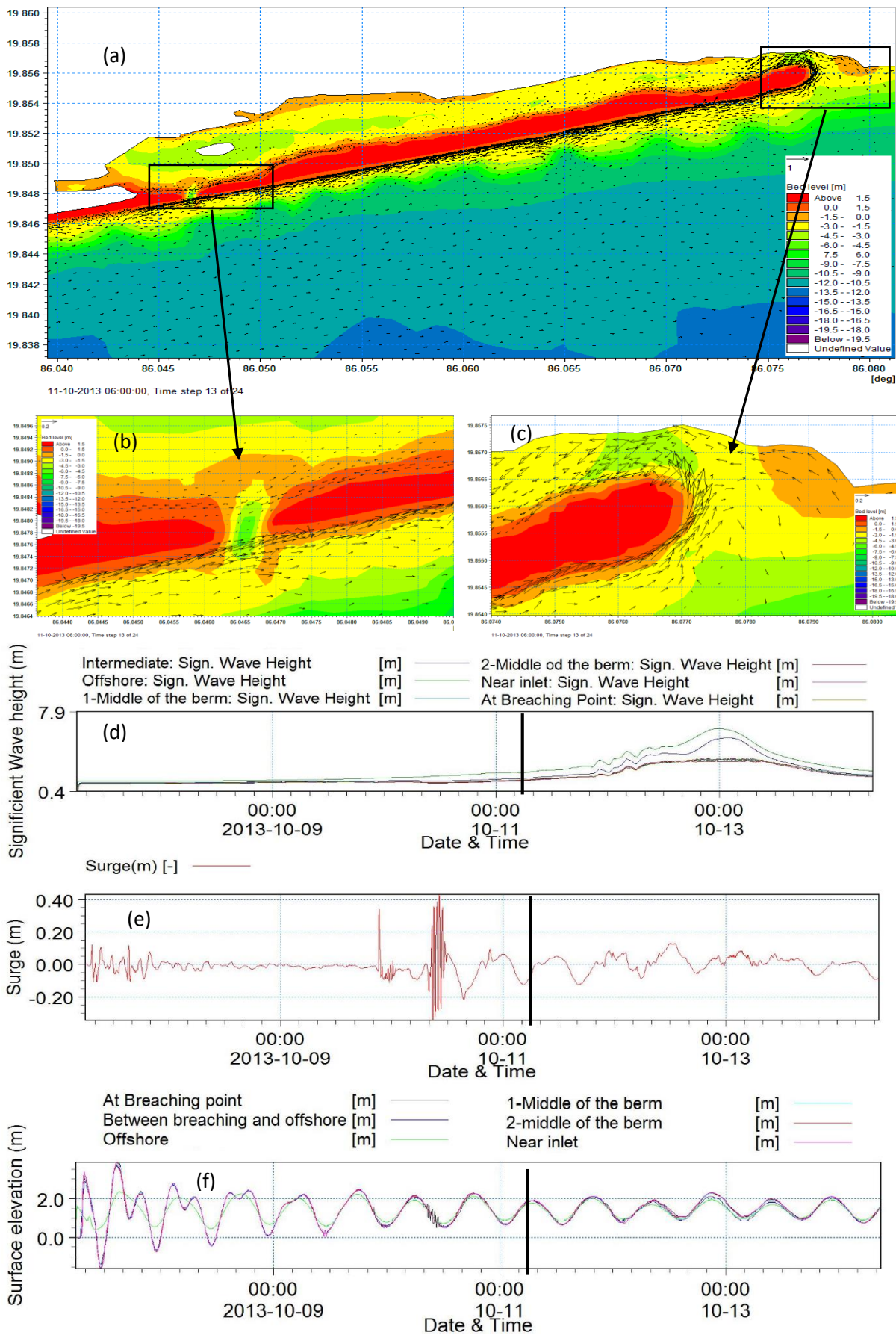


Figure A4.7 At 11-10-2013 06:00:00 time step the Figure shows vector plot (a) whole model domain, (b) near breach, (c) near inlet with time series plots of (d) significant Wave height, (e) surge and (f) surface elevation at various locations

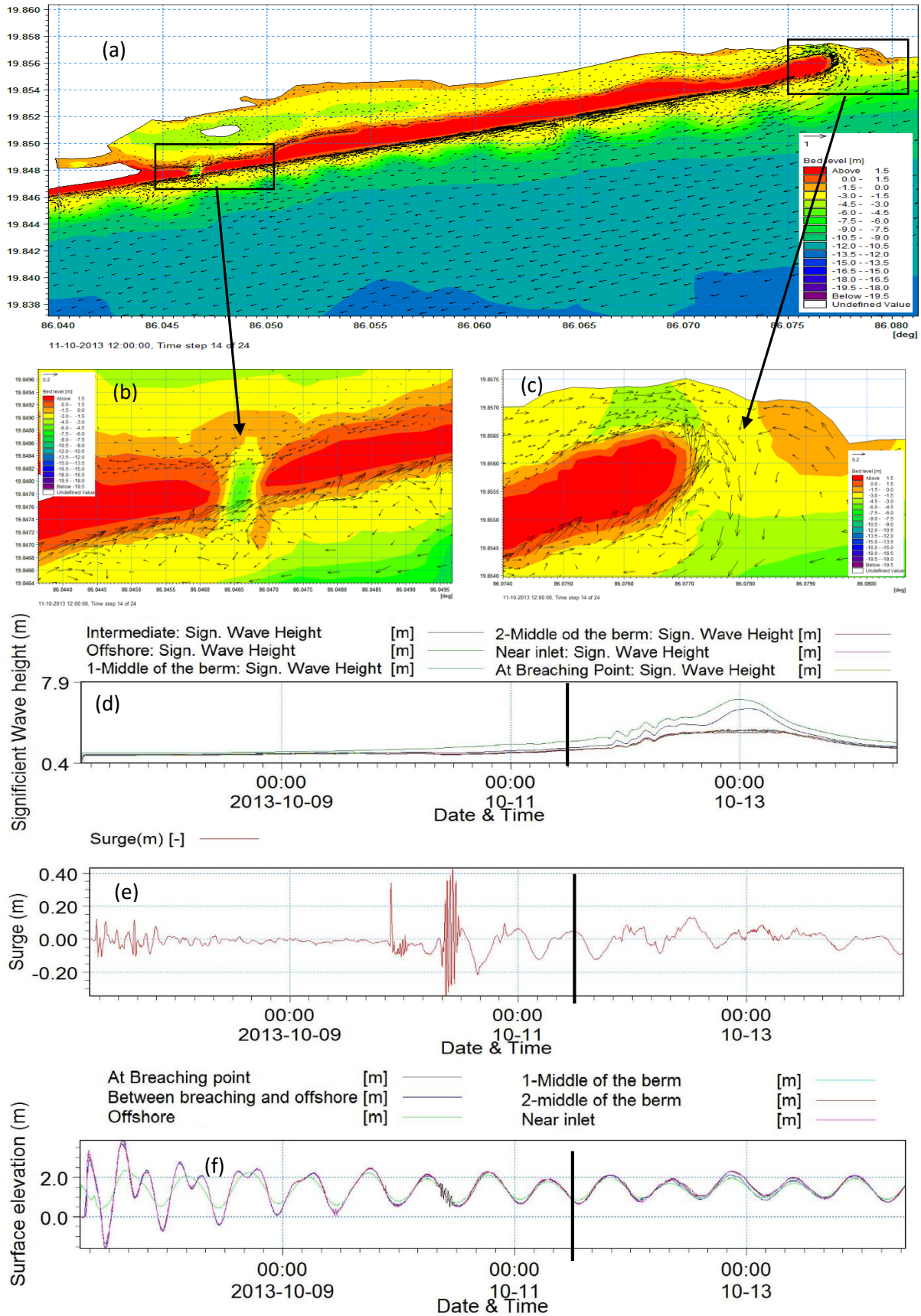


Figure A4.8 At 11-10-2013 12:00:00 time step the Figure shows vector plot (a) whole model domain, (b) near breach, (c) near inlet with time series plots of (d) significant Wave height, (e) surge and (f) surface elevation at various locations

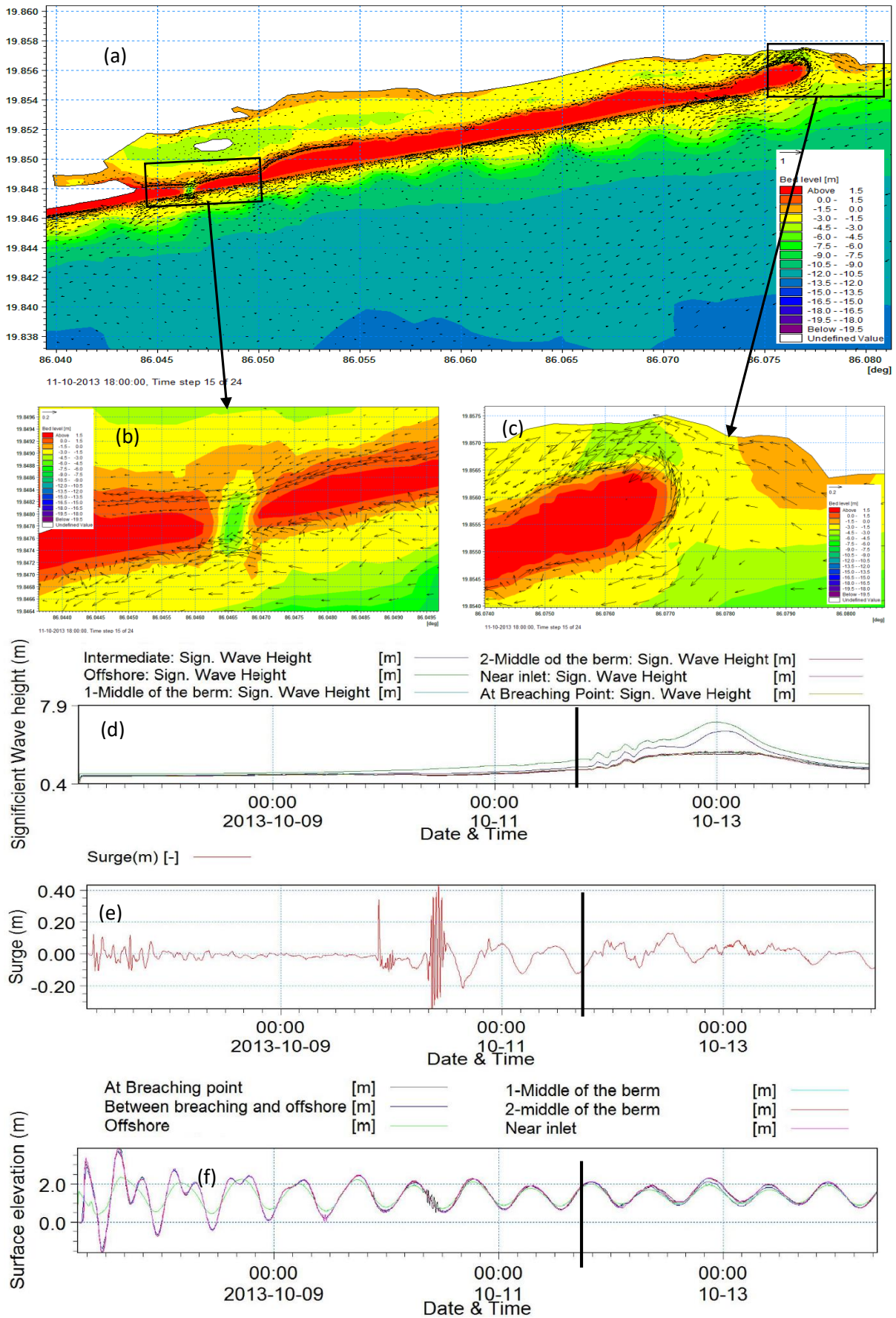


Figure A4.9 At 11-10-2013 18:00:00 time step the Figure shows vector plot (a) whole model domain, (b) near breach, (c) near inlet with time series plots of (d) significant Wave height, (e) surge and (f) surface elevation at various locations

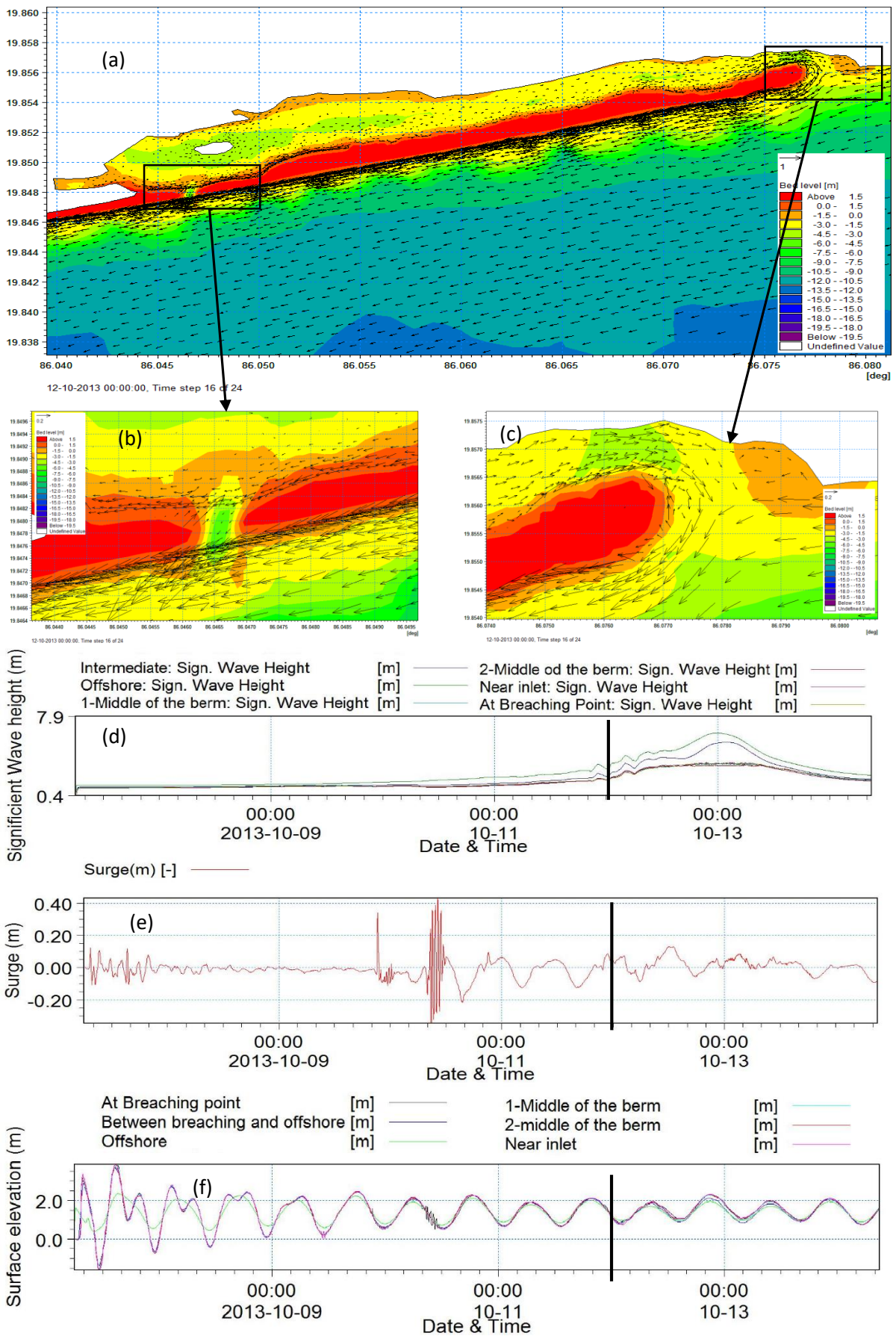


Figure A4.10 At 12-10-2013 00:00:00 time step the Figure shows vector plot (a) whole model domain, (b) near breach, (c) near inlet with time series plots of (d) significant Wave height, (e) surge and (f) surface elevation at various locations

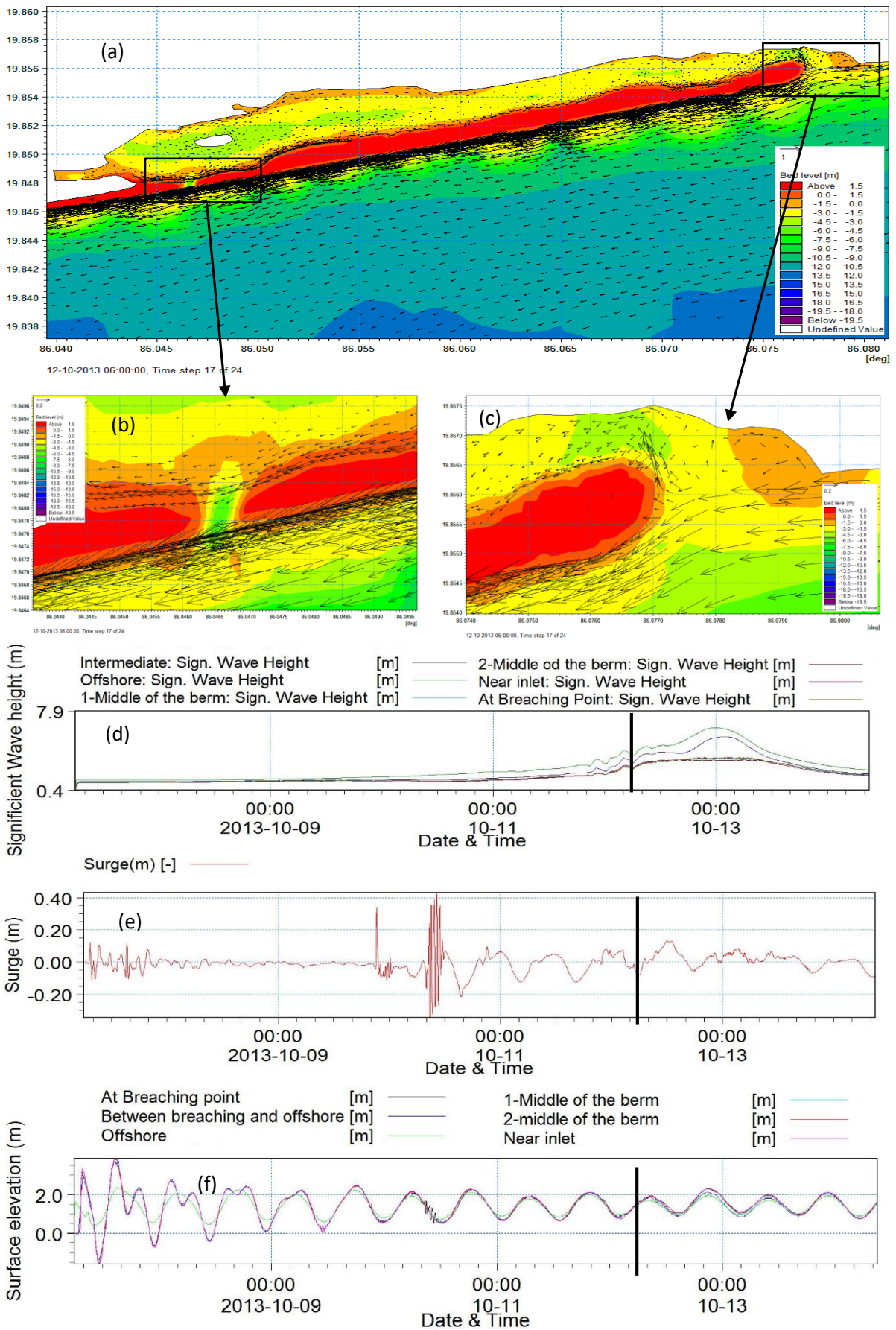


Figure A4.11 At 12-10-2013 06:00:00 time step the Figure shows vector plot (a) whole model domain, (b) near breach, (c) near inlet with time series plots of (d) significant Wave height, (e) surge and (f) surface elevation at various locations

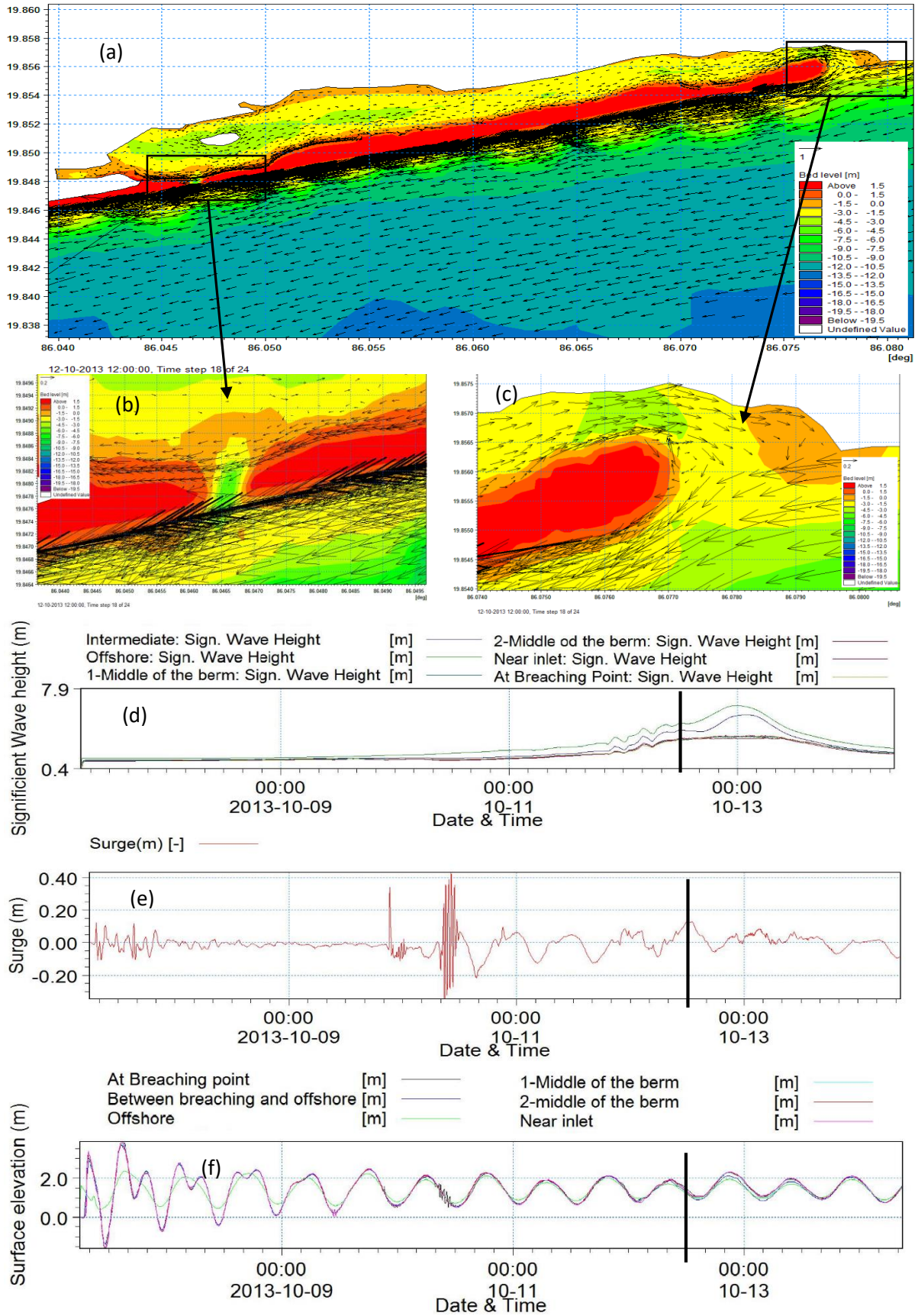


Figure A4.12 At 12-10-2013 12:00:00 time step the Figure shows vector plot (a) whole model domain, (b) near breach, (c) near inlet with time series plots of (d) significant Wave height, (e) surge and (f) surface elevation at various locations

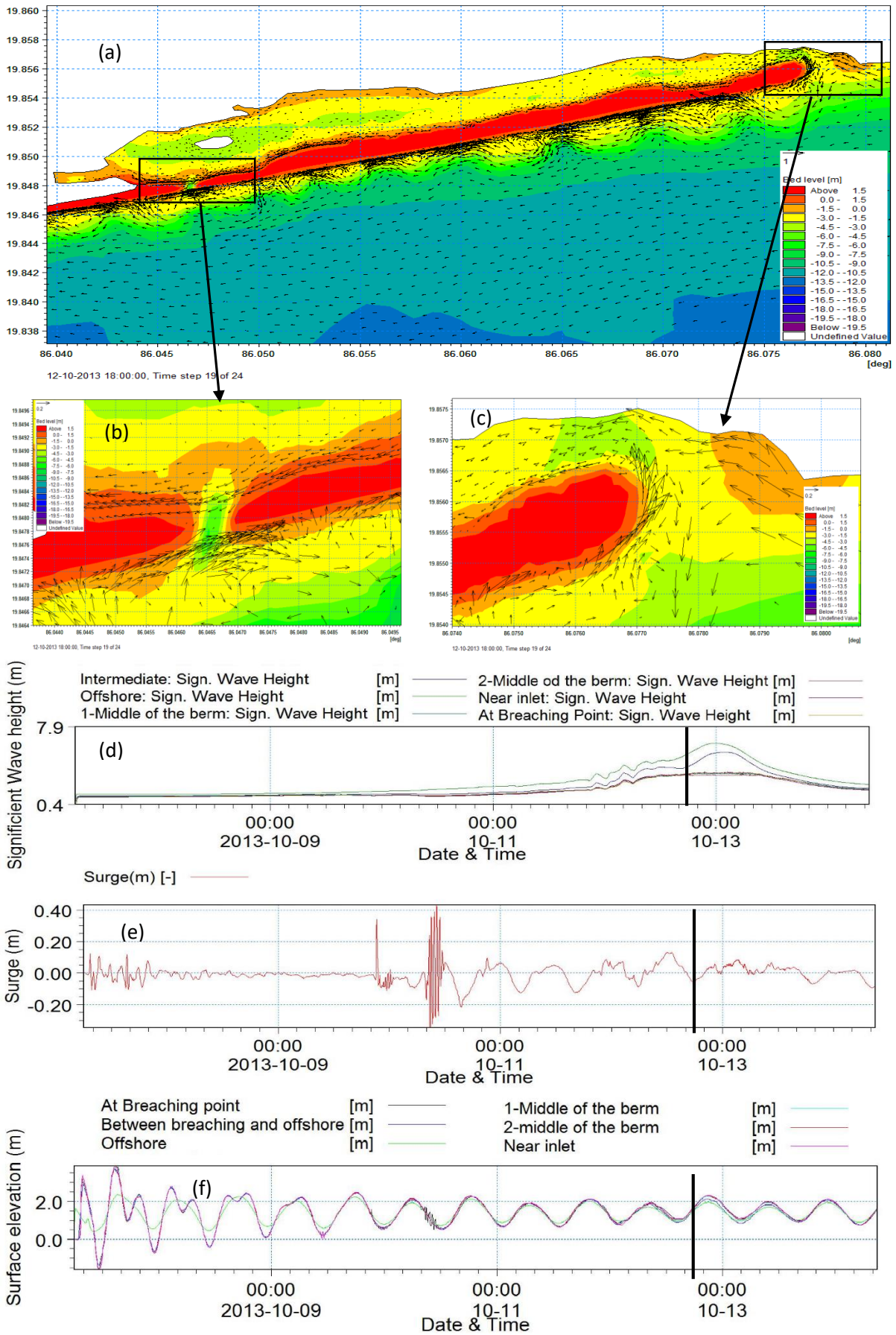


Figure A4.13 At 12-10-2013 18:00:00 time step the Figure shows vector plot (a) whole model domain, (b) near breach, (c) near inlet with time series plots of (a) significant Wave height, (e) surge and (f) surface elevation at various locations

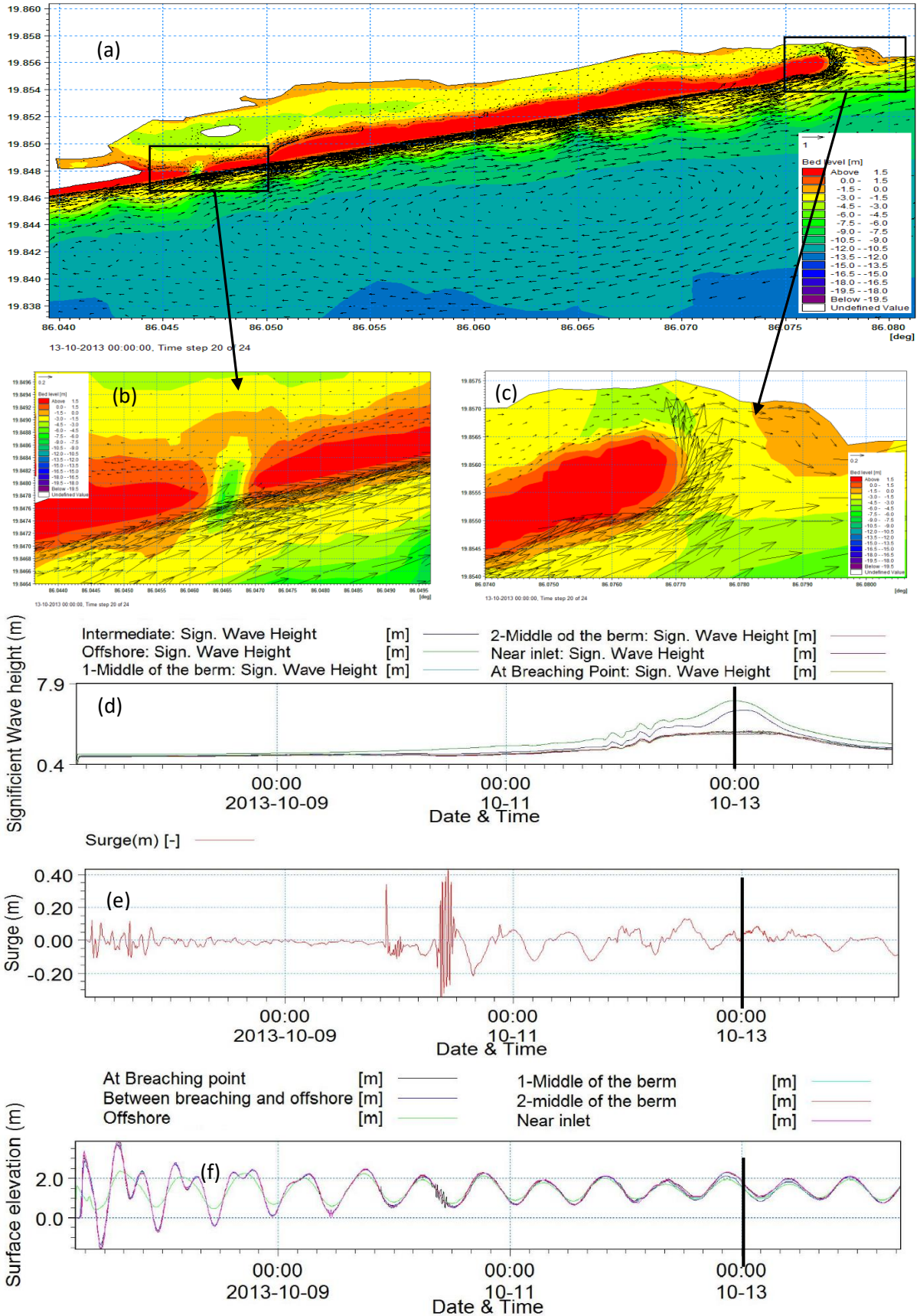


Figure A4.14 At 13-10-2013 00:00:00 time step the Figure shows vector plot (a) whole model domain, (b) near breach, (c) near inlet with time series plots of (a) significant Wave height, (e) surge and (f) surface elevation at various locations

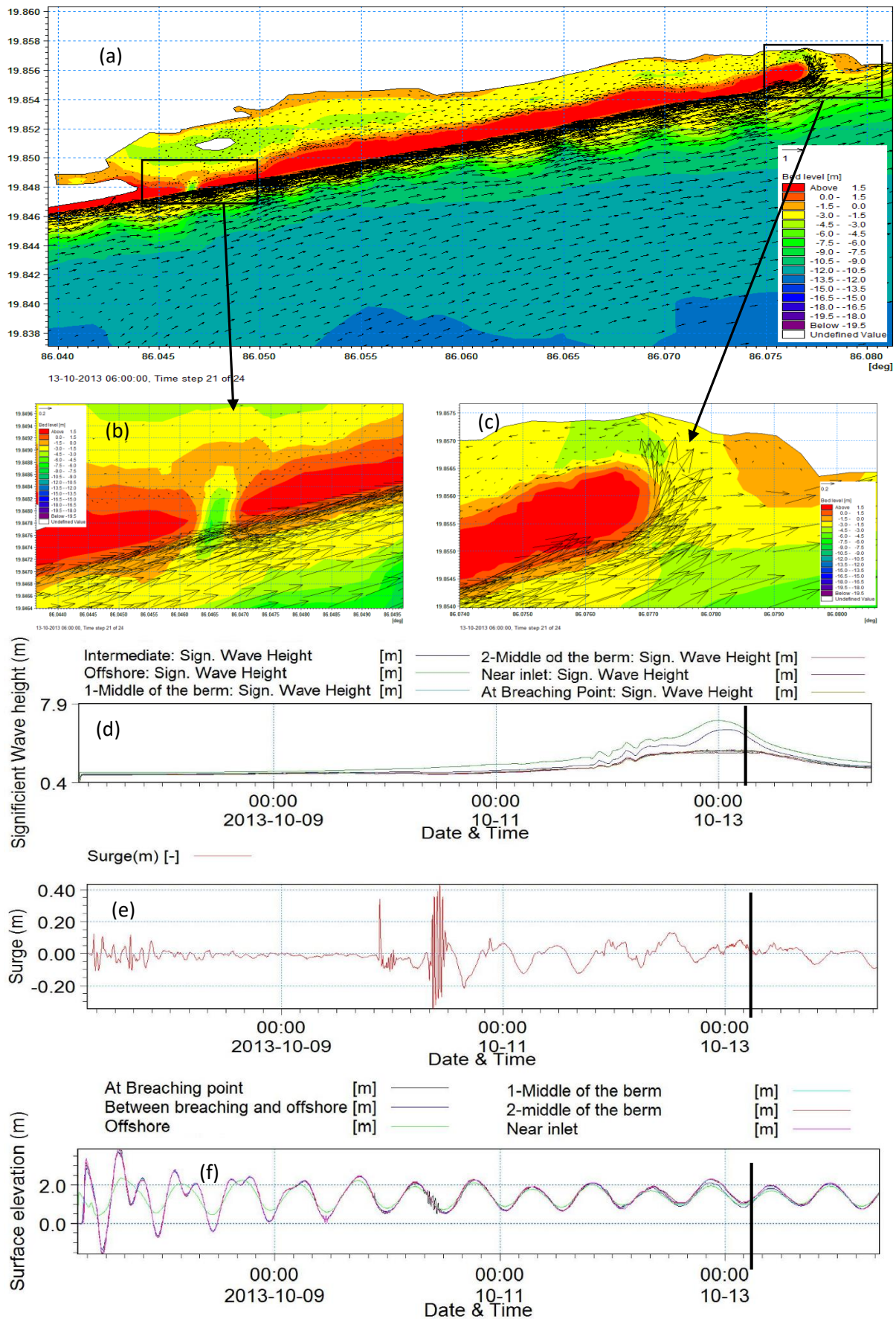


Figure A4.15 At 13-10-2013 06:00:00 time step the Figure shows vector plot (a) whole model domain, (b) near breach, (c) near inlet with time series plots of (a) significant Wave height, (e) surge and (f) surface elevation at various locations

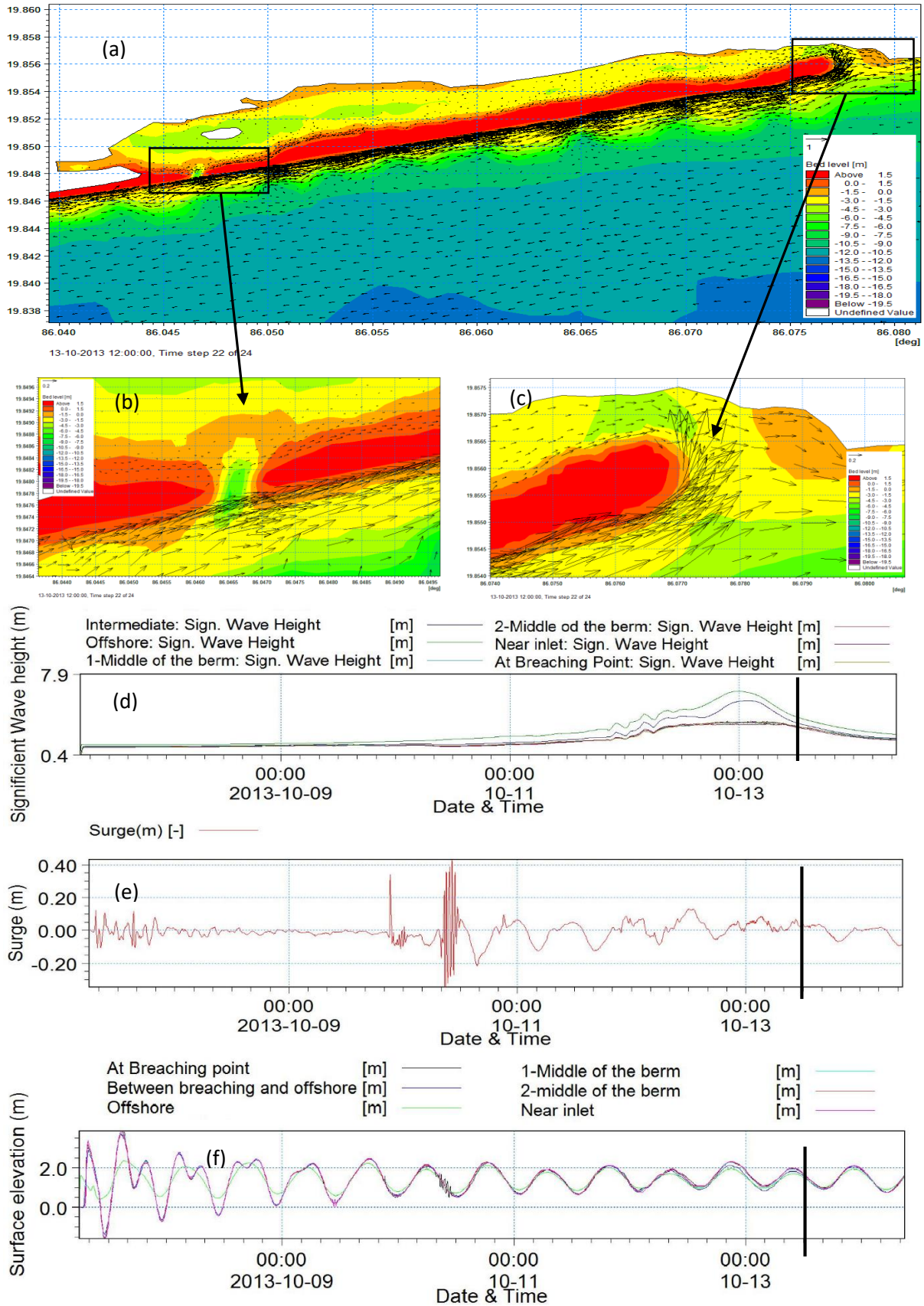


Figure A4.16 At 13-10-2013 12:00:00 time step the Figure shows vector plot (a) whole model domain, (b) near breach, (c) near inlet with time series plots of (a) significant Wave height, (e) surge and (f) surface elevation at various locations

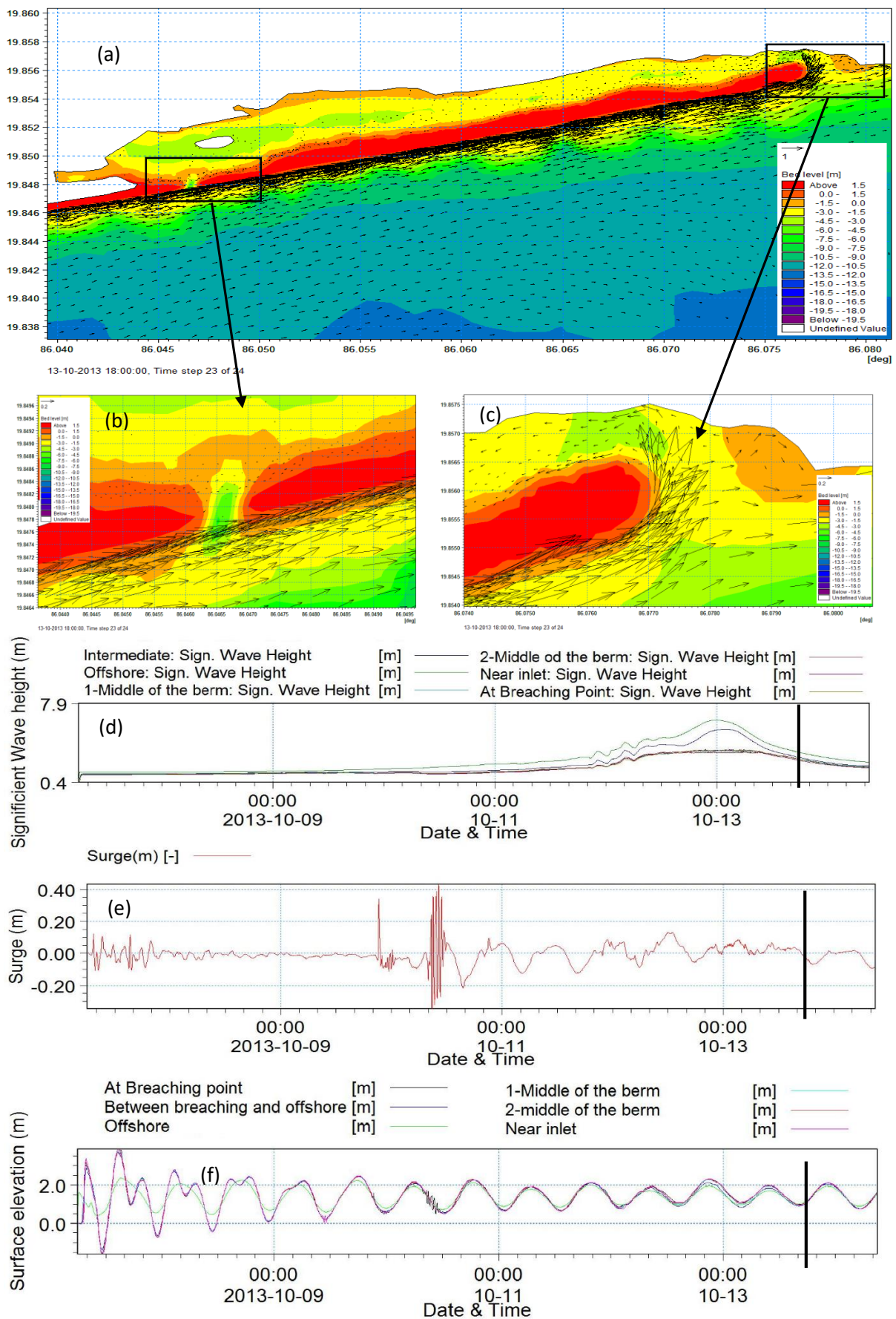


Figure A4.17 At 13-10-2013 18:00:00 time step the Figure shows vector plot (a) whole model domain, (b) near breach, (c) near inlet with time series plots of (a) significant Wave height, (e) surge and (f) surface elevation at various locations

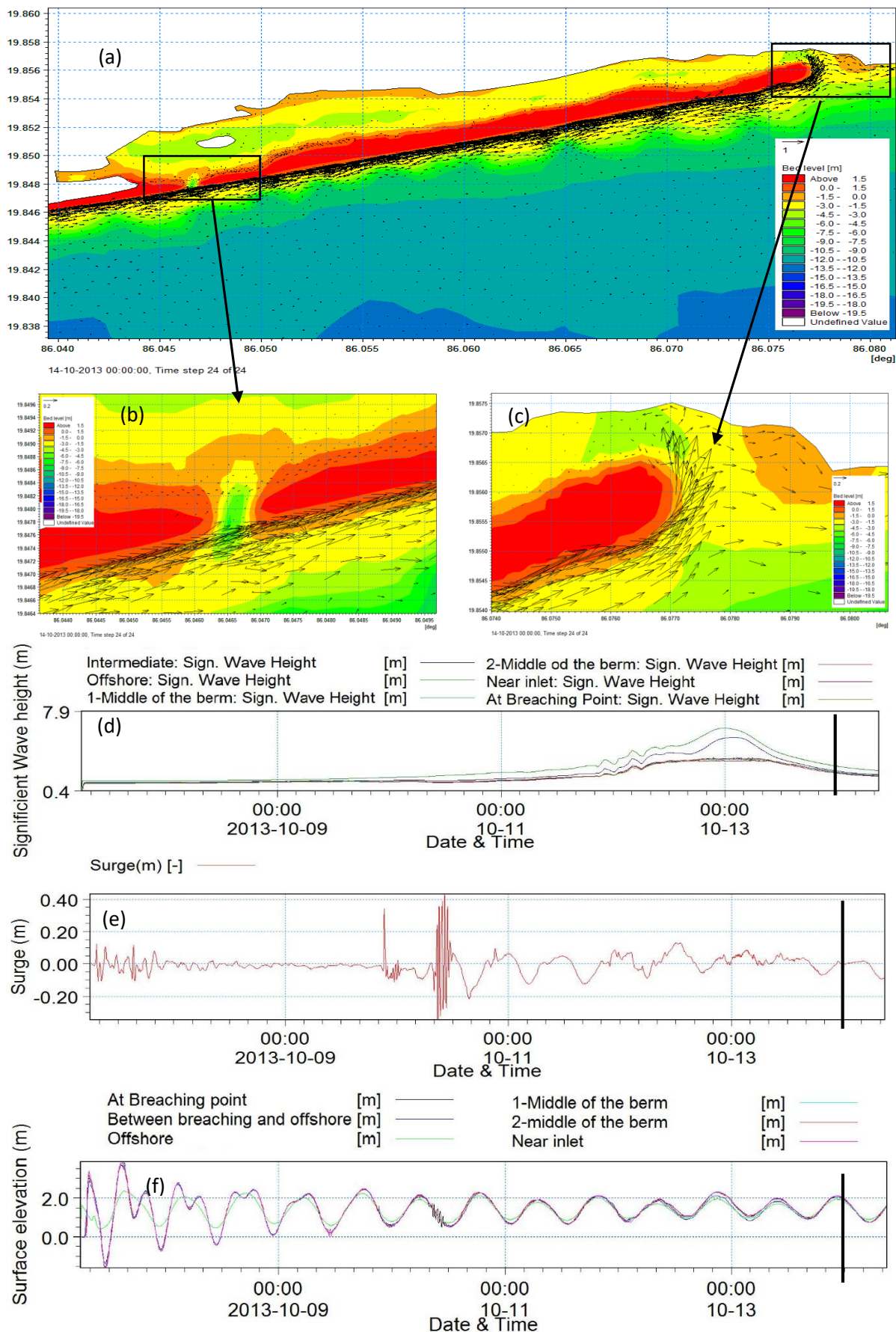


Figure A4.1 At 14-10-2013 00:00:00 time step the Figure shows vector plot (a) whole model domain, (b) near breach, (c) near inlet with time series plots of (a) significant wave height, (e) surge and (f) surface elevation at various locations

REFERENCES

Amarnatha Reddy, N. et al. (2015a). "Classification of tidal inlets along andhra pradesh coast on the central east coast of india." *8th International Conference on Asia and Pacific Coasts, APAC2015*, Indian Institute of Technology Madras, Chennai, India.

Amarnatha Reddy, N., Vikas, M., Seelam, J.K. and Rao, S., 2015b. A study on seasonal morphological changes and classification of tidal inlets along gujarat and kerala, 4th National conference of the Ocean Society of India (OSICON2015), Goa, India.

Andersen, O.B. (1995). "Global ocean tides from ers 1 and topex/poseidon altimetry. *Journal of Geophysical Research.*" 100(C12), 25249–25259.

Arora, M. et al. (2005). "Regional flow duration curve for a Himalayan river Chenab." *Nordic Hydrology*, 36(2), 193-206.

Barton, J. et al. (2007). "Development of a methodology for assessing estuary pressures: Relationships with catchment conditions, Stage 2 linking catchments to the sea - understanding how human activities impact on victorian estuaries." *Milestone 3 report*, the National land and Water Resources Audit: review and expand the Victoria-wide classification.

Bhaskaran, P.K. et al. (2013). "Performance and validation of a coupled parallel ADCIRC-SWAN model for THANE cyclone in the Bay of Bengal." *Environmental Fluid Mechanics*, 13(6), 601–623.

Bhaskaran, P.K. et al. (2014). "A numerical study of coastal inundation and its validation for Thane cyclone in the Bay of Bengal." *Coastal Engineering*, 83, 108–118.

Bhaskar, N.R. et al. (1997). "Flood Estimation for Ungauged Catchments Using the GIUH." *Journal of Water Resources Planning and Management*, 123(4), 228-238.

Bhunya, P.K. et al. (2003). "Simplified two-parameter Gamma distribution for derivation of synthetic unit hydrograph." *J. Hydrol. Eng.*, 8 (4), 226-230.

Bhunya, P.K. et al. (2005). "Hybrid model for derivation of synthetic unit hydrograph." *J. Hydrol. Eng.*, 10(6), 458-467.

Bhunya, P.K. et al. (2007). "Suitability of Gamma, Chi-square, Weibull, and Beta distributions as synthetic unit hydrographs." *Journal of Hydrology*, 334, 28-38.

Bhunya, P.K. et al. (2011). "Synthetic Unit Hydrograph methods: A Critical Review." *The Open Hydrology Journal*, 5, 1-8.

Burgess, R. et al. (2004). "Classification framework for coastal systems." 600/r-04/061, Office of Research and Development, UA, EPA.

Central Water Commission (CWC), (1992). "Flood Estimation Report for West Coast Region - Konkan and Malabar Coasts [Subzone – 5(a) and 5(b)]: A method based on unit hydrograph principles." *Design office report No. K&M/19/1992*, Hydrology (Small Catchments) Directorate, CWC, New Delhi, India.

Central Water Commission (CWC), (2001). "Manual on Design Flood Estimation." Hydrology Studies Organization, CWC, New Delhi, India.

Chant, R.J. et al. (2011). "The shaping of an estuarine superfund site: Roles of evolving dynamics and geomorphology." *Estuaries Coasts*, 34, 90–105.

Chien, H. et al. (2011). "Sediment dynamics observed in the Jhoushuei River and adjacent coastal zone in Taiwan Strait." *Oceanography*, 24(4), 122-131.

Chowdhury, P. and Behera, M.R. (2016). "Morphological evolution of a tidal inlet located along the west coast of India." *IX International Conference on Coastal and Port Engineering in Developing Countries (COPEDEC2016)*, Rio de Janeiro, Brazil, 16-21 October.

Chow, V.T. (1964). "Handbook of Applied Hydrology." McGraw-Hill, New York.

Cooper, J.A.G. (1993). "Sedimentation in a river dominated estuary." *Sedimentology*, 40, 979–1017.

Cooper, J.A.G. (2002). "The role of extreme floods in estuary-coastal behavior: Contrasts between river- and tide-dominated microtidal estuaries." *Sedimentary Geology*, 150, 123–137.

Crocker, K., M. et al. (2001). "REFRESH - Regional Flow Regimes Estimation for Small-scale Hydropower Assessment." Final Report- part 2, Himachal Pradesh, India.

Croley II. T.E. (1980). "Gamma synthetic hydrographs." *Journal of Hydrology*, 47, 41–52.

da Silva, J.F. et al. (2002). "Evaluation of the nutrient inputs to a coastal lagoon: The case of the ria de aveiro, portugal. Nutrients and eutrophication in estuaries and coastal waters." *Developments in hydrobiology*, 164. Springer, Dordrecht, 379-385 pp.

Dadouh-Guebas, F. et al. (2005). "Transition in ancient inland freshwater resource management in sri lanca affect biota and human populations in and around coastal lagoons." *Current Biology*, 15, 579-586.

Danovaro, R. and Pusceddu, A. (2007). "Biodiversity and ecosystem functioning in coastal lagoons: Does microbial diversity play any role?." *Estuarine, Coastal and Shelf Science*, 75, 4-12.

Davis, R.A. and Hayes, M.O. (1984). "What is a wave-dominated coast?." *Marine Geology*, 60(1-4), 313-329.

De Vriend, H.J. et al. (1989). "Hybrid prediction of intertidal flat evolution in an estuary." *International Conference Hydraulic and Environmental Modeling of Coastal, Estuarine and Rivers waters*, Bradford, U.K.

De Vriend, H.J. and Ribberink, J.S. (1996). "Mathematical modeling of meso-tidal barrier island coasts. Part II: Process-based simulation models. Advances in Coastal and Ocean engineering." P. L.-F. LIU, ed., *World Scientific Publishing Company*, Singapore, 150-179.

De Vriend, H. J et al. (1999). "Coastal inlets and tidal basins." Lecture notes, TU Delft.

Dissanayake, D.M.P.K. et al. (2009). "Modelled channel patterns in a schematized tidal inlet." *Coastal Engineering*, 56 (11-12), 1069-1083.

Di Silvio, G. (1989). "Modelling the morphological evolution of tidal lagoons and their equilibrium configurations." *XXII Congress of the IAHR*, Ottawa, Canada.

Dooge, J.C.I. (1959). "A general theory of the unit hydrograph." *J. Geophys. Res.*, 64(2), 241-256.

Dube, S.K. et al. (1986). “The effect of continuously deforming coastline on the numerical simulation of storm surges in Bangladesh.” *Mathematics and Computers in Simulation*, 28, 41–56.

Dube, S.K. et al. (2005). “Effect of Mahanadi river on the development of storm surge along the Orissa coast of India: a numerical study.” *Pure and Applied Geophysics*, 162, 1673–1688.

Duck, R.W. and da Silva, J. F. (2012). “Coastal lagoons and their evolution: A hydromorphological perspective.” *Estuarine, Coastal and Shelf Science*, 110 (0), 2-14.

Dyer, K.R. (1995). “Sediment transport processes in Estuaries.” *Geomorphology and Sedimentology of Estuaries*, edited by Perillo, G. M. E., Elsevier Sci., New York, pp. 423-449.

Gallo, M.N. and Vinzon, S.B. (2005). “Generation of overtides and compound tides in the Amazon estuary.” *Ocean Dynamics*, 55, 441–448.

Garde, R.J. and Kothyari, U.C. (1990). “Flood estimation in Indian catchments.” *Journal of Hydrology*, 113, 135-146.

Garel, E. et al. (2009). “Tidal and river discharge forcing upon water and sediment circulation at a rock-bound estuary.” *Estuarine Coastal Shelf Science*, 84, 269–281.

Gayathri, R. et al. (2015). “A numerical study of hypothetical storm surge and coastal inundation for AILA cyclone in the Bay of Bengal.” *Environmental Fluid Mechanics*, 16(2), 429-452.

Godin, G. (1985). “Modification of river tides by the discharge.” *Journal of Waterway Port Coastal Ocean Engineering*, 111(2), 257–274.

Goel, N.K. and Chander, S. (2002). "Regionalisation of Hydrological Parameter." State of Art Report No. INCOH/SAR-24/ 2002, National Institute of Hydrology, Roorkee, India.

Goel, N.K. (1998). "Flood Estimation in Sub-Himalayan Region Using L-Moments." International Symposium of 'Hydrology of Ungauged Streams in Hilly Regions for Small Hydro-Power Development, New Delhi, India.

Gowthaman, R. et al. (2015). "Nearshore waves and longshore sediment transport along Rameshwaram Island off the east coast of India." *International Journal of Naval Architecture and Ocean Engineering*, 7, 939-950.

Gray, D.M. (1961a). "Interrelationship of watershed characteristics." *J. Geophys. Res.*, 66, 1215-1223.

Gray, D.M. (1961b). "Synthetic hydrographs for small drainage areas." *SCE*, 87(4), 33-35.

Guo, L. et al. (2014). "The role of river flow and tidal asymmetry on 1-D estuarine morphodynamics." *Journal of Geophysical Research: Earth Surface*, 119, 2315–2334.

Hale, J. and Butcher, R. (2008). "Summary and review of approaches to the bioregionalisation and classification of aquatic ecosystems within australia and internationally."

Hayes, M.O. (Editor) (1979). "Barrier island morphology as a function of tidal and wave regime." Barrier islands from the gulf of st. Lawrence to the gulf of mexico. *Academic Press*, New York, 1-27 pp.

Heap, A. et al. (2001). "Australian estuaries and coastal ways: A geosciences perspective for improved and integrated resource management." *Australian Geological Survey Organisation*, Australia.

Holmes, M.G.R. et al. (2004). "Regional low flow estimation." United Kingdom contribution to the International Hydrological Program (IHP) of UNESCO, IHP-VI-Technical Document in Hydrology No. 68: 23-58.

Horrevoets, A.C. et al. (2004). "The influence of river discharge on tidal damping in alluvial estuaries." *Journal of Hydrology*, 294(4), 213–228.

Isla, F.I. (1995). "Coastal lagoons. In: G.M.E. Perillo (Editor), *Geomorphology and sedimentology of estuaries*." *Elsevier*, Amsterdam, pp. 241-272.

Iwasaki, S. and Shaw, R. (2008). "Fishery resource management in chilika lagoon: A study on coastal conservation in the eastern coast of india." *Coastal Conservation*, 12, 43-52.

Jain, S.K. et al. (2000). "Design Flood Estimation Using GIS Supported GIUH Approach." *Water Resources Management*, 14(5), 369-376.

Jaya Kumar, S. et al. (2006). "Tsunami height estimation in nearshore waters off Tamil Nadu coast using MIKE21 hydrodynamic model for the December 2004 Indian Ocean tsunami." *15th Congress of Asia and Pacific division of the International Association for Hydraulic Research (APD-IAHR) and International Symposium on Maritime Hydraulics*, IIT Madras Chennai, INDIA.

Jaya Kumar, S. (2012). "A numerical study on tsunami induced sediment transport in vicinity of a submarine canyon off southeast coast of India." *4th International Conference on Estuaries and Coasts (ICEC2012)*, 8-11 October 2012, Hanoi, Vietnam.

Jaya Kumar, S. and Mani Murali, R. (2014). "Storm and Tsunami induced sediment transport and morphology changes in vicinity of tidal inlets." *INDO-JAPAN Workshop on River Mouths, Tidal Flats and Lagoons*, IIT Madras, India, 78-87.

Jayantilal, N.P. and Akshay, R.T. (2016). "Synthetic Unit Hydrograph Development for Ungauged Basins Using Dimensional Analysis." *American Water Works Association Journal*, 145-153.

Kalnay, E. et al. (1996). "The ncep/ncar 40-year reanalysis project." *Bulletin of the American Meteorological Society*, 77(3), 437-471.

Karunarathna, H. et al. (2008). "Long-term morphodynamic evolution of estuaries: An inverse problem." *Journal of Estuarine, Coastal and Shelf Science*, 77(3), 385-395.

Karunarathna, H. et al. (2009). "Beach profile evolution as an inverse problem." *Journal of Continental Shelf Research*, 29(18), 2234-2239.

Kjerfve, B. (Editor). (1994). "Coastal lagoons." *Elsevier*, Amsterdam, 1-8 pp.

Kothyari, U.C. (1984). "Estimation of Annual Runoff from Catchments." M.Tech Dissertation, Department of Civil Engineering, Indian Institute of Technology Roorkee, Roorkee, India.

Kothyari, U.C. and Garde, R.J. (1991). "Annual Runoff Estimation for Catchments in India." *Journal of Water Resources Planning and Management*, 117(1), 1-10.

Kothyari, U.C. (1995). "Estimation of Monthly Runoff from Small Catchments in India." *Journal of Hydrological Sciences*, 40, 533-541.

Kothyari, U.C. (2004). "Estimation of Hydrologic Variables from Ungauged Catchments Using Artificial Neural Networks." Proceedings of Symposium on Prediction in Ungauged Basins for sustainable water resources planning and management, BITS, Pilani, India.

Krol, M. (1990). "The method of averaging in partial differential equations." *PhD thesis*, University of Utrecht, 81 pp.

Kumar, R. et al. (2003). "Development of Regional Flood Formulae using L-moments for Gauged and Ungauged Catchments of North Brahmaputra River System." *The Institution of Engineers (India)*, 84, 57-63.

Kumar, R. et al. (2004). "GIUH based Clark and Nash Models for runoff estimation for an ungauged basin and their uncertainty analysis." *International Journal of River Basin Management*, 2(4), 281-290.

Marciano, R. et al. (2005). "Modelling of channel patterns in short tidal basins." *Journal of Geophysical Research*, 100, F01001.

Nash, J.E. (1958). "Determination of runoff from rainfall." *Proc., Inst., Civ. Eng., Dublin, Ireland*.

Nash, J.E. (1959). "Synthetic determination of unit hydrograph parameters." *J. Geophys. Res.*, 64(1), 111-115.

Nielsen, P. (2009). "Coastal and estuarine processes. Advanced series on ocean engineering." *World Scientific*, New York, NJ (USA), 343 pp.

Pandey, R.P. and Ramasastri, K.S. (2003). "Estimation of lean season water availability in streams with limited data." *The Institution of Engineers (India)*, 84, 149-152.

Parida, B.P. (2004). "Delineation of Homogeneous Flood Regions in Central India using Single and Complete Linkage Methods." Proceedings of 2nd APHW Conference, Singapore. *Hydrological Sciences* 1, 56-65.

Parida, B.P. et al. (2004). "Regional Flood Frequency Analysis of Mahi-Sabarmati Basin (Subzone 3-a) using Index Flood Procedure with L-Moments." *Water Resources Management*, 12(1), 1-12.

Patra, S.K. and Jena, B.K. (2013). "Wave characteristics during severe cyclonic storm JAL, along east coast of India." *WMO International Conference on Indian Ocean Tropical Cyclones and Climate Change (IOTCCC-2012)*, New Delhi, WWRP, 4, 152-159.

Perez-Ruzafa, A. et al. (2011). "Mediterranean coastal lagoons in an ecosystem and aquatic resources management context." *Physics and Chemistry of the Earth*, 36, 160-166.

Raghuvanshi, N. et al. (2006). "Runoff and Sediment Yield Modeling using Artificial Neural Networks: Upper Siwane River, India." *Journal of Hydrologic Engineering*, 11(1), 71-79.

Ramakar, J. and Vladimir, S. (2008). "A review of methods of hydrological estimation at ungauged sites in India." Colombo, Sri Lanka: International Water Management Institute (IWMI Working Paper 130).

Ramakumar, M. (2000). "Recent Changes in Kakinada Spit, Godavari Delta." *Journal Geological Society of India*, 55, 183-188.

Ramkumar, M. (2003). "Progradation of the Godavari delta – a fact or empirical artifice? Insights from coastal landforms." *Journal Geological Society of India*, 62, 290–304.

Ramirez, J. A. (2000). "Prediction and modeling of flood hydrology and hydraulics. Chapter 11 of *Inland Flood Hazards: Human, Riparian and Aquatic Communities*." Edited by Ellen Wohl. Cambridge University Press.

Ranasinghe, R. and Pattiaratchi, C. (1998). "Flushing Characteristics of a Seasonally-Open Tidal Inlet: A Numerical Study." *Journal of coastal research*, 14(4), 1405-1421.

Ranasinghe, R. and Pattiaratchi, C. (1999). "The seasonal closure of tidal inlets: Wilson Inlet - a case study." *Coastal Engineering*, 37, 37-56.

Ranasinghe, R. and Pattiaratchi, C. (2003). "The seasonal closure of tidal inlets: causes and effects." *Coastal Engineering*, 45(4), 601-627.

Rees, H. G. et al. (2004). "Recession-based hydrological models for estimating low flows in ungauged catchments in the Himalayas." *Hydrol. Earth Syst. Sci.*, 8, 891-902.

Rengamannar, V. and Pradhan, P.K. (1991). "Geomorphology and evolution of Godavari delta." In *Quaternary Deltas of India* (ed. Vaidyanadhan, R.), *Journal Geological Society of India*, 22, 51-64.

Roy, P.S. et al. (2001). "Structure and function of south-east australian estuaries." *Estuarine, Coastal and Shelf Science*, 53(3), 351-384.

Roelvink, J.A. (2006). "Coastal morphodynamic evolution techniques." *Coastal Engineering*, 53, 277- 287.

Sahoo, B. et al. (2006). "Flood Estimation by GIUH-Based Clark and Nash Models." *Jr. of Hydrologic Engineering*, 11(6), 515-525.

Salami, A.W. et al. (2009). "Evaluation of synthetic unit hydrograph methods for the development of design storm hydrographs for Rivers in South-West, Nigeria," *J Am Sci.* 5(4), 23-32.

Sastry, J.S. (1991). "Morphological changes at Godavari delta region due to waves, currents and associated physical processes." In Quaternary Deltas of India (ed. Vaidyanadhan, R.), *Geological survey of India*, 22, 139–151.

Sassi, M.G., and Hoitink, A.J.F. (2013). "River flow controls on tides and tide-mean water level profiles in a tidal freshwater river." *Journal of Geophysical Research: Oceans*, 118, 1–13.

Savenije, H.H.G. (2005). "Salinity and Tides in Alluvial Estuaries." *Elsevier Science*, Amsterdam, Netherlands, 208pp.

Seelam, J.K. et al. (2014). "Seasonal dynamics of a tidal coastal inlet on east coast of india - measurements and modelling." *19th Congress of the Asia Pacific Division of the Congress of the International Association for Hydro-Environment Engineering and Research (IAHR)*, IAHR-APD 2014, Hanoi, Vietnam.

Shaji, C. et al. (2014). "Storm surge studies in the North Indian Ocean: A review." *Indian Journal of Geo-Marine Sciences*, 43(2), 125-147.

Singh, V.P. (1988). "Hydrologic systems: Rainfall-runoff modelling." Vol. 1, Prentice Hall, Englewood Cliffs, New Jersey.

Singh, S.K. (2000). "Transmuting synthetic unit hydrographs into gamma distribution." *Journal of Hydrologic Engineering*, 5 (4), 380–385.

Singh, R. D. et al. (2001). "Regional Flow-Duration Models for Large Number of Ungauged Himalayan Catchments for Planning Micro-hydro Projects." *Journal of Hydrologic Engineering*, 6(4), 310- 316.

Singh, P.K. et al. (2014). "A Review of the synthetic unit hydrograph: from the empirical UH to advanced geomorphological methods." *Hydrological Sciences Journal*, 59(2), 239-261.

Sivakholundu, K.M. et al. (2009). "Role of Tidal asymmetry on the Morphology of the estuarine navigational channel." *Proceedings of International Conference in Ocean Engineering (ICOE 2009)*, IIT Madras, Chennai, India.

Snyder, F.F. (1938). "Synthetic unit hydrographs." *Trans Am Geophysics Union*, 19, 447-454.

Soil Conservation Service (SCS), (1957). "Use of storm and watershed characteristics in synthetic hydrograph analysis and application." U.S. Dept. of Agriculture, Soil Conservation Service, Washington, D.C.

Stive, M.J.F. et al. (1998). "Morphodynamics of a tidal lagoon and adjacent coast." *Proceedings of 8th International Biennial Conference on Physics of Estuaries and Coastal Seas*, The Hague, 397-407.

Stive, M.J.F. and Wang, Z.B. (2003). "Morphodynamic modelling of tidal basins and coastal inlets." In C. Lakkhan (Ed.) *Advances in coastal modelling*, Elsevier Sciences, pp. 367-392.

Sudhakar, B.S. (2015). "Snyder Unit Hydrograph and GIS for Estimation of Flood for ungauged catchments in Lower Tapi Basin, India" *Hydrology: Current Research*, 6(1), 1-10.

Swamee, P.K. (1995). "Mean Annual Flood Estimation." *Journal of Water Resources Planning and Management*, 121(6), 403-407.

Takeda, I. and Sunamura, T. (1982). "Formation and height of berms." *Transactions-Japanese Geomorphological Union*, 3, 145–157.

Taylor, A.B. and Schwarz, H.E. (1952). "Unit hydrograph lag and peak flow related to basin characteristics." *Trans Am Geophys Union*, 33, 235-46.

Tung T.T. et al. (2008). "Morphological stability of tidal inlets using process-based modeling." *Proceedings of International Conference on Coastal Engineering*.

Tung, T.T. et al. (2009). "Morphological modelling of tidal inlet migration and closure." *Journal of Coastal Research*, 56, 1080–1084

Tung, T.T. (2011). "Morphodynamics of seasonally closed coastal inlets at the central coast of Vietnam." *PhD Thesis*, Faculty of Civil Engineering and Geosciences, Delft University of Technology.

Van der Wegen, M. and Roelvink, J.A. (2008). "Long-term estuarine morphodynamics evolution of a tidal embayment using a 2 dimensional process based model." *Journal of Geophysical Research*, 113, C03016.

Van der Wegen M. (2010). "Modeling morphodynamic evolution in alluvial estuaries." *Ph.D. Thesis*, UNESCO-IHE /TU Delft, CRC Pres.

Van der Wegen, M. et al. (2008). "Long-term morphodynamic evolution and energy dissipation in a coastal plain, tidal embayment." *Journal of Geophysical Research*, 113, F03001.

Van der Wegen, M. and Roelvink, J.A. (2008). “Long-term estuarine morphodynamics evolution of a tidal embayment using a 2 dimensional process based model.” *Journal of Geophysical Research*, 113, C03016.

Van der Wegen, M. et al. (2011). “Bed composition generation for morphodynamic modeling: Case study of San Pablo Bay in California, USA.” *Ocean Dynamics*, 61 (2-3), 173-186.

Van Dongeren, A.D. and De Vriend, H.J. (1994). “A model of morphological behaviour of tidal basins.” *Coastal Engineering*, 22, 287-310.

Vikas, M. (2015). “Classification of tidal inlets along indian coast.” *M.Tech Thesis*, National Institute of Technology Karnataka, Surathkal.

Vikas, M. et al. (2015a). “Classification of tidal inlets along central west coast of india.” *8th International Conference on Asia and Pacific Coasts, APAC2015*, Indian Institute of Technology Madras, Chennai, India.

Vikas, M. et al. (2015b). “A study on the classification of select tidal inlets along the east coast of india.” *20th International Conference on Hydraulics, Water Resources and River Engineering - HYDRO 2015*, IIT Roorke, India.

Vikas, M. et al. (2015c). “Tidal inlet classification along the coasts of goa and karnataka.” *4th National conference of the Ocean Society of India (OSICON2015)*, Goa, India.

Vu, T.T.T. (2013). “Aspects of inlet geometry and dynamics.” *Ph.D. Thesis*, The University of Queensland, Brisbane, Australia.

Wang, Z.B. et al. (1995). “Morphodynamic modeling for a tidal inlet in the Wadden Sea.” *Marine Geology*, 126, 289-300.

PUBLICATIONS

INTERNATIONAL JOURNALS

1. Amarnatha Reddy, N., Jaya Kumar, S., Subba Rao and Nagaraj, M.K. (2018). “Flood estimation at ungauged catchments of western catchments of Karnataka, West coast of India.” *ISH Journal of Hydraulics Engineering*, 1-11. <https://doi.org/10.1080/09715010.2018.1426055>
2. Amaranatha Reddy, N., Vikas, M., Jaya Kumar, S. and Subba Rao. (2015). “Classification of tidal inlets along Andhra Pradesh coast on the central east coast of India” *Procedia Engineering*, 116, 922-931. <https://doi:10.1016/j.proeng.2015.08.382>
3. Vikas, M., Amaranatha Reddy, N., Jaya Kumar, S. and Subba Rao. (2015). “Classification of tidal inlets along central west coast of India” *Procedia Engineering*, 116, 922-931. <https://10.1016/j.proeng.2015.08.381>
4. Jaya Kumar, S., Amarnatha Reddy, N., Vikas, M., Jyothi, P.K., Vu, T.T.T. and Subba Rao. (2018). “Classification of tidal inlets along the coast of India.” *Journal of Geomorphology*, Elsevier Publication (Under Review).

INTERNATIONAL CONFERENCES/ SYMPOSIUMS

1. Amarnatha Reddy, N., Vikas, M., Jaya Kumar, S. and Subba Rao. (2018). “Non-dimensional methods to classify the Tidal inlets along the Karnataka coastline, West coast of India.” *4th International Conference in Ocean Engineering (ICOE-2018)*, IIT Madras, Chennai, India.

2. Amarnatha Reddy, N., Jaya Kumar, S., Subba Rao and Nagaraj, M.K. (2016). “Application of synthetic unit hydrograph to determine flood discharge along the tidal inlets of Karnataka coastline.” *10th International Symposium on Lowland Technology (ISLT-2016)*, Mangalore, Karnataka, India.
3. Jaya Kumar, S., Vikas, M., Amarnatha Reddy, N. and Subba Rao. (2015). “Classification of tidal inlets along the Indian coast.” *International Indian Ocean Expedition (HIOE)*, National Institute of Oceanography, Goa, India.
4. Vikas, M., Amarnatha Reddy, N., Subba Rao and Jaya Kumar, S. (2015). “A study on the classification of select tidal inlets along the east coast of India.” *20th International Conference on Hydraulics, Water Resources and River Engineering*, IIT Roorkee, India.
5. Jaya Kumar, S., Amaranatha Reddy, N., Ramana Murthy, M.V., Mani Murali, R., Arun Kumar, A. and SubbaRao. (2014). “Seasonal Dynamics of a Tidal coastal inlet on East coast of India – Measurements and Modelling.” *19th IAHR-APD Congress*, WRU, Hanoi, Vietnam.
6. Jaya Kumar, S., Amaranatha Reddy, N. and Jyoti, K. (2018). “Cyclone Induced Berm Breaching in the Bay of Bengal Under Climate Change Conditions - a Case Study Off Konark Coast During Cyclone Phailin.” *15th annual meeting Asia Oceania Geosciences Society (AOGS)*, Honolulu, Hawaii, US. (Abstract accepted)

NATIONAL CONFERENCES

1. Amaranatha Reddy, N., Vikas, M., Jaya Kumar, S. and Subba Rao. (2015). “A study on seasonal morphological changes and classification of tidal inlets along Gujarat and Kerala Coast.” *4th National conference of Ocean Society of India (OSICON-15)*, CSIR-NIO, Goa, India.

RESUME

Name : Amaranatha Reddy N.
Date of Birth : 06-09-1982
Address : Assistant Professor
Department of Civil Engineering
Madanapalle Institute of Technology & Science
Kadiri Road, Angallu (V), Chittoor (Dist.)
Madanapalle, Andhra Pradesh – 517325.



Mobile : (+91) 8686151727/7890526220

Email(s) : amaranathareddyn@mits.ac.in / amarmtech@gmail.com

Qualification : B.Tech. (Civil Engineering),
M.Tech. (Offshore Structural Engineering)

Journal Publications : International – 5

Conference Publications : International – 13 National - 1